DESIGN AND DEVELOPMENT OF A SMART INVERTER SYSTEM

by

ADEKOLA, OLAWALE IBRAHIM

Thesis submitted in partial fulfilment for the award of the requirements for the degree

Master of Technology: Electrical Electronic and Computer Engineering

in the Faculty of Engineering

at the Cape Peninsula University of Technology

Supervisor: DR AK RAJI

Bellville Campus

December, 2015

CPUT copyright information

This dissertation/thesis may not be published either in part (in scholarly, scientific or technical journals), or as a whole (as a monograph), unless permission has been obtained from the University.

DECLARATION

I, Olawale Ibrahim ADEKOLA, declare that the contents of this dissertation/thesis represent my own unaided work, and that the dissertation/thesis has not previously been submitted for academic examination towards any qualification. Furthermore, it represents my own opinions and not necessarily those of the Cape Peninsula University of Technology.

Signed **Date**

ABSTRACT

The growing interest in the use of solar energy to mitigate climate change, reduction in the cost of PV system and other favourable factors have increased the penetration of the PV(Photovoltaic) systems in the market and increase in the worldwide energy supply. The main component in a DG is a smart inverter connected in a grid-tied mode which serves as a direct interface between the grid and the RES (Renewable Energy System).

This research work presents a three phase grid-tied inverter with active and reactive power control capabilities for renewable energy sources (RES) and distributed generators (DG). The type of the inverter to be designed is a Voltage Source Inverter (VSI). The VSI is capable of supplying energy to the utility grid with a well regulated DC link at its input.

The solution this project proposes is an implementation of the designed filter to effectively reduce the harmonics injected into the grid to an acceptable value according to standards and also an approach to control the real and reactive power output of the inverters to help solve the problems of instability and power quality of the distribution system. The design, modelling and simulation of the smart inverter system is performed in MATLAB/SIMULINK software environment. A 10 kW three-phase voltage source inverter system connected to the utility grid was considered for this research. Series of simulations for the grid-connected inverter (GCI) model was carried out using different step changes in active and reactive power references which was used to obtain the tracking response of the set power references. The effectiveness of the control system which was designed to track the set references and supply improved power quality with reduced current ripples has been verified from the simulation results obtained.

ACKNOWLEDGMENTS

- I wish to thank Almighty Allah for giving me the opportunity and strength to effectively carry out my research work.
- My sincere appreciation goes to my supervisor Dr A.K Raji for his support, supervision and guidance. His mentoring and motivation has facilitated me in completing this research work.
- I would also like to express my profound gratitude to my beloved parents, Prof and Dr (Mrs) ADEKOLA, for their endless love and affection showed to me during my toughest and most trying period.
- I will also like to appreciate my siblings, Tola, Kamal, Mariam, Abdullahi and Abdulrahman as well for their moral support. May Allah reward you abundantly (Amin).
- My sincere gratitude also goes to the members of Faculty of Engineering: Akim, John, Martial, Makani, kunle, Clement, Khader, Alli and Al-jadeed for their support and helpful suggestions during my Master's program.
- My gratitude goes to Seyi, Qazeem, Aisha, Bukola, Damola, Benji, Sodiq, Afolabi, Ife, Mumba and others just to mention a few for helping me in one way or the other. God's blessings shall not depart from you all.

TABLE OF CONTENTS

LIST OF FIGURES

LIST OF TABLES

DEDICATION

This thesis is dedicated to almighty Allah and to my parents Prof. & Dr (Mrs) ADEKOLA for their continuous motivation and support from the beginning of my studies.

RESEARCH OUTPUTS

1. Adekola, O.I., & Atanda, A.K., 2015, March. Design and Development of a Smart inverter. In *Cape Peninsula University of Technology (CPUT) Faculty of Engineering Postgraduate Seminar*, *Cape Town 2015.*

2. Adekola, O.I., & Atanda, A.K., 2014, November. Design and Development of smart inverter system. In *Cape Peninsula University of Technology (CPUT) Poster presentation for CPUT research day, Cape Town 2014.*

3. Adekola, O.I. & Raji, A.K., 2015, August. Functionalities of Smart Inverter System for Grid-Connected Applications. In *Industrial and Commercial Use of Energy (ICUE), International Conference on the. IEEE,*. pp. 340–344.

4. Adekola, O.I. & Raji, A.K., 2015, December. Design of a smart inverter system for photovoltaic application. In *Energy Technologies (ENTECH), International Conference, Istanbul 2015.*

5. Adekola, O.I. & Raji, A.K., 2015, December. Controller design for renewable energy power electronics converter using Simulink control design tool. In *Energy Technologies (ENTECH), International Conference, Istanbul 2015.*

LIST OF ABBREVIATIONS

AC	Alternating Current
CSI	Current source inverter
DC	Direct Current
DER	Distributed energy resources
DES	Distributed energy source
DG	Distributed generation
dq	direct-quadrature
EMI	Electromagnetic interference
ES	Energy storage
FFT	Fast Fourier transform
GCI	Grid-connected inverter
GHG	Greenhouse gas
GTO	Gate turn off thyristor
HVDC	High voltage direct current
IGBT	Insulated gate bipolar transistor
IGCT	Integrated Gate-Commutated Thyristor
kW	Kilowatts
LCL	inductor-capacitor-inductor
LV	Low-Voltage
MATLAB	Matrix laboratory
MFI	Multifunctional inverter
MG	Micro-grid
MPPT	Maximum power point tracker
MW	Megawatts
PCC	Point of common coupling

PR	Proportional resonant
PV	Photovoltaic
SHSs	solar home systems
VSC	Voltage source converter
VSI	Voltage source inverter
IEEE	Institute of Electrical and Electronics Engineers
P	Active power
PLL	Phase-locked loop
PI	Proportional-integral
PQ	Power quality
PWM	Pulse width modulation
Q	Reactive power
RES	Renewable energy sources
SPWM	Sinusoidal pulse width modulation
THD	Total harmonic distortion

GLOSSARY OF TERMS

Distributed resource (DR)	This is a source of electrical power that is not directly connected to a bulk power transmission system. Examples of DR are generators.
Generator	An electric machine that converts mechanical energy to electrical energy
IEEE 1547	A standard of the Institute of Electrical and Electronics Engineers for interconnection of distributed generation resources into the grid.
Inverter	A device or system that converts direct current to alternative current
MegaWatt (MW)	A unit of power (rate of energy consumption) 1 MegaWatt is equal to 1 000 000 Watts 1 000 MegaWatts is equal to 1 GigaWatt.
MATLAB	A multi-paradigm mathematical processing environment and fourth-generation programming language
Model	A representation of real world systems in a software environment such as Simulink for better understanding.
Simulink	An environment for block diagrams where multi-domain simulations and Model-Based Designs are carried out.

LIST OF SYMBOLS

C_b	Base capacitance
C_f	Filter Capacitor
f_g	Grid frequency
f_{res}	Resonance frequency
f_{sw}	Switching frequency
i_i	Inverter output current
i_g	Grid current
I_{rms}	Root mean square current
K_p	Proportional gain
K_i	Integral gains
L_i	Inverter-side inductor
L_g	Grid-side inductor
L_T	Total inductance
PF	Power factor
P_n	Nominal power
r	Relation factor between inductances
R_i	Inverter-side inductor resistances
R_g	Grid-side inductor resistances
R_f	damping resistor
v_i	inverter output voltage
v_c	Filter capacitor voltage
V_{dc}	Nominal direct current voltage
v_g	Grid voltage
V_{rms}	Root mean square voltage
ω	Angular speed

ω_n	Natural frequency in rad/secs
Z_b	Base-impedance

CHAPTER 1

INTRODUCTION

1.1 Background

In recent times, there has been continuous increase in energy consumption which has also led to the increase of renewable energy production. There are different sources of energy currently in use but unfortunately, most of the energy sources come from conventional fossil fuels (Ross & Jordan 2012.). The use of conventional fossil fuels for the production of electricity in South Africa contributes more than 90% of our total consumption making us the biggest polluter on the continent. The environmental impacts of fossil fuels such as oil, coal and gas are very enormous and hazardous. Apart from contaminating the air, polluting and harming the environment, it has been identified as the main culprit in increasing greenhouse gases (GHGs) in the atmosphere, which is causing global climate change. The greenhouse gases (GHGs) such as carbon dioxide, nitrous oxide and methane are released when we use fossil fuels. One of the most immense methods of generating electricity without emissions or noise is through PV solar electricity by converting abundant sunlight to electrical energy(Hoffmann 2006). Solar photovoltaic (PV) systems are used for several applications since the maintenance required is low and no pollution discharged. The Fig 1.1 shows that South Africa uses a very high percentage of coal to generate electricity than any other source of energy (Adekola & Raji 2015). The decrease in the cost of renewable energy technology in the past years till the next 6 years is also shown in the graph in Fig 1.2.

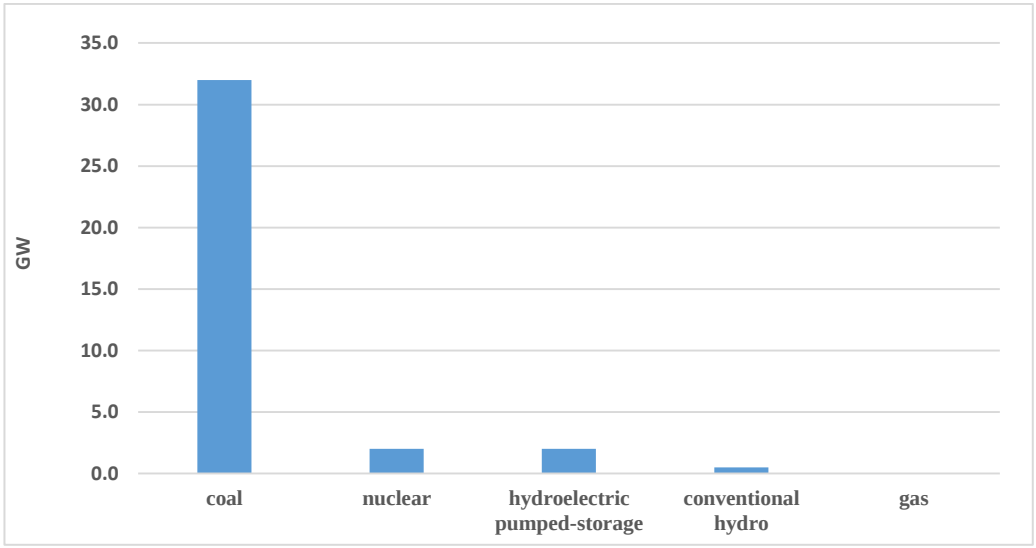

Figure 1.1: Energy mix in South Africa

(Pegels 2010)

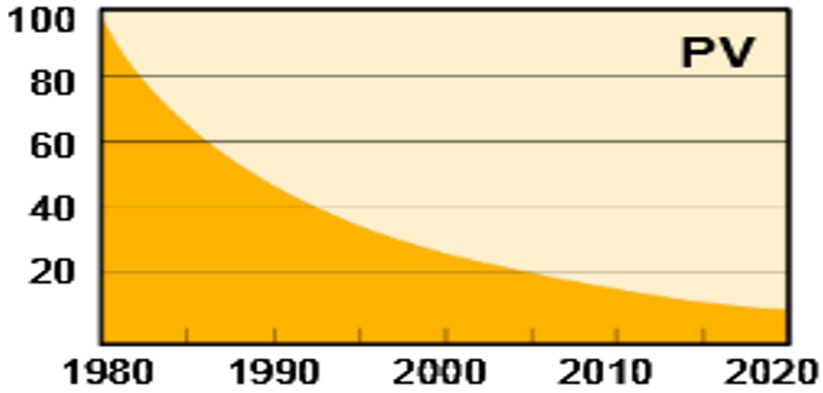

Figure 1.2: Cost reduction curve for renewable energy technology (Banks & Schaffler 2006)

The South African government initiative in ensuring that substantial percentage of our energy mix is renewable is evidenced in the renewable energy independent power producer programme (REIPPPP) with close to 3 GW generation capacities of approved deals as at the close of the third bidding window. Also construction is set to start on Eskom's 100 MW concentrated solar plant, in the Northern Cape according to the Electricity report for year 2015 (Powertech & Creamer Media's research channel Africa 2014). The use of alternative renewable energy will reduce the rate at which greenhouse gases are being released to the atmosphere resulting in a healthier environment(Ross & Jordan 2012). Renewable energy is produced from sources that are replenished naturally. Some of the different energy sources are sun, wind and water. All these sources can be converted to electricity through conversion technologies such as wind turbine and photovoltaic which are still in the process of achieving high technological efficiency and market penetration level (Sissine 2007). Electricity is generated from sunlight through PV devices using semiconducting materials such as silicon such that when sunlight strikes the solar panel, electrons in the silicon start to move around creating energy (Ross & Jordan 2012). However, the intermittency and variability nature of renewable energy sources may result into power system instability if intelligent interface is not provided.

A power electronics inverter system should have a digital design, robust software facilities and a two-way communications ability in order to make the system intelligent. The system typically comprises of a reliable, robust and proficient silicon-based hardware, which can be controlled by an adaptable software environment by integrating a control structure capable of advanced performance monitoring. The intelligent or smart interface can be developed by employing Power electronics technology. Recently, there has been continuous growth in power electronics field and the main aspects of this field are; system engineering, semiconductor device

technology and rising technology which consist of control, cooling and protection. The improvement in the reliability and efficiency of the utility grid is facilitated by the smart inverter which makes it a very significant unit of the distributed generation (DG) interface (Carnieletto et al. 2009). Lately, the use of renewable energy has been of high concern to the Distributed generation generators as their source. Various types of renewable energy sources are used by the distributed generations but the challenges with these sources is that the power output are not reliable. The significant features to operate the DG are the Smart technologies and Power Electronics. Therefore, in order to effectively achieve reliability with the power output, a power electronics interface system such as a smart inverter system is required. The world market share for inverter systems in the past few years has been plotted in Fig. 1.3 below which shows the continuous spread of the smart technology in the market

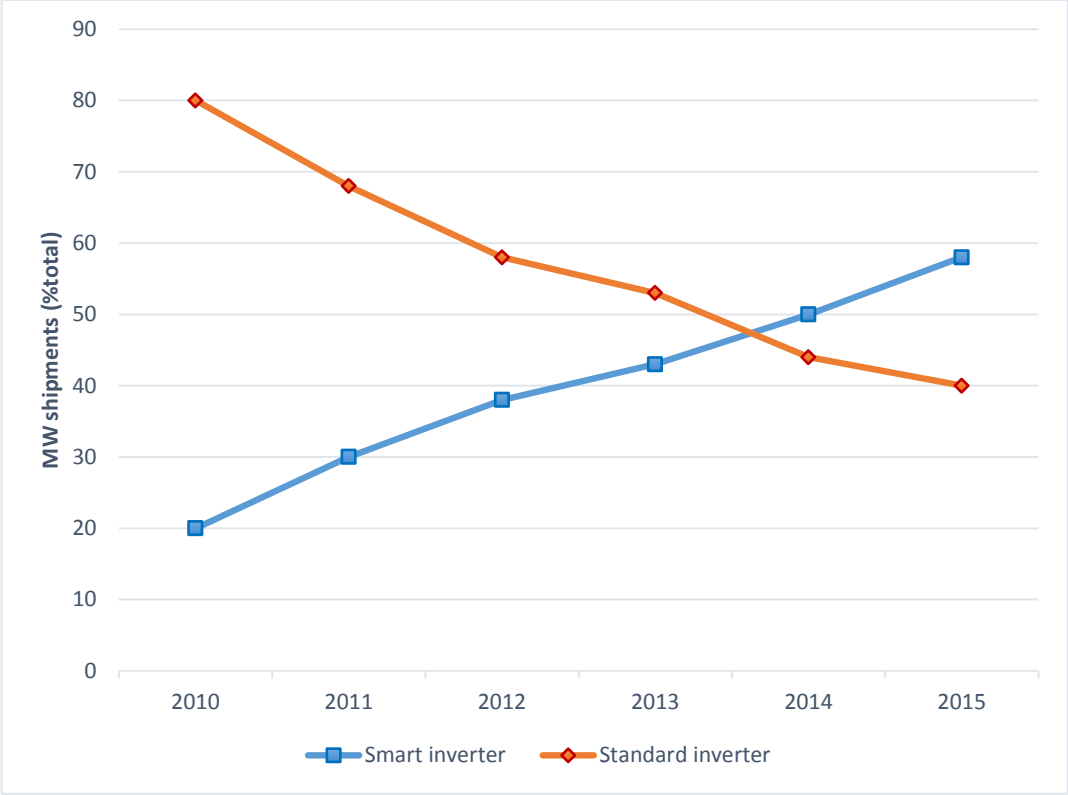

Figure 1.3: World market share of standard inverter and smart inverter graph

(Bouzguenda et al. 2011; B. Craciun et al. 2012)

1.2 Benefits of Using the Renewable Energy Systems

- An example of the Renewable energy sources (RES) is solar energy systems and it receives sunlight at no cost and converts this sunlight to an AC power energy which can be used.
- The RES is accessible most of the time.
- The fossil fuel is getting depleted and will no longer be sustainable as compared to the RES which cannot be depleted.
- The amount paid for electricity bills to utility shareholders will be minimized.
- The maintenance needed by the renewable energy sources is less and no emission of pollution, however, the main cause of global warming is the emission of greenhouse gases when fossil fuels are used.

1.3 Smart Inverters

The photovoltaic (PV) inverter converts direct current generated by the solar panels into alternating current, before it can be used by the electric grid. For both central and distributed power installations, the solar inverters are indispensable for connecting to the electric grid. The integration of solar power into the grid is presumed to have a negative impact on the resiliency and reliability of the electricity system according to the grid operators. This is due to its non-dispatchable and intermittent nature i.e. the sun cannot be controlled and cloudiness as a result of dynamic characteristics of the atmosphere. Considering an instance whereby the solar photovoltaic panel experiences cloudiness, the light intensity which the panel receives reduces, resulting in the output voltage to drop. On the other hand, problems of such are pervasive in all solar installations due to the distributed solar generation which supplies energy directly to the distribution grid, compared to the central generation which supplies into the transmission system, as a result, it presents mostly difficult system control issues for grid operators. Nevertheless, the solution to these problems has been made possible through advanced technology, which is the smart PV inverter (Johnson 2013).

The reliability of the electric grid is improved through the integration of smart solar inverter by allowing distributed solar sources to stay connected to the grid when there are slight instabilities in voltage and frequency**.** According to the Institute of Electrical and Electronics Engineers (IEEE) 1547 standard, it is required that the smart solar inverter should trip and disconnect from the grid when there is an incidence of voltage or frequency fluctuation whereas the traditional inverters are not capable of doing so. Unexpected disconnections as a result of conforming to the IEEE 1547 standard can cause more instability in the grid rather than reducing it**.** Disturbances can either be a

major or minor disturbance in voltage or frequency, which the Smart solar inverter is capable of differentiating between them. The need for disconnection from the grid when there is an occurrence of minor voltage or frequency fluctuations is not necessary, since a smart solar inverter is built in such a way that it can maintain a suitable range of voltage and frequency. As regards to the IEEE 1547 standard, even though the smart solar inverter is capable of handling slight fluctuations in voltage and frequency, it is essential that the smart PV inverter trips and disconnects during conditions of major disturbances in voltage and frequency. However, it is important to conform with the standard for interconnecting distribution resources IEEE 1547, in order to let the smart PV inverter to stay connected to the grid in case of minor voltage and frequency fluctuations, before commencing major installation of smart PV inverters for new and existing projects.

The reliability of the grid can be improved using the smart PV inverter by generating and absorbing reactive power together with real power, apart from being able to withstand voltage and frequency disturbances, which as a result reduces the voltage instabilities linked with distributed solar power. Transmission assets can be destroyed by these voltage instabilities resulting from distributed sources. Voltage fluctuations can be stabilized at the distribution level when the smart PV inverter increases flexibility of transmission network. Permitting grid operators to remotely allow and deactivate functions and modify set points of controlled voltage and frequency as needed by the grid is as a result of the flexibility of the grid being enhanced by the smart solar inverters enabling real-time communication between grid operators and distributed solar sources(Americans for a clean energy grid 2014). Smith (2013) also identified some efforts towards the smart inverter functions which are summarized in the table 1.1 below.

Table 1.1 Smart Inverter Functions

	Smart Inverter Functions	Summary	Applications
1	Connect/Disconnect	Utility control for connect/disconnect	PV/ES
2	Maximum Generation Unit	Reduce maximum output of DER	PV/ES
3	Charge /Discharge Management	Managing charge/discharge of ES	ES
4	Fixed Power Factor	Fixed power factor regardless of voltage or watt output	PV/ES
5	Intelligent Volt-ampere reactive	Volt-ampere reactive output based upon local voltage and output	PV/ES
6	Volt-watt	Watt output based upon local voltage and watt output	PV/ES
7	Frequency-watt	Frequency-based watt control	PV/ES
8	Watt-Power Factor**	Watt-based PF control	PV/ES
9	Low/High Voltage Ride Through	Ability to remain online during low and high voltage events	PV/ES
10	Dynamic Reactive Current	‘’fast’’ volt-ampere reactive response to sudden voltage condition	PV/ES
11	Real Power Smoothing	Controlling charge/discharge to reduce watt fluctuations	ES
12	Dynamic Volt-Watt	‘’fast’’ watt response to sudden voltage condition	ES
13	Load/Generation Following	Dispatching of DER to match load and/ or other generation	ES

1.4 The Smart Grid

The connectivity, automation and synchronization between the suppliers, consumers and networks that implement a distant transmission or performs local distribution is intensified by the Smart grids. The smart grid theory is the incorporation of digital architecture to distribution and long distance transmission grids to both improve current operations by minimizing the losses, and also to create new markets for the generation

of alternative energy (Vijayapriya & Kothari 2011). The existing grid lacks ability to communicate compared to a smart grid infrastructure which is made up of enhanced sensing and advanced communication and computing capabilities. Each of the units of the system are connected together with communication paths sensor nodes and integration of smart inverters to provide the ability to inter-operate between them for example, distribution, transmission and other substations like residential, commercial and industrial locations (Güngör et al. 2011). Smart grid can also be referred to as other names such as Smart Electric Grid, Intelligent grid, Smart Power Grid and Future Grid (Weedall 2000).

"The smart grid is a modern electric power grid infrastructure for improved efficiency, reliability and safety, with smooth integration of renewable and alternative energy sources, through automated control and modern communications technologies" (Güngör et al. 2011).

1.5 Statement of the research problem

Power generation in South Africa is majorly through coal making South Africa one of the most environmental unfriendly countries in the world. For this reason, it has become crucial to look at different methods of increasing the techniques of generating power through the implementation of renewable energy sources (RES). However, the stability of the real power output from the RES is not suitable. Therefore, the integration of intelligent grid systems are very essential in order to overcome the unpredictable and varying nature of the renewable energy which typically depends on the weather for its source of power. For the effective operation of the grid-connected system such that the reliability of the system is enhanced, new control approaches need to be developed in order to gain reliability and consistency in the energy generated through renewable energy sources. It is necessary to integrate in the grid system the monitoring and control of fluctuations in the flow of energy due to the periodic nature of renewable energy and to arrange for backup capacity to take in the intermittent generation.

1.6 Justification for the research

The increased number of grid connected solar PV inverters gave rise to different problems in the grid. Some of them are; power quality issues and problems relating to stability and safety of the utility grid due to the intermittent nature of the RES (Renewable energy sources) (Teke & Latran 2014). Some of the challenges affecting

the state of the grid is lack of secure, reliable communications infrastructure for interconnecting the distributed resources to the utility side (Boulder 2012). Over the last ten years, there have been various factors responsible for the continuous increase in the penetration of the solar power systems which are; increase in social acceptance of solar modules, rising utility rates for electricity and the decrease in the cost of manufacturing solar modules. The effect of this continuous penetration of distributed, intermittent renewable energy generation has made it a necessity for the grid system to become more intelligent to enable the flow of electricity in a steady and reliable manner. A Major component that will enable the effective transition is the smart solar inverter, which will gradually become the mastermind of the solar-empowered smart grid (Belur, 2014; Khadkikar et al. 2012). The smart inverter has become essential to the grid system because they can be used to improve the stability, reliability and quality of power supply by the grid. They will also function tremendously in the applications of peak load shaving and power regulation of intermittent energy resources. To help improve the grid stability, there is need to control the active power in the smart inverter to help in lowering the frequency. It is also important to keep the frequency in the transmission network stable as much as possible. The control of voltage is important by adding and penetrating Voltage-Ampere reactive (VARs) at different periods throughout the transmission and distribution network even though the reactive power can be controlled in huge generation stations. Equipment and loads can be negatively affected when there is redundant voltage. The stability of the grid can be improved and transmission losses can be minimized through VAR control. (Zuercher-Martinson, 2012).

For a grid system to be considered efficient, it must have the capability to operate both in grid-tied operation and anti-islanding operation modes due to factors like grid outages, economical convenience or even planned disconnection(Salam et al. 2010). This study resulted in the design and development of a power electronics interface that will improve the stability and reliability of the grid through appropriate design and development of an effective control algorithm.

1.7 Objectives of the research

The following specific objectives will be used to achieve the overall aim of the research work.

- To design the output filter of the inverter and the power stage of the system.
- To develop a system that will improve the power quality of the renewable energy systems.

- To develop an inverter capable of controlling both reactive and active power flow in either direction.
- To design and develop the current controller for the inverter which is capable of operating in grid-connected mode.
- To design a very efficient and reliable grid-connected inverter.

1.8 Delineation of the research

This research work will consider the following limitations:

- For the purpose of this study, a single loop control algorithm will be implemented.
- Only one inverter topology is used for this research purpose.

1.9 Outline of thesis

The chapter one of this thesis briefly introduces the thesis giving a little background of the smart grid technology, the justification and the aim of carrying out this research was also highlighted.

Chapter two gives a comprehensive literature on the past works that have been done in this area of research.

Chapter three also contains literature on the basic knowledge of power electronics, which are applicable for the study of inverter systems.

In chapter four, the design procedures used for the LCL filter and the controller design for the inverter was done.

Chapter five is where the simulations of the developed model using the designed parameters from chapter four were given.

Chapter six gives the conclusion of this work and some recommendations were given for future research.

CHAPTER 2

LITERATURE REVIEW

2.1 Introduction

This study was carried out due to the unsustainable use of fossil fuels, which are now limited resources and gradually running out depending on the rate at which we use them. At the present rate at which oil and gas is being consumed, it is presumed that known world reserves will run out of oil and gas in a little over 40 years from now. Even though new places are being discovered for oil and gas, they are still not enough to supply as much oil as the recognized reserves, which are gradually running out, would produce. Therefore, an effective switch period is required globally to move from oil to alternative sources of energy. The solar photovoltaic (PV) cell has been regarded as the most suitable energy conversion system. The solar PV harness the solar radiation which is the most abundant source of energy (Marafia 2001).

In the last few years, there has been tremendous growth in the amount of DG systems connected to the grid due to favourable regulatory policies with its main objective which is to increase the renewable energy production (Sun & Zhang 2012; Xue et al. 2011). Renewable Energy (RE) technologies play an essential role in generating energy with little or no greenhouse gases. These renewable energies also referred to as an alternative to conventional source of energy, are being used for different applications. In addition, the use of DC to AC inverters in Distributed Generation (DG) systems such as photovoltaic, wind, gas turbines etc. is gradually moving towards large scale energy generation which was inaccurately defined as small-scale electricity generation systems so many years back (Doukas et al. 2006; Marafia 2001; Trabelsi & Ben-Brahim 2011; Trabelsi et al. 2013). The grid system requires additional systems to monitor the voltage and current regulation unlike the previous years when the inverter is required to disconnect during strange grid conditions and faults waiting for normal grid conditions for reconnection to the grid. The advancement in smart inverter has been faced with new challenges which are to ensure the grid stability and avoid anti-islanding (Walling et al. 2010; Paál et al. 2011; Ullah et al. 2007). This section discusses further on the background and literature of the grid-tied system, distributed generation, different types of VSI control such as controls implemented in stationary reference frames, synchronous reference frame, grid synchronization possibilities for these control techniques and harmonic filtering. The impact of the grid-tied PV systems on the distribution generation such as power systems frequency, voltage, power flow and reliability is also discussed.

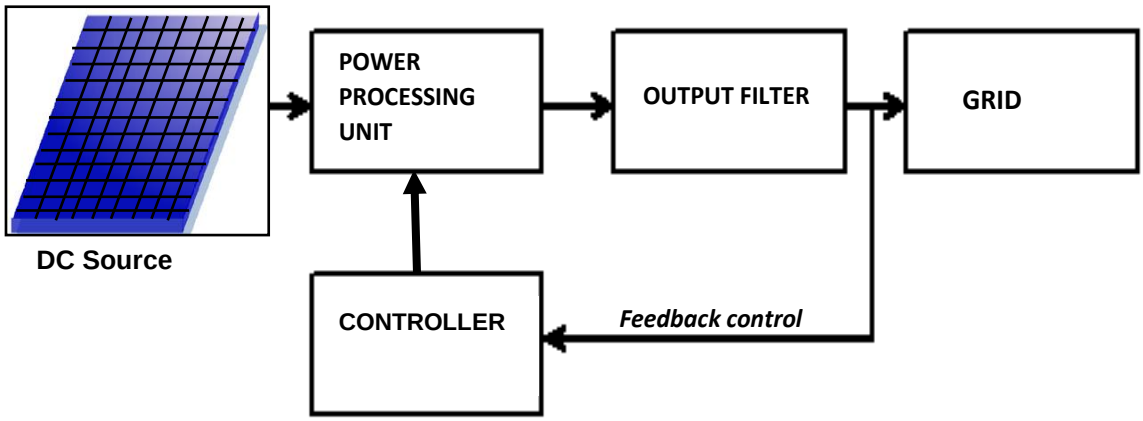

Figure 2.1: Experimental block diagram of the smart inverter system

2.2 PV Array Model

The representation of a PV panel which captures the sunlight through the PV cells is shown in Fig 2.2 below. The PV cells comprises of silicon p and silicon n layers. The atoms of the silicon and the internal field between the positive and negative charges are ionized by the light with precise wave length inside the photovoltaic device. There is a better interaction between the atoms when there is a high irradiance resulting into a high production of potential difference (Trejos et al. 2012; petrone et al. 2007; Gow and Manning 1999). Disturbances such as solar irradiation is a factor in which the output voltage of the solar cell relies on during the course of its operation which is also a function of the photocurrent. The solar cells' output current is represented in equation (2.1) for a PV array which comprises of N_s modules in series connection and N_p parallel connected modules. Equation (2.2) and (2.3) represents the voltage and current of the PV array respectively. The power output of the PV array is given in equation (2.4) which is the product of output current in (2.3) and output voltage in (2.2) of PV (Salam et al. 2010; Bellini et al. 2009).

$$I_c = I_{ph} - I_o = I_{ph} - I_{sat}\left[e^{\frac{q}{AKT_c}(V+IR_s)} - 1\right] \quad (2.1)$$

$$V_{pv} = N_s \times \left[V_{ref} - \beta\left(T - T_{ref}\right) - R_s\left(T - T_{ref}\right)\right] \quad (2.2)$$

$$I_{pv} = N_p \times \left[I_{ref} + \alpha\left(\frac{G}{100}\right)\left(T - T_{ref}\right) + \left(\frac{G}{100} - 1\right)I_{sc}\right] \quad (2.3)$$

$$P_{pv} = I_{pv} \times V_{pv} \quad (2.4)$$

Where,

I_c = Output current of the solar panel

I_{ph} = Light generated current in a solar cell

I_o = Reverse saturation current of diode

G = Irradiance

α = Current temperature coefficient

K = Boltzman constant

q = Electron charge

T_c = Cell temperature in kelvin

β = Voltage temperature coefficient

A = Ideality factor

N_p = Number of modules connected in parallel

N_s = Number of modules connected in series

T = Stack temperature

P_{pv} = Output power of the PV array

I_{pv} = Output current of the PV array

V_{pv} = Output voltage of the PV array

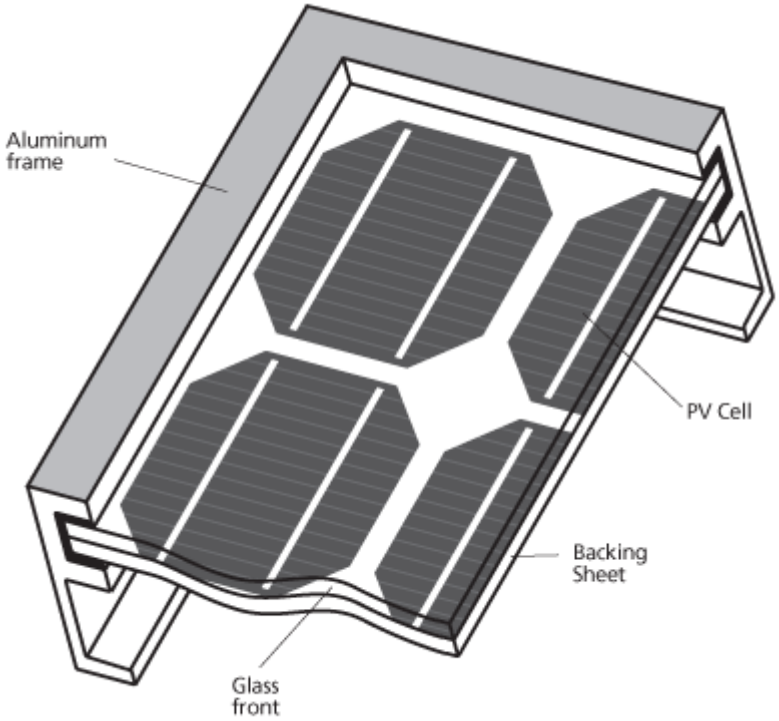

Figure 2.2: Representation of a PV Panel

2.3 Classification of Inverters

The general classification of Multifunctional inverter (MFI) based on circuit power structure is summarized in figure 2.3 below (Khadkikar 2012).

2.3.1 Classification of Inverter Based on The Type of Power Source:

Depending on whether the system is fed by a single phase (2-wire) or three phase (3-wire or 4-wire) source, AC loads or devices in the power system can be categorised into single phase and three phase. Different types of inverter configurations are used to reduce PQ disturbances from the system (Jena et al. 2011). The PQ disturbances associated with voltage that occur in both single-phase and three-phase systems share almost the same features. In addition, three phase systems need voltage unbalance compensation to satisfy the improved PQ. The compensation for the reactive power and harmonic currents is the main concern of the single-phase system. The current unbalance expected from the reactive current and current harmonics must be considered for a three phase three-wire system. In a three-phase four-wire (3P4W) system, there is need for a neutral current compensation loop (Alatrash et al. 2012; Trujillo et al. 2010; Goyal et al. 2009; Renders et al. 2009; Kim & Choi 2008; Macken et al.2004).

The GCI (grid-connected inverter) system configuration that is most common which compensates for PQ disturbances in a single-phase two-wire supply system is made up of two H-bridge inverters i.e. total of four semiconductor switches. Grid-connected inverter topologies in single-phase system usually do not have large capacities mostly used in small scale RESs application (Paál & Tatai 2010).

The single-phase GCIs have low capacities as stated earlier and are mostly used in residential PV systems. Furthermore, the methods of detecting harmonics in three phase GCIs is much simpler compared to single phase GCIs. Also the single phase GCI is known to be usually an unbalance source, which poses more problems to the utility in managing the problem of the unbalance source. Hence, three phase GCI have many advantages which makes it adequate for a wide-range of applications. The three phase GCIs are also available in single-stage and two-stage GCI system (Teke & Latran 2014; Maris et al. 2007).Some of the advantages of using a three-phase system in high-power applications are:

- It reduces the stress on the inverter switches.
- Decrease in size and ratings of reactive components.
- There is increase in the frequency of output current, therefore, reducing the size of output filter.

- It creates a uniform distribution of losses.

Hence, a three-phase single-stage grid-connected PV system has been considered in this work. Inverter interfacing PV module(s) with the grid involves various requirements and standards which will be discussed in the latter part of this chapter (Malek 2014).

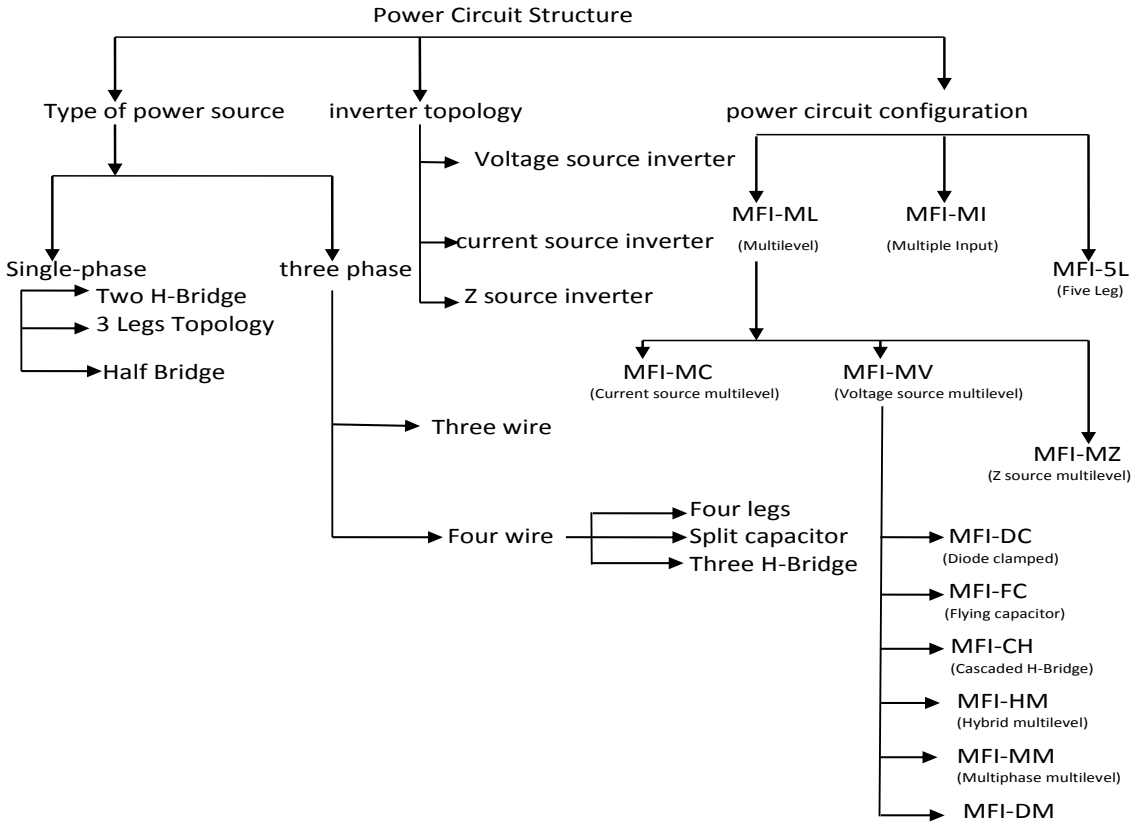

Figure 2.3: General classification of MFI Based on Circuit Power Structure (Teke & Latran 2014)

2.3.2 Classification of inverter structure or topology:

The grid-connected inverter ensures that the DC link value is maintained at its set reference value. Hence, a current source inverter (CSI) is a type of inverter where the current at the DC side maintains the identical polarity, and as a result, the polarity of the DC side voltage determines the direction of flow of average power through the converter. The DC side of a CSI is normally in series connection with a comparatively large inductor, which retains the current continuity and is more typical of a current source. The inverter can be formed with a pulse width modulated current source inverter (CSI), which uses a common inductor L_{DC} to create the DC bus. The Fig. 2.4 below shows the structure of a CSI-based GCI system.

Generally, the CSI has not been widely used for power system applications compared to the VSI. This is due to the bipolar electronic switches which are needed by the CSI. Also, the CSI-based GCI topology is not used often because of the losses and high

cost involved. The power semiconductor industry is however yet to entirely produce a widespread supply of fast, fully controllable bipolar switches commercially. Even though bipolar types of the GTO and the IGCT are obtainable commercially, they are not adequate in respect with the switching speed and are mostly designed for very high power electronic converters (Teke & Latran 2014; Yazdani & Iravani 2010; Dai & Wu 2009).

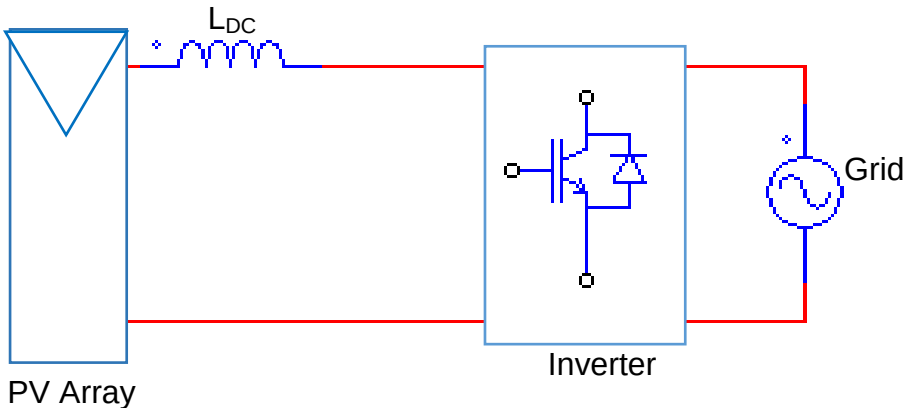

Figure 2.4: Topology of grid connected system: (a) Current Source inverter (Teke & Latran 2014)

The Voltage source inverters (VSI) which is the most commonly used GCI is the second topology of the GCI. In this topology, the common capacitor C_{DC} is used. The DC source voltage maintains the same polarity in a voltage source inverter (VSI) and the polarity of the DC source current determines the direction of the converter average power flow. Typically, the terminals of the DC source of a VSI are in parallel connection with a comparatively large capacitor that is representative of a voltage source. In contrast to the CSI, a VSI needs reverse conducting switches or switch cells. The switch cells are obtainable as the IGBT or the reverse conducting IGCT commercially. Each of the switches in a VSI was achieved by connecting a GTO in antiparallel with a diode before the widespread use of the IGBT and the IGCT (Yazdani & Iravani 2010).

VSI are used for converting energy from a DC source to an AC output, both in a standalone mode or when in grid-connected mode. The Fig. 2.5 below shows the single-line structure of a VSI-based GCI. The VSI-based topology is mostly used in GCIs. Blocking diode is not needed in VSI topology. VSI is cheaper, lighter in weight, and enables better control which is more flexible than the CSI topology (Teke & Latran 2014; Dasgupta et al. 2013; Yazdani & Iravani 2010).

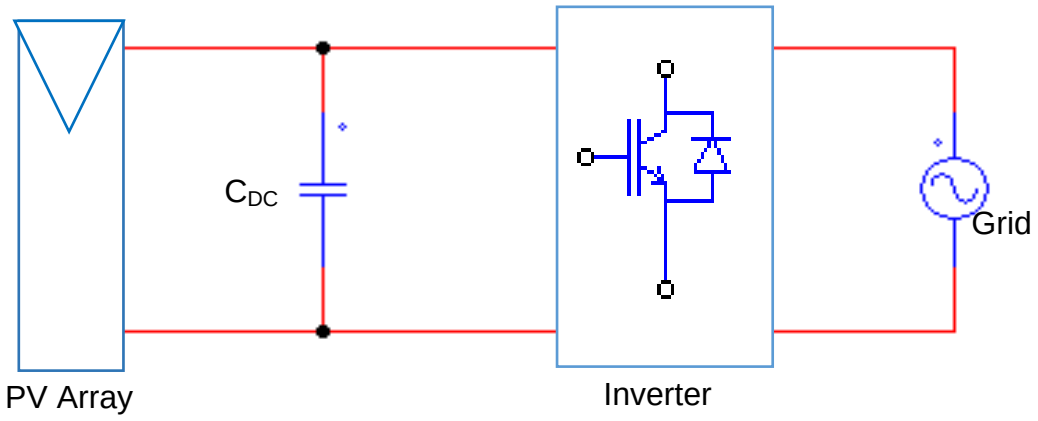

Figure 2.5: Voltage source inverter

The Z-source inverter (ZSI) is the third type of inverter structure that uses common energy storage capacitor and an inductor. ZSI consist of X-shaped LC impedance, which makes it different in structure from the conventional VSI or CSI as it can be seen in Fig. 2.6 below (Teke & Latran 2014). The ZSI was mostly used in 3 phase systems in the past, and the presence of the LC impedance in the full bridge inverter boosts up the voltage (Yang & Blaabjerg 2015; Gajanayake et al. 2009; Chen et al. 2009; Gajanayake et al. 2007)

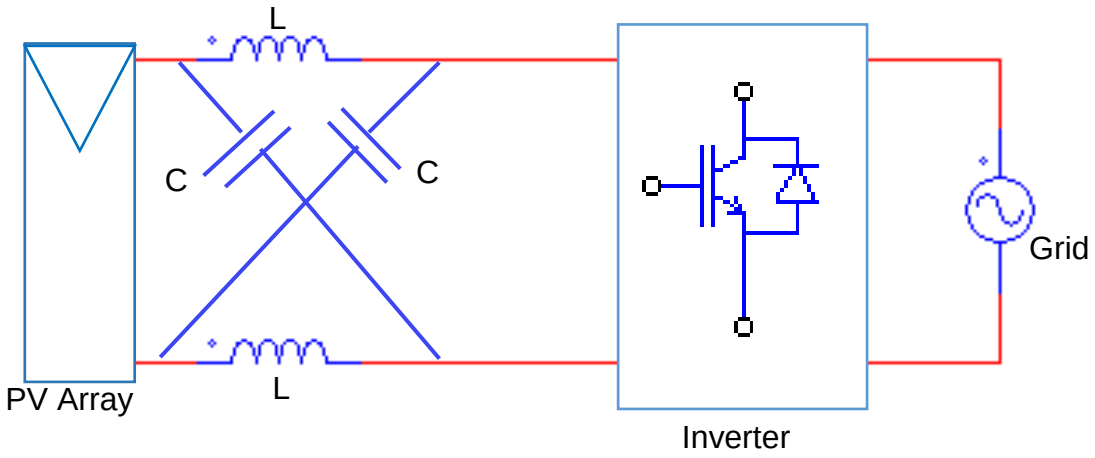

Figure 2.6: Topology of grid-connected system: (a) Z Source inverter

2.3.3 Classification of Inverter Configurations

Inverter configurations can be categorised majorly into three different types depending on the number of power stages present in the system:

- Single-stage inverters
- Dual-stage inverters
- Multi-stage inverters

In a single-stage inverter, the maximum power point tracking current control loops and voltage control loops are implemented all in one stage as shown in the Fig. 2.7a. However, in a dual-stage inverter, the maximum power point tracking is performed by a DC to DC converter in between the PV panels and inverter, and control loops are implemented by the inverter as seen in the Fig. 2.7b. And finally, each string has a DC to DC converter connected to it which performs the maximum power point tracking control but one control inverter implements the control loops for a multi-stage inverter as depicted in figure 2.7c (Malek 2014).

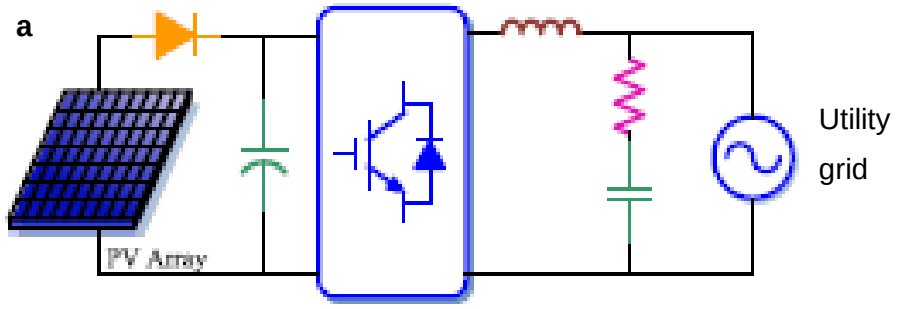

Figure 2.7a: Configuration of different PV application circumstances (a) single-stage structure

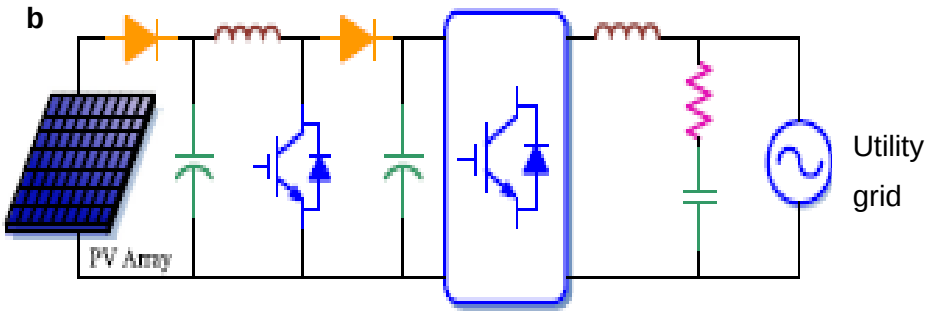

Figure 2.7b: Two-stage structure
(Zeng et al. 2013)

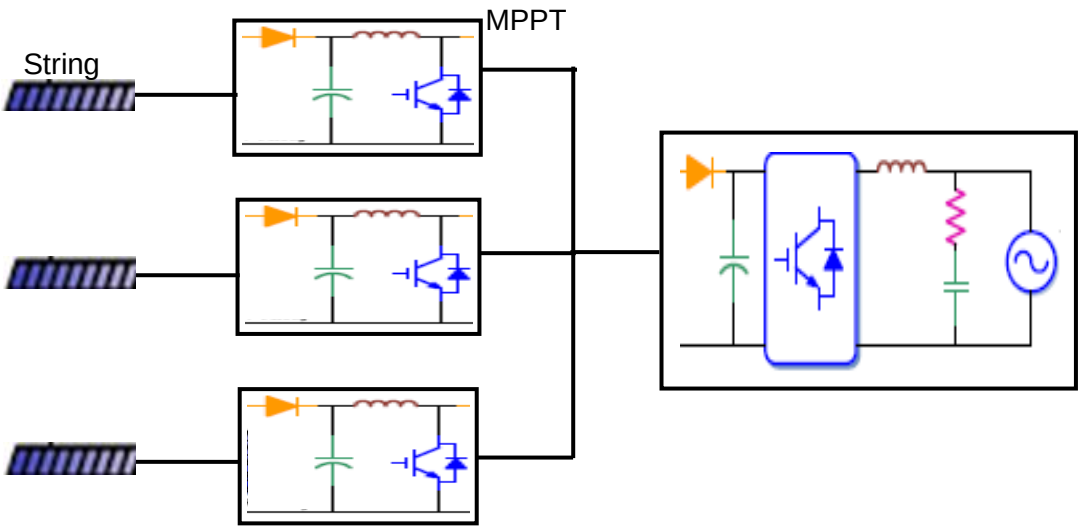

Figure 2.7c: Multi-Stage Inverter

2.4 Topologies of grid-connected inverter configurations

The multifunctional inverters are basically power electronics interface system which are used in converting DC power to AC. The inverter connects to the grid ensuring its performance at MPPT (maximum power point tracking). The power conversion system has to be supplied with a maximum power point tracker (MPPT) so as to make use of the maximum power generated by the PV modules. This MPPT is a mechanism which tracks the voltage at the period when the maximum power is consumed at all times (Massawe 2013; Hamadi et al. 2011). The classification of the inverter topologies is based on the features and functions of the conversion phase of the GCI.

2.4.1 Central Inverters

In this kind of inverter, the PV arrays are connected in parallel to one central inverter. A central inverter is mostly used in three phase grid-connected system with power ratings of 10 kW to 1000 kW. High DC voltage cables are required, for this type of inverter but it has a reasonably high efficiency due to low losses in the power conversion stage but the disadvantage of this configuration it is quite expensive due to the long cables which are needed in the connection of the PV array to the GCI and the centralized MPPT. In addition to that, the cost of installing and managing the system is high.. Another issue in this configuration is power mismatch. Apart from the central inverter, which is the major solution for three-phase, all other configurations, are the most common solutions for single-phase PV applications. A typical solar PV system provides DC voltage to a central inverter for local distribution and to the utility grid. The efficiency in transformerless PV converters is quite high compared to the conventional PV systems

where isolation transformers are being used (Bouzguenda et al. 2011; Craciun et al. 2012; Massawe 2013; Yang & Blaabjerg 2015).

2.4.2 String Inverters

To improve on the drawbacks of the central inverters, the string inverters have been introduced. Each of the PV strings are connected to individual inverters for this configuration. In order to improve the power supplied by individual string to the central inverter, a DC to DC converter can be implemented. When this topology is compared to the central inverters where a single inverter is employed, there is better efficiency and reliability of the PV modules and the complete system. The response of the poor performance of a solar panel is limited to its string, thus the whole system is not affected. There is a separate inverter that converts from DC to AC at the output of the individual string, thus, the utilization of a central inverter is excluded. For this configuration, the MPPT control is achieved independently i.e. at each string providing overall energy of better-quality. More power electronic converters need to invested in due to the power mismatches which is still present in this configuration (Bouzguenda et al. 2011; Craciun et al. 2012; Yang & Blaabjerg 2015).

2.4.3 Multi-String Inverters

This topology is a combination of the string inverters and module inverters. The configuration which is an improvement on the string inverter is represented in Fig. 2.4 below. Each string implements a DC to DC conversion before it is connected to a central inverter and the power limit is 5 kW for this topology. However in this configuration, MPPT is implemented for each string as well thereby improving the efficiency of the system. Power mismatch is still present in this configuration which also needs investing in more power electronics converters (Craciun et al. 2012; Yang & Blaabjerg 2015).

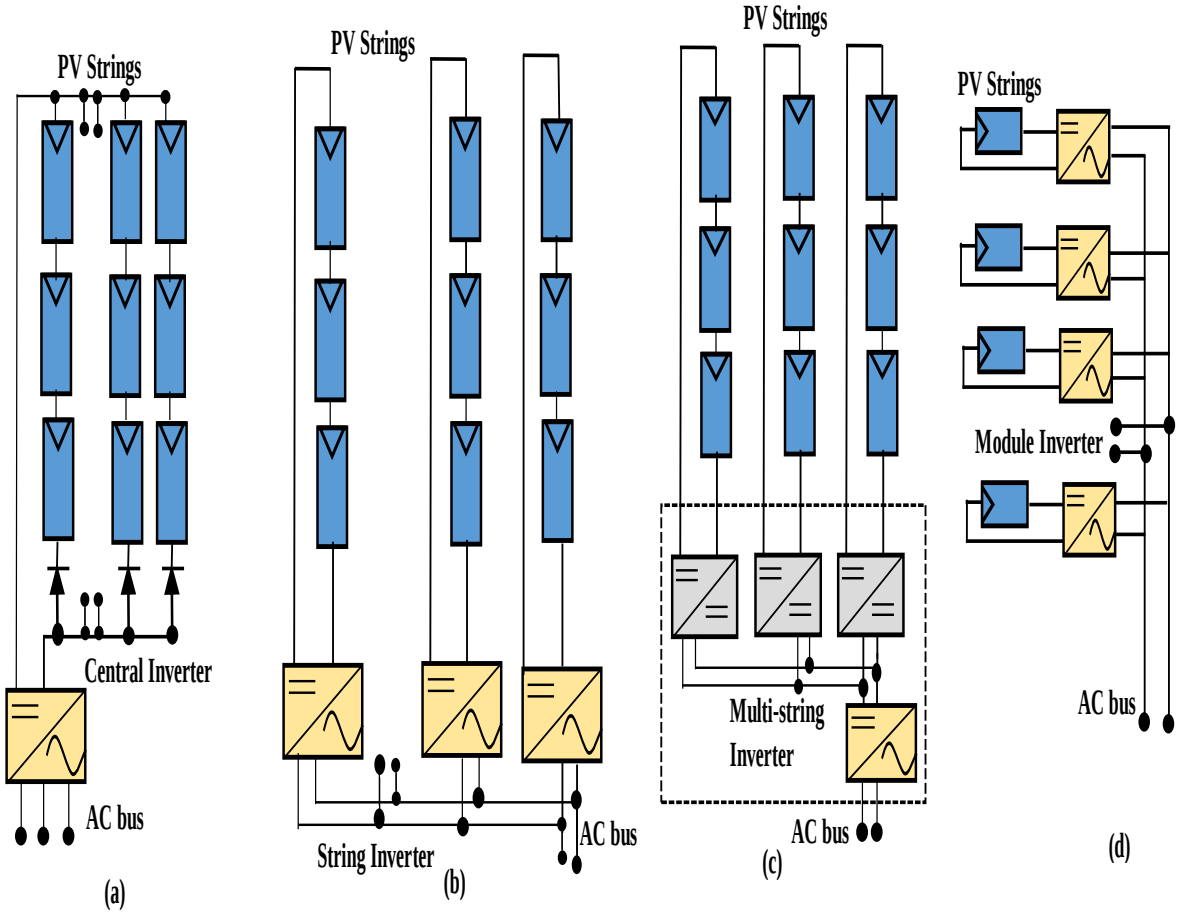

Figure 2.8: PV grid connected systems configurations a. Central Inverterb. string Inverter c. Multi-string Inverter d. Module Inverter
(Craciun et al. 2012; Massawe 2013)

2.4.4 Module Inverter System (Micro Inverters)

Each solar panel comprises of a separate inverter at their outputs for this topology which is the most recent technology. Each panel thus employs MPPT at the individual panel. Considering the drawbacks with other configurations, the module converters were developed being another means for solving the issues of low power ratings in PV systems. The effects of mismatches are minimal in this configuration since the module uses a single PV panel with a separate MPPT control. It provides DC to AC conversion from each individual panel rather than an entire string (Bouzguenda et al. 2011; Craciun et al. 2012; Massawe 2013; Yang & Blaabjerg 2015).

2.4.5 Transformerless AC Module Inverters (Module Integrated PV Converters)

Several works have been done to cut down on the number of power conversion stages resulting in reduction in cost and higher reliability of the single stage PV inverters in order to have a better efficiency and power density in total. A buck-boost or boost converter is integrated into the AC module inverters to realize the DC-link voltage that

is needed since the power of a single PV module is not so high and it depends on the ambient conditions. LCL filter is used to achieve the acceptable total harmonic distortion of the current. The major setback of the integrated boost AC module inverter is that a zero cross current distortion will be present. The buck-boost AC module has been proposed to be a way out to this problem. The buck-boost AC module produces a DC biased voltage which is 180° out of phase to the other so as to diminish the zero cross current distortion (Yang & Blaabjerg 2015; Tang et al. 2012).

2.4.6 Transformerless Single-stage String Inverters

The single-phase full-bridge string inverter is used for higher power applications between 1 KW to 5 KW because it has fewer power switching devices and less complicated. LCL filter is used to improve the power quality for this configuration. To minimize the leakage current that occurs in transformerless topology a precise modulation technique is designed. In order to remove the leakage current, bipolar modulation technique is used thereby improving the modulation patterns. Introduction of AC or DC paths to transformerless full-bridge inverters using additional switches results in isolation. Low current is injected due to this isolation between the PV modules and the grid all through zero-voltage states.

2.4.7 DC-Module Converters in Transformerless Double-Stage PV Systems

The double-stage PV Systems consists of a DC to DC converter for increasing the low voltage of the PV module to a voltage level that is required for the inverter stage. This solves the issue of limited output voltage range of the single-stage PV technology. The DC to DC converter carries out the MPPT control of the PV panels. It comprises of a DC-link Capacitor used for power decoupling, and the filtering is done by a PV capacitor. Leakage current can be minimized in this topology using time-sharing boost converter resulting to a system with suitable efficiency. The impedance network based DC-DC converters is an upcoming solution for single-phase double-stage PV systems (Yang & Blaabjerg 2015).

2.5 Modes of operation of Inverter

2.5.1 Grid-Connected Mode

Grid connected inverters are very important components in DGSs. They are used as interfaces for distributed renewable energy sources or micro-sources such as photovoltaic arrays, wind turbines, micro-gas turbines, energy storage devices etc., to connect to the utility grid, as shown in Fig. 2.9a below. The major concerns in grid connected inverters are high efficiency and low cost. Generally, grid-connected inverters can be categorized into two typical configurations which are the single-stage

and the two-stage or multiple-stage. However, the more stages present in a GCI, the lower the efficiency of the GCI; the multiple-stage GCI mainly has two stages. A two-stage GCI usually comprises of a DC/DC stage and a DC/AC stage, as depicted earlier in Fig. 2.7b. The function of the two-stage is to boost the PV array voltage and track the maximum power; and secondly to allow the conversion of this power into high-quality ac voltage. In essence, the DC to DC stage is used to realize maximum power point tracking (MPPT) for the wind turbine, PV systems, or control of bidirectional flow of power for the purpose of energy storage. However, the control of the power and current that is being injected into the grid is done at the DC to AC stage. On the other hand, the GCI with just a single stage comprises of only the DC to AC stage without the DC to DC stage, but the single-stage will perform the whole functions that are being carried out by the two-stage GCI. Although, fewer electronic components are used in a single-stage GCI compared to the two-stage, as a result, making it less expensive, reduction in weight and more reliable with greater efficiency. The presence of several power stages affects the whole efficiency, reliability, and compactness of the system as well as rise in the cost. The single-stage has several advantages, such as simple topology, high efficiency and so on. However, the control strategy is more complex but it has to be designed so that it can extract the maximum power obtainable and to accurately transmit it from the PV array to the grid instantaneously. In this case, an important consideration in the controller design is required (Kadri et al. 2011; Mahmood & Jiang 2012). In contrast, the two-stage GCI requires a control algorithm that is less complicated since different tasks are being performed by two different stages that do not depend on each other. Moreover, one of the advantages of the two-stage GCI over the single stage is that the DC to DC stage is capable of boosting the DC voltage from the micro-source if it is low thereby meeting up with the voltage required by the DC to AC stage. Both the single-stage and two stage GCIs have benefits and drawbacks over each other, which makes it difficult to conclude on which is better than the other. The conditions in which both are used are different. Mostly, the two-stage GCI is employed in grid-connected systems with low capacity range because of its flexible characteristic; on the other hand, single-stage GCI systems with wide limit range are generally used in single-stage GCI systems to achieve a better reliability and efficiency. For PV application, as previously seen in Fig. 2.7b, the two-stage GCIs are generally utilized in single-phase utility grid and the capacities are typically small compared to the single-stage grid-connected inverter systems which are predominantly used in three-phase utility and the capacities are comparatively bigger. The two-stage GCIs are commonly used in single-phase utility grid and they don't have capacities for large PV applications compared to the single-stage (Zeng et al. 2013).

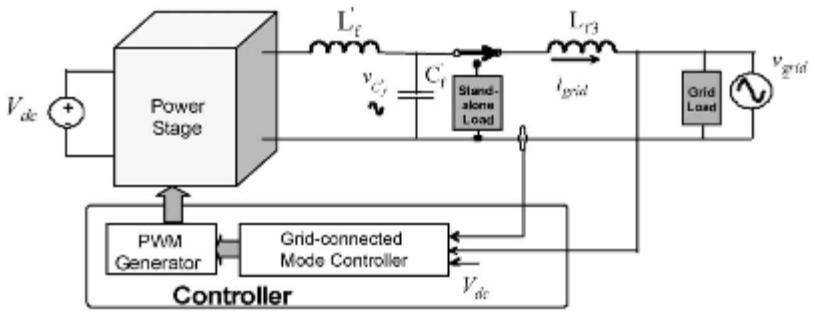

Figure 2.9a: Representation of grid-connected mode inverter operation (Mazumder et al. 2010)

2.5.2 Stand-Alone Mode (Off-Grid System)

Difficulty in storing generated solar electricity is one of the main shortcomings of the solar generated energy. There is need for substantial running costs in off-grid systems for current storage technologies due to their limited life. Nevertheless, the cost of storage is expected to reduce considerably with the new technologies such as super capacitors, flywheels and fuel cells, as well as improved chemical batteries. There is typically an energy storage system in the standalone PV system, during times of darkness or foul weather; energy is supplied to the loads by batteries that are charged during PV operation. This enables consistent supply of power at all times if the storage capacity is huge enough and the geographic location provides adequate energy from the sun. (Banks & Schaffler 2006) (Leslie 2003).

There are presently a number of uses of renewable energy in off-grid photovoltaic mode, amongst which are solar cooking and water heating. In distant areas from the grid, PV systems are used as standalone sources of electricity, but the grid-connected electricity is cheaper compared to the off-grid system in South Africa. A number of the implemented tasks are seen in houses, schools and electrification of hospitals delivered by off-grid energy services with solar home systems (SHSs) to facilities in the community (Lin & Chen 2006; Winkler 2005). The mode of operation of the standalone inverter is illustrated in Fig 2.9b below.

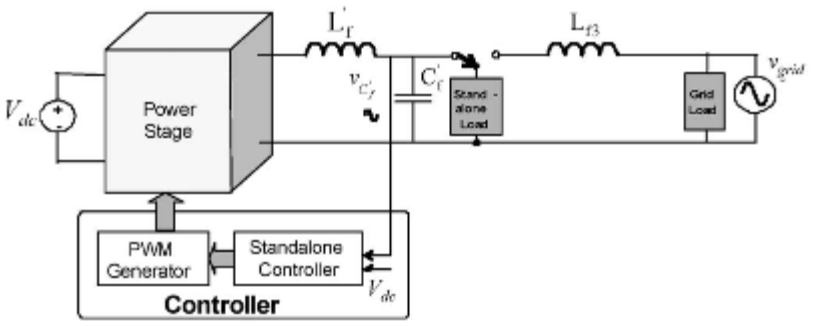

Figure 2.9b: Representation of standalone inverter operation (Mazumder et al. 2010)

However, grid-connected applications have gained more interest in the leading international market for PV technology. The grid connected system can be implemented for storage purpose in this instance together with other storage choices like pumped storage systems and distributed storage.

2.6 PV Technology

This section concentrates on the study of the recent developments of power electronic converters and the latest technologies in the PV systems that are being used. Due to the increase in research and development work in the area of renewable energy source PV systems as an alternative energy source to complement the grid systems is becoming feasible. (Smith 2013) defines a PV system as a system that converts sunlight into electricity. The system comprises of one or more solar cell modules where several cells are connected to make up a panel, which take insolation from the sun and convert that into a DC signal that is sent to an input filter capacitor. After the connection of the input filter capacitor is a DC to AC inverter that converts the current from the DC stage into an AC signal which is synchronized with the grid. Insignificant loads such as lighting systems and DC motors may be directly supplied by the electricity obtainable at the terminals of a photovoltaic array or panel. Electronic converters i.e. power conditioners is needed for most PV uses for the electricity from the photovoltaic device to be processed. The voltage and current control is done by the converters at the load side which is not constant due to the solar irradiation and temperature which constantly changes, primarily to track the maximum power point (MPP) of the device and to regulate the flow of power in grid connected systems (Trabelsi & Ben-Brahim 2011). (Salam et al. 2010) also enumerates that solar cells are assembled into bigger units to form PV modules, which are then connected in a parallel-series architecture and make up arrays of PV modules. The output voltage of the solar cell is a function of the photocurrent which is dependent on the level of solar illumination when it is conducting. The PV topologies to be proposed must have a high reliability, a reasonable cost, and a user-friendly design in order to achieve an overall highly efficient PV system. In order to supply normal load demand to customers or supply electricity to the grid, the need for power conditioning systems, such as inverters and DC to DC converters are highly essential. For conditions where there is no grid available or alternative means of power supply, the photovoltaic modules can be used for a number of applications. Such applications are power for institutions, telecommunication relay stations and customer equipment, households, water heaters, water pumps and security systems (Banks & Schaffler 2006). The PV module connection must conform to the standards set by the utility companies. Nowadays, one of the international standards the grid connected

systems must conform to is the IEEE1547 (IEEEStandards 2009; Blaabjerg et al. 2006). These standards are created to deal with problems such as power quality, detection of islanding operation, grounding, etc. They outline the present and future PV module features (Carrasco et al. 2006).

In order to minimize stability issues, the generating systems should have the following:

- System management: production units should implement security analysis for current and anticipated circumstances, availability analysis in generation of power and additional services, information about short-term restriction, or to carry out actions that have been planned.
- Stability of voltage: operators of the grid network need to instruct the power production units to supply reactive power with the aim of keeping the voltage profile steady.
- System robustness: there is need for the power systems to be powerful in an instance of irregularities in the power system,
- Stability of frequency: there is need for the power systems to supply the required control so as to stabilize the demand and generation imbalance.
- System restoration: after a disruption or power failure, voltage has to be restored by the power plant or to operate in voltage control mode if it is technically feasible

Since inverters interface all PV systems, there should be improvement in the control strategies applied to them so as to satisfy the obligatory requirements. The grid interface requirements, power quality and anti-islanding should be considered while integrating the PV system to the network (Yafaoui et al. 2012; Craciun et al. 2012).

2.7 International Standards for Grid-Connected Systems and DES

The quality of the distributed power is one of the demands existing in all standards with regard to grid-tied systems. As regards to the standards in this field, 5% of total harmonic distortion is allowed in the injected current into the grid (Blaabjerg et al. 2006). In order to connect to the grid, the standards given by the utility companies must be obeyed. Therefore the grid-connected inverter has to adhere to these standards. The current standards EN61000-3-2 and IEEE1547 and the prospective international standard IEC61727 are some of the standards worth considering. The mentioned standards deal with issues like power quality, islanding operation detection and grounding (Kjaer et al. 2005). Some of these standards have been summarized in the tables 2.1 to 2.4 below. The time required for the GCI to disconnect from the grid when the nominal power is greater or lesser than 30 kW and when there is frequency variation is given in Table 2.1 below.

Table 2.1: IEEE1547 interconnection requirements

DR size	Frequency range (Hz)	Clearing times (s)
≤ 30 kW	>60.5	0.16
	<59.3	0.16
≥ 30 kW	>60.5	0.16
	<59.8 to 57 (adjustable)	Adjustable 0.16 to 300
	<57.0	0.16

The variations in voltage should not exceed the limits set by the standards and for abnormal conditions, the disconnection time for the GCI system is presented in Table 2.2 below (IEEEStandards 2009).

Table 1.2: Voltage Requirements for LV PV Systems

IEEE 1574		IEC 61727		VDE-AR-N 4105	
Voltage Range %	Disc (Sec)	Voltage Range %	Disc (Sec)	Voltage Range %	Disc (Sec)
V < 50	0.16	V < 50	0.10	V < 80	0.1
50 ≤ V < 88	2.00	50 ≤ V <88	2.00	V ≥ 110	0.1
110 < V < 120	1.00	110 < V < 135	2.0		
V ≥ 120	0.16	V ≥ 135	0.05		

In order to safeguard human lives and equipment, the GCI is required to disconnect from the grid within a certain period when there is variation in frequency which is given in Table 2.3 below.

Table 2.3: Frequency Deviations and Disconnection Time

IEEE 1574		IEC 61727		VDE-AR-N 4105	
Frequency Range (Hz)	Disc (Sec)	Frequency Range (Hz)	Disc (Sec)	Frequency Range (Hz)	Disc (Sec)
59.3 < f < 60.5	0.16	49 < f < 51	0.20	47.5 < f < 51.5	0.10

The GCI is required to reconnect back to the grid after the fault has been ride-through for a certain time delay as given in Table 2 below (Craciun et al. 2012).

Table 2.4: Reconnection Requirements

IEEE 1574	IEC 61727	VDE-AR-N 4105
88 < V < 110 (%) AND 59.3 < f < 60.5 (Hz) AND Delay of 5 minutes	85 < V < 110 (%) AND f_n-1 < f < f_n+1 (Hz) AND Delay of 3 minutes	80 < V < 110 (%) AND 47.5 < f < 51.5 (Hz) AND Delay of 5 seconds

2.8 Electricity demand and generation developments

As a result of the fast growing population, the worldwide energy demand and environmental safety has been a major concern resulting to a need for an environmental friendly source of energy. The energy sector is a key factor in the generation of greenhouse gases, majorly carbon dioxide and methane. Energy generation through renewable energy technologies releases minimal or no GHGs. Different alternative sources of energy have been discovered for various applications such as renewable energies. However, the universal use of a lot of these renewable sources is still at their premature stages due to their conversion rate which is not efficient enough (Trabelsi & Ben-Brahim 2011).

The demand and generation trends in the past years of energy policy is monitoring how people use energy and how energy use changes over time whereby electricity shareholders are finding it difficult to generate enough electricity that will meet the demand. In the past years, there have been significant changes in the electricity industry towards deregulation and completion with the aim of improving economic efficiency. There is competition among different firms to provide generation services at a price set by the market due to demand rate and communication between the firms. Analysis is also carried out by regulatory agencies to monitor and supervise market behaviour (Ventosa et al. 2005).

It is very important to plan for both the total energy required yearly and to ensure that generation capacity of energy generation is adequate and available at all times to meet the peak demand for power. The two available peaks in electricity consumption are the lower peak which occurs during early hours of the morning, and the other peak is greater, and sudden which arises late in the evening. These are predominantly caused by domestic activity at these times, and also due to plant start-ups in industries and commercial places. These peaks are seasonal, with the peak consumption occurring during winter period. In view of the different technologies and resources, it is therefore important to examine their capability to produce power when needed apart from their

ability to also generate a particular amount of energy over the year (Banks & Schaffler 2006).

Solar energy is regarded as one of the cleanest sources of energy resources that does not contribute to global warming. The sun radiates more energy in one second than what can be used by consumers from its time of existence. Solar energy is also known as alternative energy to fossil fuel energy sources such as oil, gas and coal. It is a cheap and abundant source of energy with less environmental hazards during the generation and conversion of energy. The gradual extinction of fossil fuels has given rise to interest in the integration of solar energy around the world (Solangi et al. 2011; Selvaraj & Rahim 2009).

Solar energy demand has increased over the past 20 years, at a steady rate of 20% to 25% per year as a result of the decreasing costs. Some of the reasons for the increase in the use of solar energy to generate electricity were identified as follows; improvement in the efficiency of solar cells; advanced manufacturing-technology; and economies of scale. 350 MW of solar equipment was sold in 2001 to complement the solar equipment producing a clean energy at this time. In addition, 574 MW of PV was installed in 2003. This increased to 927 MW the following year. The European Union was on a path to fulfilling its own goal of 3 GW of renewable energy from PV sources for 2010 (Carrasco et al. 2006).

Electricity demand by customers is getting higher. Therefore, there is the need for the most suitable technology which calls for further development of the PV system to contribute to the global electricity demand, resulting to the reduction in emission of carbon by decreasing the use of fossil plants. Terrestrial applications of PV market are; Consumer, Off-grid (mostly used in isolated industrial and developing countries for supplying the rural regions with electricity) and On-grid use (Hoffmann 2006). The key objective of having a storage capability in a grid connected system is to enable the system to function as an uninterruptible power supply to the loads when the utility grid cannot supply. During the day when there is excess energy generated, if a system lacks an energy storage, the excess energy will be sold back to the utility. The PV system without storage would not function during periods when there is no sunshine, therefore, limiting the overall utilization of the system to daytime periods. One usual way of increasing operation of the system is to model the DC to AC converter control to facilitate bidirectional flow of power and use the converter to supply reactive and harmonic compensation to the grid. When the PV is not capable of producing for a period, this function can still continue, as a result, system utilization is increased (Leslie 2003).

With the integration of the energy storage system(ESS) with the utility grid, the electricity produced at times of low demand and from intermittent renewable energy sources is shifted for times when the demand for electricity is high or when there is no other generation available. Adequate integration of the renewable energy sources with energy storage systems gives opportunity for higher market penetration (Serban & Marinescu 2010; Carrasco et al. 2006).

The growing interest in the number of investors in solar energy has intensified the research that involves the development of a multifunctional inverter for stability of the grid. Solar photovoltaic technology could generate energy from the sun to provide large-scale, domestically safe, and global friendly electricity. Solar PV installation was projected to supply 15GW in 2010 as compared to 2.7GW in 2006. The need for silicon to produce solar cells is estimated to rise from 41,000 tons to 120,000 tons from 2006 to 2010 and an estimated increase of 400,000 tons in 2015. The Fig. 2.10 below shows the projected growth and installation of solar PV energy in some countries and worldwide till 2030.

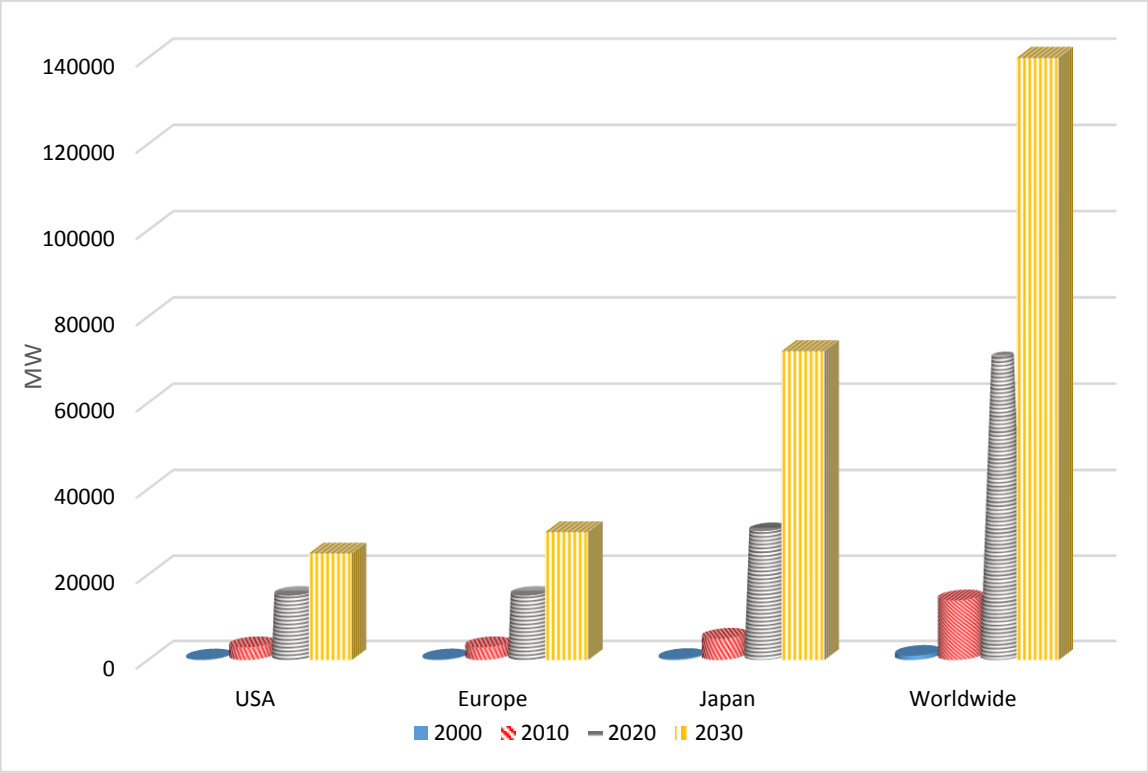

Figure 2.10; Growth and installation of solar PV energy in various countries

The effect of PV in the electric power system is eventually limited by electricity demand that is not matching with normal solar PV production, resulting into unusable PV generation. In order not to incur so much cost by increasing the usefulness of solar PV

generation, the electric power system will require modification to take in surplus production of solar PV.

the usefulness of this excess PV generation can be increased through some of the following ways (Denholm & Margolis 2007):

- Increased flexibility: permits more of the normal load to be met by the PV by dropping the system minimum.
- Load shifting: normal load to be deviated to periods of larger PV output.
- Energy storage: electricity generated by solar to be stored and use of this stored energy at periods of minimal or no output by the solar.

2.9 Energy Storage in Distributed Energy Source (DES)

Energy storage is regarded as an important element of energy planning in electricity sector and for other energy options. There have been major difficulties in storing electricity in large quantities. Due to the intermittent nature of most RES and the variability in electricity load requirements storing of electricity is quite essential in renewable energy systems. The combination of these problems is one of the most challenging issues being experienced in the small and large-scale use of renewable energy. As the electricity supply sector advances, there is better prospect in the use of distributed generation, and many of the renewable energy technologies provide themselves predominantly well to distributed generation applications. This may reduce the necessity for storage and can help to cut down on transmission and substation investments (Banks & Schaffler 2006).

Energy storage allows the decoupling of electricity generation from demand in an electricity generation and supply system. During the periods of low energy demands, low generation cost or energy from intermittent renewable energy sources, the energy is stored with storage equipment by converting the electricity into thermal power, chemical energy, etc. which is further released during periods of increased energy demand, high generation cost and when no other means of generation is available. Through changing the way of consuming energy, they can transfer the peak power and increase the low valley power on the basis of meeting the requirements of users. Consequently, it is usually known as "peak load-shifting" technology. Improved market penetration resulting into primary energy and emission savings is obtainable when there is proper integration of renewable energy sources with storage systems (Carrasco et al. 2006; Xiao-Hong 2009).

There are different conditions where the single-stage and two-stage GCIs are appropriate for energy storage application. A single-stage PWM converter can be supplied directly by energy storage cells if the dc voltage is sufficient. However, in

order to match the output voltage of cells and the input voltage of the DC/AC stage, a DC/DC stage with step-up feature might be required. According to the topologies of GCIs for RESs application that were mentioned earlier, it can be seen that there is a DC/AC stage in both two-stage and single-stage GCI. The essential part of the GCI is the DC to AC stage which converts the DC energy of RESs into an adequate AC energy interfaced to the utility (Alepuz et al. 2006). The representation of the GCI with energy storage is showed in Fig. 2.11.

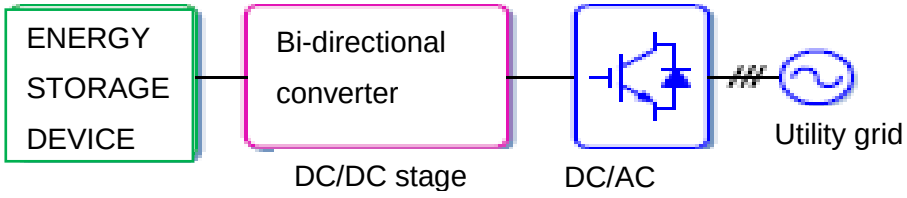

Figure 2.11: Grid-connected system of Energy storage device (Zeng et al. 2013)

2.10 Role of a Smart Grid

The application of smart grid tools and technologies applied in the electrical grid infrastructure allow bidirectional flow of energy and communication between the grid and the PV. These functions can result into having an improved efficiency, reliability, safety, and interoperability. The growth of technology and services regarding smart grid has been rising and was estimated to increase between 2009 and 2014 to nearly 43 billion dollars in the United States and worldwide increase greater than 171 billion dollars.

The effects of renewable energy on the operation and planning of the system are known quite well. Though, the study of existing smart grid capabilities such as communication and controls for managing the effects of integrating and optimizing the future power system with high levels of solar and wind energy is not satisfactory. The objective of the future grid is to increase integration of RES at a very fast rate to be driven by cost improvements, favorable policies etc.

However, the inconsistency in load type is an important concern in smart grid technology. The major type of loads that affect energy efficiency, demand response and load control of the smart grid consist of residential, commercial, industrial, agricultural and plug-in electric vehicles (Boulder 2012; Amin & Mohammed 2011).

2.11 Advantages and Applications of Solar Energy in Generating Electricity

It has been regarded that solar applications i.e. PVs are the best and one of the cheapest means of providing the elementary energy services that are not sufficient to every individual in the area. However, some of the advantages and applications of

solar energy in generating electricity are the following (Solangi et al. 2011)(Parkpoom et al. 2004):

- There are no release of greenhouse or toxic gases such as carbon dioxide (the greenhouse gases in the atmosphere tend to trap heat and, despite the fact that changes in levels have occurred naturally in the past, it is the amount of releases of unnatural greenhouse gas that is of major concern, with high probability of resulting in climate change).
- Decrease in the amount of transmission lines from electricity grids.
- Quality of water resources is enhanced.
- Rise in regional and independence of national energy;
- Diversification and security of energy supply;
- Rapid growth in electrification of rural communities in developing countries.
- Used in solar home systems by supplying power for domestic lighting and other DC appliances such as radios, TVs, sewing machines, etc.
- For home lightings and community buildings as well as in telecom towers using PV modules.
- For commercial applications such as solar cooling systems in supermarkets, theatres and cinemas, since air-conditioner is one of the appliances that consumes electricity the most.
- Solar water heaters to minimize the electricity being consumed by heating water for various domestic and industrial applications of hot water.
- Huge solar power plants providing off-grid desert communities.

  Additionally, one of the most optimistic applications of RES to seawater desalination is the use of solar energy in thermal desalination processes (Doukas et al. 2006).

2.12 Demands for Grid-Connected Photovoltaic Systems

There has been growing interest in the use of free renewable natural energy such as solar or wind energy. For remote locations, the solar PV systems are becoming the smartest alternatives. Due to the infinite availability of solar irradiation, the solar PV systems as compared to other sources of renewable offer improved performance.

The main source of power electricity generation in some regions in the nearest future will be through PV systems. The requirements for PV system are becoming much tougher (Trabelsi & Ben-Brahim 2011). Solar PV inverter is one of the key component in the PV system which is used to convert dc power generated by the PV modules into ac power so as to supply the grid (Selvaraj & Rahim 2009) . The demands at the PV side, power output maximization, a desirable DC voltage should be maintained for the inverter, and panel monitoring and diagnosis have to be enhanced. At the grid side, a

desirable THD of the output current should be attained. PV system should not violate grid voltage and frequency, grid faults ride-through. High demands for efficiency in order to reduce PV energy cost. With the use of advanced semiconductor devices, intelligent control, transformerless PV technology, high efficiency is achieved. Other demands for the PV grid-connected system are temperature management, which increases the reliability of the system. A grid-friendly system can be developed through advanced monitoring, forecasting and communication(Yang & Blaabjerg 2015; Braun et al. 2012)

2.13 Problems related to PV Array connection to the Grid

The power conditioning system (PCS) that is needed to convert the DC output voltage to 50 Hz AC voltage at the proper level to interface to the utility at the stated distribution level is one of the key issues that must be resolved in connecting the PV arrays to the utility grid. Line frequency converters or high frequency converters can be used to convert from DC to AC. During the operation of the line frequency converters there is a poor lagging power factor which introduces harmonic currents to the grid, thus, considering the modern technology, the high frequency converter is of higher interest. A good sinusoidal voltage waveform can be generated with high frequency converters. The system can be operated at a desired power factor by controlling the high frequency converter. During the period of transmitting reactive power, there is voltage drop resulting in the utility grid tending to have a voltage that is low at the outputs of feeders. The voltage can be improved back to the appropriate values at the ends of the feeders by ensuring the PV generation systems with power factor control is positioned close to the end user (Dasgupta et al. 2013; Karmiris et al. 2012; Singh et al. 2011; Delfino et al. 2010).

The inverter control should have the ability to identify a fault or blackout in the utility grid and disconnect from the system. During islanding mode when there is an outage if the converter continues to operate, there is a possibility that the reclosing of utility breakers for fault clearance would connect to the unsynchronized system. There could be huge voltage surges occurring on the utility grid during lightning strikes, hence, the inverter must have the ability to protect itself during this period.

Introducing a DC to DC converter between the PV array and the input to the DC to AC inverter is one usual approach of connecting a PV system to the grid. The DC to DC converter functions as a buffer and creates more choices in selecting the nominal output voltage of the PV array. When generating a high DC voltage by connecting an immense quantity of PV cells in series, there is a risk of one cell shorting and destroying other cells in the array. This issue can be prevented by using the DC/DC

converter which allows a low voltage PV array to be interfaced to a high voltage AC system(Leslie 2003).

2.14 Harmonics

From so many years back, when there has been continuous rise in the use of static converters, the harmonic problem has been predominant, thereby having a direct effect on the quality of the electricity supply.

Generally, the issue of harmonics can be identified as a type of disturbance that is caused when there are components which are not linear in the electrical systems, determines a permanent alteration of the voltage and current sinusoidal waveforms, such as sinusoidal components at a frequency that varies from the nominal frequency.

Decrease in the quality of electricity and the performances of other equipment sensitive to voltage harmonics will be altered as a result of PV generators that are connected to the distribution network through static converters and therefore harmonics is potentially generated (Abo-Al-Ez et al. 2012). However, due to harmonic voltage distortion, the static converters may not operate properly as they are sensitive to harmonics.

Furthermore, in order to improve the quality of the electric service thus, adding value to the PV energy and making PV systems more engaging, the use of filters for harmonic reduction is of extreme importance.

The major disturbing residential loads are:

- Computers
- Television receivers
- Thyristor-controlled devices such as lamp dimmers
- Fluorescent lamps

A large number of residential loads significantly contribute to network harmonics even though the residential loads connected to the LV network have a limited power. The harmonic current content from each equipment can reach 100% and these can cause distortions on the network voltage of about 4% with the current utilization of electronic devices if the equipment are in phase with other generators. There will be increase in distortion as these devices increase (Verhoeven & KEMA 1998). The harmonic impedance should be limitless under perfect condition for all low order harmonics so as to reduce the harmonic current distortion generated by the converter system when it is in a condition where the supply is distorted. However, for all values of harmonic supply distortion, zero harmonic current should be supplied by the inverter (Twining & Holmes 2003).

2.14.1 Harmonic Effects

There can be losses in the utility network and potential breakdown of equipment connected to it as a result of harmonic effects. The effect of harmonics is gradual even though PV systems are usually small, they should not be ignored. Recent inverter equipment operating on PWM switching is usually very good, generating very slight harmonics. On the other hand, many small sources of harmonics can have a significant effect on the whole levels in the utility network. Example is found in TV sets (Verhoeven & KEMA 1998).

Some of The key effects of voltage and current harmonics on the different network components are:

- System efficiency is reduced.
- Excess voltage and currents as a result of parallel and series resonance.
- The insulation of the system components is destroyed resulting into shorter life span of components.
- Malfunction of the electrical system components.

2.14.2 Harmonic Filtering

There has been a huge development in semiconductor based devices over the past years which has given rise to additional power electronic applications which includes high voltage DC systems, computer power supplies, and adjustable speed motor drives. However, the mode of operation of these devices is creating problems with the power distribution system as their use increased even though these systems improved existing applications and created new applications. These systems which draw non-linear currents from the sinusoidal distribution system use diode and semiconductor device on the front end. The non-linear currents drawn by the device contain harmonics of the line frequency and reactive elements that interfere with the line voltage of the distribution system due to the impedance of the distribution lines. The neutral line, which is not designed to carry large currents, can experience voltage unbalance and excessive currents due to the non-linear currents in three-phase systems. The rate at which the non-linear systems that are present in a distribution system increase, the more obvious the effects of the harmonic and reactive “pollution” on the system become. The occurrence of huge current in the neutral lines causes unnecessary tripping of protection equipment, overheating, and destruction of the insulation. The disturbances caused as a result of the non-linear currents exist as harmonics in the distribution system voltages. Any delicate electronic equipment that is connected to the distribution system can be affected by the harmonics present in the system voltage,

e.g. telecommunications systems, computer systems, and control systems. The communications systems can experience interference due to harmonic currents and voltages through electrostatic and electromagnetic coupling from the transmission lines. In order to limit the amount of harmonic current that can be introduced into the distribution system depending on the type of equipment, the IEEE and IEC initiated some standards. Some of the standards are the IEC International Standard 1000-3-2 which comprises of equipment limited to less than 16A per phase, and 1000-3-4 that comprises of equipment limited to between 16 and 75A per phase. These standards are being integrated into the regulations of most power generation companies that must be abided by. In order to limit the amount of harmonic and reactive currents drawn by the equipment, most power electronics systems that convert AC to DC that are being developed recently have been designed with a power factor correction (PFC) stage on the front end due to these regulations. One way to correct the problem at the source is the PFC method, but another means is to place a vast harmonic filter or reactive compensating system at the input to a facility that draws non-linear currents.

Large reactive loads draw current that is out of phase with the source voltage such as a huge number of motors at a manufacturing facility. This results into a greater apparent power, and added current which is essential to charge and discharge the reactive loads generates I^2Rlosses in the utility generation equipment and transmission lines. Commercial customers that draw excessive reactive currents are mostly penalized to pay charges by the utilities. Manufacturing companies place reactive compensation equipment at the utility connection to the facility most times in order to avoid paying charges (Leslie 2003).

The harmonic content in the inverter can be minimized by improving the output waveform of the inverter therefore, reducing the size of the filter to be used and the level of electromagnetic interference (EMI) produced by switching operation of the inverter(Selvaraj & Rahim 2009). The filtering systems used for reduction of harmonics are passive and active filtering systems. A number of research is ongoing to enhance the power distribution system requirement in terms of the reliability and quality of voltage. The variation in the solar and wind output power generation can result into irregularities and voltage disturbances. The use of LCL (inductor-capacitor-inductor) filter in GCIs has gained more attention due to its improved capability to reduce harmonics resulting to the utilization of a switching frequency that is lower which does not exceed the harmonic limits, and the electromagnetic interference is minimized also specified by the IEEE-1547 and IEEE-519 standards (Mohamed 2011).

Some considerations such as conformity of the power quality with interconnection standards is involved while designing the GCI. The voltage source inverter (VSI) is

usually used for the GCI however the output from this inverter is a modulated voltage, therefore, it is essential to filter out the harmonics before it is connected to the grid as regards to the grid requirements. The LCL filter is widely used due to its enhanced performance to reduce harmonics, power consumption is minimal and electromagnetic interference is minimized. Various research are still ongoing on the analysis of LCL filter for the purpose of designing (Reznik 2012; Singh et al. 2011; Marei et al. 2004).

2.15 Filter Topology

The function of the filter is to supply the grid with current that is free of harmonic distortion. Therefore, it is important to have a filter connected to the inverter before it is connected to the utility grid. The efficiency and weight of the filter needs to be considered before choosing the inverter to be used. The L and LC filters have poor high frequency noise damping capabilities as compared to LCL filter which dampens the high frequency noise due to its extra inductance (Massawe 2013). Therefore the LCL filter design is considered in this study for smoothing the output current as proposed in (Blaabjerg et al. 2006).

In the operation of grid connected VSI the filter functions in dual mode. Firstly, the filter should have an overriding inductive behaviour to enable the suitable operation of the VSI if connected to a voltage source type system such as the utility grid. In this case, the eminent behaviour of synchronous generators and of transmission lines is imitated by the grid connected inverter where the control of active and reactive power transmission is associated to the control of phase and magnitude of the electromagnetic force (Dasgupta et al. 2011). Secondly, the grid-connected inverter generates PWM carrier and side-band voltage harmonics. These voltages may result to the flow of current into the grid and if adequate filters are not employed to prevent this flow, it can affect other sensitive loads or equipment and there will be more losses. In order to conform to these requirements, a filter comprising of a simple inductor is the easiest way out. The switching frequency is low for applications about several hundreds of kW and more, such as wind turbine systems so as to reduce losses. In order to meet the demands of standards and grid codes thereby mitigating the harmonics in the current, the use of a high value of input inductance could not be sufficient, and it becomes quite expensive to realize higher value filter reactors and sometimes also the strain of the inductor could pose as a problem. Furthermore, the dynamic response of the system may become worse. The switching frequency is higher for applications about a few kW, such as most commonly found photovoltaic systems. Thus, even smaller inductors could achieve the requirements, but there is still

problem of strain of the inductors since the converter and its passive elements are integrated.

The major issue at the system level is related to the instabilities produced by some specific harmonics like in the case of wind or photovoltaic systems. Therefore a means of reducing or eliminating these harmonics is to use a bank of tuned LC trap filters, thereby preventing the voltage quality from getting worse.

However, limitations that are very strict for frequencies more than a certain threshold should be adhered to as recommended by the standards and grid codes. The use of high-order filters like LCL, which provide 60 dB per decade attenuation for the PWM carrier and side-band voltage harmonics, is a preferred solution since low-pass filter attenuation will be necessary. Best results can be gotten using relatively small values of inductors and capacitors with this solution. Some of other benefits of the LCL filter include: small distortion in the grid current and reactive power production; and the option of using a comparatively small switching frequency for a specified harmonic attenuation.

The most implemented approaches to reduce PWM carrier and side-band harmonics are the use of a tuned LC filter or a low-pass LCL filter as identified previously. The tuned LC filter functions as a group of trap filters to reduce selective harmonics. For power converters switching at hundreds of Hz, this solution is particularly practicable since they generate PWM harmonics that has a very low frequency, which makes it difficult to tune a low-pass filter like the LCL filter.

The figures of the kinds of filter previously mentioned are represented below. There is possibility of having different kinds of trap filters by connecting an inductor and a capacitor in parallel and some other combinations of these two types of filters. The robustness of the filter must be considered in designing and of the LC filters so as to reduce a certain frequency. Alternatively, there is a certain degree of freedom in designing the low-pass LCL filter (Ahmed et al. 2007; Teodorescu et al. 2011).

2.15.1 L Filter (First-order):

The simple inductor filter represented in the Fig. 2.12 below has an attenuation of -20 dB per decade through the entire frequency range. in order to mitigate the inverter harmonics adequately, the switching frequency of the inverter has to be high to employ this filter (Ahmed et al. 2007).

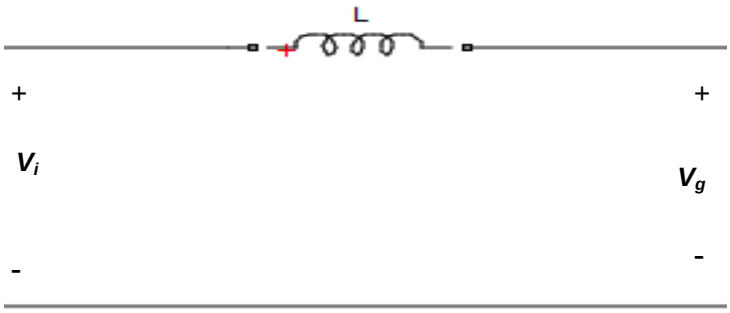

Figure 2.12: Configuration of L filter

2.15.2 LC Filter (Second-order):

The output voltage and the grid voltage synchronized is synchronized together, thus ripple current is supplied to the grid by the PWM inverter. The connection of the output LC filter removes the high switching frequency components from the output current of the inverter. The current ripple determines the inductor to be designed for the filter. The lesser the ripple, the lower the switching and conduction losses. The ripple current is usually chosen to be 10% to 15% of rated current. the designed value of the inductor in a system where 10% ripple of the rated current is chosen gives the equation (2.5) below (Bhutia, M. Ali, et al. 2014; Sangita Nandurkar & Rajeev 2012)

$$\Delta iL_{max} = \frac{1}{8} \times \frac{V_{dc}}{L \times f_{sw}} \qquad (2.5)$$

The reactive power supplied by the capacitor at fundamental frequency determines the capacitor to be designed. Considering 5% of the rated power for the design of reactive power gives the equation (2.6):

$$C = 15\% \times \frac{P_{rated}}{3 \times 2\pi f \times V_{rated}^2} \qquad (2.6)$$

The LC(second order) filter represented in the Figure below yields -40 dB/decade attenuation. a shunt element is required to mitigate the switching frequency components more since low attenuation of the inverter switching components is realized by the L filter. in order to generate low reactance at the switching frequency, the shunt component must be selected. However, this element must present a large magnitude impedance within the range of control frequency. A capacitor is used as the shunt element. The resonant frequency is calculated from the equation (2.7)(Hassan & Bhuiyan 2010):

$$f_o = \frac{1}{2\pi} \frac{1}{\sqrt{LC}} \qquad (2.7)$$

The LC filter in the Fig. 2.13 below has been experimented in UPS systems with a resistive load. in a case where the load impedance through C is quite large more than the switching frequency, the LC filter is suitable for such configurations. Due to the introduction of shunt in LC filter, it consumes more reactive power and cost more than the L filter (Ahmed et al. 2007).

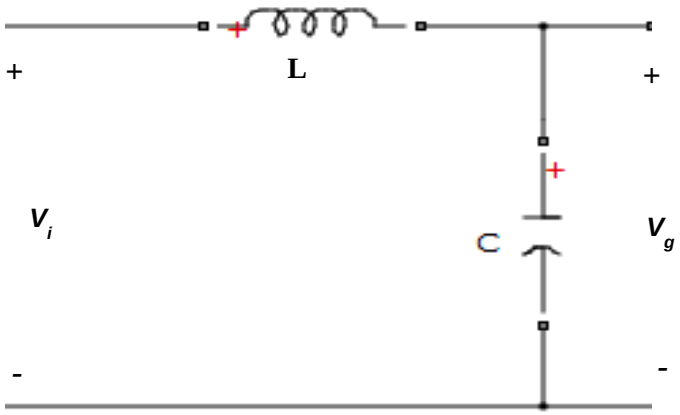

Figure 2.13: Configuration of LC filter

2.15.3 LCL Filter (Third-order):

One of the most important benefits for high power applications is the introduction of the LCL low-pass filter represented in the Fig. 2.14 below which has a better harmonic performance at lower switching frequencies. It yields better reduction of inverter switching harmonics compared to the L and LC filters. A more complex current control strategy is however required by systems integrating LCL filters to maintain stability in the system, and is subject to interference due to grid voltage harmonics as a result of resonance risks and lower harmonic impedance injected to the grid (Vodyakho & Mi 2009; Raoufi & Lamchich 2004). It is challenging to obey the IEEE-519 standards without an LCL filter with low inductance on the inverter side. Minimized harmonic distortion levels with lower switching frequencies and less total energy stored can be realized using the LCL filter. However, due to resonance, the LCL filter may lead to both dynamic and steady state input current distortion (Twining & Holmes 2003; Ahmed et al. 2007; Chetty & Ijumba 2009; Shen et al. 2009).

The LCL filter's resonant frequency is given by equation (2.8):

$$f_o = \frac{1}{2\pi}\sqrt{\frac{L_1+L_2}{L_1L_2C}} \qquad (2.8)$$

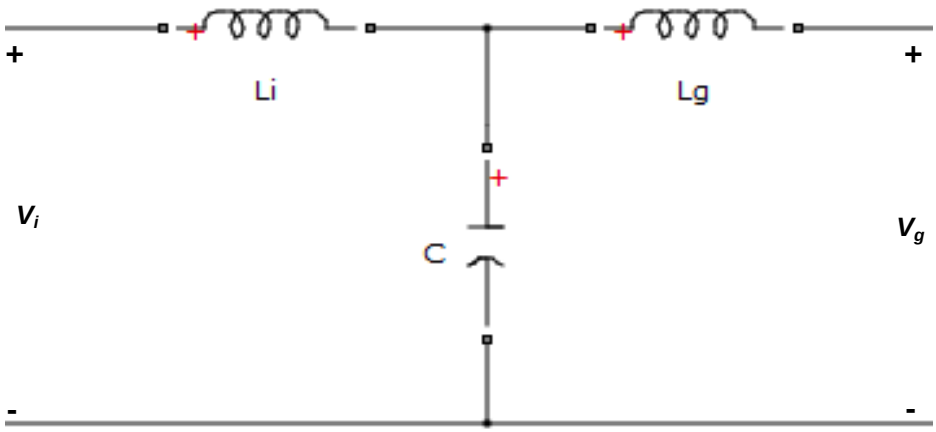

Figure 2.14: configuration of LCL filter

LCL frequency response: An essential transfer function is $H_{LCL} = \frac{i_g}{v_i}$ where the grid voltage is expected to be an ideal voltage source which is able to discard the harmonic frequencies. If $v_g = 0$, which is the condition for current-controlled inverters, the transfer function of LCL filter i.e. when the system is not damped is:

$$H_{LCL}(s) = \frac{1}{L_1 C_f L_2 s^3 + (L_1 + L_2)s} \qquad (2.9)$$

However, employing some simple algebraic procedures, the transfer function for the damped system is stated as:

$$H_{LCL}(s) = \frac{sC_f R_f + 1}{s^3 L_1 L_2 C_f + s^2 R_f C_f (L_1 + L_2) + s(L_1 + L_2)} \qquad (2.10)$$

2.16 Maximum Power Point Tracking

The V-I characteristic of photovoltaic cells is non-linear which depends on solar intensity and cell temperature. It is challenging to control the output of the PV cells due to its non-linear characteristics so that the maximum power that is available will be fed to the grid. The process of maximizing the power output of the PV array is identified as maximum power point tracking (MPPT) (Leslie 2003).

However, Maximum Power Point Tracking is one of the most essential things that must be considered while working with PV panels. (Trabelsi & Ben-Brahim 2011) further explained MPPT as a means of finding a method to extract the maximum power obtainable from the PV panel. This subject is very crucial when dealing with solar energy. The knowledge of MPPT originated from maximum power transfer which means that the maximum power is transferred from the source to the load when the internal resistance of the source is the same with the resistance of the load. The transfer of maximum power will not be possible if the load resistance is fixed. Hence, the DC to DC converter will be used as a variable load while changing the duty cycle in

order to reach the maximum power point. It is worth nothing to note that MPPT is carried out by the DC to AC inverter for a single stage inverter.

2.17 EMI Problems

EMI (electromagnetic interference) problems are caused by sudden fluctuations in voltage (dv/dt) or current (di/dt) levels in a waveform. Most fast switching power semiconductor devices found in GCIs generate high dv/dt and di/dt in their waveforms. The radiated high-frequency wave generated from a conductor having a high dv/dt wave which works like an antenna, may combine with a sensitive signal circuit and appear as noise known as radiated EMI. This noise signal may be carried by a dependent coupling capacitor through the ground wire (conducted EMI). A high di/dt current wave may also produce conducted EMI by combining through a dependent common inductance. The problems related to EMI include interference in the communication line and faults in sensitive signal electronic circuits. EMI problems can be resolved through adequate shielding, noise filtering, careful equipment layout, and grounding. Several standards relating to EMC (electromagnetic compatibility) have been defined to control EMI problems (Bose 2002).

2.18 Non-Controlled Grid Connected Inverter

The modelling of the inverter is implemented through its nominal input impedance in parallel with a current perturbation during this operating state, which signifies the current needed by the inverter to introduce sinusoidal power to the grid. Hence, the power conversion structure can be modeled as a single system comprising of the PV panel, the DC to DC converter, and the inverter as a whole system. Standard grid-connected inverters need DC-link voltages higher than the usual PV voltages; therefore, a boost DC to DC converter was implemented. Boost converters are non-minimum phase systems in voltage mode, hence, the inductor current control must also be implemented instead of voltage control. The inductor current i_L and the state variables chosen are the input and output capacitors voltages V_{Ci} and V_{Co} for the system. In addition, the sources of perturbation are the PV panel short-circuit current I_{SC} that models the changes in irradiance, the perturbation of the load current I_O and the variable used is the duty cycle of the inverter d ($0 \leq d \leq 1$) (Gonzalez et al. 2012; Wang et al. 2011).

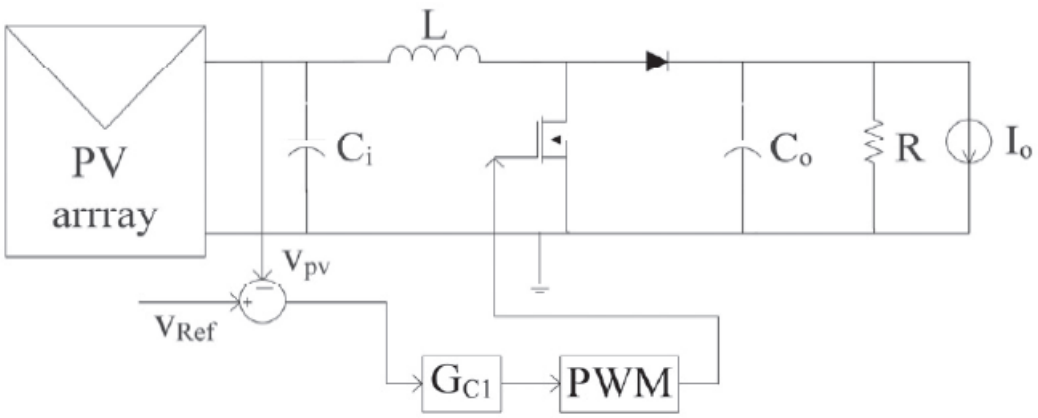

Figure 2.15: Electrical model of PV system with non-controlled inverter connected to the grid

From the electrical models of Fig. 2.15 above, the following relations defines the semi-period where the MOSFET is turned ON:

$$v_l = v_{Ci} \tag{2.11}$$

$$i_{Ci} = I_{sc} - \frac{v_{Ci}}{R_{MPP}} \tag{2.12}$$

$$i_{Co} = -\frac{V}{R} - I_o \tag{2.13}$$

where v_L and v_{Ci} are the voltages of the inductor and input capacitor, i_{Co} signifies the output capacitor current, the DC link nominal voltage is represented by V, R and I_o represents the grid connected inverter load current and resistance, and I_{SC} and R_{MPP} represents the Norton equivalent of the PV panel around its MPP. Likewise, the relations for the semi-period where the MOSFET is turned off:

$$V_L = v_{Ci} - v_{Co} \tag{2.14}$$

$$i_{Ci} = I_{SC} - \frac{v_{Ci}}{R_{MPP}} - i_L \tag{2.15}$$

$$i_{Co} = i_L - \frac{V}{R} - I_o \tag{2.16}$$

where i_L and i_{Co} signify the inductor and input capacitor currents.

2.19 Control Strategies Used In Grid-Connected Inverter

One of the main problems that occur while using grid-connected VSI is that it is very sensitive to disturbances present in the grid. This is commonly found in variable speed

wind turbines and other RES, which are usually situated in rural regions and linked to the grid by long overhead lines, and are prone to faults easily.

Grid disturbances that occur during a short period often cause the turbine to stop compulsorily resulting to production losses. The reduction of voltage sag by using a dynamic voltage restorer (DVR) is another application which is more difficult, where power is generated to the dc-link through a shunt-connected VSI. The VSI which is shunt-connected is necessary to operate through faults for this application. The power needed by the DVR can also fluctuate a lot. It is necessary to ensure adequate operation of the VSI when the supply condition is disturbed, resulting to the need for a robust controller. The performance of the VSI can be severely affected by voltage dips amongst other power quality instabilities. A voltage dip is a decrease in voltage with time interval between one half-cycle and one minute, caused majorly by a short-circuit fault (Saccomando & Svensson 2001).

The power electronics interface is necessary to achieve the control and flexibility required by the micro-grid. The control strategy of the DC to AC stage primarily comprises of an outer dc bus voltage loop and an inner current loop(Zeng et al. 2013).

2.19.1 CSI Controls

The AC output is a current waveform and the waveform is most times not affected by load. The AC output voltage should be more than the initial DC voltage that is fed into the DC inductor or the supplied DC voltage is usually lesser than the AC input voltage. Hence for the conversion of DC to AC power, the CSI serves as a boost inverter. A further DC to DC conversion will be necessary for applications where the voltage limit is large. However, the efficiency of the system is reduced and the system becomes more expensive due to the presence of another power conversion process. Also, the source of the CSI is from an adjustable current from a DC source with very high impedance as compared to VSI where the DC source has negligible impedance. It is mostly used in medium voltage industrial applications (Massawe 2013; Peng 2003).

2.19.2 PQ (Active Power-Reactive Power) Controls

The power control mode is employed to regulate the active and reactive powers independently when the inverter operates in grid-connected mode(Salam et al. 2010). In this case, the inverter is used to supply a given active and reactive power set point. During transient state, such as load changes or power variations in renewable energy sources (RES), the power quality of inverter is significantly not affected due to the nature of the control mode. The mode of operation of this inverter is by injecting the available input power into the grid. The value of the reactive power injected correlates

with the specific value that has been locally or centrally defined from the MGCC (Micro Grid Central Controller). In PQ control method, it only allows a simple control over the output current of the inverter during short-circuit conditions by limiting the total gain of the PI (proportional integral) controllers(Lopes et al. 2006). The inverter uses the power control mode to regulate the active and reactive power independently when in grid-connected mode. However, when the inverter works in islanding mode, it uses the voltage control scheme (Salam et al. 2010).

2.19.3 VSI Controls

The VSI controls is one of the most important control approaches employed in operating an inverter. VSI control can be defined as a technique where the inverter is controlled to deliver definite values of voltage and frequency to the load. The real and reactive power output of the VSI is determined according to the amount of load (Lopes et al. 2006; Barsali et al. 2002). The three phase voltage source inverter (VSI) is commonly used as the interface between RES-based DG generators and the grid system in designing applications. The switching signals for VSI which are mostly the current signals when designing a smart inverter, may have information on the active power supplied from the RES and the reactive power needed to compensate for the power quality disturbances at the PCC (point of power coupling) (Teke & Latran 2014; Geibel et al. 2009; Arai et al. 2008). A completely controlled synchronous generator is not frequently found in a microgrid and in typical power systems, the control of frequency and voltage depends on it. Due to the kind energy generated by the RES technologies which are usually installed in a microgrid (MG) it is not adequate to be connected straight to the grid network. Therefore, the use of inverter which serves as a power electronic interface will be applicable. It is required that the VSI are able to sustain over currents for a larger time interval than the time required for fault clearance. Hence, when there is a case of short-circuits of induction machines the VSI will provide reactive power within the specified current limits and this behavior will be sustained until the induction machines recover(Lopes et al. 2006). This control technique consists of the inner current loop and the outer voltage loop to realize a fast dynamic response. The inner current loop regulates the active and reactive power from the grid thereby monitoring the power quality of the system. However, the outer voltage loop controls the DC link voltage which is responsible for the flow of power in the system. The stability of the system with slow dynamics is of utmost importance in the control strategy. Grid-side control was also proposed by some authors based on the fact that the dc-link voltage loop can be cascaded with an inner power loop instead of a current loop, so the current is controlled indirectly (Saccomando & Svensson 2001; Agirman & Blasko 2003; Teodorescu & Blaabjerg 2004; Blaabjerg et al. 2006; Kadri et al. 2011;

Reznik 2012). The basic building component of the three-phase VSI is the half-bridge inverter, and the three-phase VSI control involves the control of three half-bridge inverters at the same time.

Categorically, there are two major methods of controlling the active and reactive power of a voltage source inverter (VSI) system which are voltage-mode control and current-mode control. The voltage-control mode has been mainly employed in high voltage and power applications such as in Flexible Alternating Current Transmission System (FACTS) controllers, even though industrial applications of this mode have also been stated. the real and reactive power components P and Q of The VSI system is exchanged with AC system at the point of common coupling (PCC) (Reznik 2012; Jena et al. 2011)

For controlling of the real and reactive power in the VSI system in current-mode control, the current at the AC side of the VSI is first controlled through the VSI terminal voltage by a dedicated control system. Afterwards, the real and reactive power are both controlled with respect to the PCC voltage by the phase angle and the amplitude of the VSI line current. As a result, for cases of overloading, the VSI is protected due to the current control system. The current-mode control provides other benefits such as robustness against variations in parameters of the VSI and AC system, superior dynamic performance, and the control precision is better (Al-Saedi et al. 2011). The general structure of the current control methods available is showed in the Fig 2.16 below:

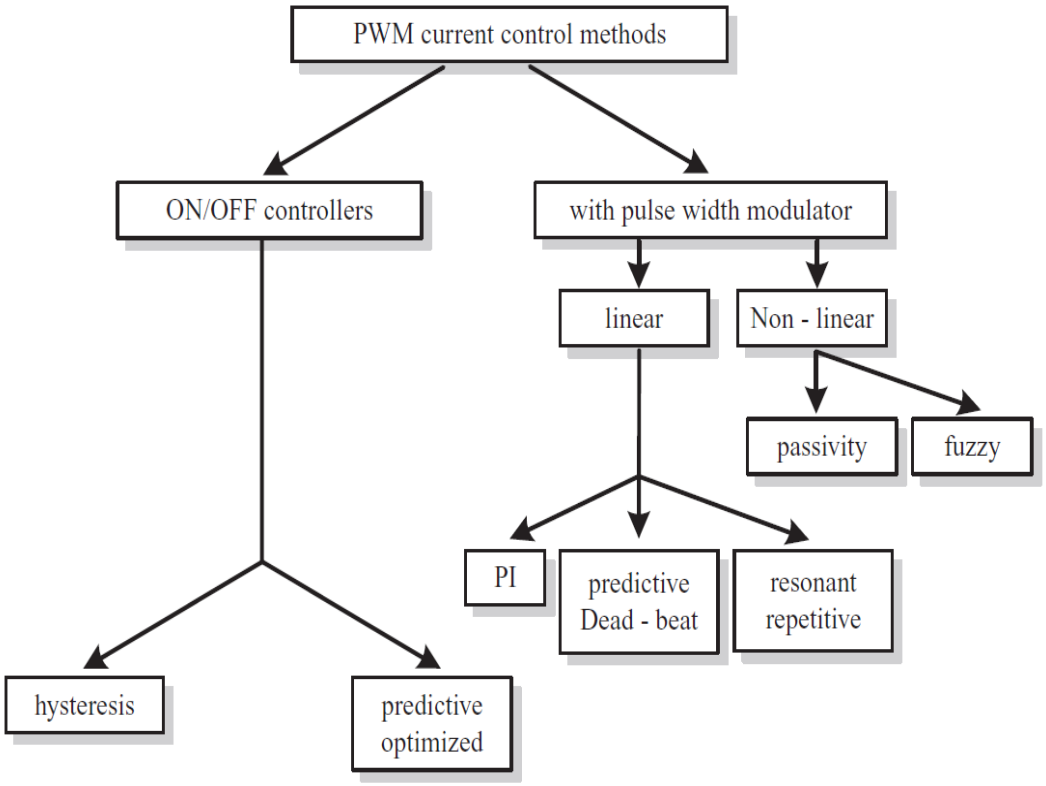

Figure 2.16: Classification of current control methods

(Teodorescu et al. 2011)

Sensitive loads and grid-tied inverters are affected by voltage sags which is one of the major problems regarding power quality resulting to current overshoot and distortions. Therefore, high performance should be achieved for both normal operating conditions of the grid and during fault conditions through the control approaches for inverters (Rodriguez et al. 2009).

Moreover, for the effective operation of power electronic-based MFI systems, there is need for advanced control system. The control systems for VSI calculate the current and voltage reference signals and define the switching sequence of the inverter switches. Due to the large computation time and delay in calculating the reference signals, frequency domain approaches like fast Fourier transform are not used often. Instantaneous derivation of compensating currents or voltage signals is possible through time domain approaches. A large number of control techniques have been applied to MFIs in the time domain effectively. The time domain control methods mostly used for MFIs are instantaneous active and reactive power and synchronous reference frame methods. These methods convert the current and voltage signals in the ABC frame into the stationary reference frame or the synchronously rotating frame for the fundamental and harmonic quantities to be extracted. Instantaneous active and reactive powers are calculated in PQ theory; however the concern of dq theory is with

the free current of the source voltage. Real and reactive powers are concerned with fundamental components. The fundamental components in the distorted voltage or current are DC quantities (Teke & Latran 2014; Dasgupta et al. 2011; Chen et al. 2005).

The major categories of dimensional/reference frames in VSI control are:

- Stationary reference frame control (αβ frame control)
- Synchronous/ rotating reference frame control (dq frame control)
- Natural reference frame control

Stationary Reference Frame

The Stationary reference frame allows transformation of controlling a system of three half-bridge converters to an equivalent control of two equivalent subsystems. However, the reference, feedback, and feed-forward signals are in general sinusoidal functions of time. Therefore, to realize a performance that is satisfactory with small steady state errors, there may be the need of the compensators to be of high orders, and the closed-loop bandwidths must be sufficiently larger than the frequency of the reference commands. Thus, the compensator design is not an easy task, especially if the operating frequency is variable though this problem is addressed in dq frame. In addition, the concept of instantaneous reactive power can be defined in stationary reference frame (Vasquez et al. 2013; Rocabert et al. 2012; Yazdani & Iravani 2010). This frame is one of the techniques used to structure the control loops as represented in the Fig. 2.17 below. The grid currents are transformed into stationary reference frame using the ABC to αβ module in this technique. The use of other controller types is required because of the issue associated with PI controller in failing to eliminate the steady-state error when controlling sinusoidal waveforms since the control variables are sinusoidal in this case.

Over the last few years, the use of Proportional resonant (PR) controller has increased due to large acceptance in regulating current of grid-tied systems. The transfer function of the PR controller in stationary reference frame in matrix form is given by;

$$G_{PR}^{(\alpha\beta)}(s) = \begin{bmatrix} K_p + \dfrac{K_i s}{s^2 + \omega^2} & 0 \\ 0 & K_p + \dfrac{K_i s}{s^2 + \omega^2} \end{bmatrix}$$

Where K_p and K_i are the proportional gain and integral gain of the controller respectively while ω is the resonance frequency of the controller. This controller has the capability of eliminating the steady-state error between the controlled signal and its

reference since it is able to obtain a very high gain around the resonance frequency. The width of the frequency band around the resonance point is dependent on the integral time constant K_i. The lower the value of K_i, the smaller the band, while the band is bigger if the value of K_i increases. Past works also identified high dynamic characteristics of PR controller (Sangita Nandurkar & Rajeev 2012; Dash et al.2012; Blaabjerg et al. 2006; Timbus et al. 2005).

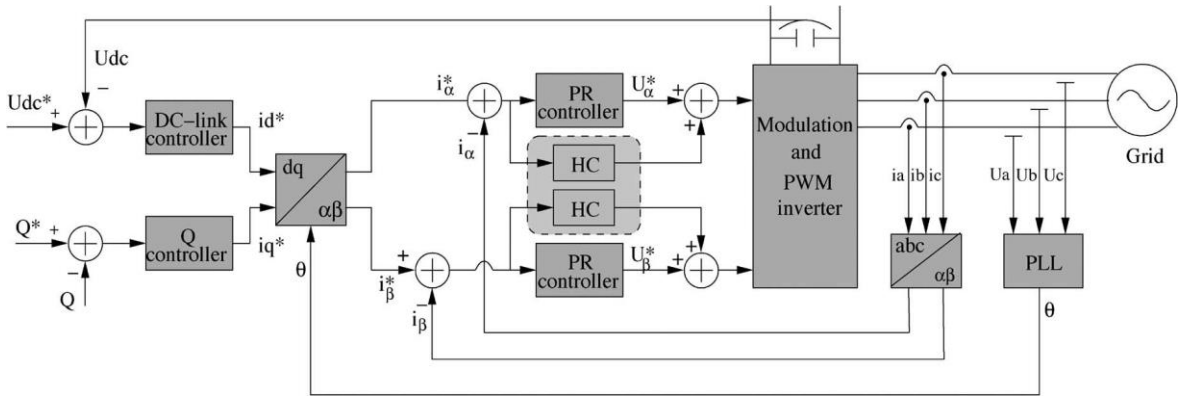

Figure 2.17: Typical structure of a stationary reference frame

Synchronous Reference Frame

Synchronous reference frame control is also known as dq frame control. The grid current and voltage waveforms are transformed into a reference frame that rotates synchronously with the grid voltage using a reference frame transformation module i.e. ABC to dq. Therefore, filtering and controlling can be carried out easily since the control variables are in form of dc values (Blaabjerg et al. 2006).

The signals in dq frame assume DC waveforms under steady-state conditions. This allows application of compensators with simpler structures and lower dynamic orders. Additionally, integral terms can be included in the compensators to realize a zero steady-state tracking error. A more suitable analysis and control design tasks is possible through the dq frame representation of a three-phase system (Zamani et al. 2012; Yazdani & Iravani 2010).

A representation of the dq control is shown in the Fig. 2.18 below. The dc-link voltage in this configuration is controlled in respects to the output power required. The reference for the active current controller is the output, while the reference for the reactive current is typically set to zero, if the reactive power control is not allowed. A reactive power reference must be introduced to the system in a situation where the control of reactive power is required (Tsengenes & Adamidis 2011).

The performance of the proportional integral (PI) controllers when regulating dc variables is very adequate which is why it is usually linked with the dq control structure.

The transfer function of the controller in dq coordinates can be written in matrix form as;

$$G_{PI}^{(dq)}(s) = \begin{bmatrix} K_p + \frac{Ki}{s} & 0 \\ 0 & K_p + \frac{Ki}{s} \end{bmatrix} \qquad (2.17)$$

Where K_p and K_i represents the proportional gain and integral gain of the controller respectively. The phase angle used by the ABC to dq transformation module has to be derived from the grid voltages since the current being controlled have to be in phase with the grid voltage. Hence, there is a probability of filtering the grid voltages and using arctangent function to derive the phase angle. Furthermore, the phase-locked loop (PLL) technique is now the most recent method of deriving the phase angle of the grid voltages in the case of distributed generation systems. As represented in the structure below, the performance of PI controller can be improved mostly by using cross-coupling terms and voltage feed-forward. The main problem with using the PI controllers in grid-connected systems even with these improvements is that it has an inadequate compensation capability of the low-order harmonics (Savaghebi et al. 2013; Sangita Nandurkar & Rajeev 2012; Blaabjerg et al. 2006; Timbus et al. 2005; Twining & Holmes 2003).

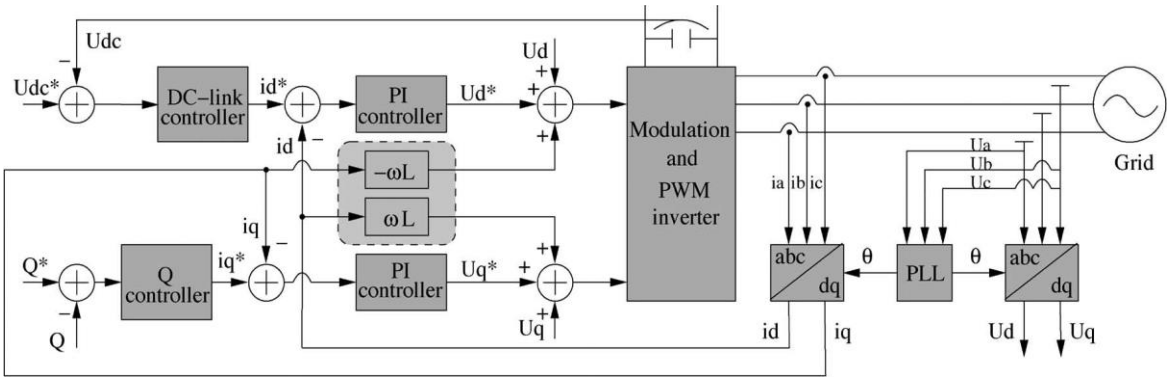

Figure 2.18: Representative structure of a rotating reference frame

The dq frame has the same advantages as the αβ frame, in addition to the following (Yazdani & Iravani 2010; Evju 2006):

- If the control is implemented in the dq frame, a sinusoidal command tracking problem is transformed to a corresponding DC command tracking problem. Therefore, the control can be done using PI compensators.
- Particular types of models of electric machine exhibit time-varying, equally coupled inductances when in ABC frame. If the model is formulated in dq frame, the time-varying inductances are transformed to the same constant parameters.

- Huge power systems components are usually expressed and analyzed in synchronous reference frame. Therefore, VSI systems that are represented in this frame allow analysis and design tasks based on procedures that are usually used for power systems, in a combined framework.

Natural Reference Frame

The concept of ABC control is to have a separate controller for each grid current. On the other hand, when designing the controller, the different methods of connecting the three-phase systems is an issue to be considered such as delta, star with isolated neutral and star without isolated neutral connections. The phases interact with one another In the case of isolated neutral systems; therefore, only two controllers are required since the third current is given by the Kirchhoff current law. However, it is possible to have three independent controllers by having additional considerations in the controller design as commonly found in hysteresis and dead-beat control.

ABC control is a configuration where nonlinear controllers like hysteresis or dead beat are usually preferred due to their high dynamics. The performance of these controllers is identified to be proportional to the sampling frequency. Therefore, the fast growth of digital systems like digital signal processors or field-programmable gate array is a benefit for such an application.

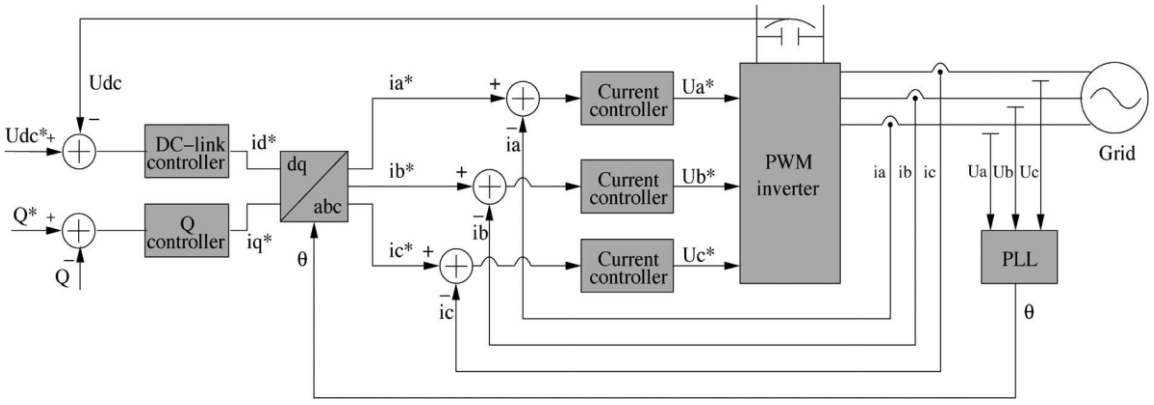

Figure 2.19: Representative structure of a natural reference frame

The Fig. 2.19 above shows the possibility of implementing ABC control where the output of the dc-link voltage controller sets the active current reference. Three current references are generated which utilizes the phase angle of the grid voltages supplied by a PLL system. Each of the current reference is compared with the corresponding measured current, which produces tan error that goes into the controller. The modulator will not be required if hysteresis or dead-beat controllers are utilized in the current loop (Babu et al. 2011; Jena et al. 2011). The switching state for the switches in

the power converter is the output from these controllers. In a situation where three PI or PR controllers are employed to generate the duty cycles for the PWM pattern, the need for a modulator will be required.

1) PI Controller: The combinations of PI controller with dq control are widely used, but it is also possible to implement it in ABC frame. in this instance, equation (2.18) represents the transfer function of the controller and the complexity of the controller matrix, due to the important off-diagonal terms that expresses the cross coupling between the phases which is obvious (Blaabjerg et al. 2006). A converter system can convert a sinusoidal waveform to DC through the use of a proportional-integral (PI) compensator, however, for a sinusoidal command to be tracked, the compensator must be of higher order and bandwidth. tracking of sinusoidal voltage or current commands is the main concern in a three-phase VSI system (Yazdani & Iravani 2010; Fukuda & Yoda 2001).

$$G_{PI}^{(abc)}(s) = \frac{2}{3} \cdot \begin{bmatrix} K_p + \frac{K_i s}{s^2+\omega_0^2} & -\frac{K_p}{2} - \frac{K_i s+\sqrt{3}K_i\omega_0}{2\cdot(s^2+\omega_0^2)} & -\frac{K_p}{2} - \frac{K_i s-\sqrt{3}K_i\omega_0}{2\cdot(s^2+\omega_0^2)} \\ -\frac{K_p}{2} - \frac{K_i s-\sqrt{3}K_i\omega_0}{2\cdot(s^2+\omega_0^2)} & K_p + \frac{K_i s}{s^2+\omega_0^2} & -\frac{K_p}{2} - \frac{K_i s+\sqrt{3}K_i\omega_0}{2\cdot(s^2+\omega_0^2)} \\ -\frac{K_p}{2} - \frac{K_i s+\sqrt{3}K_i\omega_0}{2\cdot(s^2+\omega_0^2)} & -\frac{K_p}{2} - \frac{K_i s-\sqrt{3}K_i\omega_0}{2\cdot(s^2+\omega_0^2)} & K_p + \frac{K_i s}{s^2+\omega_0^2} \end{bmatrix} \quad (2.18)$$

2) PR Controller: it is easy to apply PR (proportional resonant) controller in ABC since the controller is already in stationary frame and equation (2.19) below shows the possibility of applying three controllers. For this instance, it is necessary to consider the impact of the isolated neutral in the control; therefore, the third controller is not required in (2.19). Nevertheless, it can be observed that the complexity is reduced significantly in this controller as compared to (2.18) (Blaabjerg et al. 2006).

$$G_{PR}^{(abc)}(s) = \begin{bmatrix} K_p + \frac{K_i s}{s^2+\omega_0^2} & 0 & 0 \\ 0 & K_p + \frac{K_i s}{s^2+\omega_0^2} & 0 \\ 0 & 0 & K_p + \frac{K_i s}{s^2+\omega_0^2} \end{bmatrix} \quad (2.19)$$

3) Hysteresis Controller: It is important to note that in implementing the hysteresis control, an adaptive band of the controller has to be designed to achieve fixed switching frequency. Past literatures discussed the various techniques and algorithms for achieving fixed switching frequency. There is need to consider the isolated neutral again since the output of the hysteresis controller is the state of the switches. in the formula of the hysteresis band (HB), an a' term was included to justify for the load (transformer) connection type, as expressed in (2.20) below (Blaabjerg et al. 2006).

$$HB = \frac{0.25a\prime U_{dc}}{f_{sw}L_T}\left[1 - \frac{L_T^2}{a'^2 U_{dc}}\left(\frac{U_g}{L_T} + \frac{di^*}{dt}\right)^2\right] \qquad (2.20)$$

4) Dead-Beat Controller: The dead-beat controller tries make the error insignificant with one sample delay. The controller in its digital application is as expressed as:

$$G_{DB}^{(abc)} = \frac{1}{b} \cdot \frac{1-az^{-1}}{1-z^{-1}} \qquad (2.21)$$

where a and b are represented as;

$$a = e^{-\frac{R_T}{L_T}T_S} \qquad (2.22)$$

$$b = \frac{1}{R_T}\left(e^{-\frac{R_T}{L_T}T_S} - 1\right) \qquad (2.23)$$

The controller employs one sample time delay since dead-beat controller controls the current in such a way that it can reach its reference at the completion of the subsequent switching period. The delay can be compensated for by employing an observer in the structure of the controller, so that the current reference can be modified to compensate for the delay. The discrete transfer function of the observer is expressed as:

$$F_{DB}^{(abc)} = \frac{1}{1-z^{-1}} \qquad (2.24)$$

therefore, the new current reference is given as:

$$i^{*\prime} = F_{DB}^{(abc)}(i^* - i) \qquad (2.25)$$

As a result, a very fast controller with no delay is achieved. In addition, it is acceptable for microprocessor-based application since the algorithms of the dead-beat controller and observer are quite simple (Mohamed & El-Saadany 2007; Blaabjerg et al. 2006).

2.20 Summary of Grid Synchronization Methods

As regards to the standards in this specialty, the current introduced into the utility network has to be synchronized with the grid voltage. As a result, in distributed power generation systems (DPGSs), the grid synchronization procedure plays a significant part. The control variables such as grid currents with grid voltages using other transformation modules like ABC to dq are synchronized by the synchronization algorithm which produces mainly the phase of the grid voltage vector. Various approaches of extracting the phase angle have been established and shown in many

works till date. The relationship between the major methods used for identifying the phase angle of the grid voltages on various grid conditions was carried out in (Timbus et al. 2005). Benefits and drawbacks in addition to an evaluation of performance were also identified (Blaabjerg et al. 2006).

2.20.1 Grid Voltages Filtering Technique

As shown in Fig. 2.20a and 2.20b below, filtering of the grid voltages in different reference frames such as dq or αβ is an alternative option. The filtering method runs into a huge challenge extracting the phase angle when grid variations or faults arise in the utility network, even though it has been reported as an improved performance over the zero-crossing method. To get the phase angle of the utility voltage in this technique, it involves the use of the arctangent function. A delay is introduced in the processed signal in using filtering generally. It is not adequate in a situation where it is used for extracting the grid voltage angle. Therefore, it is necessary to design a suitable filter (Sangita Nandurkar & Rajeev 2012; Blaabjerg et al. 2006) (Timbus et al. 2005).

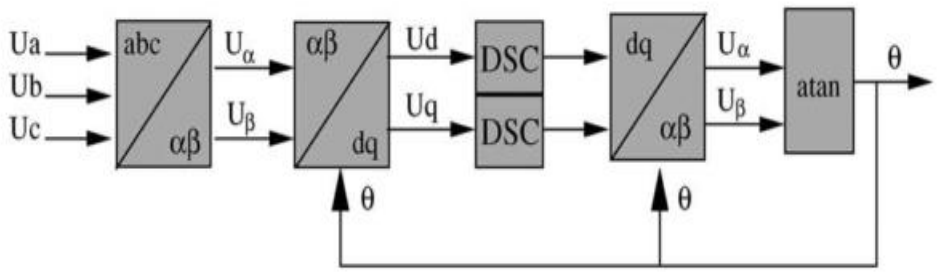

a)

Figure 2.20a Synchronization method using filtering on the dq synchronous rotating reference frame

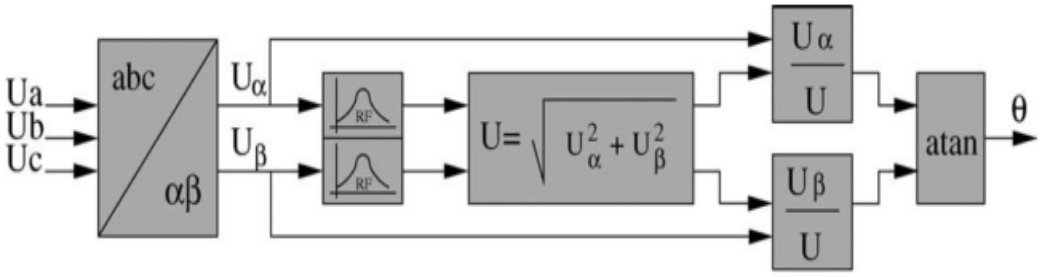

b)

Figure 2.20b: Synchronization method using filtering on the $\alpha\beta$ stationary reference frame

2.20.2 Zero-Crossing Technique

The zero-crossing technique is the easiest to implement among all the methods; Just like the grid voltages filtering technique, performances are also reported not be impressive when applying it, mostly if deviations are registered by grid voltages e.g. harmonics or notches.

2.20.3 PLL (Phase-locked loop) Technique

The PLL technique is the advanced method of extracting the phase angle of the grid voltages in recent times. Grid synchronizations is very essential in grid connected systems. The output frequency and phase of grid voltage is synchronized with grid current using different transformation. There are a number of approaches to extract phase angle which has been established. One signal can track the other when PLL technique is utilized. The output signal is maintained and synchronized with a reference input signal in frequency and phase. PLL can be employed using the dq transformation and adequate loop filter design in a three phase grid-connected system. The PLL is employed in dq synchronous reference frame, which can be seen in the representation in Fig. 2.21 below. It can be observed from this structure that it requires the coordinate transformation from ABC to dq, and by setting the reference to zero, the lock can be achieved. A PI regulator is commonly used to control this variable, and the frequency of the grid is the output from this regulator (Umland & Safiuddin 1990). The utility voltage angle is derived after the integrating the grid frequency and this is supplied back into the αβ to dq transformation block to transform into the synchronous rotating reference frame. This procedure has a better rejection of different types of disturbances such as grid harmonics, notches etc. however, to resolve the problem unbalance in the grid, further improvements have to be made. The second harmonics generated by the negative sequence will transmit through the PLL system when the voltage faults are not balanced and will have an effect on phase angle that was extracted. A number of filtering methods are required to resolve this issue, thus filtering out the negative sequence. The PI loop filter is a low pass filter. It is used to override high frequency component and supply a controlled DC signal to voltage controlled oscillator (VCO) which serves as an integrator. The inverter output frequency that is integrated to get the inverter phase angle ‘θ’ is the PI controller output. PLL becomes active when the difference between grid phase angle and inverter phase angle is decreased to zero leading to synchronously rotating voltages Ud = 0 and Uq which is the magnitude of grid voltage. The three phase dq PLL configuration can therefore evaluate the phase angle of the positive sequence of the grid voltages when there is unbalanced situations

(Sangita Nandurkar & Rajeev 2012; Blaabjerg et al. 2006; Timbus et al. 2005; Pádua 2005).

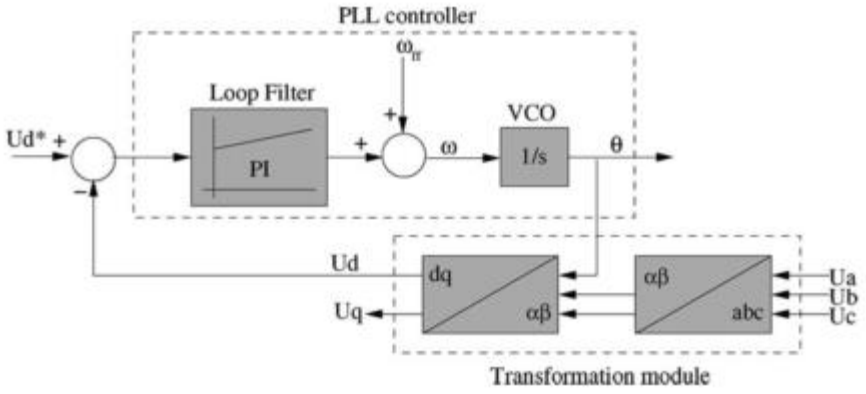

Figure 2.21: Representation of three phase dq PLL method

2.21 Control Structures Evaluation

The key problems of the control configuration employed in synchronous reference frame is the need for voltage feed-forward and cross-coupling terms. The phase angle of the grid voltage is also important in this application. If PR controllers are used for current regulation, it becomes easier to apply the control when the control configuration is employed in stationary reference frame, compared to the configuration employed in dq frame. Besides, the phase angle information is not a requirement, and filtered grid voltages can be used as model for the reference current waveform. The control can be more complex if an adaptive band hysteresis controller is used for current regulation in a situation where the control configuration is employed in natural frame. Alternatively, a less complex control system can be obtained by employing a dead-beat controller (Yoo & Wang 2011). The phase angle information is also optional as it is also the case with stationary frame control. The fact that independent control of each phase can be obtained if grid voltages or three single-phase PLLs are used to create the current reference is evident for this control structure.

2.22 Pulse Width Modulation

The PWM modulators are open-loop voltage controllers, and the commonly used techniques for PWM modulation is carrier based PWM, space vector modulation and random PWM. However, other methods of PWM are included in the classification below. The only technique to be described here will be sinusoidal carrier based PWM, since only this PWM is used in this work.

PWM CLASSIFICATION

There are various techniques of PWM proposed in literature, namely;

- Sinusoidal PWM (SPWM)
- Random PWM
- Minimum ripple current PWM
- Space-Vector PWM (SVM)
- Selected harmonic elimination (SHE) PWM
- Sigma-delta modulation
- Sinusoidal PWM with instantaneous current control
- Delta modulation
- Hysteresis band current control PWM

Conventional inverter utilizes pulse width modulated (PWM) as control strategy. PWM inverters can control their output voltage and frequency at the same time. The harmonic components in the load currents can also be decreased when PWM is implemented. Due to these characteristics, they have become a major practice in several industrial applications such as variable speed drives, uninterruptible power supplies, and other power conversion systems. Although, the major concern is to mitigate the harmonic components in output currents, in order to reduce the influences of electromagnetic interferences or noise and vibrations. In the three-phase inverter, there is significant reduction of the harmonic currents compared to the single-phase PWM inverter. Nowadays, the standard single-phase inverters implement the full-bridge system whereby the power circuits used is approximate sinusoidal modulation technique. Then the three output voltage values are zero, positive (+Vdc) and negative supply dc voltage levels (-Vdc). Hence, the carrier frequency and switching functions determines the harmonic components of their output voltage. Therefore, the harmonic is reduced only to a certain level.

(Selvaraj & Rahim 2009; Park et al. 2003) proposed an inverter topology that uses two reference signals, in place of one reference signal, to produce PWM signals for the switches. A proportional-integral (PI) current control technique is used to maintain the output current sinusoidal, to have high dynamic performance when the atmospheric conditions is changing rapidly and to maintain the power factor close to unity since the inverter is used in a PV system.

2.22.1 Sinusoidal Pulse Width Modulation (SPWM)

The current injected into the grid is filtered by a filtering inductance L_f and it must be sinusoidal with low harmonic distortion. One of the most effective methods used in

producing sinusoidal current is sinusoidal PWM. A high-frequency carrier and a low-frequency sinusoid are compared to achieve sinusoidal PWM, which is the modulating or reference signal. The switches have constant switching frequency due to the constant period of the carrier. the crossing of the carrier and the modulating signal determines the switching constant(Selvaraj & Rahim 2009; Park et al. 2003).

The sinusoidal PWM technique is easy to apply resulting in the widespread use of the technique for industrial converters. The PWM technique of controlling the output voltage is described in Fig. 2.22a below. The basic principle of SPWM is described as the comparison between high frequency isosceles triangular waveform which is the carrier signal and slow-varying sinusoidal waveform which is the modulating signal at the fundamental frequency and the switching points of power devices is determined by the points of intersection of the waves. The periodic waveform of the carrier signal has a period of T_s and varies between −1 and 1. This technique can alternatively be identified as triangulation, sub oscillation or sub harmonic procedure. The pulse widths of Vao wave vary in a sinusoidal way in order to have the fundamental component frequency average and the modulating signal frequency to be equal and its amplitude is proportional to the command modulating voltage (Reznik 2012; Yazdani & Iravani 2010; Marwali & Keyhani 2004). The same carrier wave can be used for all three phases, as shown on Figure 2.22b and 2.22c below.

The PWM process is shown in Figure 2.22 below, where the switch has its switching function defined as:

s(t) = 1, if the switch is commanded to conduct
s(t) = 0, if the switch is turned off.

Therefore, as Figure 2.22c shows when the modulating signal is greater than the carrier signal, a turn-on command is issued for one switch, and the turn-on command is cancelled for the other switch. The reverse of this happens when the modulating signal is lesser than the carrier signal. However, when a switch is ordered to turn on, it does not imply that it has to conduct; the switch conducts on the condition that the turn-on command is provided and the current direction agrees with the characteristics of the switch. For instance, an IGBT can only conduct when the current flow is from the collector to the emitter, in response to a turn-on command.

Similarly, the periodic saw-tooth waveform can also be used as a carrier signal. Although, for high-power converters, a triangular carrier signal is frequently used (Panda et al. 2009; Yazdani & Iravani 2010).

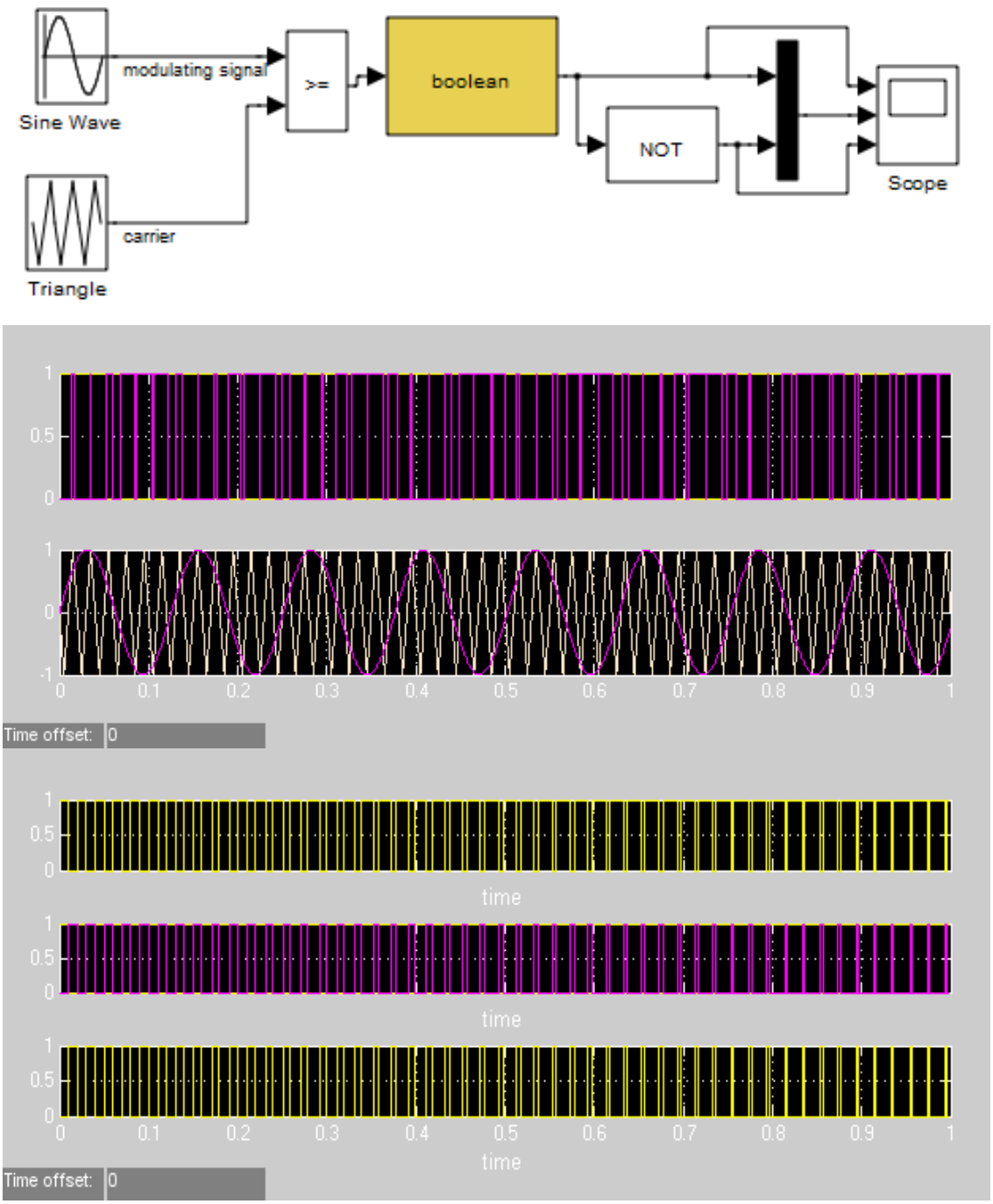

Figure 2.22a: Schematic representation of the mechanism of generating PWM gating pulses for inverter switches in Simulink

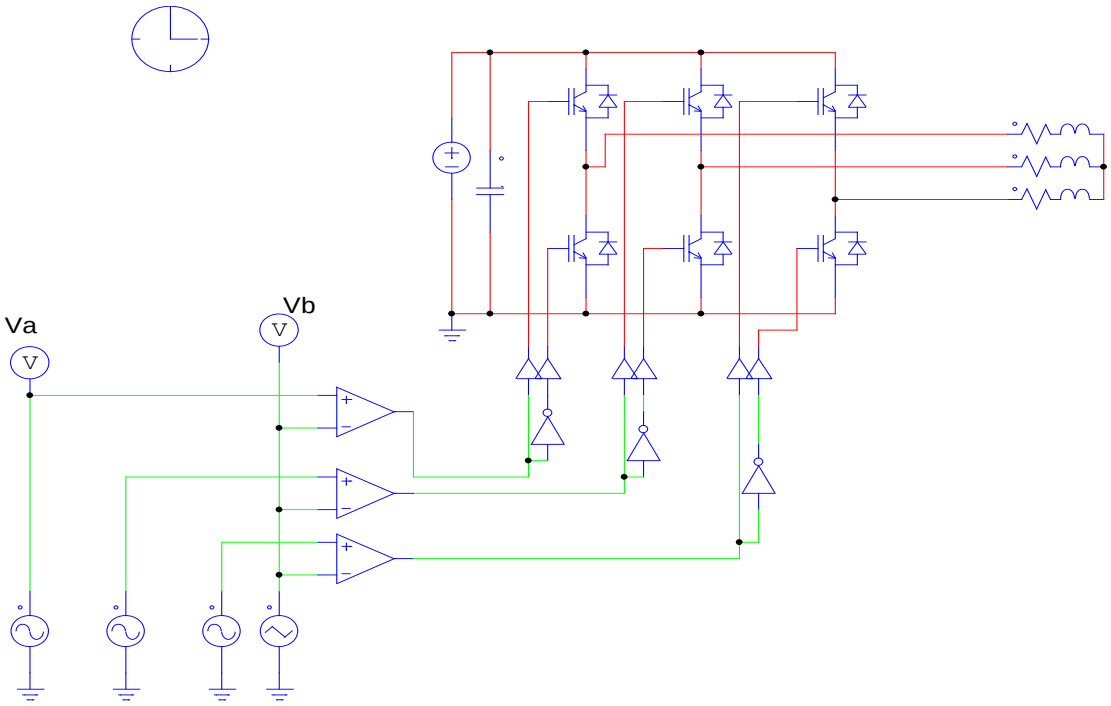

Figure 2.22b: Three-phase VSI system with SPWM

The maximum output voltage in the linear region when modulation index q is between 0 and 1 for SPWM is:

$$V_{LL} = \frac{\sqrt{3}}{\sqrt[2]{2}} = 0.612V_{DC} \qquad (2.26)$$

$$m = \frac{V_p}{V_T} \qquad (2.27)$$

Where V_p peak value of the modulating wave and V_T peak value of the carrier wave

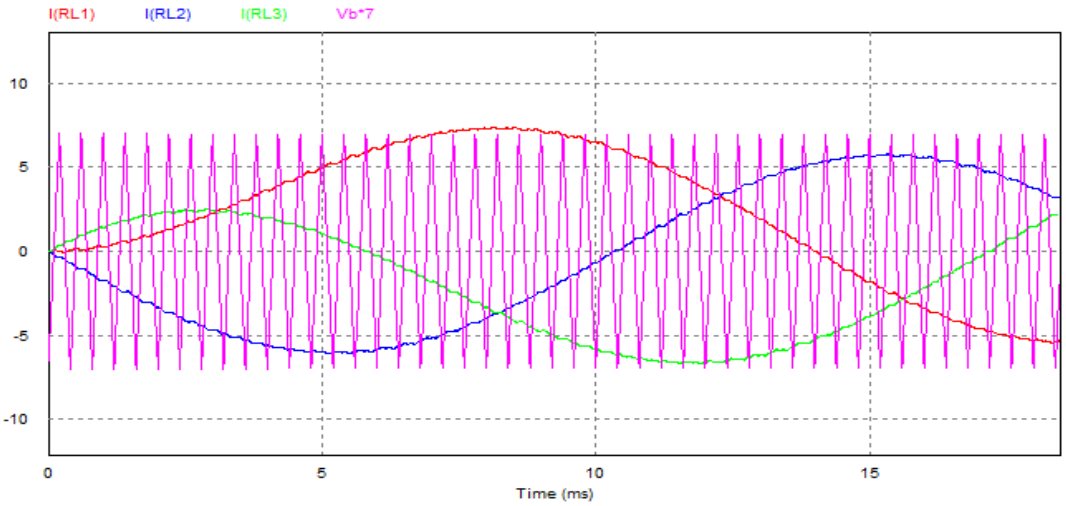

Figure 2.22c: Sinusoidal PWM for three phase VSI

2.23 Power Quality Issues

The power quality at the point of common coupling (PCC) and DGs can be affected because of the presence of several power electronic devices such as reactive local loads and local loads that are nonlinear or unbalanced. However, the stability and economical operation of GCIs are dependent on the power quality of DGs and MGs. Moreover, in the nearest future, the quality of the electricity sold to the utility will determine the price of electricity in a competitive electricity market. Therefore, the power quality of DGSs and MGs will directly proportional to the price of electricity sold, resulting to their economic benefits being affected. The stability of GCIs will be affected immensely by the power quality at PCC. The nonlinear loads are the main cause of distortion of PCC voltage because the GCIs are usually connected to the secondary side of the transformers. This distorted voltage will directly deteriorate the voltage and current control loops of a GCI, resulting to distorted current. This can also result to unplanned trip off of the GCI in some critical situations. Also, from the electric power system perspective, power quality problems may lead to further loss and power equipment may overheat, sensitive loads faults, boring noises from torque oscillations of electric machines and the interference of communication network (Zeng et al. 2013).
All the deviations produced by the interface between the grid and its customers from the ideal supply features are related by power quality. The PV generation has a huge impact on the distribution system because an increase in disturbance emissions will have direct effect on the local performance of the network with the probability of transmitting to higher levels if they are not kept under safe conditions. The impact of low emissions should result in minor losses, possibility of false tripping is minimized, lifecycle of the equipment is prolonged or the damage for some parts of the system is avoided (Craciun et al. 2012).

2.24 Anti-Islanding

Islanding is defined as the continued operation of a distributed generation unit while the grid is tripped arising from fault conditions in the grid or for maintenance purposes (Reznik 2012). In (Salam et al. 2010; Craciun et al. 2012) which explained Islanding as a situation when the PV generation is disconnected from the grid but continues to power locally, i.e. there is no interruption in the generation of energy to the loads connected to the islanded part. The islanding problem is dominant in LV networks, therefore, it is recommended for the generation units to disconnect at a frequency band of 49 Hz to 51 Hz. Islanding that occurs when the grid line fails but the connected photovoltaic system is still in operation, is dangerous to the personnel and equipment that is required to be detected and prevented (Massawe 2013).

Unintentional islanding of the inverter system is not desirable because it can damage equipment which remains connected to the inverter, and it can lead to dangerous situations since the grid may be assumed to have disconnected (Reznik 2012).When unintentional islanding occurs whereby a portion of the area EPS (Electric power system) is being energized by the distributed resource through the PCC. The DR interconnection system will detect the islanding operation and stop to energize the area EPS within 2s of formation of Island (IEEEStandards 2009).

However, the grid no longer regulates the voltage during the islanding mode, since the system is disconnected from the main grid. As a result, there is the need for an inverter control scheme to actively regulate the local voltage (Salam et al. 2010).

2.25 Conclusion

The literature involved in this research has been given in this chapter. The inverter topologies have been reviewed. The different control algorithms and filter topologies, which are available for inverter, have also been discussed. The following chapter will discuss fundamental inverter configurations in power electronics and the switching technologies for inverter.

CHAPTER 3

POWER ELECTRONICS TECHNOLOGY

3.1 Introduction

All through the past number of years, two major causes have influenced the fast development of power electronics. One of the major causes is the improvement of fast semiconductor switches, which are capable of fast switching and high power conduction. The introduction of real-time computer controllers that can implement advanced and complex control systems is another major influence in the development of power electronics. These factors have resulted to the development of economical and grid-friendly converters

Power electronic converters have been used widely for domestic, industrial, and information technology applications. However, over the past few years, their application in power systems has significantly increased due to advancement in power semiconductor and microelectronics technologies. As a result, the use of power-electronic converters in power conditioning, compensation, and power filtering applications is rising gradually.

A power electronic converter comprises of a power circuit and a control or protection system. On the other hand, the power circuit can be achieved through different types of configurations of power switches and ancillary components. The power circuit and the control system are connected through gating or switching signals and feedback control signals. Therefore, the transfer of energy in a converter system is achieved through adequate switching of the semiconductor switches by the control scheme, based on the total performance that is needed, the regulatory commands, and the feedback from a host of system variables (Yazdani & Iravani 2010; Satoh & Yamamoto 2001).

3.2 Power Electronic Converter Systems

Power electronic converter can be defined as a circuit with multiport that is composed of semiconductor switches and can also consist of auxiliary components and apparatus, such as inductors, capacitors, transformers etc. The role of a converter is mainly to allow the exchange of energy between two or more subsystems, in accordance to the required performance conditions. The subsystems often have different characteristics in terms of voltage or current waveforms, phase angle, number of phases and frequency and thus can only be interfaced through power-electronic converters. In the case of wind turbine or generator unit, a power-electronic converter is required as an interface, i.e. an electromechanical subsystem that produces variable-

frequency or variable voltage electricity, with the constant-frequency or constant-voltage utility grid.

Converters are generally classified depending on the type of electrical subsystems that they interface that is, AC or DC according to technical literature. Hence, a DC to AC converter interfaces a DC subsystem to an AC subsystem, a DC to DC converter interfaces two DC subsystems and an AC to AC converter interfaces two AC subsystems (Mohan & Undeland 2007).

The conventional diode-bridge rectifier is an example of an AC to DC converter. An AC to DC converter is called a rectifier if the flow of average power is from the AC side to the DC side. Otherwise, the converter is known as an inverter if the average power flow is from the DC side to the AC side. Some types of DC to AC converters have the capability to transfer power in bidirectional mode, precisely; they can operate either as an inverter or as a rectifier. However, the diode-bridge converter can only operate as a rectifier.

The DC to DC converter can also be referred to as DC converter while the AC to AC can be identified as an AC converter. A DC converter can interface two DC subsystems directly, or it can use an intermediate AC link. For the second scenario, the converter comprises of two consecutive DC to AC converters, which are integrated through their AC sides. Likewise, an AC converter can be direct, such as the matrix converter, or it may implement an average DC link. The implementation of DC link consists of two consecutive DC to AC converters, which are integrated through their DC sides. This type is also referred to as AC to DC to AC converter, which is commonly, used in AC motor drives and variable-speed wind-power conversion systems (Gidwani et al. 2013).

3.2.1 Applications of Power Electronic Converters in Power Systems

In the past, there were limitations in implementation of high-power converter systems in electric power systems to high-voltage DC (HVDC) transmission systems and limitation is even higher with the typical static VAR compensator (SVC) and electronic excitation systems of synchronous machines. However, for electrical power systems over the past 2 decades, applications to generate, distribute, transmit and supply of electric power have been increasing constantly. Fast and continuous improvements in power electronics technology and the various types of semiconductor switches for high-power applications, which are easily obtainable, have been the major factors. Advanced signal processing and control methods and the corresponding techniques for several applications have been accomplished through continuous advancements in microelectronics technology.

Problems such as power line congestion are solved using power electronic-based equipment, which is needed in restructuring trends in the electric utility sector.

Constant increase in energy demand has led to the use of the electric power utility structure to almost reach the limit, therefore to improve stability there is the need for the utilization of electronic power device.

In order to deal with the problems of global warming and other environmental issues linked with centralized power generation has resulted to the drift toward additional application of renewable energy. The drift has gained more attention due to modern technological advancements and has led to economic and technical sustainability of renewable energy resources. Electric power system are used to interface these energy resources through power electronic converters., development of operational models and strategies which are still new, such as micro grids, smart grids and active networks also shows that there will considerable growth in the performance and significance of power electronics in electric power systems (Su et al. 2011; Braun 2007).

Improvement of efficiency and reliability of the power generation, transmission, distribution, and structure for delivery, huge renewable energy resources and storage systems integration to electric utility grids, integration of distributed energy resources (distributed generation and distributed storage units) at sub-transmission and distribution voltage levels majorly, maximum increase in the rate of penetration of renewable energy sources are some of the anticipated prospective functions of power-electronics converter systems in power systems (Pouresmaeil et al. 2013; Yazdani & Iravani 2010).

In electric power systems, power electronic converter systems are used for;

Active Filtering: The major role of a power electronic-based active filter is to produce and inject or receive definite amount of current or voltage components in order for the power quality to be improved in the host power system (Li et. al 2011).

Compensation: increase in power-transfer capability of the line, maximization of the power transfer efficiency, voltage and angle stability improvement, power quality enhancement, or to achieve a combination of the above-mentioned aims, are some of the roles of a power-electronic (static) compensator, in a transmission or distribution line. According to flexible AC transmission systems (FACTS) and custom-power controllers several static compensation methods have been discussed at length in the technical literature (Song & Johns 1999). Some of The FACTS controllers are the semiconductor-controlled phase shifter, the static synchronous series compensator (SSSC), the static synchronous compensator (STATCOM), the intertie power flow controller (IPFC) and the unified power flow controller (UPFC).

Power Conditioning: The role of an electronic power conditioner is primarily to facilitate the exchange of power between two electrical or electromechanical

subsystems in a controlled mode. The power conditioner has to check that specific requirements of subsystems are met regularly. Such requirements include voltage magnitude, frequency, power factor, and velocity of rotating machines.

Some of these electronic power conditioning systems are;

- The DC to AC converter system: DC power transfer from a DC distributed energy resource (DER) system such as the photovoltaic (PV) solar array, a battery storage unit, or a fuel cell to the grid.
- The AC to DC to AC converter system: AC power transmission from a variable-frequency wind-power unit to the utility grid.
- The HVDC rectifier or inverter system: it conveys electrical power through a DC tie line between two electrically isolated AC subsystems.

3.3 Semiconductor-Device Technology

The reliability and performance of power-electronic applications have recently improved due to the power semiconductor devices that are more obtainable, improved electrical quality and cheaper cost since factors such as size, weight and price of the complete power electronics interface implemented in RES depends on the performance of the device (Carrasco et al. 2006). One of the most popular component used for power electronics and also for renewable energy applications of recent is the insulated gate bipolar transistor (IGBT). The inverter topologies have improved from the use of large thyristor grid connected inverter configurations to smaller IGBT configured inverters due to the advancement in transistors used as switches. These transistors are configured to allow increase in the power switching frequency in order to extract more energy and satisfy the connecting standards. The standards also requires that the inverters must be able to detect an islanding condition and take applicable measures in order to safeguard persons and equipment (Verhoeven & KEMA 1998) . In this condition, the grid has been disconnected from the inverter, and continues to supply the local loads. PV cells can either be used as isolated power supplies or grid connected applications. The applications of PV energy are shown in the Fig. 3.1 show.

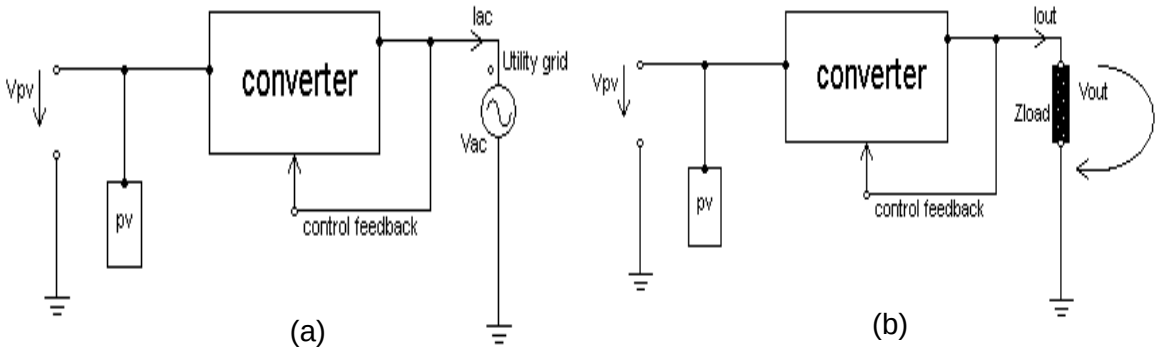

Figure 3.1: PV energy applications. (a) grid-connected application (b) power supply application

(Carrasco et al. 2006)

3.3.1 Power Semiconductor Switches

The main components that make up the power electronic converters are the Power electronic semiconductor switches. They are implemented in power electronic converters in form of conditions to turn on and off switches and aid the conversion of power from ac to dc (rectifier), dc to ac (inverter), dc to dc (chopper) and ac to ac at the same (ac controller) or different frequencies (cycloconverter). A power electronic semiconductor switch is a device that can allow and disturb the current flow by applying a gating signal through the host circuit branch. This is different from the mechanical switch operation in which the on and off transition is realized through a mechanical method, such as the mechanical arm movement. A switch that is mechanical is not planned to switch repeatedly due to its slow mode. This basically includes moving parts leading to lifetime loss during each switching action and it provides a limited number of on and off operations, compared to an electronic switch. It also injects fairly low power loss while it is conducting, such that it can almost be represented practically as an ideal switch.

On the other hand, an electronic switch is fast and proposed for continuous switching and does not include any moving part and therefore, no lifetime loss is experienced during turn-on and turn-off modes; leading to switching and conduction power losses.

Combining both mechanical and electronic switches can provide an optimum solution in terms of switching speed and power loss for some applications according to the characteristics of the mechanical and electronic switches mentioned above. However, the drift towards the development of power semiconductor switches is due to the continuous increase in the use of electronic switches. the focus of most research and development programs of the power semiconductor switch industry is the determination

to increase the maximum acceptable switching frequency and to reduce switching and conduction losses (Yazdani & Iravani 2010). The switching mode power conversion yields high efficiency, however the drawback is that there is generation of harmonics at both the supply and load sides due to the nonlinearity of switches, they are non-ideal switches and they have conduction, turn-on and turn-off switching losses (Bacha et al. 2013). Some of the common applications of converters are; heating and lighting controls, dc and ac motor drives, static VAR generation, ac and dc power supplies, electrochemical processes and active harmonic filtering. In order to design efficient, reliable and cost effective systems with the best performance, even though the cost of power semiconductor devices in power electronics equipment may hardly exceed 2% to 3%, the total cost and performance of the equipment may highly be determined by the features thoroughly. It is worth noting that the present technology advancement in power electronics has generally been influenced by the development of power semiconductor devices. The knowledge of power device components, processing, manufacturing, packaging, modelling and simulation has been greatly influenced by the improvement of microelectronics. Modern power semiconductor devices are mostly made up of silicon material (Eltamaly 2012; He et al. 2011; Bose 2002).

3.4 Classification of Switch

It is essential to discuss briefly on the types of switches as the behaviour of a power-electronic converter mainly depend on the type of its semiconductor switches.

3.4.1 Uncontrollable Switches

The only uncontrollable switch available is the power diode and it is a two-layer semiconductor device. The current conduction and disturbance periods are determined by the host electrical circuit, which makes the switch uncontrollable. Power diodes are widely used in power-electronic converter circuits either as separate components or as basic parts of other switches (Yazdani & Iravani 2010). Power diodes are used for uncontrolled rectification of power and are also utilized in applications such as electroplating, welding, anodizing, variable frequency drives, battery charging and dc and ac power supplies. Additionally, they are used for feedback and freewheeling roles in converters and snubbers. The power diode usually has a P-I-N structure, which is a P-N junction with a semiconductor layer (I-layer) in the middle close to intrinsic to tolerate reverse voltage. The symbol for diode and its volt-ampere characteristics is illustrated in the Fig. 3.2 below. The diode can be represented by A junction offset drop and a series-equivalent resistance that gives a positive slope in the V-I characteristics can be used to represent a diode in forward-biased condition. The typical forward conduction drop is usually 1.0 V. the drop will lead to conduction loss and the device

must be cooled by a suitable heat sink to limit the junction temperature. In the reverse-biased condition, there is a small leakage current flow which increases steadily with voltage due to minority carriers. The device goes through avalanche breakdown when the reverse current becomes higher if the reverse voltage goes beyond a threshold value (breakdown voltage), leading to large power dissipation in the junction and the diode being destroyed by heating (Buticchi et al. 2012; Bose 2002).

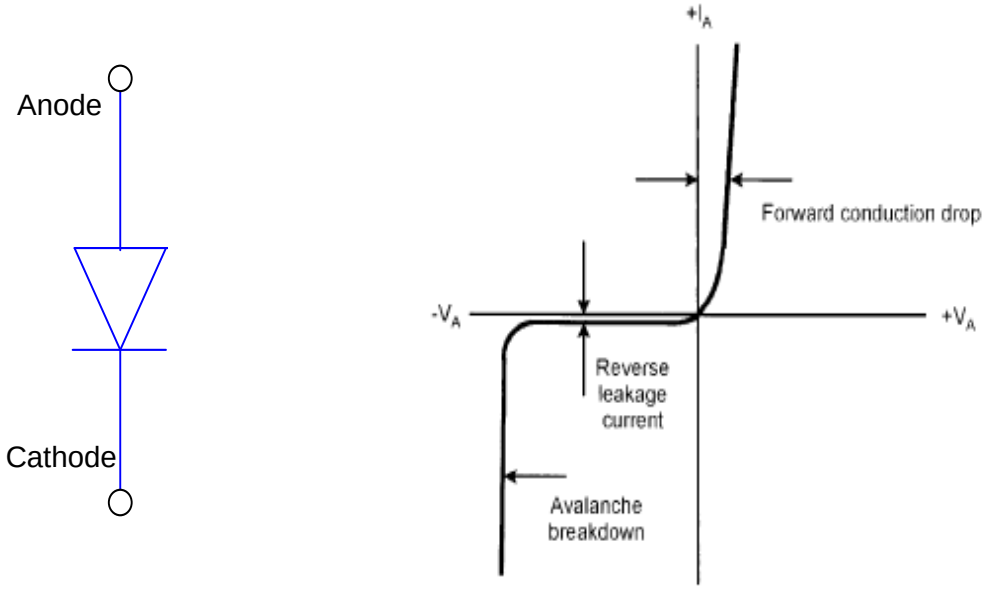

Figure 3.2: Diode symbol and volt-ampere characteristics

3.4.2 Semi-controllable Switches

The thyristor or the silicon-controlled rectifier (SCR) is the commonly used semi-controllable electronic switch. The thyristor is a four-layer semiconductor device that is semi-controllable, and on the condition that the device is voltage biased correctly, then the only period at which its current conduction starts can be determined by a gating signal. However, the host electrical circuit determines the current disturbance period of the thyristor. even though fully controllable switches have also been considered and utilized for HVDC applications in recent times, the thyristor is usually used for HVDC converters (Yazdani & Iravani 2010). The traditional pillars for bulk power conversion and control in industry used to be the thyristors. The introduction of this device in the late years of 1950 brought about the modern power electronics. The word “thyristor” was gotten from thyration which corresponds to the gas tube. It usually comprises of the SCR, IGCT, triac, MCT and GTO. The classes of thyristors are standard or slow phase-control-type and fast-switching voltage-fed inverter-type. The inverter-type has become obsolete in recent times. The thyristor symbol is shown in Fig. 3.3 below. It is

essentially a three-junction P-N-P-N device, and the P-N-P and N-P-N component transistors are connected in regenerative feedback mode. The device blocks voltage in both forward and reverse directions known as symmetric blocking. The device conducts when the anode is positive, but the gate loses its control to turn off the device the moment the device starts conducting. A thyristor can also be turned on by extreme anode voltage, rate of voltage increase ($^{dv}/_{dt}$), by an increase in junction temperature(T_j) or by the light shining on the junctions. Present thyristors are obtainable in very huge voltage and current ratings. Emitter current is induced into the component transistors leading to switching mode, when forward voltage is applied across a device firstly, then the off-state or static $^{dv}/_{dt}$ forms displacement current in the depletion layer capacitance of the central junction. The device can be damaged by the concentration of heavy current when the anode current $^{di}/_{dt}$ is too much resulting from the turn-on of the device. There is large conduction loss in a thyristor just like a diode, but the switching loss is quite small (Bose 2002).

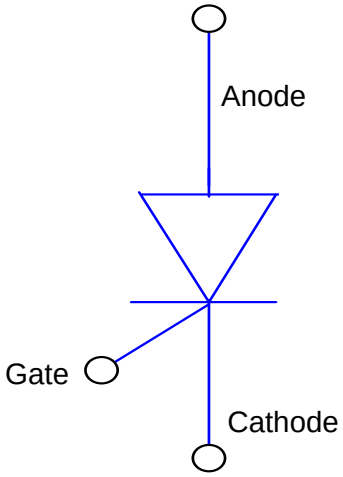

Figure 3.3: Thyristor symbol

3.4.3 Fully Controllable Switches

The gating command determines the current conduction and disturbance times of a fully controllable switch. The types of fully controllable switches that are commonly used are;

Metal Oxide Semiconductor Field Effect Transistor (MOSFET):

The power MOSFET is a three-layer semiconductor device. The current and voltage ratings of power MOSFETs are quite limited when compared to other fully controllable power switches. Thus, the application of power MOSFETs is limited to fairly lower power converters where the major condition is a high switching frequency (Yazdani &

Iravani 2010). A power MOSFET is a unipolar, majority carrier, “zero junction”, voltage-controlled device compared to other semiconductor devices. The Fig. 3.4 below depicts the symbol of an N-type MOSFET. An N-type conducting channel will be induced if the gate voltage is positive and more than the threshold value, therefore allowing current flow by majority carrier (electrons) between the drain and the source. The operational gate-source capacitance will require a pulse current during turn-on and turn-off even though the gate impedance is exceptionally high at steady state. The device has the ability to block voltage in asymmetric mode, and has an integral body diode which can transmit full current in the reverse direction as represented. The diode is categorised by slow recovery and an external fast-recovery diode is usually used to bypass in high-frequency applications. It is worth noting that conduction resistance of MOSFETs tend to be reduced by the modern trench gate technology. Parallel operation of MOSFET is much easier due to the positive temperature coefficient of this resistance. Huge MOSFETS are actually made-up by parallel connection of many devices. The conduction loss of a MOSFET is quite large for higher voltage devices but its turn-on and turn-off switching times are very small leading to minimal switching loss. The device does not have the minority carrier storage delay issue related with a bipolar device. The capability of the drive to charge and discharge a small input basically determines its switching times. A MOSFET is usually driven by a current source dynamically followed by a voltage source even though it can be statically controlled by a voltage source. In order to reduce switching delays, the common practice is to drive it by a current source dynamically followed by a voltage source. MOSFETs are commonly used in low-voltage, low-power and high-frequency switching applications such as switching mode power supplies (SMPS), brushless dc motors (BLDMs), solid-state dc relays and stepper motor drives (Bose 2002).

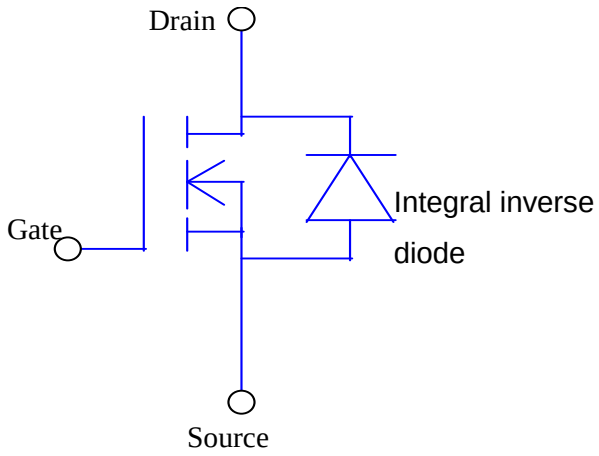

Figure 3.4: MOSFET symbol

Gate Turn Off Thyristor (GTO):

The structure of GTO device consists of a four-layer semiconductor and the external gating signals can be used to turn on and turn off the device. A small positive gate current pulse is required to turn on the device while a fairly high, negative current pulse is needed to turn off the GTO. This condition calls for a complex drive scheme. The diversion of PNP collector current by the gate has led to the ability of a GTO to turn-off, therefore the regenerative feedback effect of the PNP and NPN is broken. GTOs are obtainable with ability to block voltage in asymmetric and symmetric mode, which are used in voltage-source converters respectively. The turn-off current gain of a GTO, which is very small usually 4 or 5, is referred to as the ratio of anode current before turn-off to the negative gate current needed for turn-off. For example, a 6000 A GTO will need as large as 1500 A gate current pulse. However, the period of the pulsed gate current and the equivalent energy related to it is small and can be produced by low-voltage power MOSFETs easily. Some of the applications of GTOs whose symbol is represented in Fig. 3.5 below can be found in static VAR compensators (SVGs), motor drives and ac to dc power supplies with high power ratings. The introduction of large-power GTOs displaced the force-commutated, voltage-source thyristor inverters (Bose 2002).

Though in the past years, the GTO used to be the preferred switch for high-power applications among the fully controllable switches. However, the IGBT has also overthrown the use of GTO in recent times (Yazdani & Iravani 2010).

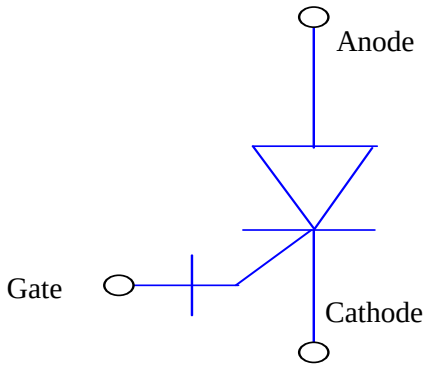

Figure 3.5: Symbol of a GTO

Integrated Gate-Commutated Thyristor (IGCT):

The IGCT is simply a GTO switch with reduced turn-off drive requirements both theoretically and structurally. Furthermore, the IGCT switches faster compared to the

GTO and also have a lesser on-state voltage drop. Due to the voltage and current handling abilities of the IGCT, it has gained significant consideration for high-power converters in the past few years (Yazdani & Iravani 2010). It was also mentioned in (Bose 2002) that The IGCT was presented by ABB in 1997 and is one of the most recent member of the power semiconductor family at this time. It is essentially a high-voltage, high-power, hard-driven, asymmetric-blocking GTO with turn-off current gain as unity. For instance, a turn-off negative gate current of 3000 A is needed by a 4500 V IGCT with a controllable anode current of 3000 A. Several MOSFETs connected in parallel with ultra-low leakage inductance in the drive circuit can provide such a gate current pulse of very short period and very high di/dt which has low energy content. The device component holds the built-in gate drive circuit. The device is made of an integrated anti-parallel diode. Compared to the GTO, the conduction drop, turn-on *di/dt*, gate driver loss, minority carrier storage time, and turn-off *dv/dt* of the device are presumed to be greater. Faster switching of the device allows operation without snubber and switching frequency higher than that of the GTO. For higher power applications, series or parallel connection of several IGCTs can be employed. The device has been used in power system inter-connected installations and medium power up to 100 MVA and 5 MW industrial drives respectively.

Insulated Gate Bipolar Transistor (IGBT):

The IGBT is also a semiconductor device consisting of three layers. Since about 2 decades ago, the power IGBT has considerably developed with respect to the switching frequency, current rating and the voltage rating. it is used for a wide range of applications in electric power systems at the moment (Yazdani & Iravani 2010). One of the most significant innovative in the history of power semiconductor devices was the introduction of insulated gate bipolar transistors (IGBTs). They are devices which are commonly used in power electronics of medium power ranging from a few KWs to a few MWs and are widely utilized in dc to ac drives and power supply systems (Baliga 2001). They overthrew BJTs in the upper power range, and are getting rid of the GTOs in the lower power range at the moment. An IGBT exhibits the benefits of both a MOSFET and BJT which is essentially a hybrid MOS-gated turn-on and turn-off bipolar transistor. The basic structure of an IGBT and the device symbol are shown in Fig. 3.6 below. Its structure is basically similar to that of a MOSFET, except an additional positive P layer has been included at the collector instead of the negative drain layer of the MOSFET. The IGBT has the high-input impedance characteristics of a MOSFET but conduction characteristics of a BJT. An N-channel is induced in the P region if the gate is positive in relation to the emitter. This forward-bias the base-emitter junction of the PNP transistor, turning it on and leading to conductivity modulation of the negative

region, which reduces the conduction drop considerably compared to that of a MOSFET. The driver MOSFET in the corresponding circuit of the IGBT transmits most of the total terminal current at on state. The thyristor-like latching action as a result of the parasitic NPN transistor is avoided by adequately minimizing the resistivity of the positive layer and averting most of the current through the MOSFET. To turn off the device, the gate voltage is decreased to zero or negative, thereby the conducting channel in the P region is shut off. The current density of the device is greater than that of a BJT or MOSFET. Its input capacitance C_{iss} is considerably smaller compared to that of a MOSFET. The ratio of gate-emitter capacitance is also lesser, resulting to an improved Miller feedback effect. The present IGBT uses trench-gate technology to further decrease the conduction drop. However, a snubber is optional when designing the IGBT converter (Wu 2006; Bose 2002).

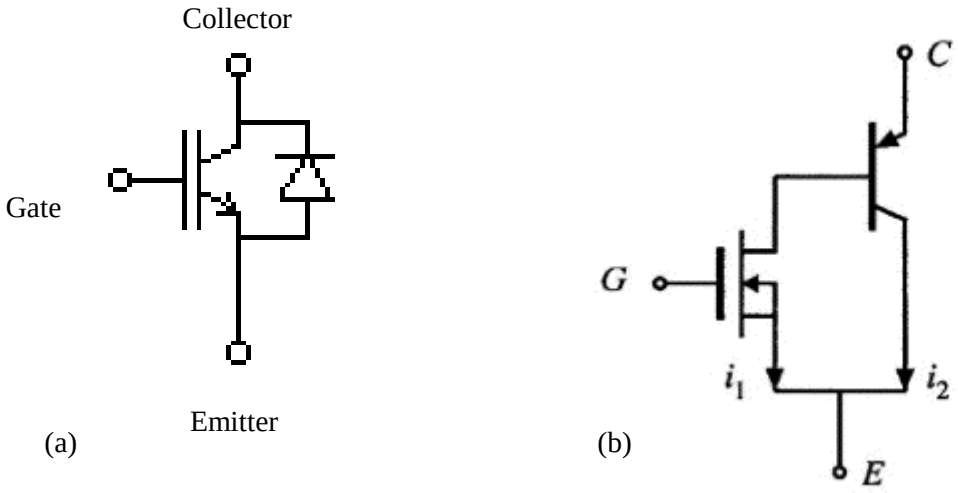

Figure 3.6: The IGBT; (a) the schematic symbol (b) Equivalent circuit (Erickson 2000)

For high-power applications, the IGBTs that are competing with the gate turn-off thyristors (GTOs) are presently advanced technology turn-on components improved to a very high power (6 kV - 1.2 kA). The GTO is converted into a new high-performance component with a large safe operation area (SOA), lower switching losses, and a short storage time by an integrated gated control thyristor (IGCT) which is developed as a mechanical integration of a GTO with a delicate hard drive circuit recently. Some of the comparison between IGCT and IGBT are stated below(Carrasco et al. 2006).

- The switching frequency of the IGBTs is higher than IGCTs, so they introduce less distortion in the grid.
- IGBTs are manufactured in form of modular devices. The silicon is isolated to the cooling plate and for reduced electromagnetic emission; it can be connected to ground

with high switching frequency. The base plate of this module is built from a distinct material that has almost the same thermal behaviour as silicon leading to slightest thermal stress. This increases the lifetime of the device by ten folds approximately. In contrast to the IGBTs, IGCTs are manufactured like disk devices. a cooling plate is used to cool them by electrical connection on the high-voltage side. This will result into high electromagnetic emission that is a major concern. Another approach is the number of permitted load cycles. The silicon chip will continuously experience mechanical stress by Heating and cooling the device which can damage the device.

- The major benefit the IGCTs have is that they have a lower voltage drop during ON-state, which is approximately 3 V for a 4500 V device. The power dissipation for such instance will be 2400 W per phase for a 1500 kW converter due to the voltage drop. However, for the IGBT, the voltage drop is higher compared to the IGCTs. The power dissipation due to the voltage drop for a condition of 1500 kW will be 5 kW per phase for a 1700 V device having a drop of 5 V. In summary, with the recent semiconductor technology, for renewable energy applications and converters, IGBTs generally have more benefits compared to the IGCTs.

The semi-controllable and fully controllable switches can be categorized into the following with respect to their voltage and current handling capability:

3.4.4 Unidirectional Switch: A unidirectional switch has the ability to conduct current in only one direction. Thus, the switch turns off and adopts a reverse voltage when it's current reaches zero and tries to go negative. The unidirectional switch can either be bipolar (symmetrical) or unipolar (asymmetrical). A bipolar switch can tolerate a moderately high reverse voltage. An example of a bipolar switch which is unidirectional is a thyristor. On the other hand, a unipolar switch has a comparatively low reverse breakdown voltage resulting in a reverse in-rush current that can destroy the switch when the voltage is more than the switch reverse breakdown voltage. Therefore, a diode can be connected in antiparallel with the unipolar switch which also makes the switch reverse conducting to avoid the reverse breakdown and the damage caused. The GTO and the IGCT can both be obtained in form of unipolar and bipolar types commercially. A current source converter (CSC) usually needs bipolar, unidirectional switches (Yazdani & Iravani 2010).

3.4.5 Reverse Conducting Switch: to achieve a reverse-conducting switch, unidirectional switches which can either be unipolar or bipolar is connected in antiparallel with a diode. A reverse-conducting switch is therefore known as a unipolar switch whereby the reverse breakdown voltage is almost the same with the forward voltage drop of a diode. The reverse-conducting switch is thus reverse biased by fairly low volts when

the switch begins to conduct in the reverse direction. Some of the types of reverse-conducting switches are the power MOSFET, the IGBT and the Reverse conducting IGCT switches which are obtainable commercially. The figure of the fully controllable reverse-conducting switch, which is also commonly regarded as a switch cell is shown in Fig. 3.7 below. The VSI requires reverse-conducting switches. The symbolic illustration of a switch cell where the gate control terminal is hidden is represented in Fig. 3.7 (b) below.

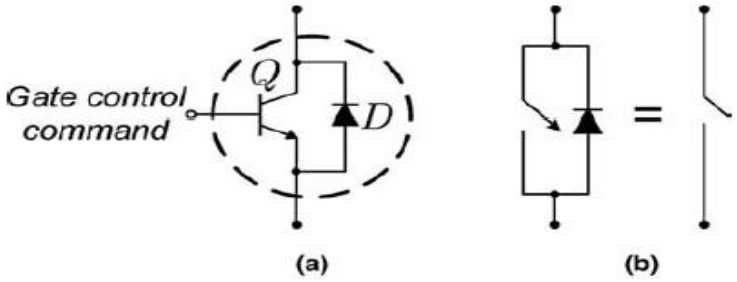

Figure 3.7: a) basic representation of a switch cell. b) Symbolic illustrations of a switch cell

3.4.6 Bidirectional Switch: A bidirectional switch can conduct and stop the flow of current in both directions. Furthermore, a bidirectional switch when in the off state, it must tolerate both forward and reverse voltage biases which is basically a bipolar switch. Two thyristors that are connected in antiparallel can be regarded as an example of a semi-controllable bidirectional switch. It is important to note that there is no fully controllable bidirectional single-device switch technology. Therefore, to achieve such switching technology, two bipolar unidirectional switches are connected in antiparallel. Application of fully controllable bidirectional switch can be found in matrix converters.

3.5 Voltage Source Inverters (VSI)

This thesis will focus on modeling and control of the VSI system and the most common VSI system configurations are enumerated. As found in (Bose 2002), it explained the voltage source converter as a device which receives DC voltage at the source and converts to an AC voltage on the load side. Depending on the application the AC voltage can either be constant or variable. The converter circuit can operate as either inverter or as a rectifier. A voltage source inverter should have a constant voltage source at the input. An inverter can require a large capacitor to be connected at the input to make the source voltage inflexible. The dc voltage which can be obtained from solar photovoltaic array can either be constant or flexible. The output of the inverter can be single phase or multiphase and the wave form at the output can have square wave,

sine wave, PWM wave or stepped wave (Beser et al. 2010). Due to the DC voltage at the converter input, the power semiconductors conduct in forward-biased. Therefore the use of IGBTs and other devices such as MOSFETs, IGCTs, BJTs and GTOs are preferred because of their asymmetric blocking capability. In the past, the forced commutated thyristor converters were used before they became outdated. There is a free reverse current when a diode is connected to the device. It is important to know that the AC generated voltage wave is not affected by the load factors in a voltage source converter. Some of the applications in which voltage source inverters are being used are;

- AC power supply from PV array or battery
- AC uninterruptible power supply (UPS)
- Active harmonic filter
- Induction heating
- AC motor drives
- Static VAR generator (SVG) or compensator

3.6 Fundamental Configurations

3.6.1 Single Phase Inverters

Half-Bridge Inverter

The half-bridge single-phase, two-level VSI is known as one of the simplest inverter configurations as shown in the Fig. 3.8 below. The circuit is made up of a pair of semiconductor devices connected in series across the dc supply(Bose 2002). The half-bridge VSI comprises of an upper switch cell and a lower switch cell. Each of the switch cells is made of an entirely controllable, unidirectional switch connected in antiparallel with a diode. This switch configuration creates a reverse-conducting switch that is found easily, such as it is the case in commercial IGBT and IGCT. A DC source, a battery unit, or a more detailed structure such as the DC side of an AC to DC converter can be the DC system which keeps the net voltage of the split capacitor.

The Figure of the half-bridge VSI below is referred to as a two-level converter since the switched AC-side voltage, at any point, depending on which switch cell is on is either at the voltage of node p or at the voltage of node n. the pulse-width modulation (PWM) technique is generally used to control the basic component of the AC-side voltage(Yazdani & Iravani 2010).

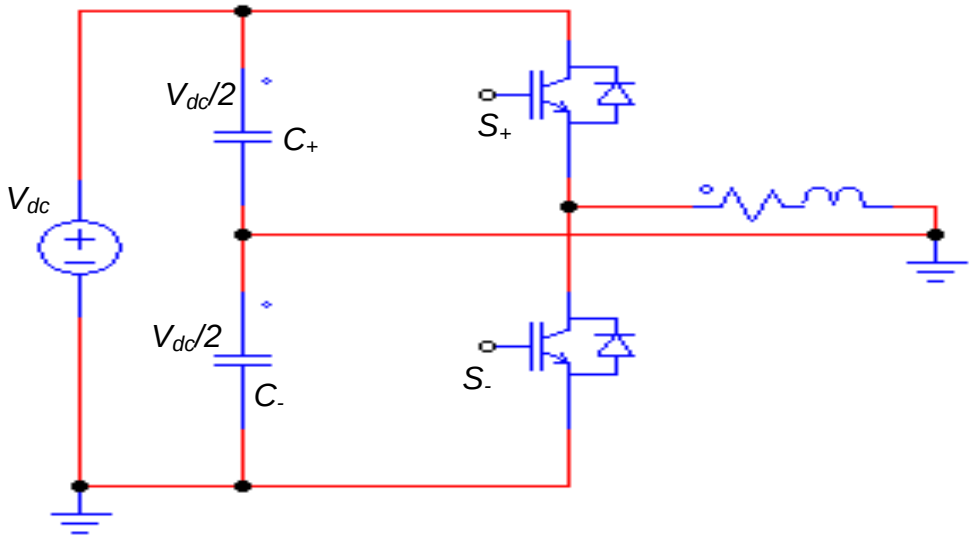

Figure 3.8: Schematic of the half-bridge, single-phase, two-level VSI

Full Bridge Inverter

The Fig. 3.9 below shows a full-bridge single-phase VSI which is obtained if two half-bridge VSIs are in parallel connection through their DC sides. Hence, the AC system can be interfaced with the AC-side terminals of the full-bridge inverter. The alternate switches pair to generate the output square wave voltage. The diodes and IGBTs are designed to be able to sustain the supply voltage. The benefit of the full bridge VSI is that, for a specified DC voltage, the AC voltage generated by the full-bridge VSI is two times larger compared with the half-bridge VSC, which means a more effective use of the DC voltage and switch cells. The full-bridge VSC of Fig. 3.9 is also referred to as H-bridge converter (Yazdani & Iravani 2010; Bose 2002).

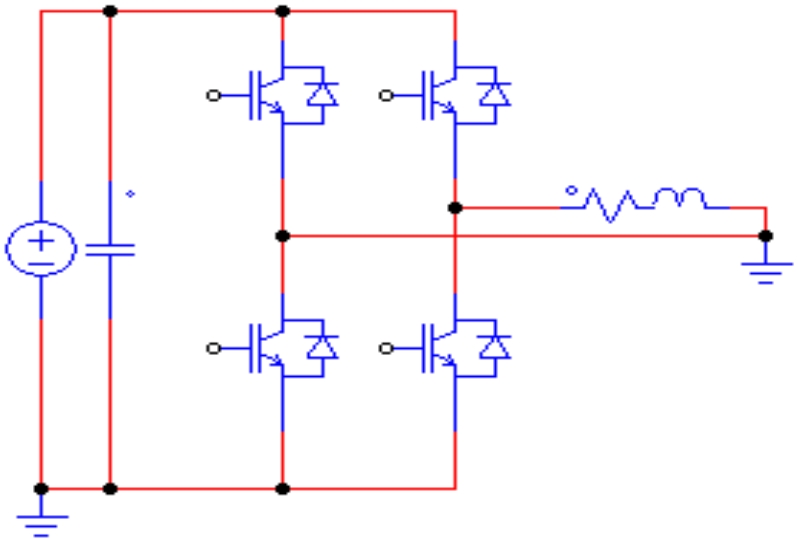

Figure 3.9: Schematic of the full-bridge, single-phase, two-level VSC (or an H-bridge converter)

3.6.2 Three Phase Bridge Inverters

The representation of a three-phase two-level VSI is shown in Figure 3.10 below. The three-phase VSI is an extension of the half-bridge VSI in Fig. 3.9 above. Three phase bridge inverters are commonly used for ac motor drives and general purpose ac supplies. The three-phase VSI is usually interfaced with the AC system through a three-phase transformer, according to three-wire connection in power system applications. Generally, a single phase or three phase utility power supplies a DC input through LC or C filter. However, the VSI must allow connection to the midpoint of its split DC-side capacitor, through the fourth wire which is known as the neutral wire if it is necessary to have a four wire interface. Otherwise, it must be amplified with an additional half-bridge converter, to indicate the fourth leg matching with the other three legs, whereby the AC terminal is connected to the fourth wire (Bose 2002) (Yazdani & Iravani 2010). The PWM technique for switching the three-phase two-level VSI is described in the previous chapter.

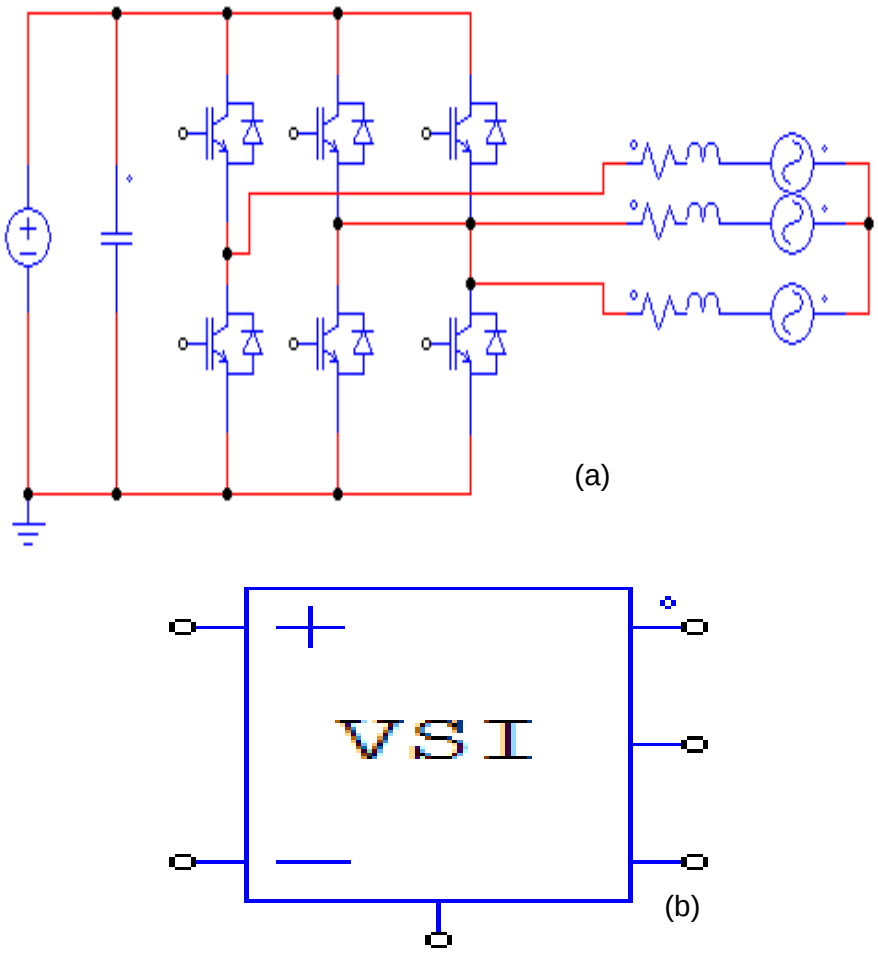

Figure 3.10: Schematic representation of the three-wire, three-phase, two-level VSI (b) the symbolic representation of the three-phase VSI.

The inverter circuit as depicted in the Fig. 3.10 above comprises of three half-bridges, which have an equal phase shift with an angle of 2π/3 to produce the three-phase voltage waves. The square wave phase voltages considering the invented dc center tap can be expressed by Fourier series as(Bose 2002);

$$v_{ao} = \frac{2V_d}{\pi}\left[\cos\omega t - \frac{1}{3}\cos 3\omega t + \frac{1}{5}\cos 5\omega t - \cdots\right] \quad (3.1)$$

$$v_{bo} = \frac{2V_d}{\pi}\left[cos\left(\omega t - \frac{2\pi}{3}\right) - \frac{1}{3}\cos 3\left(\omega t - \frac{2\pi}{3}\right) + \frac{1}{5}\cos 5\left(\omega t - \frac{2\pi}{3}\right) - \cdots\right] \quad (3.2)$$

$$v_{co} = \frac{2V_d}{\pi}\left[cos\left(\omega t + \frac{2\pi}{3}\right) - \frac{1}{3}\cos 3\left(\omega t + \frac{2\pi}{3}\right) + \frac{1}{5}\cos 5\left(\omega t + \frac{2\pi}{3}\right) - \ldots\right] \quad (3.3)$$

Where V_d = dc voltage supply. Therefore, the line voltages can therefore be derived from the equations (3.1) to (3.3) as;

$$v_{ab} = v_{ao} - v_{bo}$$

$$= \frac{2\sqrt{3V_d}}{\pi}\left[cos\left(\omega t + \frac{\pi}{6}\right) + 0 - \frac{1}{5}\cos 5\left(\omega t + \frac{\pi}{6}\right) - \frac{1}{7}\cos 7\left(\omega t + \frac{\pi}{6}\right) + \cdots\right] \quad (3.4)$$

$$v_{bc} = v_{bo} - v_{co}$$

$$= \frac{2\sqrt{3V_d}}{\pi}\left[cos\left(\omega t - \frac{\pi}{2}\right) + 0 - \frac{1}{5}\cos 5\left(\omega t - \frac{\pi}{2}\right) - \frac{1}{7}\cos 7\left(\omega t - \frac{\pi}{2}\right) + \cdots\right] \quad (3.5)$$

$$v_{ca} = v_{co} - v_{ao}$$

$$= \frac{2\sqrt{3V_d}}{\pi}\left[cos\left(\omega t + \frac{5\pi}{6}\right) + 0 - \frac{1}{5}\cos 5\left(\omega t + \frac{5\pi}{6}\right) - \frac{1}{7}\cos 7\left(\omega t - \frac{5\pi}{6}\right) + \cdots\right] (3.6)$$

However, it is important to note that the amplitude of the fundamental line voltage is $\sqrt{3}$ times the phase voltage and $\pi/6$ is the leading phase shift.

3.6.3 Multi-module VSI Systems

In high-voltage, high-power VSI systems, the switch cell of Fig. 3.10 above which is composed of a fully controllable, unidirectional switch and a diode, may not be able to tolerate the voltage or current that is required. Thus, the switch cells are connected in series or in parallel in order to overcome this problem which forms a composite switch structure also known as a valve. Two valve structures made up of parallel and series connection of identical switch cells is shown in Fig. 3.11 below. The present power semiconductor switches can tolerate the current requirements for most applications. To meet the voltage requirements for most applications, series-connected switch cells are certainly needed. The number of switch cells connected in series within a valve is controlled because of the challenges encountered during practical implementation such

as unequal off-state voltage distribution, unacceptable form factor and simultaneous gating requirements. Hence, a two-level VSC system cannot be produced for any voltage level and the maximum upper voltage applies. The maximum voltage allowed for a VSI system can be increased by series connection of equivalent three-phase, two-level VSI modules to form a multi-module VSI (Yazdani & Iravani 2010; Saeedifard et al. 2007).

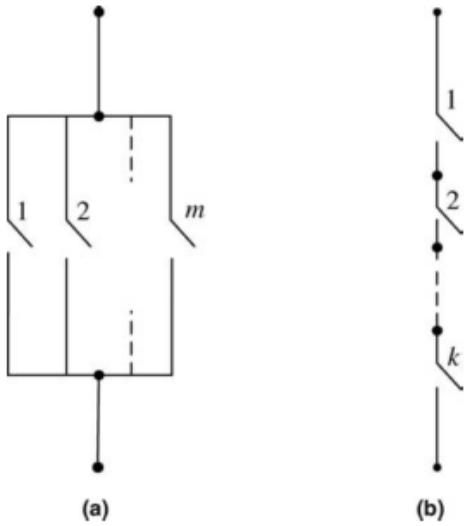

Figure 3.11: Representation of the symbols of valve made up of (a) *m* parallel-connected switch cells and (b) *k* series-connected switch cells. (Yazdani & Iravani 2010)

3.7 Conclusion

Different inverter configurations in power electronics has been discussed in this chapter. The semiconductor switches used to achieve the DC to AC conversion for the inverters have also been highlighted in this chapter.

CHAPTER 4

MODELLING AND ANALYSIS

4.1 Objective

This chapter describes the approach used to achieve this research. The modelling of a smart inverter system capable of operating in grid-connected mode using Matlab/Simulink software is also presented.

Modelling is important in order to determine the dynamic performance, robustness and stability of the control approach employed. To achieve these features the inverter control design, with improved LCL output filtering and grid synchronization through a PLL is also presented in this chapter. Firstly, the PLL is described and supplies the signals for the current loop, which is realized using the proportional-integral (PI) controller. The design approach for the LCL filter used for the system is also given. The block diagram of the inverter model with the control system considered for this project is shown in the figure 4.1 below. This system consists of the following building components as it can be depicted in the GCI representation.

- DC energy source
- DC to AC Voltage-source inverter(made up of IGBT)
- Pulse width modulation.
- LCL filter
- Grid Synchronization
- Three-phase transformation

In this section, the operation of the entire blocks will be described.

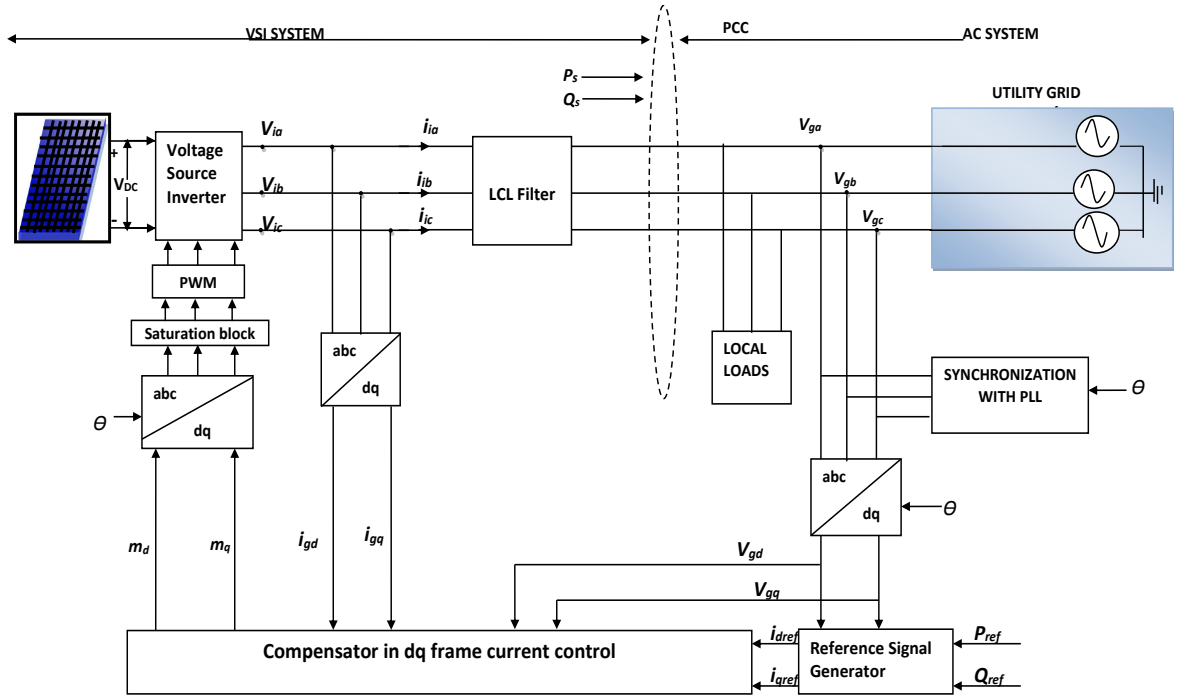

Figure 4.1: Three Phase Grid-Connected Inverter System with Control Algorithm Representation

4.2 DC Energy source

The direct conversion of the solar energy into electrical power is achieved using solar PV cells (Makhlouf, M Messai, Nabti, K and Benalla 2012). A PV cell is usually a simple P-N junction diode that converts the solar irradiation into electricity. A simple of the corresponding circuit of a PV cell is depicted in the figure below. This model is made up of a current source which signifies the current which is generated from the PV cell. The current source is in parallel a diode, a shunt resistance and a series resistance.

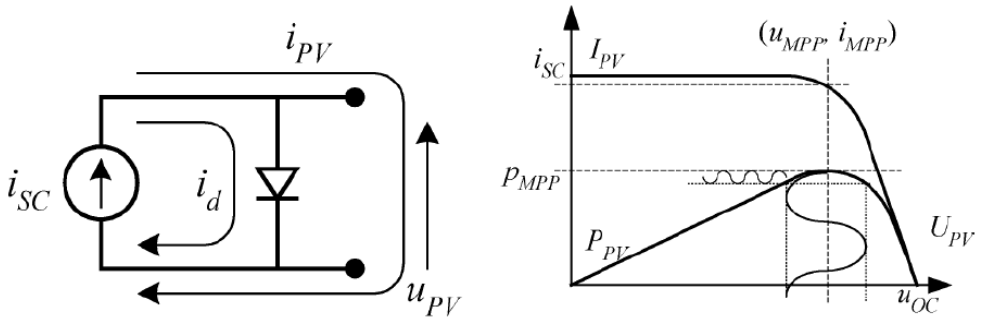

Figure 4.2: Equivalent circuit of a PV cell and its characteristics (Kjaer et al. 2005)

The Voltage-current curve characteristic has a non-linear shape. the characteristics curve tends to slide down as the solar intensity falls, and as the cell surface

temperature rises, the curve tends towards the left as it can be seen in the Fig. 4.2 above (Leslie 2003).

The diode current for this model is represented as:

$$I_D = I_s\left(e^{\alpha\left(v_{pv}+R_s i_{pv}\right)} - 1\right) \qquad (4.1)$$

Where I_s represents the saturation current, $\alpha = \frac{q}{AkT_c}$, v_{pv} and i_{pv} are the voltage and current output of the cell output, R is the resistance value, q is the electron charge, A is the ideality factor, k is the Boltzman's constant and T_c is the operation temperature (Schonardie & Martins 2008; Malek 2014; Makhlouf, M Messai, Nabti, K and Benalla 2012).

Using the Kirchhoff's law (KCL), the output current of the PV cell (4.2) can be obtained;

$$i_{pv} = I_L - I_s\left\{e^{\frac{q(v_{pv}+R_s i_{pv})}{n.k.T}} - 1\right\} - \frac{v_{pv}+R_s i_{pv}}{R_{sh}} \qquad (4.2)$$

The relationship between the solar irradiation and temperature to the current source I_L can be derived from equation (4.2) as:

$$I_L = \frac{G}{100}\left\{I_{sc} + k_i(T_c - T_{ref})\right\} \qquad (4.3)$$

Where G represents the solar irradiation, I_{sc} is the short circuit current, k_i is the coefficient for the short circuit current while T_c and T_{ref} are the operating temperature and reference temperature of the cell respectively. The relationship between the cell's saturation current I_s and with the operating and reference temperatures can be represented as:

$$I_s = I_{RS}\left(\frac{T_c}{T_{ref}}\right)^3 e^{\frac{qE_g}{Ak}\left(\frac{1}{T_{ref}} - \frac{1}{T_c}\right)} \qquad (4.4)$$

Where I_{RS} represents the reverse saturation current in the reference temperature and solar irradiation while E_g is the bandgap energy of the PV semiconductor.

There might be need for the combination of cells in series and parallel to be connected together in a case where the output voltage and current of one PV cell are quite low, so as to supply higher current and voltage. The cells are protected with a transparent material to shield them against unfriendly environmental conditions which forms a PV module. However, for high power applications, a selected number of PV modules is

required to be connected to form a PV array so as to derive a higher voltage and current.

4.2.1 DC Link Voltage Design

The power stage designed in this thesis converts the 800V DC output voltage of the three-phase converter to the grid voltage of 380 V AC at 50 Hz frequency. The output AC voltage of the inverter is specified to 380 V as three-phase VSI and the flow of power in the inverter can be in either direction.

When the DC link voltage is lesser than the peak grid voltage, it is not easy to control the grid current with the voltage drop across the semiconductor devices and filter voltage. This is the purpose of choosing a high DC link voltage.

4.3 The Inverter model

The proposed inverter for this thesis is a three-phase bidirectional DC to AC inverter topology with PWM technique. The three phase inverter basically converts DC power into AC power at desired output voltage and frequency. This can be realized using different inverter topologies and control schemes with each having their benefits and drawbacks. However, the inverter to be designed and modelled for the purpose of this research work is a PV grid-connected inverter having a DC power as input which is produced by solar panels and the output of 50 Hz three phase AC power interfaced to the grid. The simple electrical representation of the inverter studied is shown in the Fig. 4.3 below. The bidirectional feature of the inverter is very essential in this proposed grid-connected PV system, because it permits the processing of active and reactive power from the generator to the load and vice versa, depending on the application. Therefore, with a suitable control of the power switches it is possible to control the flow of active and reactive power (Eren et al. 2012; Schonardie & Martins 2008).

Basically for this design, a six switch three-phase inverter topology is used. The topology is made up of six switches that are arranged in three parallel branches, and consist of two switches in series on each branch with each switch cell made up of a transistor and a diode connected in anti-parallel. The DC input is applied to the three upper and lower parallel branches of the inverter. The generation of the three phase AC output takes place in between the two switches of each branch. This inverter configuration is simple, widely used, and a very good topology to integrate additional inverter features which makes it desirable for this thesis. The input of the inverter is in form of an ideal, balanced, three-phase voltage source, which is connected to the grid. This description of the utility grid model is based on a basic idea that the utility voltage is stiff and thus the inverter output current is not affected. The IGBTs with anti-parallel

diodes are the switches existing in the switching network, which allow flow of current in both directions and voltage blocking in one direction. The switches must meet the operating condition of the switching function so as to guarantee that the filter inductor current is not disturbed.

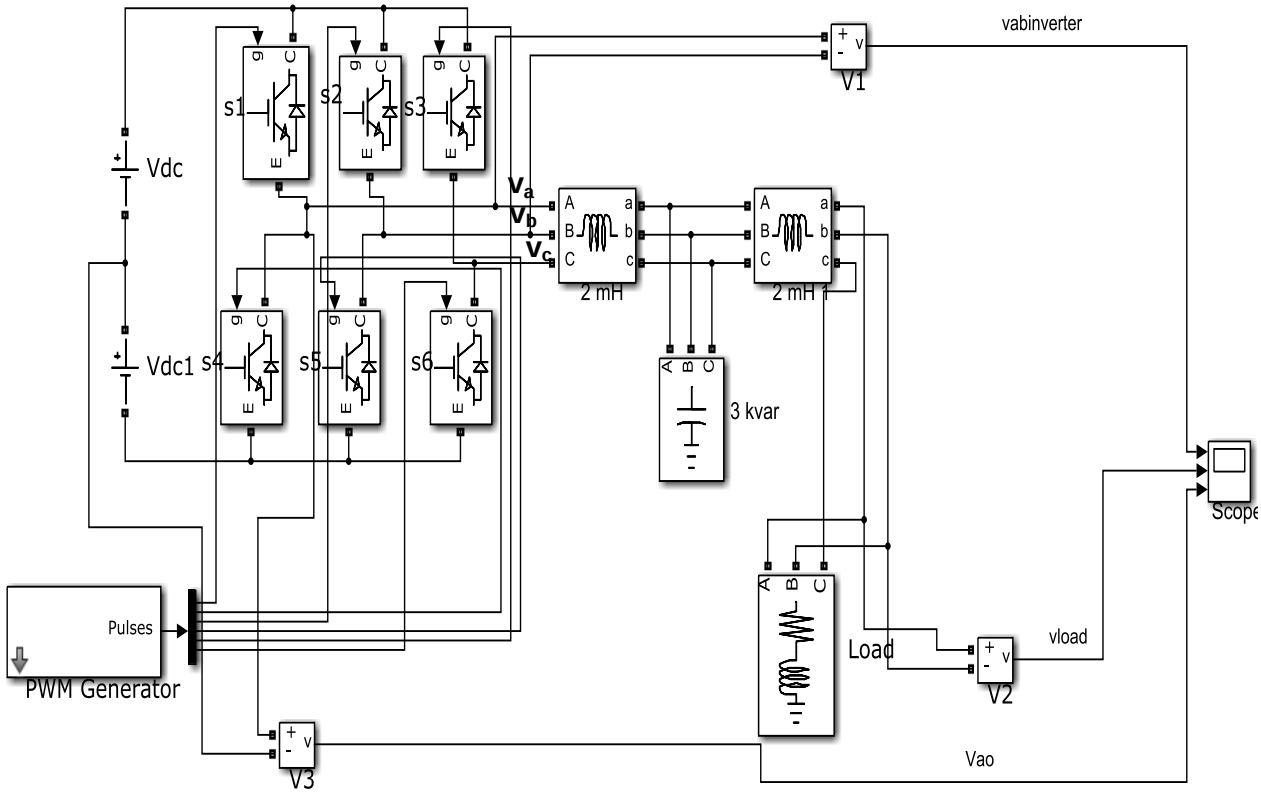

Figure 4.3: Bidirectional DC to AC PWM VSI

The Switching of the inverter is controlled by PWM in a proper sequence to generate an unfiltered output voltage. The whole inverter system is enhanced by PWM switching approach. Sinusoidal pulse width modulation (SPWM) is used to generate the switching signals for the inverter at the desired magnitude and frequency by comparing a three-phase sinusoidal wave with a triangular wave. The frequency of the inverter is set by the frequency of the triangular signal resulting into pulses which drives the gate signal. The modelling of reference sinusoidal waveforms gives:

$$v_{a\_ref} = Asin\,(2\pi ft + \theta)$$

$$v_{b\_ref} = Asin\,(2\pi ft + \theta - 120°) \qquad (4.6)$$

$$v_{c\_ref} = Asin\,(2\pi ft + \theta + 120°)$$

Where A represents the amplitude of the reference sinusoidal waveform, f is the frequency of the output waveform, θ is the phase shift V_s and V_T is the sinusoidal and triangular reference waveform varying from 1 to -1 respectively. The table 4.1 below shows the switching pattern of the inverter switches.

Table 4.1: Switching pattern of SPWM

Switch	Applicable Sine Wave	$V_s > V_T$	$V_s < V_T$
S_1	v_a	ON	OFF
S_4		OFF	ON
S_2	v_b	ON	OFF
S_5		OFF	ON
S_3	v_c	ON	OFF
S_6		OFF	ON

Hence, the inverter switches, which are on each leg of the inverter, are switched off alternatively resulting to the flow of output current continuously. The modulating index is set between 0 and 1 to limit the voltage magnitude of the inverter on the AC side. The fundamental AC side voltage waveform magnitude and amplitude of the inverter when SPWM is applied can be determined by equations (4.7) and (4.8) (Ned Mohan 2003; Bhutia, S. M. Ali, et al. 2014).

$$V_{rms} = \frac{1}{\sqrt{2}} \times V_{dc} = 0.707\, V_{dc} \qquad (4.7)$$

$$V_{rms} = \frac{\sqrt{3}}{2\sqrt{2}} \times V_{dc} = 0.612\, V_{dc} \qquad (4.8)$$

There can be an instance of short circuit across the DC source, which could damage the switches or the complete inverter when there is simultaneous switching of the inverter switches on each leg. However, switching is done transversely; the combination of the two diagonal switches gives the unfiltered output voltage. The freewheeling diodes present in the switches conduct when the output voltage is 0 and the complete switch cell unit is available commercially in form of IGBT. A corresponding mathematical model of the inverter was considered after describing the power electronic VSI configuration in order to develop the control system. The

variables of the controller should be the energy storage elements, such as the interface inductor current and the variable for the control input which are the PWM gate signals.

4.4 Output filter

The state-space representation of the system when the inductor currents and capacitor voltage (i_a, i_b, i_c, $v_{dc} = v_{pv}$) are considered as the state variables of the three-phase grid-connected PV system represented in the Fig. 4.4 below is given as (Malek 2014):

$$i_a = -\frac{R}{L}i_a - \frac{1}{L}e_a + \frac{v_{pv}}{3L}\langle 2S_a - S_b - S_c\rangle$$

$$i_b = -\frac{R}{L}i_b - \frac{1}{L}e_b + \frac{v_{pv}}{3L}\langle -S_a + 2S_b - S_c\rangle \quad (4.9)$$

$$i_c = -\frac{R}{L}i_c - \frac{1}{L}e_c + \frac{v_{pv}}{3L}\langle -S_a - S_b + 2S_c\rangle$$

the switching signals associated to each phase of three-phase VSI are represented by S_a, S_b, and S_c which is defined in equation (4.9) and when KCL is applied to the DC link capacitor node, the state-space equation for capacitor voltage is represented by equation (4.10) below:

$$S_i(i = a, b, c) = \begin{cases} 1 \;\; if \quad S_i^{Upper} : on, \quad S_i^{Lower} : off, \\ 0 \;\; if \quad S_i^{Upper} : off, \quad S_i^{Lower} : on, \end{cases}$$

$$v_{dc} = \frac{1}{C}(i_{pv} - i_{dc}) \quad (4.10)$$

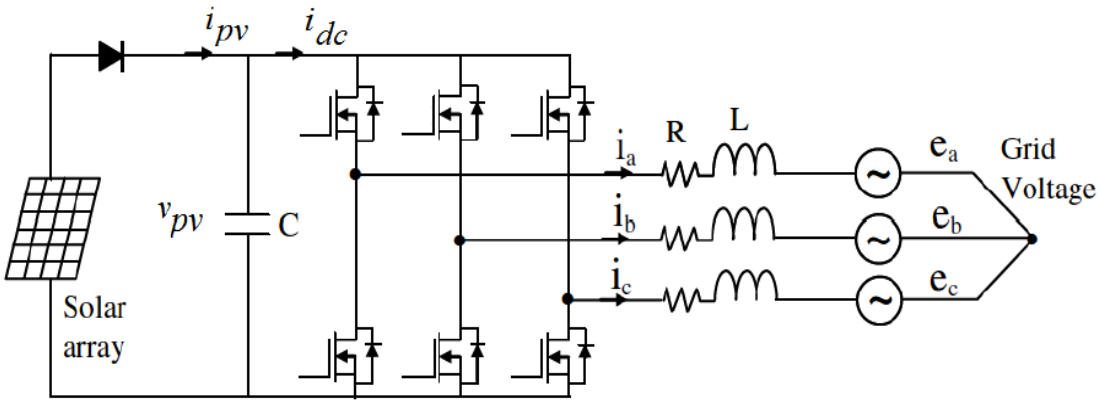

Figure 4.4: Three phase grid-connected scheme (Malek 2014)

The GCI input current is equivalent to the output current when the switching losses and conduction losses of the inverter are presumed to be negligible.

$$i_{dc} = i_a S_a + i_b S_b + i_c S_c \tag{4.11}$$

$$\Rightarrow v_{dc} = \frac{1}{C} i_{dc} - \frac{1}{C}(i_a S_a + i_b S_b + i_c S_c) \tag{4.12}$$

Hence, the following equations present the state-space representation of a lossless three-phase grid-connected PV system.

$$i_a = -\frac{R}{L} i_a - \frac{1}{L} e_a + \frac{v_{pv}}{3L}\langle 2S_a - S_b - S_c \rangle$$

$$i_b = -\frac{R}{L} i_b - \frac{1}{L} e_b + \frac{v_{pv}}{3L}\langle -S_a + 2S_b - S_c \rangle$$

$$i_c = -\frac{R}{L} i_c - \frac{1}{L} e_c + \frac{v_{pv}}{3L}\langle -S_a - S_b + 2S_c \rangle$$

$$v_{pv} = \frac{1}{C} i_{pv} - \frac{1}{C}(i_a S_a + i_b S_b + i_c S_c) \tag{4.13}$$

From the equations (4.13), it is seen that the grid-connected VSI is a nonlinear time-varying system due to the switching functions (S_a, S_b, and S_c) and diode current (i_{pv}). The later part of this chapter will present the suitable transformation and approach that will make the control procedure less complicated for this nonlinear time varying system.

4.4.1 Modelling and Design of LCL filter

During the design of the LCL filter, some critical factors such as current ripple, size of filter, switching ripple attenuation must be considered. The filter capacitance may cause resonance, which can result to instability of the system when reactive power variation is experienced by the grid. The approach of passive or active damping by introducing a resistor in series with the filter capacitor or designing of another controller is thus proposed (Reznik et al. 2012).

A LCL filter has been proved to be more effective than the L filter due to the attenuation of the L filter which is 20 dB/decade for all frequency levels. The inverter must have a high switching frequency capable of reducing current harmonics which are high. However, more switching losses is experienced depending on how high the switching frequency is. The LC filter is not suitable for a firm grid due to its variability of resonance frequency, which can affect the stability of the system (Liserre et al. 2005).

The per-phase equivalent LCL filter model is represented in the figure below. where L_i is the inductor on the inverter- side, L_g is the inductor on the grid-side, C_f is the filter capacitor with a damping resistor R_f connected in series, Ri and Rg are the inverter side and grid-side inductor resistances respectively, voltages V_i and V_g are the input (inverter voltage) and output (output system or grid voltage). Currents i_i, i_c, i_g, are

inverter output current, capacitor current and grid current respectively. A functional block diagram for the grid connected inverter using this LCL filter is depicted in Fig. 4.5.

The mathematical model for the LCL filter is indicated in the equations below which are essential for the inverter control design and dynamic analysis. This is achieved by applying KCL (Kirchhoff's current law) and KVL(Kirchhoff's voltage law to the LCL configuration depicted in the Fig. 4.5 below which enables the applicable transfer functions to be derived. Considering a three-phase system, the per-phase model of the LCL filter can be used to derive its state space model with capacitors which are wye connected. The state space model of the LCL filter with wye connected capacitors can be derived from per-phase model represented in the Fig 4.5 below (Reznik et al. 2012a; Teodorescu et al. 2011).

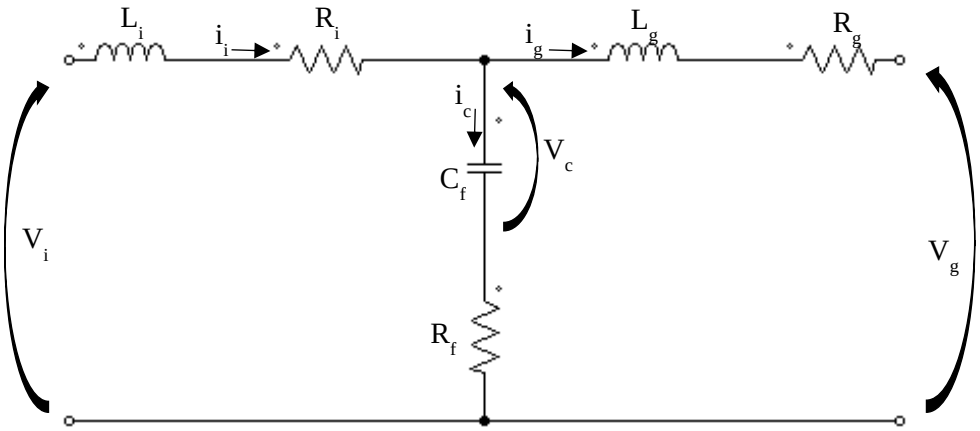

Figure 4.5: Model of LCL filter per phase

$$\frac{dv_c}{dt} = \frac{i_i - i_g}{C_f} \tag{4.14}$$

$$i_i - i_g = C_f \frac{dv_c}{dt} \tag{4.15}$$

$$\frac{di_i}{dt} = \frac{1}{L_i}\left(v_i - v_c - R_f\left(i_i - i_g\right) - R_i i_i\right) \tag{4.16}$$

$$\frac{di_g}{dt} = \frac{1}{L_g}\left(v_c + R_f\left(i_i - i_g\right) - v_g - R_g i_g\right) \tag{4.17}$$

The expression for the equations (4.14) to (4.17) in form of matrix gives:

$$\begin{bmatrix} \frac{di_i}{dt} \\ \frac{di_g}{dt} \\ \frac{dv_c}{dt} \end{bmatrix} = \begin{bmatrix} -\frac{R_i+R_f}{L_i} & \frac{R_f}{L_i} & -\frac{1}{L_i} \\ \frac{R_f}{L_g} & -\frac{R_g+R_f}{L_g} & \frac{1}{L_g} \\ \frac{1}{C_f} & -\frac{1}{C_f} & 0 \end{bmatrix} \begin{bmatrix} i_i \\ i_g \\ v_c \end{bmatrix} + \begin{bmatrix} \frac{1}{L_i} & 0 \\ 0 & -\frac{1}{L_g} \\ 0 & 0 \end{bmatrix} \begin{bmatrix} v_i \\ v_g \end{bmatrix} \quad (4.18)$$

$$\dot{x}(t) = Ax(t) + Bu(t) \quad (4.19)$$

For the three phase system, there are no cross-couplings present between the phases; therefore, the equations are equal for all phases as indicated in the matrix expression above. However, transforming the three phase system using *dq* synchronous reference frame into an equivalent two phase system in order to achieve the design of the system control easily, the equation of the system is then represented as seen in the following equation (4.20) and (4.21)(Hassan 2005).

$$\frac{d}{dt}\begin{bmatrix} i_{id} \\ i_{iq} \\ i_{gd} \\ i_{iqq} \\ v_{cd} \\ v_{cq} \end{bmatrix} = \begin{bmatrix} -\frac{R_i+R_f}{L_i} & \omega & \frac{R_f}{L_i} & 0 & -\frac{1}{L_i} & 0 \\ -\omega & -\frac{R_1+R_f}{L_i} & 0 & \frac{R_f}{L_i} & 0 & -\frac{1}{L_i} \\ \frac{R_f}{L_g} & 0 & -\frac{R_2+R_f}{L_g} & \omega & \frac{1}{L_g} & 0 \\ 0 & \frac{R_f}{L_2} & -\omega & -\frac{R_2+R_f}{L_g} & 0 & \frac{1}{L_g} \\ \frac{1}{C_f} & 0 & -\frac{1}{C_f} & 0 & 0 & \omega \\ 0 & \frac{1}{C_f} & 0 & -\frac{1}{C_f} & -\omega & 0 \end{bmatrix} \begin{bmatrix} i_{id} \\ i_{iq} \\ i_{gd} \\ i_{iqq} \\ v_{cd} \\ v_{cq} \end{bmatrix} +$$

$$\begin{bmatrix} \frac{1}{L_i} & 0 & 0 & 0 \\ 0 & \frac{1}{L_i} & 0 & 0 \\ 0 & 0 & -\frac{1}{L_g} & 0 \\ 0 & 0 & 0 & -\frac{1}{L_g} \\ 0 & 0 & 0 & 0 \\ 0 & 0 & 0 & 0 \end{bmatrix} \begin{bmatrix} v_{id} \\ v_{iq} \\ v_{gd} \\ v_{gq} \end{bmatrix} \quad (4.20)$$

$$y(t) = Cx(t) + Du(t) \quad (4.21)$$

y is the output vector which is equal to the state vector x for this instance and C is the identity matrix of dimension 6 × 6.

4.4.2 Frequency Response and Transfer Function

The transfer functions of LCL filter can be derived from the developed mathematical models above. The three phase differential equations derived previously is used to derive the transfer functions, but in these equations the inductors resistances are neglected. The extracted transfer function $H_{LCL}= i_g/v_i$ is one of the equations derived from state space equations. The grid voltage is assumed to be an ideal voltage source and it represents a short circuit for harmonic frequencies, and for the analysis of filter V_g is set to zero (V_g = 0) (Pastor & Dudrik 2013; Reznik et al. 2012). Hence, the transfer functions of LCL filter without damping and with damping are expressed in (4.22) and (4.23) below respectively:

$$H_{LCL}(s) = \frac{1}{s^3 L_i C_f L_g + s(L_i + L_g)} \tag{4.22}$$

$$H_{LCL/damp}(s) = \frac{sC_f R_f + 1}{s^3 L_i C_f L_g + s^2 C_f R_f (L_i + L_g) + s(L_i + L_g)} \tag{4.23}$$

4.4.3 LCL Filter Design procedure

The basic objective function of the LCL filter is to minimize high-order harmonics on the output side. However, inadequate design of the filter can result to increase in distortion. Hence, appropriate design of the LCL filter is very crucial. The three phase representation of the LCL filter is illustrated in the Fig. 4.6 below:

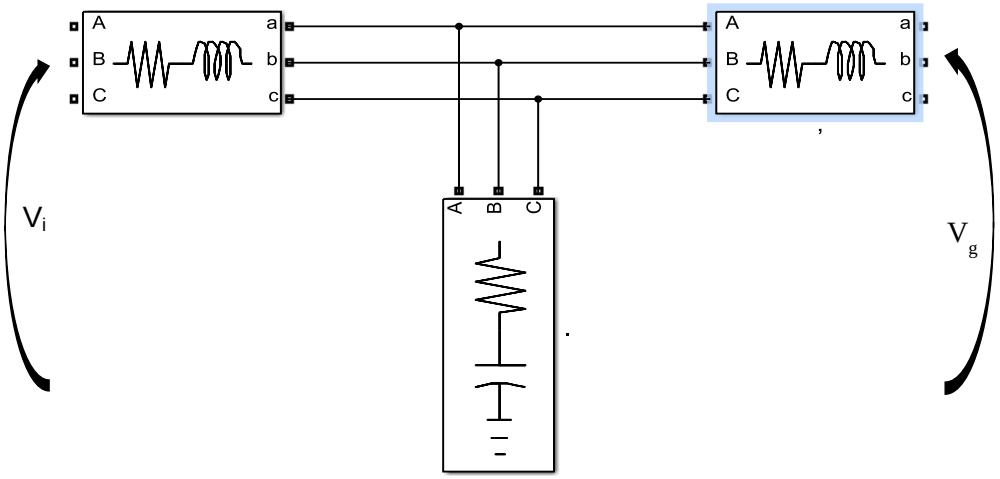

Figure 4.6: Representation of LCL filter model for three-phase VSI

Some of the factors to be considered while designing LCL filters are inverter output ripple current, inverter to grid inductor ratios and filter capacitance maximum power variations. Usually current ripple is limited to 10% to 25%, inverter to grid ratio is

usually between 0 and 1, the capacitor value is not to exceed 5% of the decrease of the rated power and ripple attenuation is limited to 20%.

The inverter to grid side inductance ratio is expressed in equation (4.27) and the relation is plotted in the figure (4.7) below. This factor is derived from the ratio between the filter impedance and the difference between resonant frequency and switching frequency. Therefore, this ratio determines primarily the desired ripple attenuation of the filter which is given as the ratio of $\frac{i_g(h)}{i_i(h_{sw})}$ (Massawe 2013).

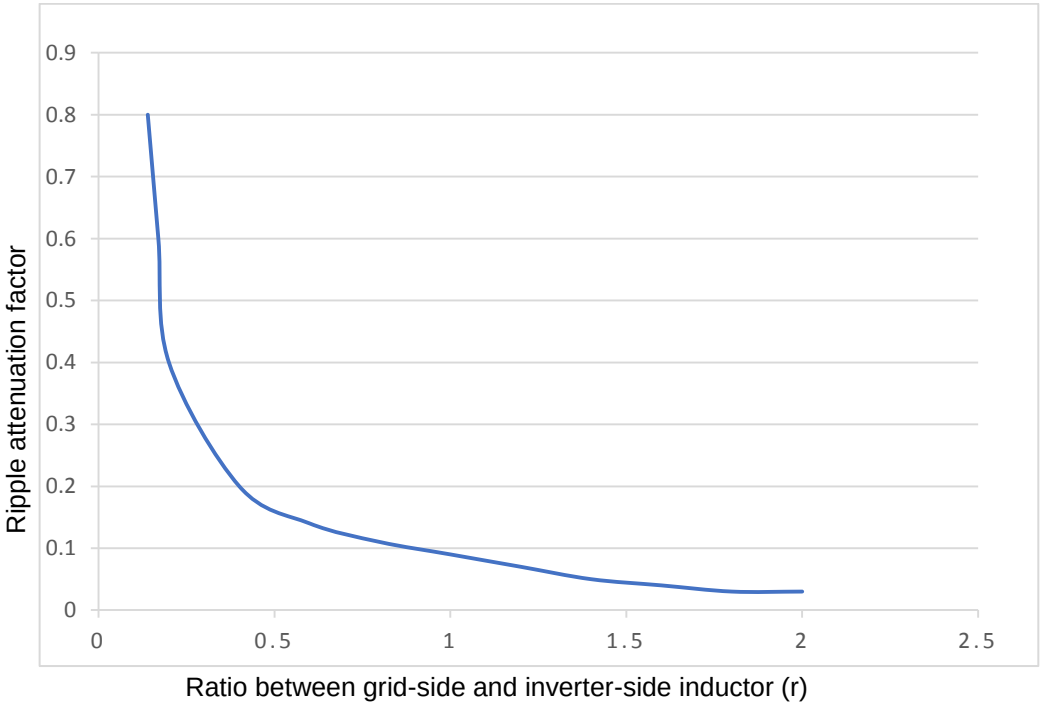

Figure 4.7: Ripple attenuation as a function of the ratio between the grid to inverter inductances
(Massawe 2013)

The procedure for the design of the filter has been described in details in this thesis, and appropriate damping can prevent resonance problems passively or actively. The power rating of the VSI, the grid frequency and the switching frequency are essential as inputs for selecting the LCL filter parameters (Mataifa et al. 2015; Reznik et al. 2012). The Fig. 4.8 below shows the flow chart summarizing the procedural design of the LCL filter. Subsequently, each stage of the algorithm is explained further and the designing of the filter used for this work.

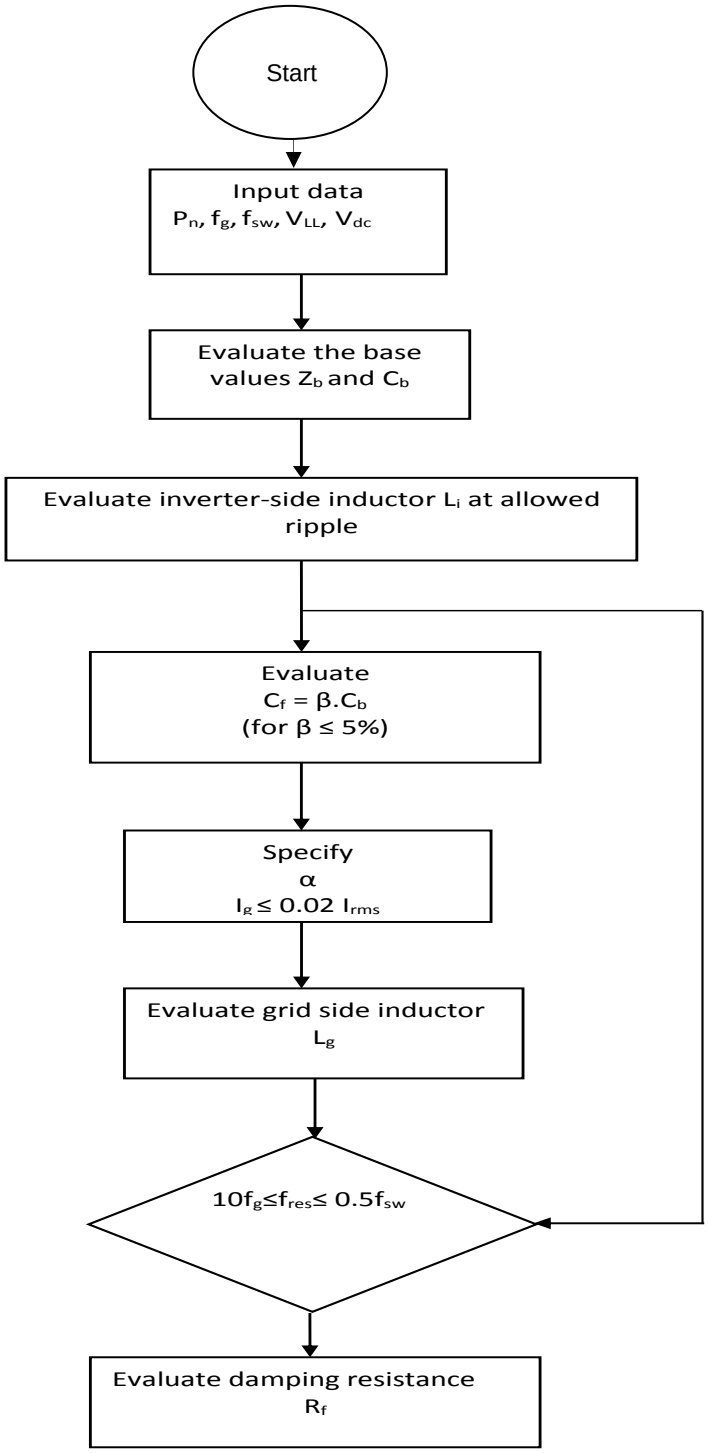

Figure 4.8: Flow chart representation of LCL filter design algorithm

In order to design the filter for this work, the following parameters will be required: V_{LL}- line to line RMS voltage (inverter output), V_{ph} - phase voltage (inverter output), P_n - rated active power, V_{dc} - DC bus voltage, f_g - grid frequency, f_{sw} - switching frequency, f_{res}- resonance frequency.

The parameters in table 4.2 below is for the calculation for the components of the filter. These parameters are the ratings of the power stage of the inverter and are essential for the design of the inverter for this work. These parameters are designed to handle an approximate power of 10 kVA. Unity power factor was assumed for this work.

Table 4.2: LCL filter design specifications

Parameter		Value
Line to line RMS Voltage	$V_{LL/rms}$	380 V
Nominal power	P_n	10 kW
DC-Link voltage	V_{dc}	800 V
Inverter configuration	3φ	Three-phase system
Nominal current	I_{rms}	15.19 A
Power factor	pf	1
Grid frequency	f_g	50 Hz
Switching frequency	f_{sw}	30 kHz
Modulation range	m_a	0 < ma < 1

The base impedance and base capacitance can be calculated by computing the values provided in table 4.2 into the respective equations (4.24) and (4.25) stated below.

$$Z_b = \frac{V_{LL/rms}^2}{P_n} \tag{4.24}$$

$$Z_b = \frac{380^2}{10000} = 14.44\ \Omega$$

$$C_b = \frac{1}{\omega_n Z_b} \tag{4.25}$$

$$C_b = \frac{1}{2\pi 50 \times 14.44} = 220.43\ \mu F$$

Minimization of the ripples in the output current of the inverter is achieved mainly by the inverter-side inductor usually 10% to 20% of the nominal current.

Choosing the inverter-side inductor to be 5% of the base impedance as allowed current ripple which meets the limit requirement of 10% of nominal current value.

$$X_{Lpu} = \frac{\omega_n L}{Z_b} \tag{4.26}$$

$$\Rightarrow L_i = \frac{X_{Lpu} \times Z_b}{\omega_n}$$

$$= \frac{0.05 \times 14.44}{2\pi 50} = 2.30\ mH$$

$$\Delta I_{Lmax} = \frac{V_{DC}}{8 f_{sw} L_i} = \frac{800}{8 \times 30 \times 10^3 \times 2.30 \times 10^{-3}} = 1.45\ A$$

$$\Rightarrow \Delta I_{Lmax} = 0.095\ I_{nrms}$$

Based on the calculation of L_i done above, the LCL filter should minimize the probable current ripple below 10% and a further reduction in ripple by 2% when the grid-side inductor is introduced which is calculated below. The ripple attenuation is determined by the constant '*r*' which defines the relationship between the inverter-side inductor and the grid-side inductor which is the main objective of the inductance at the grid side:

$$L_g = rL_i \qquad (4.27)$$

The relation between the harmonic current generated by the grid and the harmonic current generated by the inverter is expressed as:

$$\frac{i_g(h)}{i_i(h_{sw})} = \frac{1}{\left|1+r\left[1-\left(C_b\, L_i\, .\omega_{sw}^2\right)\right]x\right|} \qquad (4.28)$$

where *r*, C_b and *x* signifies the relation factor between inductances, base capacitance and the filter capacitance factor. The desired attenuation factor is determined by setting the value of r in the equation (4.27) which is a function of the ratio of the inductance on the grid side and on the inverter-side.

The total inductance for the LCL filter considering 0.09 per unit as the inductive reactance is calculated as:

$$\Rightarrow L_{Total} = \frac{X_{L\_Totalpu} \times Z_b}{\omega_n} \qquad (4.29)$$

$$= \frac{0.09 \times 14.44}{2\pi 50} = 4.137\ mH$$

Since, $L_i = 2.30\ mH$

$$\therefore L_g = 4.137\ mH - 2.30\ mH = 1.84\ mH$$

$$L_g = 1.84\ mH$$

The maximum power factor variation considered for the design of the filter capacitance seen by the grid is 5%, which is multiplied by the value of base impedance of the

system. The role of the filter capacitance C_f that serves as a sink for harmonics with high frequency is determined by setting a percentage of not more than 5% of the base capacitance C_b. The percentage chosen for this work is 5% and it is expressed as:

$$C_f = \beta . C_b \qquad (4.30)$$

$$C_f = 0.05 \times C_b$$

$$C_f = 0.05 \times 220.43\,\mu F = 11.02\,\mu F$$

The transfer function of the filter at a specific resonant frequency can be calculated based on the nominal grid impedance when the results for a number of values of '*r*' are plotted. To avoid resonance, the damping resistor R_f that is in series with the capacitor reduces the ripple on the switching frequency (Lettl et al. 2011). The value chosen for this resistor should be one third of the impedance of the filter capacitor at the resonant frequency (Reznik et al. 2012) and the filter resonance is expressed as:

$$f_{res} = \frac{1}{2\pi}\sqrt{\frac{L_i + L_g}{L_i L_g C_f}} \qquad (4.31)$$

$$\Rightarrow f_{res} = \frac{1}{2\pi}\sqrt{\frac{4.137 \times 10^{-3}}{2.3 \times 10^{-3} \cdot 1.84 \times 10^{-3} \cdot 11.02 \times 10^{-6}}}$$

$$= 1540.57\,Hz$$

$$\therefore \omega_{res} = 2\pi \times 1540.57\,Hz = 9679.68\,rad/sec$$

The value of the resonant frequency calculated in (4.31) meets the appropriate requirement which is about 5% of the switching frequency in which half of the switching frequency is allowable. It also exceeds the minimum desirable value which should be 10 times the nominal frequency. This is simply expressed in equation (4.32) (Teodorescu et al. 2011).

$$10 f_g < f_{res} < 0.5 f_{sw} \qquad (4.32)$$

Passive damping is achieved by connecting a resistor R_f which acts as the damping resistor in series with the filter capacitor C_f. The passive damping helps in stability of the control system of the VSI (Liserre et al. 2004). The higher the value of the damping resistor, the better the damping effect, however this can have a negative effect on the efficiency which is not desirable. The damping resistor value is evaluated as expressed in (4.33):

$$R_f = \frac{1}{3\omega_{res}C_f} \quad (4.33)$$

$$R_f = \frac{1}{3 \times 2\pi \times 1540.57 \times 11.02 \times 10^{-6}} \; ; \; R_f = 3.12\ \Omega$$

The parameters for the LCL filter designed are summarized in the table 4.3 below.

Table 4.3: Designed LCL filter parameter values

Parameter		Value
Grid side inductor	L_g	1.84 mH
Inverter side inductor	L_i	2.30 mH
Filter Capacitance	C_f	11.02 µF
Damping resistor	R_f	3.12 Ω
Resonance frequency	ω_{res}	9680 rad/sec
Approximated total inductor resistance	R_T	0.1

4.5 The Three-Phase grid-connected inverter synchronization

In order to decrease the dimensions of the mathematical model of the inverter system and decouple the differential equations in order to make the control design process of the three-phase grid-connected inverter system easier, the dq synchronous reference frame transformation (Park transformation) is used (Hadjidemetriou et al. 2013). The available techniques for synchronizing the inverter with the grid are zero crossing, stationary reference frame PLL and synchronous reference frame (SRF) PLL. The synchronous reference frame PLL is preferred for this thesis because of its great performance when it experiences distortion or in the course of non-ideal conditions of the grid.

4.5.1 GCI Synchronization using PLL (Phase Locked Loop) Technique

The PLL is regarded as a device, which allows one signal to track the other. The output signal synchronizes with a reference input signal in frequency and in phase. The current control loop is based on the PI (proportional integral) controller and the PLL is responsible for supplying the signals to it. In order for the PLL to synchronize the frequency of the periodic input signal and phase angle with output signal, it uses an internal oscillator identified as voltage controlled oscillator and a negative feedback. The phase angle, frequency and voltage of the grid is identified by the PLL system. In order to implement the synchronous reference frame transformations, the phase angle is needed while the frequency and voltage are necessary for the dynamic stability of

the system and to monitor the conditions of the grid. However, the currents are transformed into *dq* synchronous reference frame, which performs a decoupling process between the d and q axis. A common configuration for grid synchronization used nowadays is the phase locked loop (PLL) implemented in dq synchronous reference frame and its schematic is depicted in the Fig. 4.9 below. This configuration of PLL is made up of the phase detection and the loop filter. Implementation of the phase detection can be achieved by using abc to dq transformation in the three phase system. Alternatively, the dynamics of the system is determined by the loop filter. However, the bandwidth of the filter is an accord between the performance of the filter and the time response. As a result, quality of the lock and the PLL dynamics is highly influenced by the parameters of the loop filter (Meersman et al. 2010; Timbus et al. 2005).

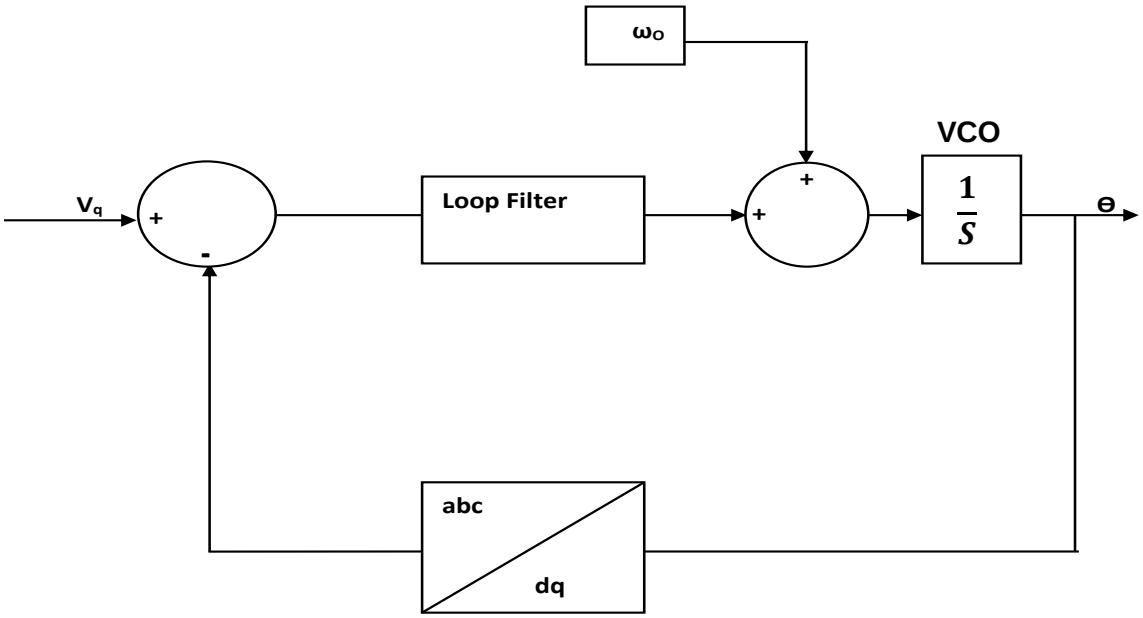

Figure 4.9: PLL representation in synchronous reference frame

Furthermore, the synchronous reference frame can easily obtain a suitable performance and small steady state errors in magnitude and phase with a simple compensator configuration since under steady state the signals are in form of DC (Reznik 2012; Chung 2000).

Usually, the utility grid is a stiff system in which any deviation in the frequency supplied results to an increase in error of the phase angle. This error is reduced to zero by employing the PI controller (Kaura & Blasko 1997). The closed loop response of the PLL algorithm can fully predict the response to fluctuations in frequency

4.5.2 Design of Synchronous Reference Frame PLL

The PLL system can be influenced by the distortions existing in the utility network when it is utilized for grid-connected applications. It is observed that the synchronization procedure dynamic is closely associated with the bandwidth of the filter. Therefore, a low dynamic filter will generate an output that is well-filtered and stable but synchronization time is increased. A design for fast dynamics will alternatively produce an output which is able to synchronize rapidly to the input however distortions present in the input signal will pass through the filter and become part of the output signal. Thus, when the synchronization system is being designed, the purpose of this system should not be overlooked. If the procedure is employed for synchronizing the control variables to the utility voltage vector in order to have an accurate synchronization required for control, then a slow dynamic procedure can be implemented. On the other hand, if the synchronization procedure is used in grid monitoring such as detecting grid faults, a fast dynamic system should be used. A tuning technique for the dq-PLL controller is given subsequently. The settling time and damping ratio of the system can be accessed through this technique. Therefore, based on these parameters, a low dynamics or fast dynamics system can be designed. The tuning method is derived from the transfer function of linearized dq-PLL depicted in Fig. 4.10 below (Timbus et al. 2005).

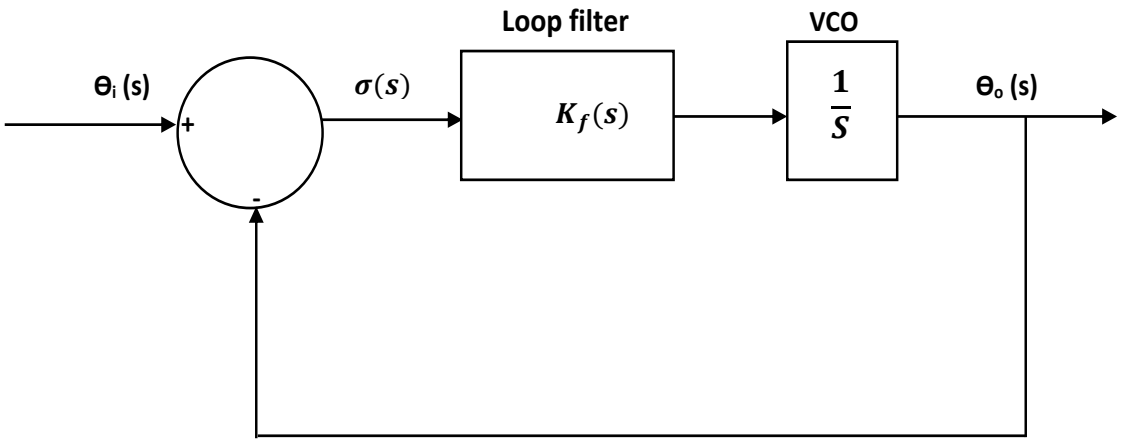

Figure 4.10: Linearized PLL system representation

The transfer function of the closed loop dq-PLL system depicted in the Fig. 4.10 above can be represented as:

$$H_c(s) = \frac{\theta_o(s)}{\theta_i(s)} = \frac{K_f(s)}{s+K_f(s)} \qquad (4.34)$$

$$H_e(s) = \frac{\sigma(s)}{\theta_i(s)} = \frac{s}{s+K_f(s)} \quad (4.35)$$

where $\theta_o(s)$ and $\theta_i(s)$ represents the Laplace transform of θ_o and θ_i respectively.

There are different ways to design the loop filter. Generally, the second-order loop is used as a good accord between the filter performance and stability of the system. Where K_p and τ represent the gains of the PI loop filter and ω_n is the PLL closed loop bandwidth The transfer function of the closed loop can be expressed in the general form of the second-order loop as (Chung 2000):

$$K_f(s) = K_p\left(\frac{1+s\tau}{s\tau}\right) \quad (4.36)$$

$$H_c(s) = \frac{2\zeta\omega_n s+\omega_n^2}{s^2+2\zeta\omega_n s+\omega_n^2} \quad (4.37)$$

$$H_e(s) = \frac{s^2}{s^2+2\zeta\omega_n s+\omega_n^2} \quad (4.38)$$

Where,

$$\omega_n = \sqrt{\frac{K_p}{\tau}} \quad (4.39)$$

$$\zeta = \frac{K_p}{2\omega_n} = \sqrt{\frac{\tau.K_p}{2}} \quad (4.40)$$

The performance of the PLL algorithm during steady state depends on the shape of the input and the order of the loop filter. The steady state error for the step change of the derivative of the frequency in which the frequency varies in time is obtained with the second order PLL with PI loop filter. Choosing a higher frequency that yields a wider bandwidth can minimize this error(Chung 2000). Although this is not the case for all conditions such as the case in distorted utility when there is an increase in bandwidth, the tracking error also increases.

Considering the following parameters for calculating the gains of the PLL system:

Damping factor ζ = 0.707

Bandwidth = 100 Hz

$$\omega_n = 2\pi f_n = 2.\pi.100 = 628.32\ rad/sec$$

Therefore,

$$K_p = 2\omega_n\zeta = 2 \times 628.32 \times 0.707 = 888.44$$

$$\tau = \frac{K_p}{\omega_n^2} = \frac{888.58}{(628.32)^2} = 2.25 \times 10^{-3}\ sec$$

$$K_p = \omega_n^2 = 628.32^2 = 394786.02$$

4.6 The Three-Phase grid-connected VSI control technique

Generally, there are two main techniques for controlling the VSI which are voltage control method and current control method. The DC instability is not a major issue when designing the GCI as this can be overcome by implementing a fast current controller. However, the current control technique which can operate in a grid-connected mode proficiently is employed in this work due to the advantages of the current control technique for grid-connected application over the voltage control method such as protection of the inverter against overcurrent and fast dynamic response. The AC-side current of the VSI is first controlled by a control structure through the VSI terminal voltage in this technique. Also the phase angle and the amplitude of the line current for the VSI controls the real and reactive power with respect to the PCC voltage. Hence, the VSI is not under the risk of overload situations due to current control system. The current controller also has some other benefits such as robustness against mismatch in parameters of the VSI and AC system, a very high dynamic performance and better control precision (Abu-Rub et al. 2012; Gabe et al. 2009; Scheuer & Stemmler 1996).

However, the current control approaches are classified into three, namely: linear controllers, hysteresis controllers and predictive controllers. An improvement of linear controllers applies to all cases where sinusoidal current and voltage are needed, by implementing PI controllers in the rotating dq reference frame. Voltage and current signals are transformed to DC quantities, when the dq-frame is synchronized with the grid voltage resulting to a fast response time (Schonardie & Martins 2008; Borgonovo 2001; Kazmierkowski & Malesani 1998).

The advantages of the grid-connected VSI system in synchronous reference frame control are that the control variables are DC quantities in steady state in addition to all the features of the stationary reference frame. This feature makes the design of the compensator extremely easy, particularly in variable-frequency conditions. A schematic representation of the current control in dq synchronous reference frame with real and reactive power controller is illustrated in Fig. 4.11 below. Therefore, the active power P_s and reactive power Q_s are controlled by the components of the line current i_{gd} and i_{gq}. The feedback and feed-forward signals which are the voltages and currents in

abc frame are transformed to the dq frame and supplied to the VSI as shown in Fig. 4.1. Typically, the reference currents i_{dref} and i_{qref} are limited by corresponding saturation blocks in order to protect the VSI system.

The addition of integral terms in the compensators in dq reference frame control facilitates the realization of zero steady state error since the control variables are DC quantities. The representation of dq reference frame and grid connected VSI system control is also constant with the technique used for the dynamic analysis of the huge power system. Usually the modelling and analysing of the small signal dynamics of the power system is done in dq reference frame. The current controller is generally well-known for its better stability, better protection and time response is reduced in an occurrence of load transients, thus, additional advantages are assured by this solution (Teodorescu et al. 2011; Balu & Lauby 1994).

4.6.1 Model of Current controller

As previously mentioned, the implementation of the synchronous reference frame is preferred because of its advantages. The dq-frame transformation is employed in order to model the three-phase grid-connected PV system in the synchronous frame. the sum of the grid-side inductor and inverter-side inductor of the output filter is modelled as L with a corresponding series resistance of R so as to have a set of linear dynamic equations for the three-phase grid-connected PV system (Malek 2014).

When dq transformation is implemented to equation (4.20) the three-phase system in synchronous frame can be expressed as:

$$L\frac{di_{gd}}{dt} = v_{id} - Ri_{gd} + \omega Li_{gq} - v_{gd} \qquad (4.41)$$

$$L\frac{di_{gq}}{dt} = v_{iq} - Ri_{gq} - \omega Li_{gd} - v_{gq} \qquad (4.42)$$

A space vector with constant magnitude rotating at the same speed of the frame, results in a constant d and q components whereas when it rotates at a different speed it has a time-variable magnitude. Differential equations for the current in the dq-frame depends on the cross-coupling terms ωi_{gq} and ωi_{gd}, and have feed forward terms V_{gd} and V_{gq} (Reznik 2012; Schauder & Caddy 1982). These are some of the specific characteristics of dq-frame. Hence, the dq-frame rotating at angular speed ω is expressed in form of matrix as:

$$\begin{bmatrix} v_{id} \\ v_{iq} \end{bmatrix} = \overbrace{R\begin{bmatrix} i_{gd} \\ i_{gq} \end{bmatrix} + L\frac{d}{dt}\begin{bmatrix} i_{gd} \\ i_{gq} \end{bmatrix}}^{\text{Filter dynamics}} + \overbrace{L\omega\begin{bmatrix} -i_{gq} \\ i_{gd} \end{bmatrix}}^{\text{Decoupling}} + \overbrace{\begin{bmatrix} v_{gd} \\ v_{gq} \end{bmatrix}}^{\text{Feed-forward term}} \quad (4.43)$$

The following equations can be obtained from (4.41) and (4.42).

$$L\frac{di_{gd}}{dt} + Ri_{gd} = u_{idq}$$

$$v_{id} = u_{id} + v_{gd} - \omega L i_{gq}$$

$$v_{iq} = u_{iq} + v_{gq} - \omega L i_{gd} \quad (4.45)$$

The dq reference frame theory is responsible for the control of power for the grid-connected inverter resulting in the determination of the power in a reference frame. The aim of the grid-connected inverter is essentially to produce or receive sinusoidal currents; hence the d and q components of the currents reference are in form of DC (Rowan & Kerkman 1986).

The current reference component i_{dref} and i_{qref} is controlled to achieve the active power control and the reactive power exchange respectively and it is usually used to influence a desired power factor. The active and reactive powers supplied to the grid can be expressed as:

$$P_{dq} = {}^{3}/_{2}\,(v_d i_d + v_q i_q) \quad (4.46)$$

$$Q_{dq} = {}^{3}/_{2}\,(-v_d i_q + v_q i_d) \quad (4.47)$$

where v_d and v_q denotes the direct and quadrature grid voltage components while i_d and i_q are the direct and quadrature output current components of the inverter.

The active power is proportional to i_d and the reactive power is proportional to i_q based on the assumption that d axis is readily aligned with the grid voltage $v_{gq} = 0$ (Reznik 2012). Therefore, (4.46) and (4.47) can further be expressed as:

$$P_{dq} = {}^{3}/_{2}\,(v_d i_d) \quad (4.48)$$

$$Q_{dq} = -{}^{3}/_{2}\,(v_d i_q) \quad (4.49)$$

The current in dq frame can therefore be deduced as:

$$i_d = {}^{2}/_{3} \cdot {}^{P}/_{v_d}$$

$$i_q = -{}^{2}/_{3} \cdot {}^{Q}/_{v_d}$$

The control structure is represented in the Fig. 4.12 below. It is important to note that all the control, feed-forward and feedback signals are DC quantities in the steady state (Karimi et al. 2011; Yazdani & Iravani 2010).

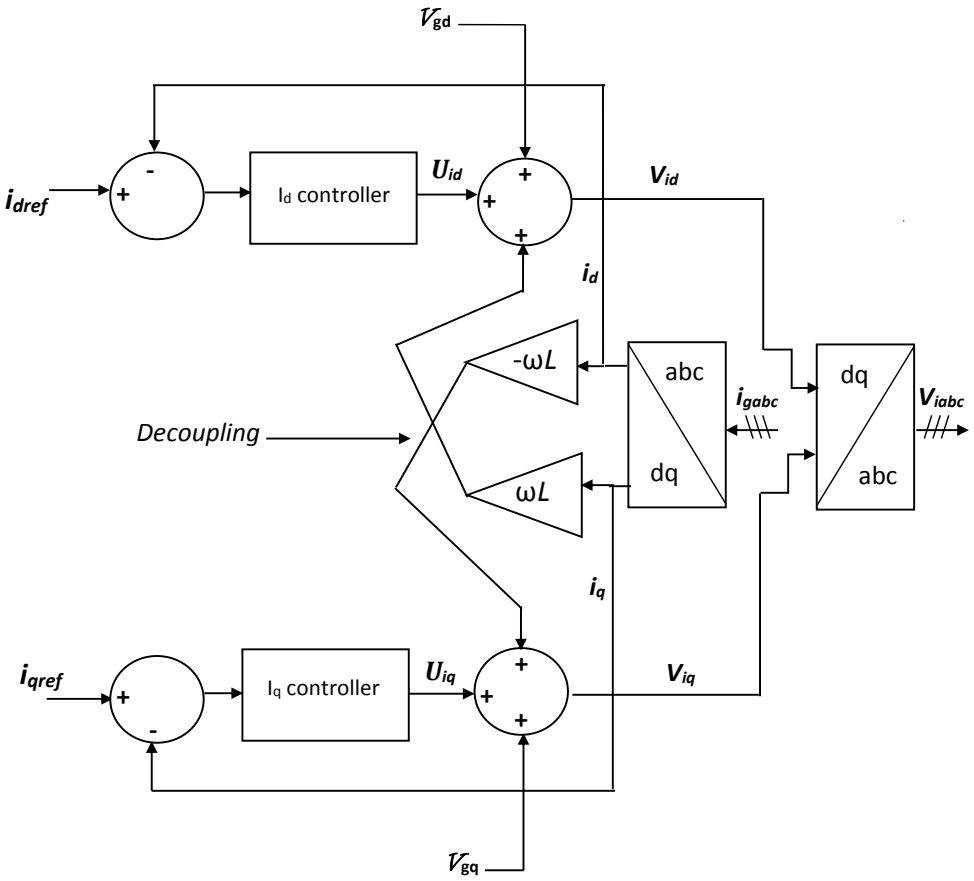

Figure 4.11: Control block representation of the current controlled VSI

4.6.2 Design of PI-Based Current Control Scheme

The PI controller is illustrated in the block representation in Fig. 4.13 below

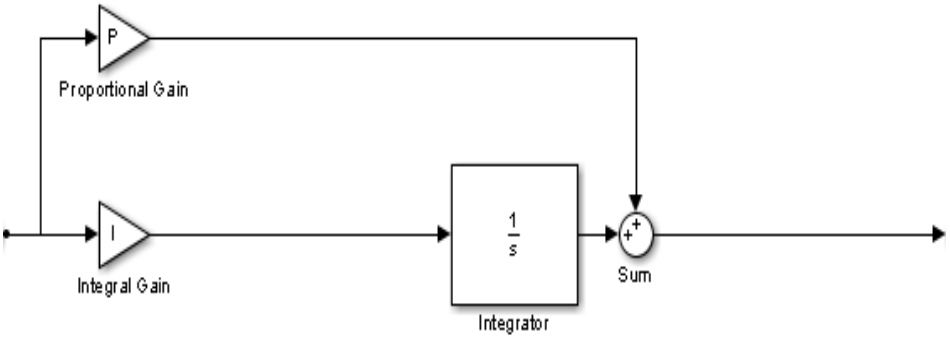

Figure 4.12: PI controller configuration

The PI control with grid voltage feed-forward v_{gd} is generally used for current-controlled VSI. However there are two problems that are associated with this solution: the PI controller lacks the capability to track a sinusoidal reference without steady state error and the inability to reject disturbance. This is as a result of the poor performance of the integral action when the disturbance is a periodic signal. the PI control is applied in a dq frame rotating with angular speed ω so as to overpower the poor performance of the PI in tracking sinusoidal reference and harmonic disturbances, where $\omega = 2\pi f_g$ and f_g signifies the grid frequency (Teodorescu et al. 2011).

The PI current controller transfer function where K_p and K_i are the proportional and integral gains respectively is defined as:

$$G_{PI}(s) = K_p + \frac{K_i}{s} \qquad (4.50)$$

$$= \frac{K_p s + K_i}{s}$$

G_d (s) is the control time delay due to elaboration of the computation device and to the PWM where T_e is the total control delay related with the computation procedure of the control system, the transfer function can be defined as:

$$G_d(s) = \frac{1}{1+sT_e} \qquad (4.51)$$

Where, $T_e = \frac{L}{R}$

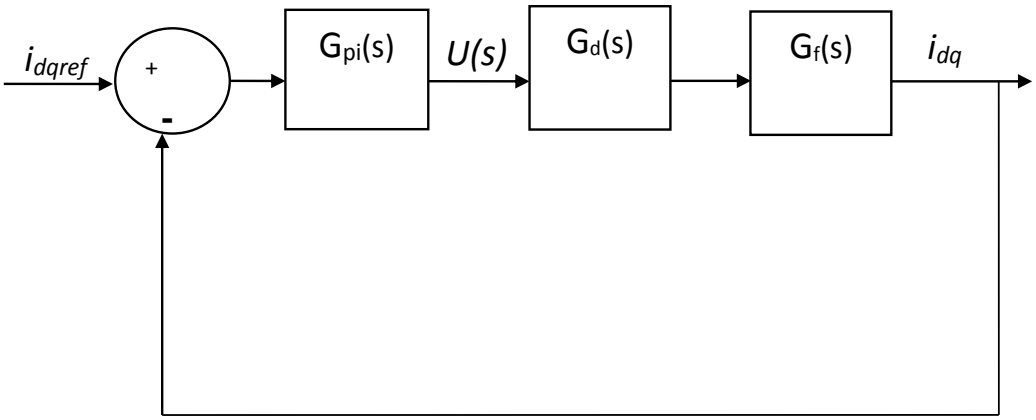

Figure 4.13: Block representation of current control loop

And G_f (s) which is the plant of the control loop is the transfer function of the filter considering the inductors and parasitic resistor values only.

$$G_f(s) = \frac{i(s)}{v(s)} = \frac{1}{R+Ls} \qquad (4.52)$$

The table 4.4 below show the parameters that will be required for the grid-connected VSI proposed for this work. The LCL filter parameters have been designed in the earlier part of this chapter.

Table 4.4: The VSI system parameters

Parameter		Value
Line to line RMS Voltage	$V_{LL/rms}$	380 V
Nominal power	P_n	10 kW
DC-Link voltage	V_{dc}	800 V
Inverter configuration	3φ	Three-phase system
Nominal current	I_{rms}	15.19 A
Power factor	pf	1
Grid frequency	f_g	50 Hz
Switching frequency	f_{sw}	30 kHz
Modulation range	m_a	0 < ma < 1

Table 4.5: Specifications of the LCL filter for VSI control algorithm

Parameter		Value
Grid side inductor	L_g	1.84 mH
Inverter side inductor	L_i	2.30 mH
Filter Capacitance	C_f	11.02 µF
Damping resistor	R_f	3.12 Ω
Resonance frequency	ω_{res}	9680 rad/sec
Approximated total inductor resistance	R	0.1 Ω

Using the parameters from the table 4.5 above, the transfer function of the plant for the control loop can be rewritten as:

$$G_f(s) = \frac{1}{R+Ls} \qquad (4.53)$$

where $L = L_i + L_g$ and $R = R_i + R_g$

$$G_f(s) = \frac{241.5}{24.15 + s}$$

Using optimal modulus criterion, from the equations above, the transfer function of the open loop current control for the system can be expressed as:

$$G_{oc}(s) = G_{PI}(s) \cdot G_d(s) \cdot G_f(s)$$

The transfer function of the open loop can be expressed in an easier form as:

$$G_{oc}(s) = \frac{K_p s + K_i}{s} \cdot \frac{1}{1+sT_e} \cdot \frac{1}{R+Ls} \qquad (4.54)$$

$$= \frac{K_p s + K_i}{s} \cdot \frac{1}{1 + sT_e} \cdot \frac{{}^{1}/_{L}}{{}^{R}/_{L} + s}$$

Evaluating further, this can be written as:

$$= \frac{K_p}{L} \cdot \frac{s + {}^{K_i}/_{K_p}}{s} \cdot \frac{1}{1+sT_e} \cdot \frac{1}{{}^{R}/_{L}+s} \qquad (4.55)$$

Setting the PI gain parameters to the following expression will eliminate large time constant:

$$\frac{K_i}{K_p} = \frac{R}{L} \tag{4.56}$$

Substituting (4.56) into the equation (4.55) gives:

$$= \frac{K_p}{L} \cdot \frac{s + {}^{R}/_{L}}{s} \cdot \frac{1}{1 + sT_e} \cdot \frac{1}{{}^{R}/_{L} + s}$$

$$= \frac{K_p}{L} \cdot \frac{1}{s} \cdot \frac{1}{1 + sT_e} \cdot$$

$$G_{oc}(s) = \frac{K_p}{Ls^2T_e + s} = \frac{{}^{K_p}/_{L}}{s^2T_e + s}$$

Let $k = {}^{K_p}/_{L}$ for easy derivation of the subsequent transfer function

$$G_{oc}(s) = \frac{k}{s^2T_e + s} \tag{4.57}$$

Therefore, the closed loop current control transfer function can be written as:

$$G_{cc}(s) = \frac{G_{oc}(s)}{1 + G_{oc}(s)}$$

$$G_{cc}(s) = \frac{\frac{k}{s^2T_e + s}}{1 + \frac{k}{s^2T_e + s}}$$

$$= \frac{k}{s^2T_e + s} \times \frac{s^2T_e + s}{s^2T_e + s + k}$$

$$= \frac{k}{s^2T_e + s + k}$$

$$\therefore\ G_{cc}(s) = \frac{{}^{k}/_{T_e}}{s^2 + {}^{s}/_{T_e} + {}^{k}/_{T_e}} \tag{4.58}$$

The second order system of the closed loop current control transfer function in the general form is expressed as:

$$G_{cc}(s) = \frac{\omega_n^2}{s^2 + 2\rho\omega_n^2 s + \omega_n^2} \tag{4.59}$$

Where ω_n denotes natural frequency of oscillation of the control system and ρ is the damping factor (Mataifa et al. 2015; Davari et al. 2009). Comparing both equations (4.58) and (4.59), the following can be deduced:

$$\omega_n^2 = {}^{k}/_{T_e}$$

$$\Rightarrow \omega_n = \sqrt{{}^{k}/_{T_e}} \tag{4.60}$$

$$2\rho\omega_n = {}^{1}/_{T_e}$$

$$\Rightarrow \omega_n = {}^{1}/_{2\rho T_e} \tag{4.61}$$

Relating equation (4.60) and (4.61), gives:

$$\sqrt{{}^{k}/_{T_e}} = {}^{1}/_{2\rho T_e} \tag{4.62}$$

Specifying ρ to be ${}^{1}/_{\sqrt{2}}$ and substituting $k = {}^{K_p}/_{L}$ back into equation (4.62) gives:

$$\sqrt{\frac{{}^{K_p}/_{L}}{T_e}} = \frac{1}{2\left({}^{1}/_{\sqrt{2}}\right)T_e}$$

$$\therefore K_p = \frac{L}{2T_e} \tag{4.63}$$

In order to compute the proportional and integral gains of the controller from the equations above, T_e was approximated to be 1 *ms* which represents the delay in the current control loop and the filter parameters in the table above is used for calculations as follow:

$$K_p = \frac{L}{2T_e}$$

$$= \frac{4.14 \times 10^{-3}}{2 \times 1 \times 10^{-3}} = 2.07$$

$$K_i = \frac{K_p R}{L}$$

$$= \frac{2.07 \times 0.1}{4.14 \times 10^{-3}} = 50$$

The PI compensator proportional and integral gain values computed above are used to start the analysis using the self-tuning tool of the PID block in Simulink control toolbox. The tool facilitates the design of the control system by getting rid of the challenges encountered during the design of the control system manually. The system was first linearized at a simulation snapshot of 0.05 before the tuning could be implemented. The tuned step response of the system shows a faster transient response with zero steady-state error. The tuned response gives a minimal overshoot for the step response and the bandwidth of the controller for the magnitude and phase response is 914rad/s. The step response and frequency response of the closed-loop current control system is depicted in the Fig. 4.15 and Fig. 4.16 below respectively.

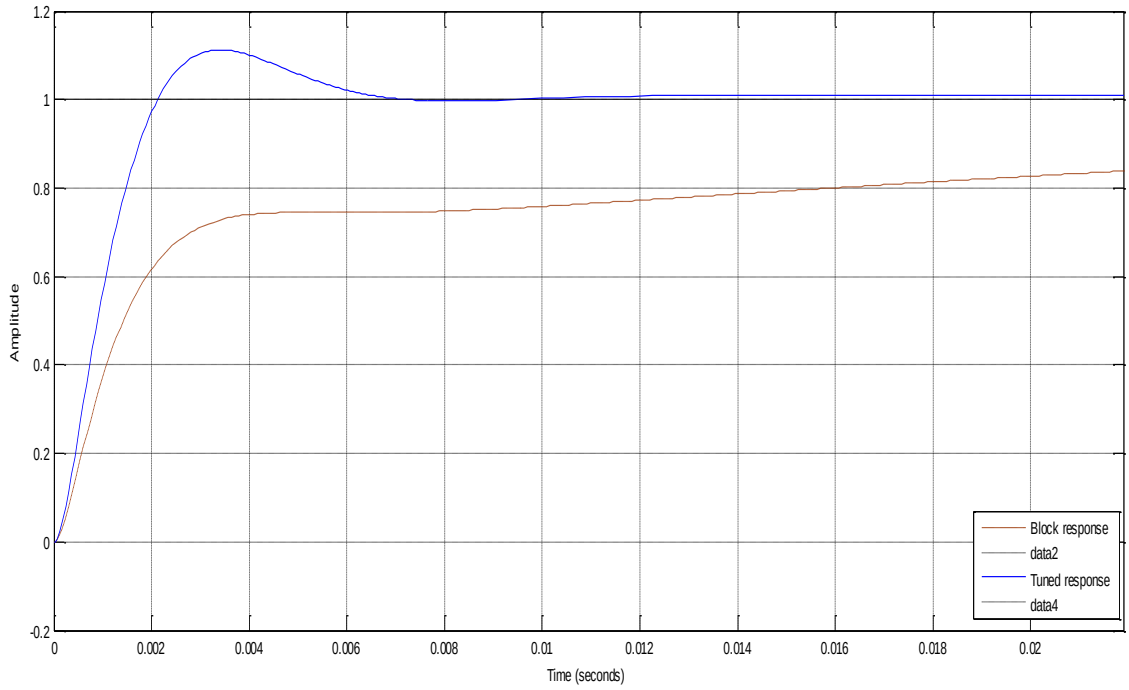

Figure 4.14: Current control loop step response

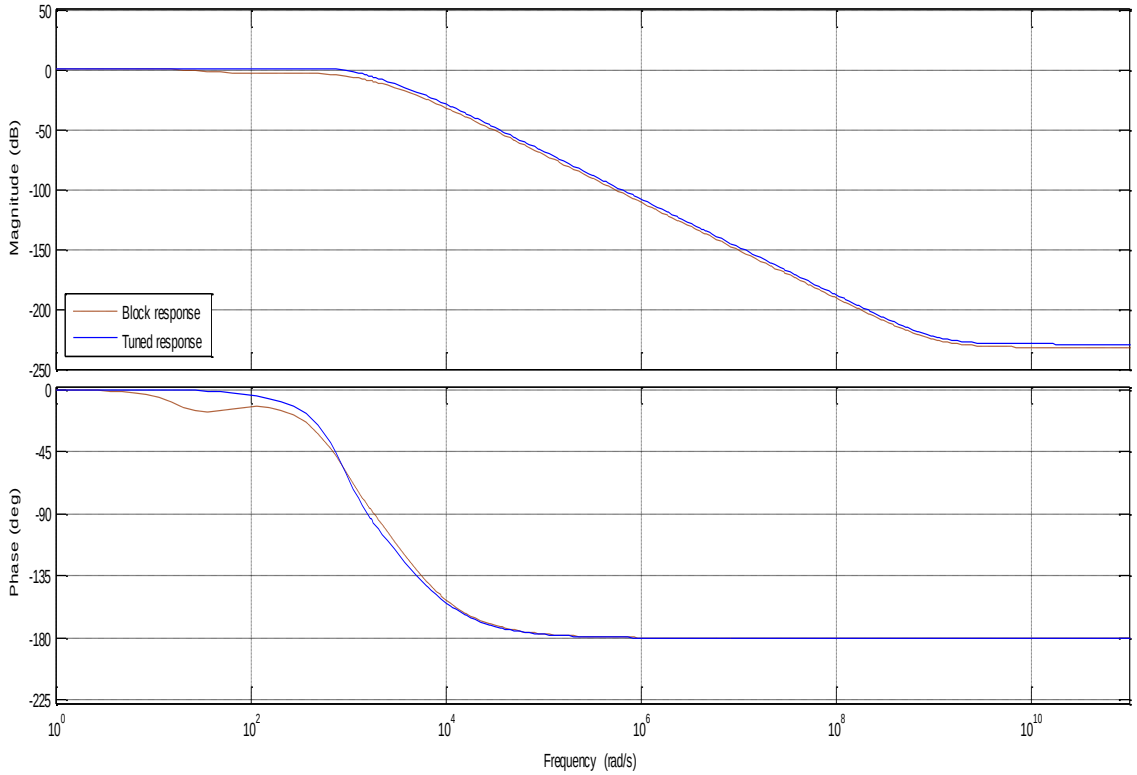

Figure 4.15: Current control loop frequency response

4.7 Conclusion

The design procedure for the LCL filter topology and the analytical description of the inverter to be developed have been described in this chapter. One of the main highlight of this chapter was also the design of the parameters of the control algorithm for the power electronics VSI system to be developed in the Simulink software. The control of GCI is essential due to the intermittent nature of the renewable energy which can results in instability of the system. The designed PI controller has been implemented in Simulink using the self-tuning tool of the PI block. The performance of the designed PI controller to work proficiently when the inverter is in grid-connected mode will be confirmed in the next chapter through various simulations.

CHAPTER 5

SIMULATION RESULTS AND DISCUSION

5.1 Introduction

This chapter concentrates majorly on the discussion of the modelling and simulation results. The design of the grid-connected voltage source inverter proficient of operating in grid-connected mode was developed and simulated using the SimPowerSystems toolbox of MATLAB/SIMULINK software.

The other part of this chapter discusses the simulation results of the inverter output voltage before the LCL filter and without the controller. The simulation results of inverter control design by implementing the PI controller and the performance of the LCL filter in grid-connected mode operation was also discussed. The simulation results of the current control of the inverter using synchronous reference frame transformation and the PI compensator is described.

5.2 Grid-connected inverter

The system as seen in the Fig. 5.1 below consists of the inverter and the LCL filter. The grid connected VSI model, which consists of building blocks from Simulink using the SimPowerSystems design tool. The universal bridge was chosen to represent the inverter model as this allows input of parameters. The block implements a bridge of selected power electronics devices in which three number of bridge arms with IGBT switches was chosen for this work. The utility grid is considered to be ideal and also the DC-link voltage which serves as the input to the grid-connected inverter system was considered to be an ideal voltage source.

The three-phase LCL filter which is made up of inductive and capacitive components has been designed in the previously in chapter four. It is connected to filter out the harmonic content by smoothing the inverter output voltage. The LCL filter is commonly used for current control algorithm in grid-connected systems.

The control of the grid-connected inverter which supplies the system with active and reactive power system is implemented using the current control approach. However, the grid connected system has to be linearized before the Self-tuning tool of the PI controller could be implemented. Due to the non-linear characteristics of the VSI block with the IGBT, the averaged model block was used for the purpose of linearizing the system. The VSI grid-connected inverter system which was simulated is depicted in the

figure 5.1 below and the current controller which was implemented is represented in figure 5.2 below. The linearized model is shown in figure 5.3 below.

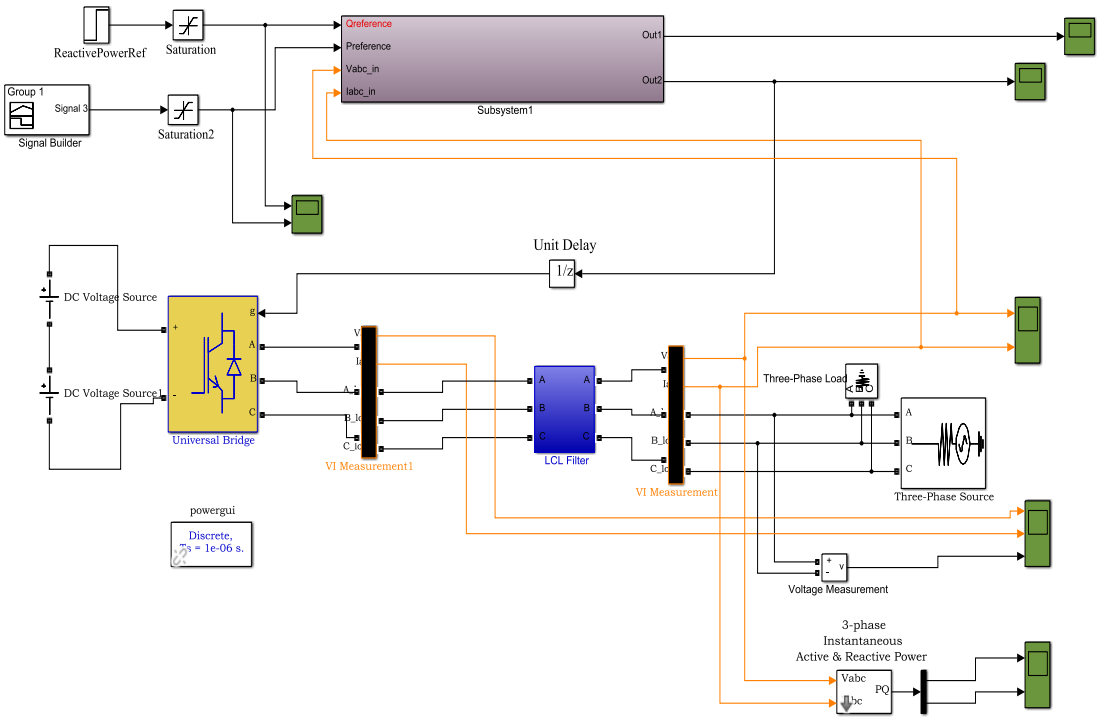

Figure 5.1: Grid-connected VSI model in Simulink

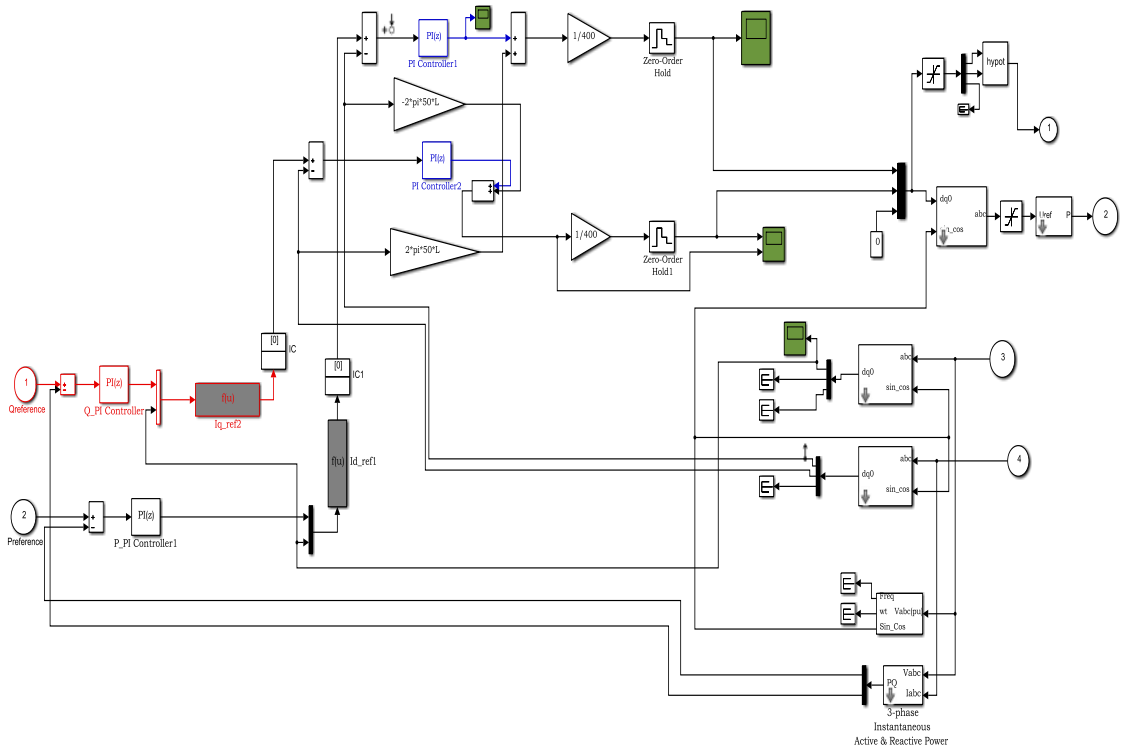

Figure 5.2: Current control system of the grid connected VSI in Simulink

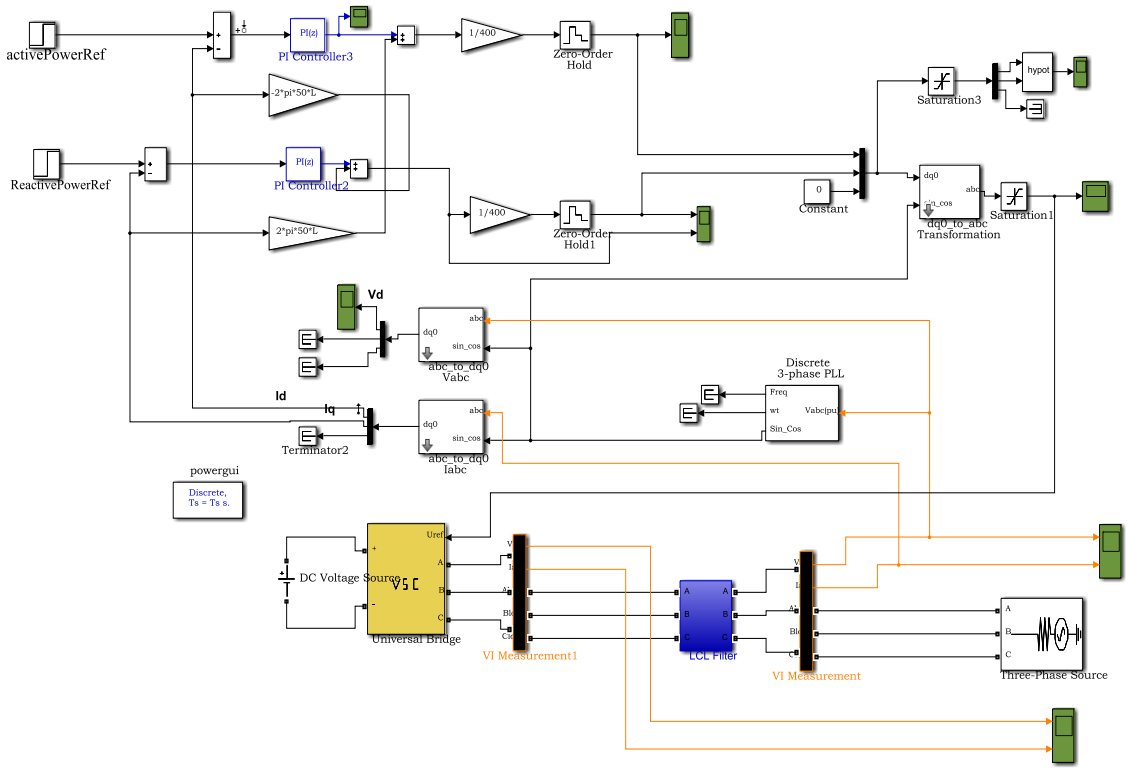

Figure 5.3: Linearized model of grid-connected VSI

5.3 Simulation Results

Different instances of the step changes in active and reactive power injected into the grid have been considered for analysis and performance evaluation of the designed grid-connected inverter model. The inverter output voltage and output current as well as the grid-side voltage and output have been studied. The harmonic analysis of the current injected into the grid was also examined.

The active power and reactive power have been varied under different states using the signal builder block from Simulink. Therefore, to monitor how the system performs under the above conditions, the simulations have been carefully carried out. In this set of simulation study, the active power of 10 kW was supplied by the inverter to the grid at nominal voltage while the reactive power remained 0 var at a simulation time of 0.5 μs.

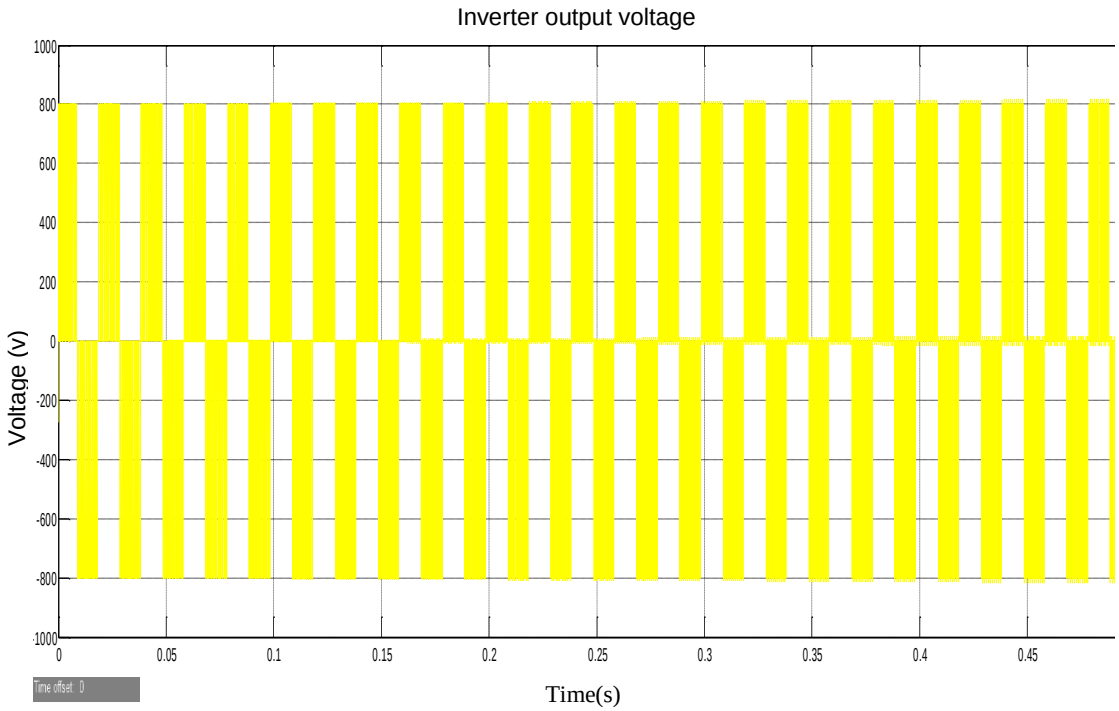

Figure 5.4: inverter switched phase voltage V_a before the filter

The conversion of the DC to AC power was implemented using inverter performing pulse width modulation at a higher switching frequency compared to the nominal frequency of the modulated signals which was used to achieve the design of the AC side. The result of phase V_a and i_a are depicted in the Fig. 5.4 and Fig. 5.5 respectively. The measurement block in Simulink was used to measure the output of the inverter which has both high and low order harmonics due to the switching influence of the IGBT switches before the LCL filter was connected. The inverter output voltage changes between -800V to 0 V and to 800 V

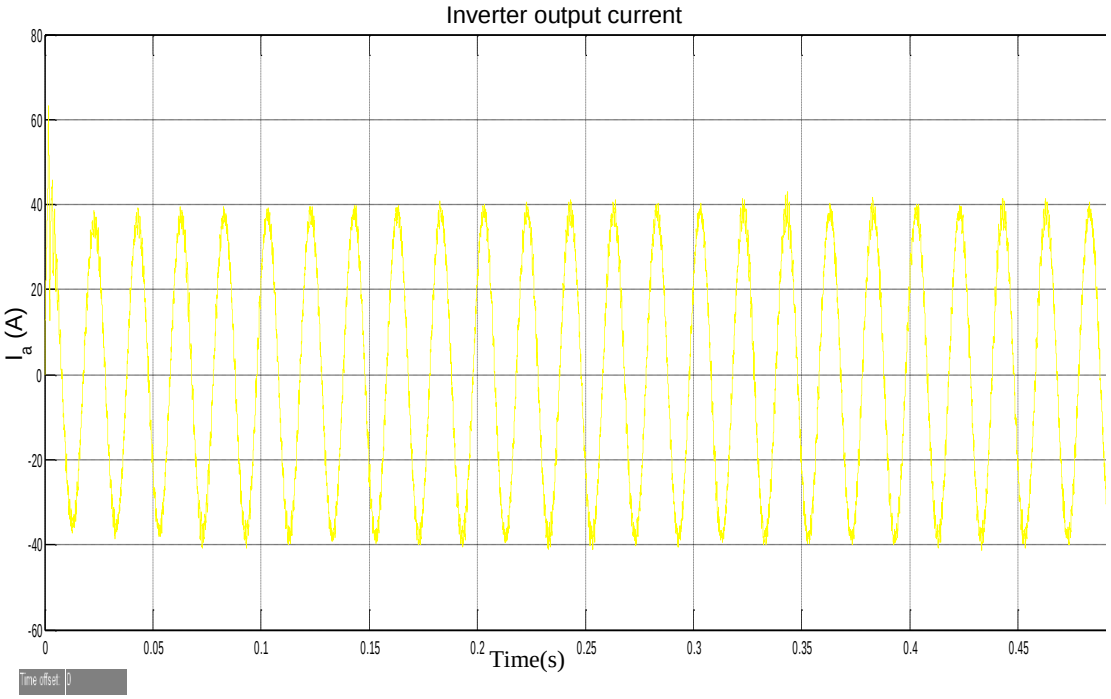

Figure 5.5: Inverter output current i_a

The harmonic contents present at the output of the inverter have been filtered out by utilizing the LCL filter. The importance of the filter is evidenced from the output waveform of the filter compare to the waveform at the input. The output waveform of the inverter contains only fundamental and low order harmonics. The ripple attenuation capability of the LCL filter to meet the interconnection standards is shown in the results obtained. The three-phase output voltage and current waveform of the grid-connected inverter after LCL filter have been connected are represented in the Fig. 5.6 and Fig. 5.7 respectively.

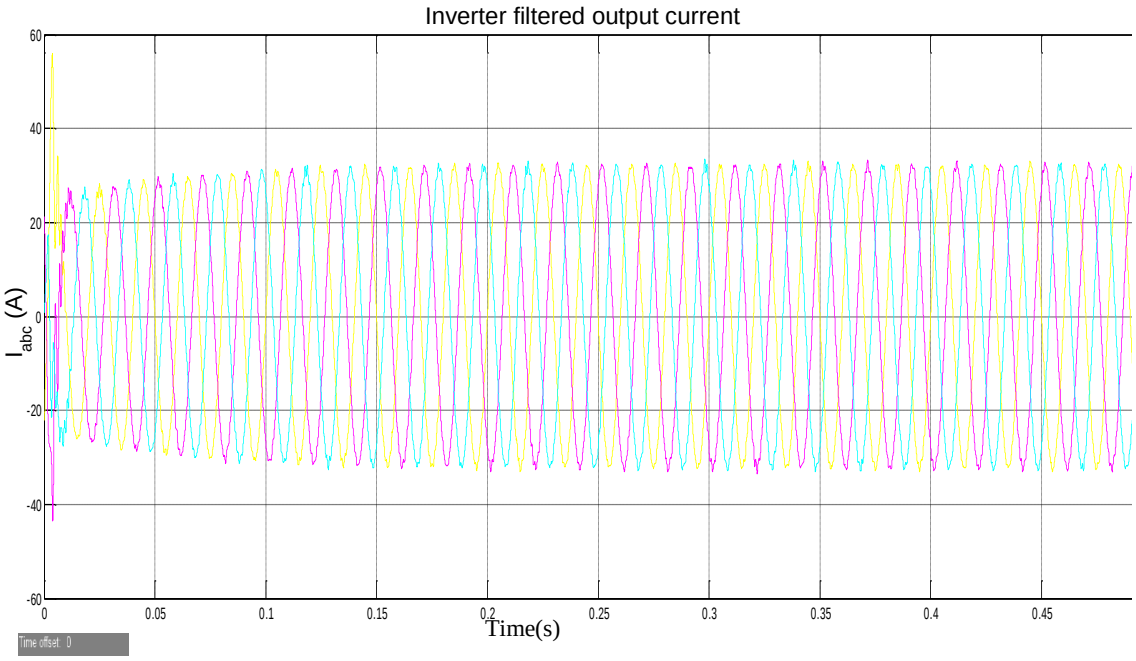

Figure 5.6: Inverter filtered output current of three-phase grid-connected inverter

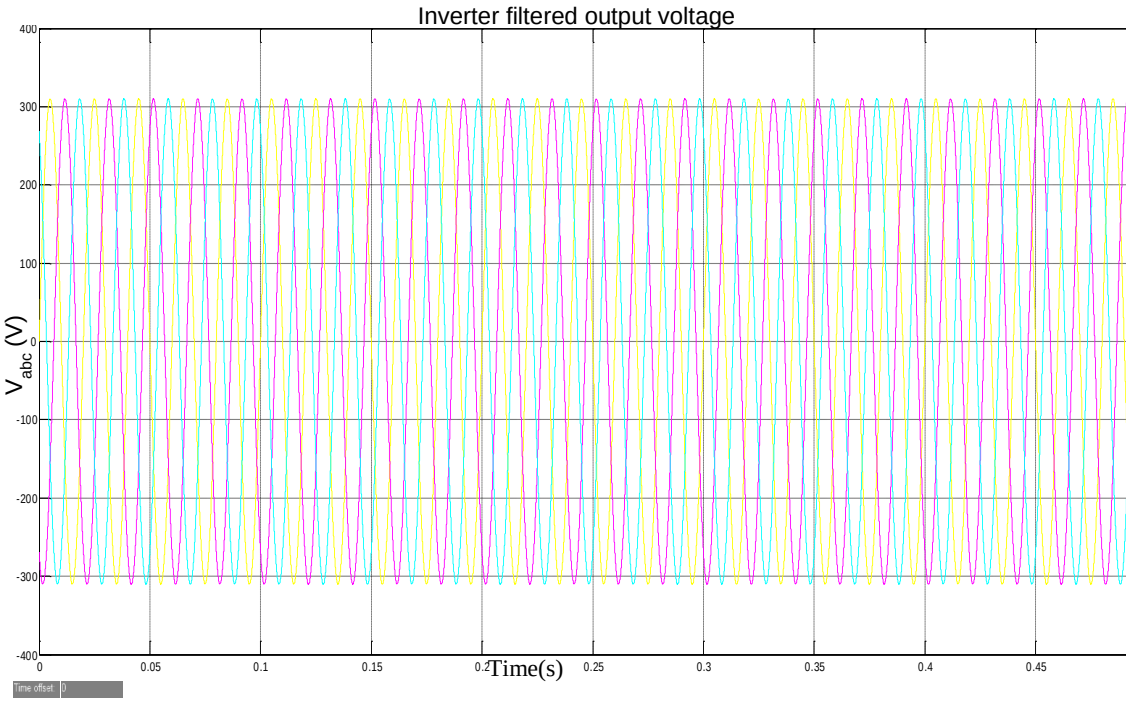

Figure 5.7: Inverter filtered output voltage of three-phase grid-connected inverter

The Phase voltage and line current at the grid-side i.e V_a and I_a are represented in Fig. 5.8 and the phase voltage and phase angle from the PLL is shown in Fig. 5.9 below. The grid-connected VSI is required to operate at unity power factor, therefore, the grid

phase voltage and grid phase current injected into the grid have been established in Fig. 5.8. The capability of the PLL (Phase locked-loop) to generate the phase angle for the adequate synchronization of the inverter terminals to grid is shown in the operation of the PLL in Fig. 5.9 below.

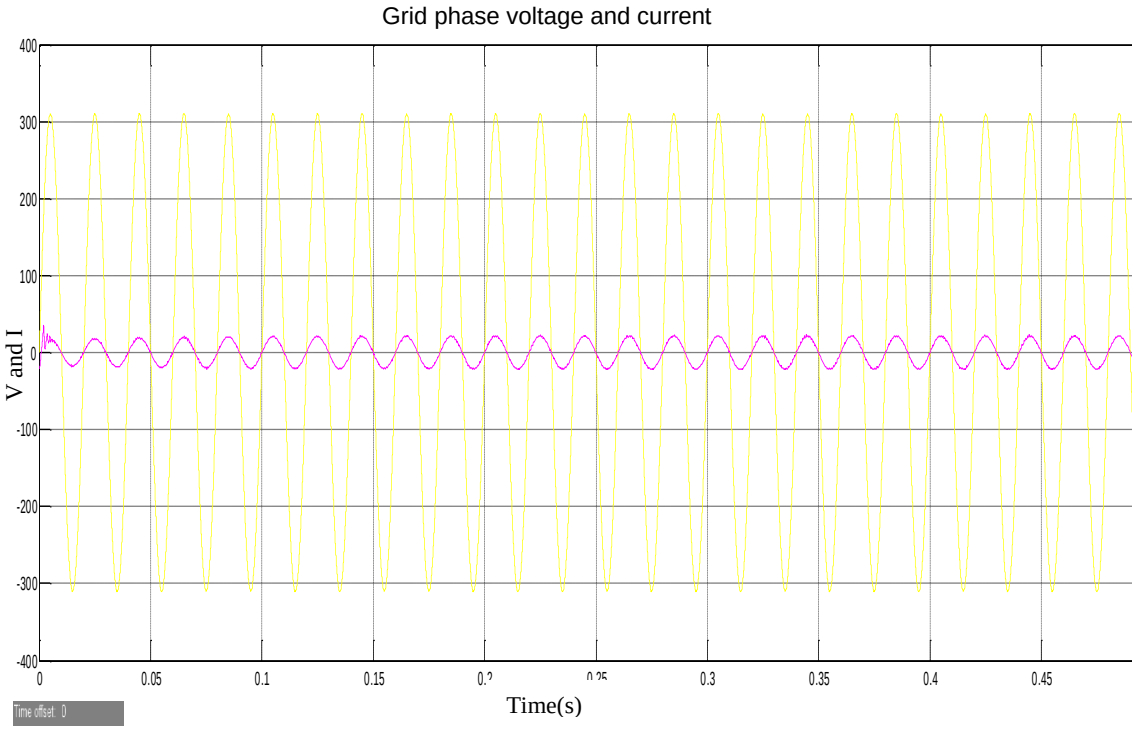

Figure 5.8: Phase voltage V_a and grid current i_a

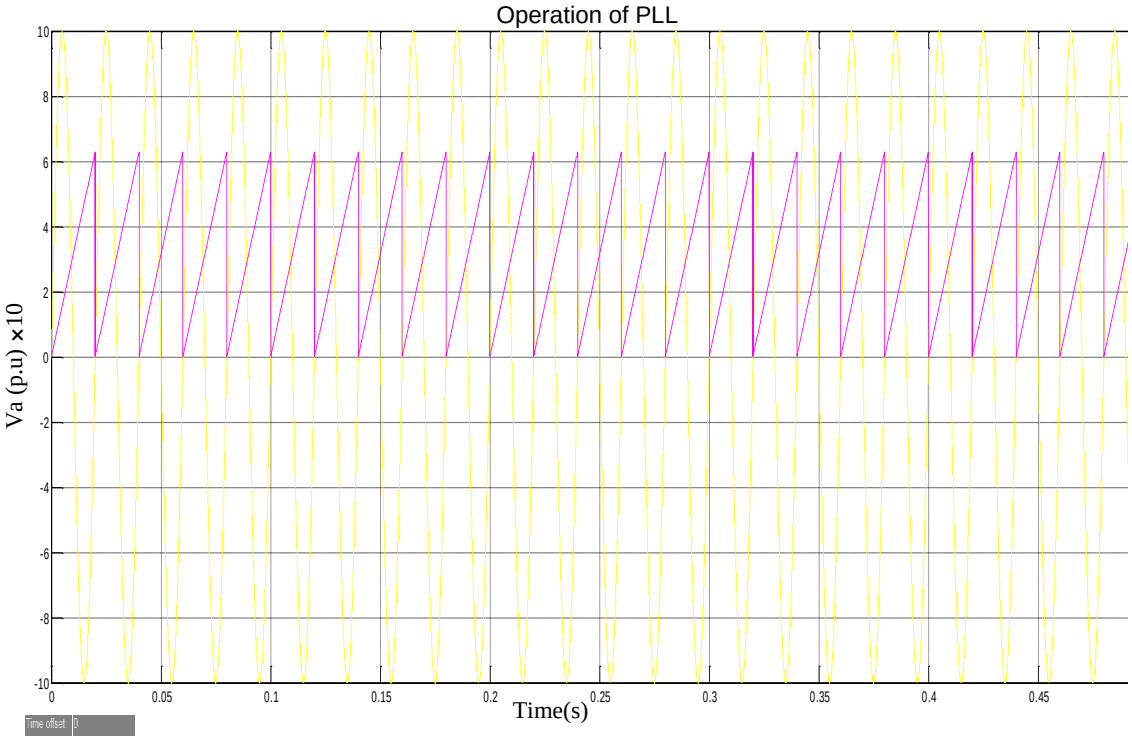

Figure 5.9: Phase voltage V_a and phase angle

The flow of active and reactive power into the grid is also displayed in Fig 5.10 and Fig. 5.11 respectively. These are the powers supplied by the GCI system.

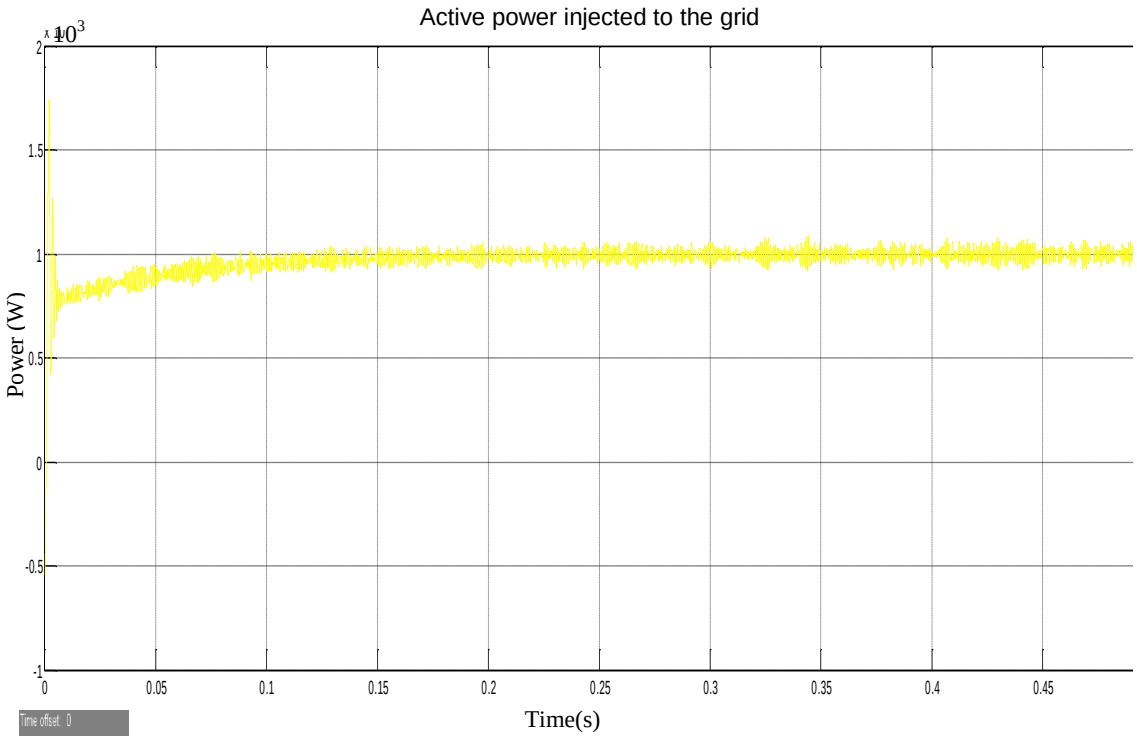

Figure 5.10: Active power 'P' injected into the grid

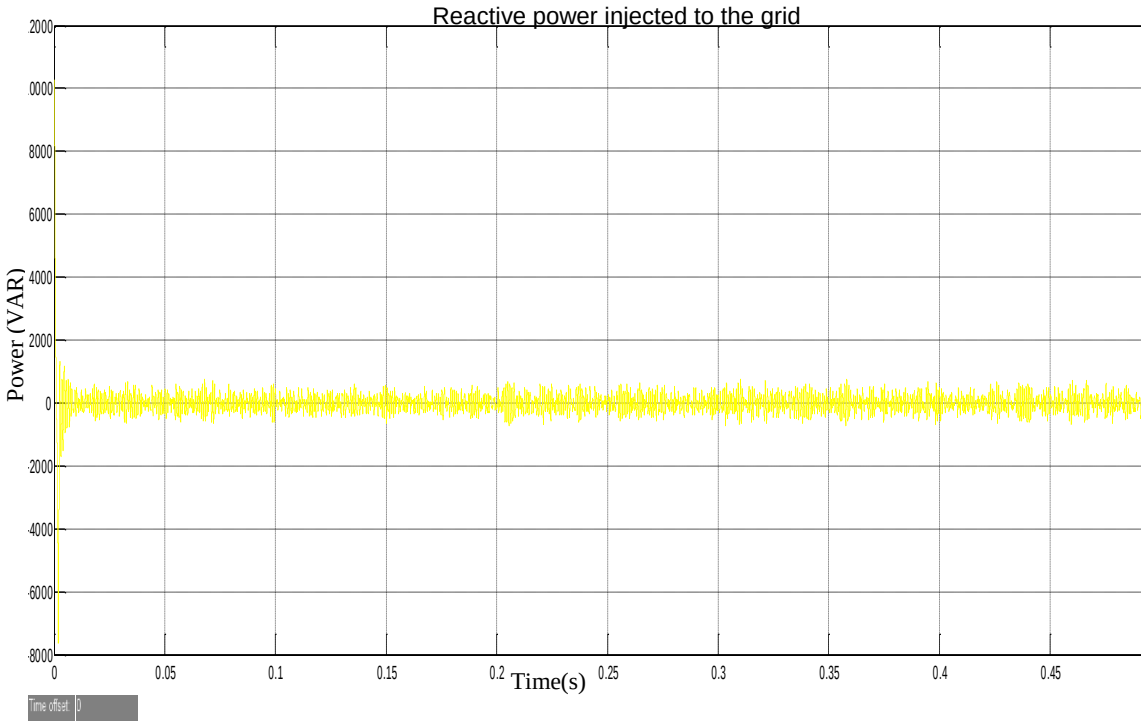

Figure 5.11: Reactive power 'Q' injected into the grid

The tracking response of the d current component is plotted in Fig 5.12. It shows the capability of the controller for the d axis in adequately tracking the set power with a steady state which is nearly zero as seen in the plot for the control loop error in Fig. 5.13 below.

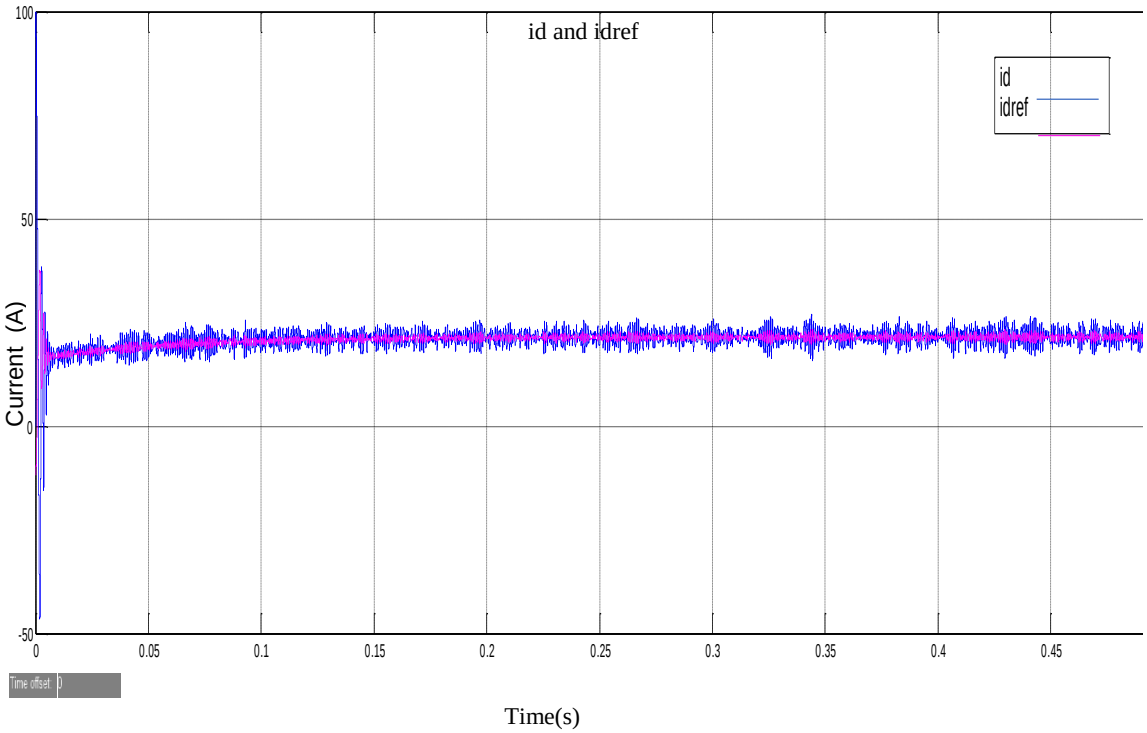

Figure 5.12: i_d current response to reference command

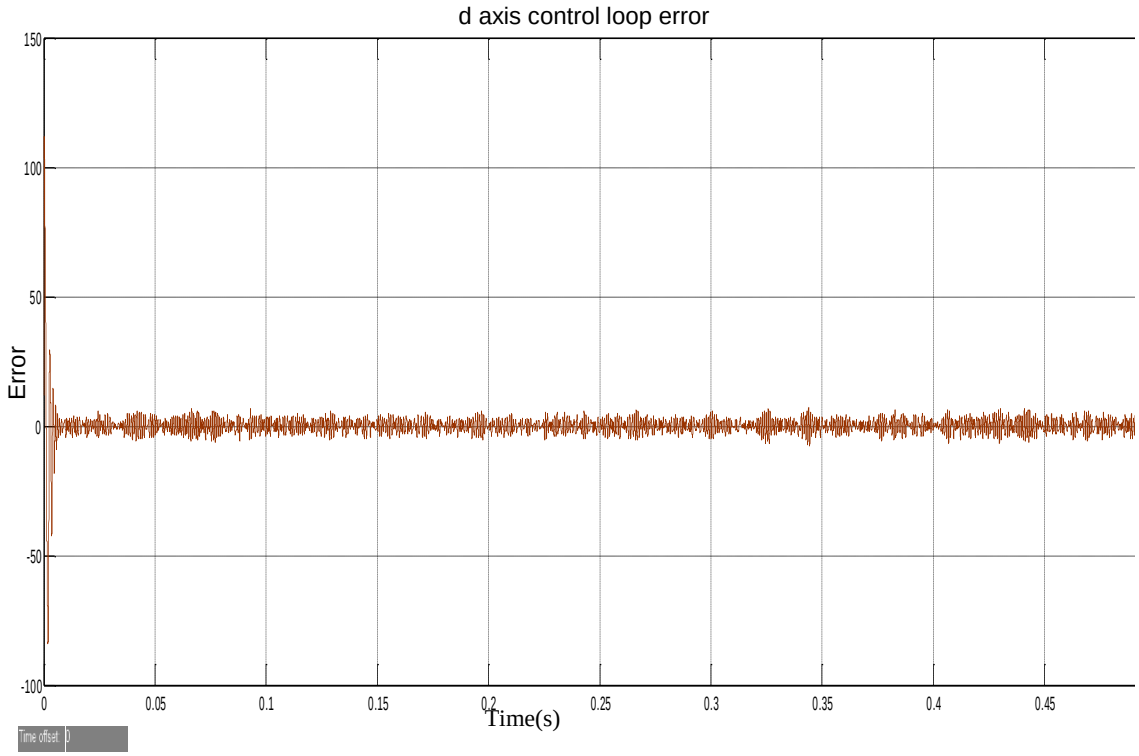

Figure 5.13: Current control loop error for i_d current

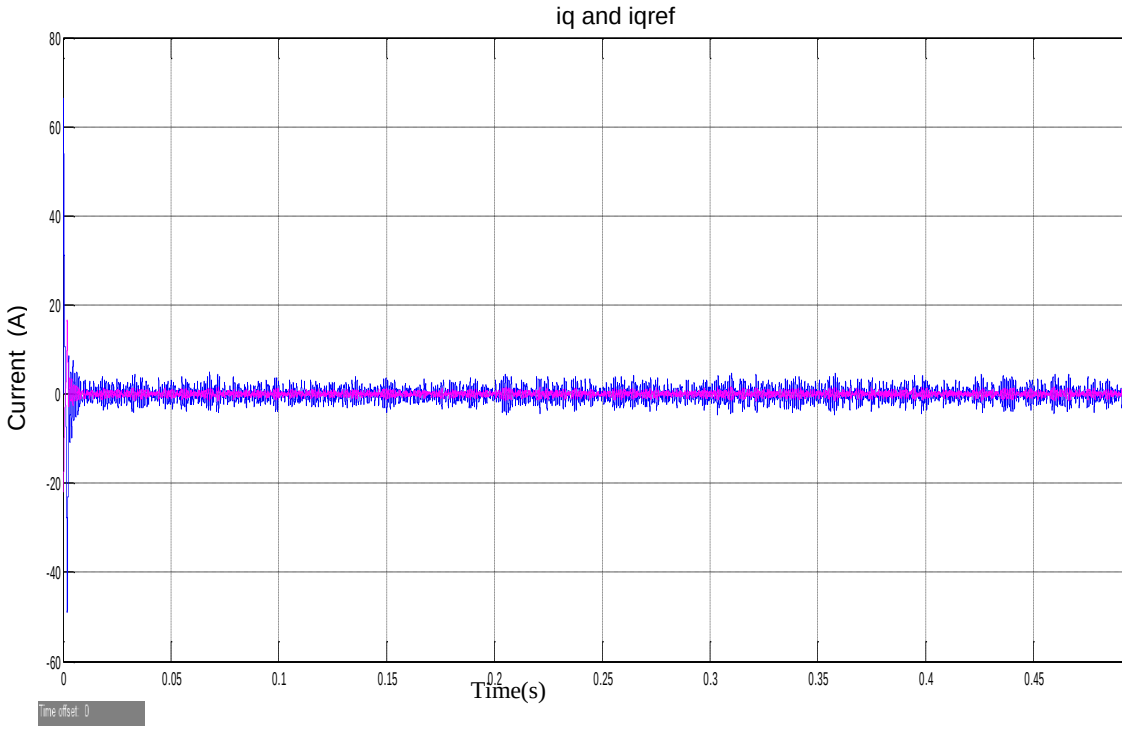

Figure 5.14: i_q current response to reference command

The tracking response of the q current component has also been plotted in Fig 5.14. It shows the capability of the controller for the q axis in adequately tracking the set power

with a steady state which is nearly zero as seen in the plot for the control loop error in Fig. 5.15 below.

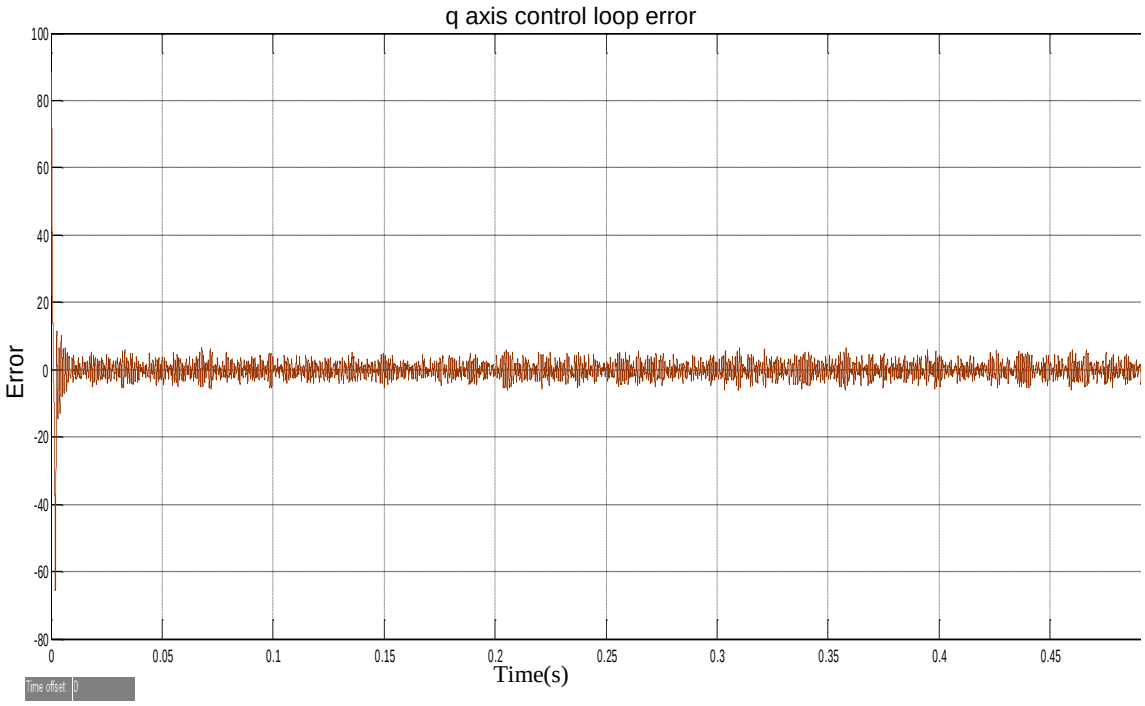

Figure 5.15: current control loop error for i_q component

The tracking response of the d and q measured voltage component has been plotted in Fig 5.16. Both d and q axis of the inverter voltage is regulated. It is significant to note that the q axis is maintained at zero for the simulations.

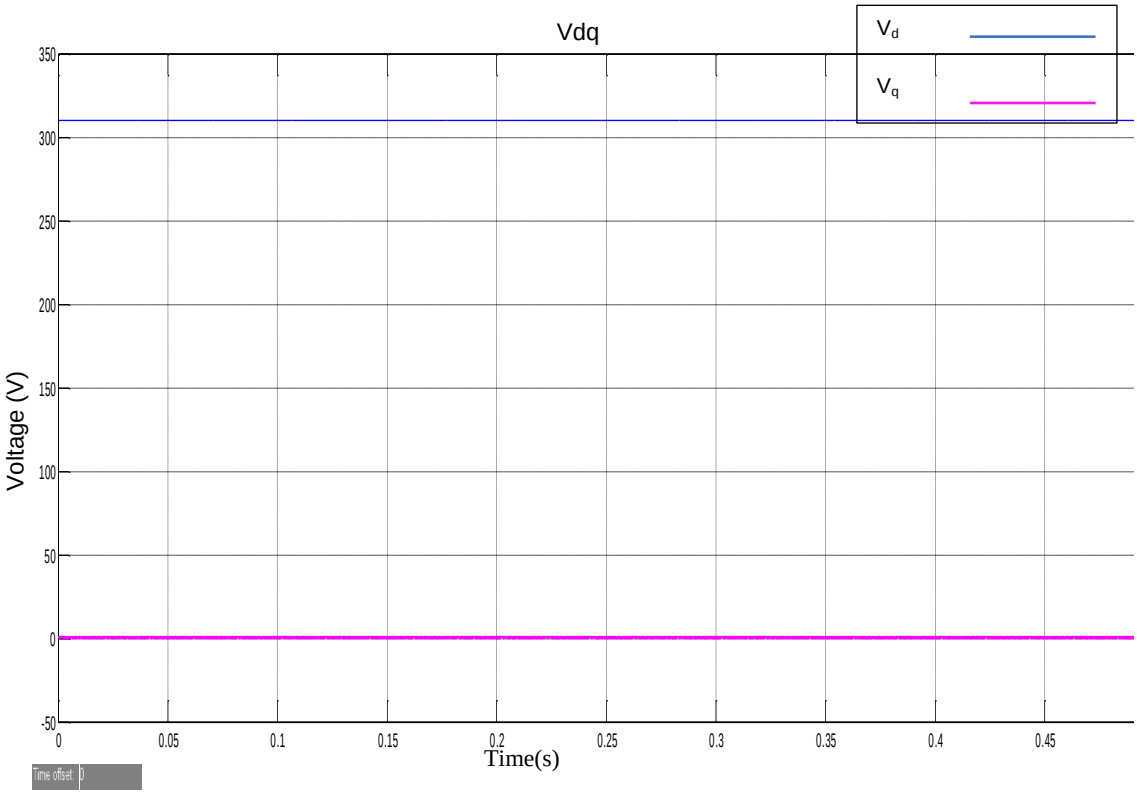

Figure 5.16: d and q components of voltage measured

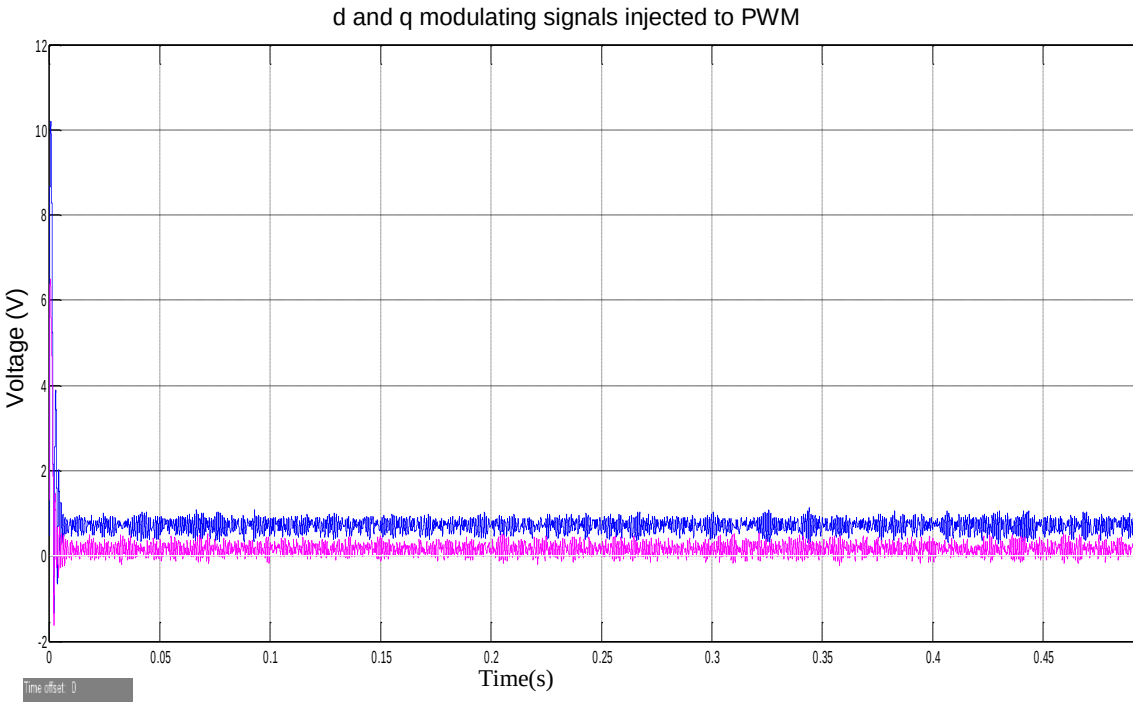

Figure 5.17: d and q components of the modulating signals directed to the PWM

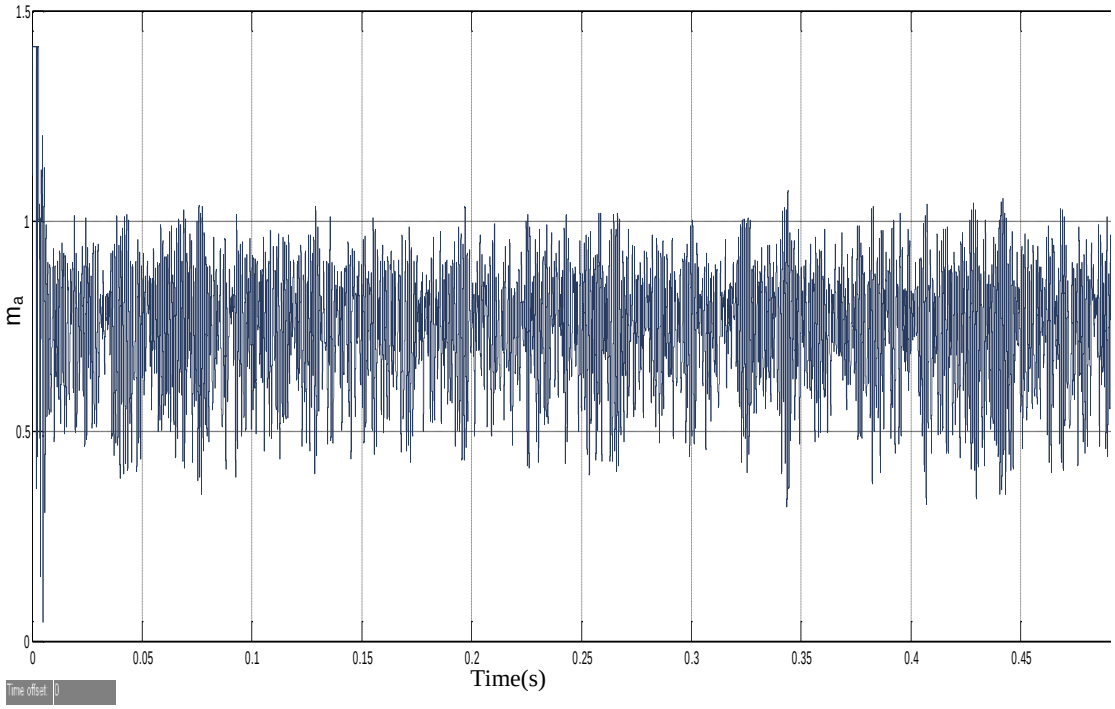

Figure 5.18: Modulation index

The Fig 5.12 and Fig. 5.14 represent the reference tracking of the d-axis current and q-axis current in response to the corresponding references. As mentioned earlier, it can be observed that the respective currents tracks the reference very close to a steady state error of zero which are displayed in Fig. 5.13 and Fig. 5.15 for the d and q current components respectively. The d and q components of the measured voltage have also been shown in Fig. 5.16. The q component of the voltage in the current controller is kept at zero as it can as well be observed. The d and q components injected into the PWM generator are also displayed in Fig. 5.17. The system requirement is that the modulation index should be between 0 and 1 and this has been presented in Fig 5.18.

The FFT (Fast Fourier Transform) analysis which was used to observe the total harmonic distortion (THD) of the grid current is displayed in Fig. 5.19 below. When 10 kW of active power and 0 VAR of reactive power are supplied by the inverter to the grid at nominal voltage, the THD injected into the grid is 3.26% as seen the FFT analysis.

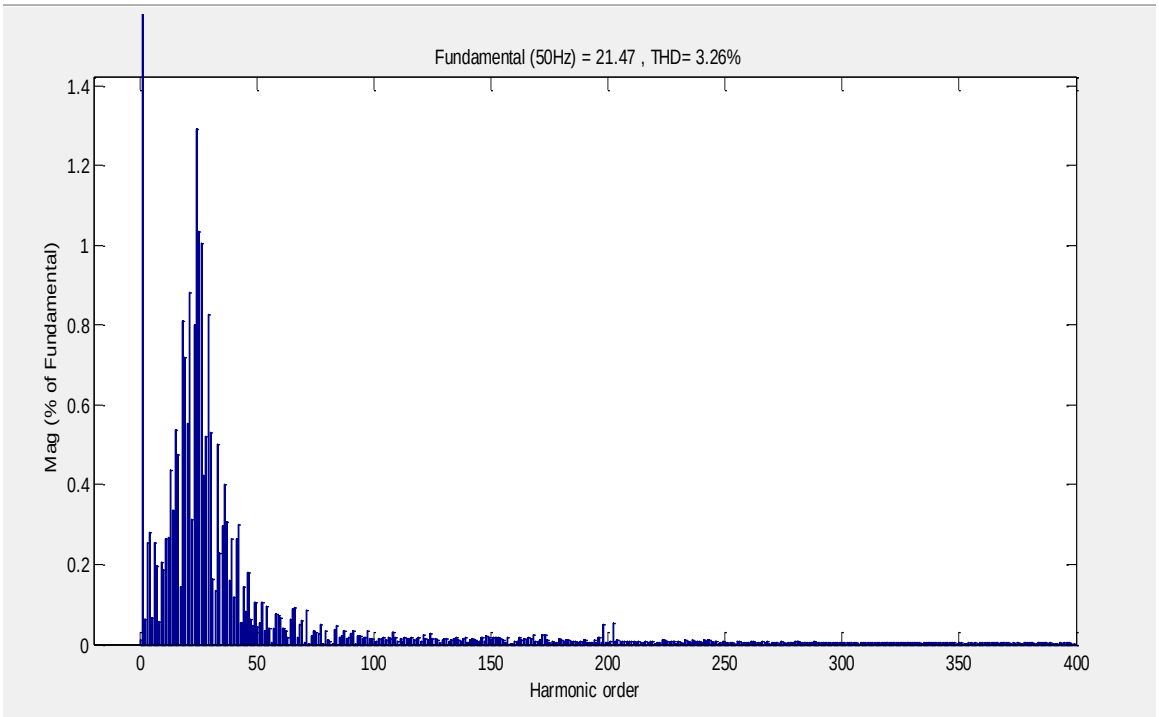

Figure 5.19: FFT Analysis showing THD of line current injected to the grid

5.3.1 System performance with step reference change in active and reactive power

The next step reference command occurs when the active power changes from 10 kW to 30 kW at time 0.2 s and the reactive power also changes to 10 kVAR at the same time. The response of the inverter phase current, grid current, phase voltage and current, active power and reactive power are displayed in Fig. 5.20, Fig. 5.21, Fig. 5.22, Fig. 5.23 and Fig. 5.24 respectively. It can be observed from Fig. 5.23 and Fig. 5.24 that the power tracks the reference smoothly and at 0.2 s when there is a step change in the injected power results into transient which is injected into the system at that time.

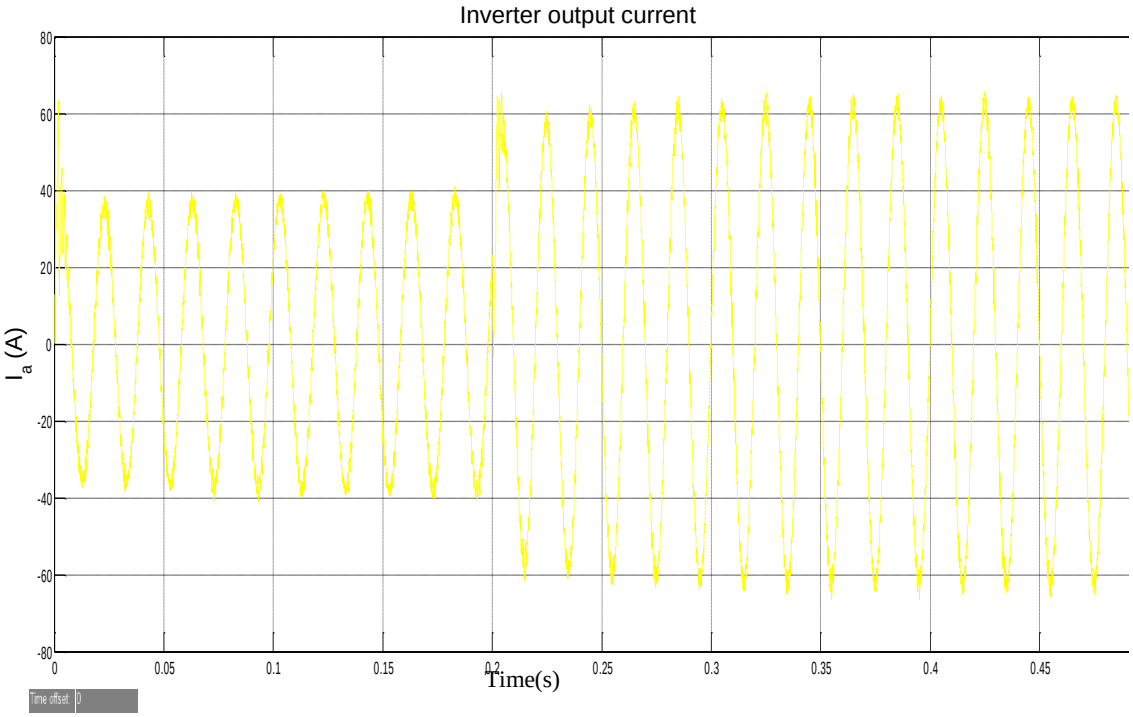

Figure 5.20: Inverter output current i_a

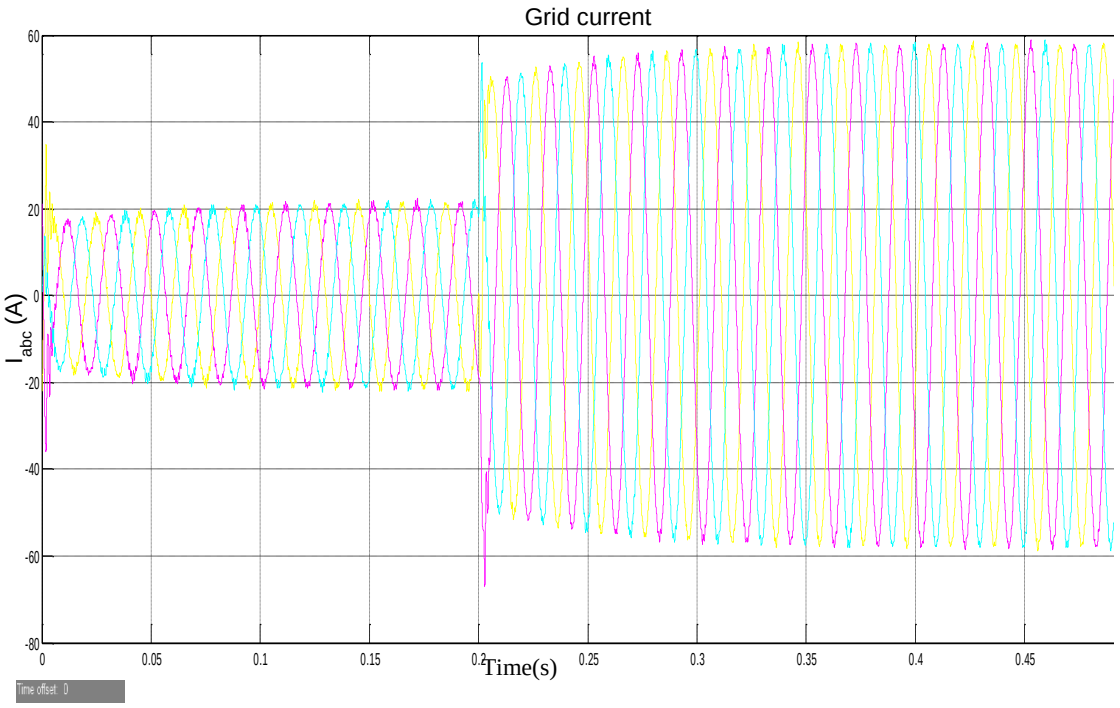

Figure 5.21: Grid current response to change in reference command of active and reactive power

The response of the inverter line current at 0.2 s is indicated in Fig. 5.20 showing a transition process occurring at that time due to step change in active power from 10 kW

to 30 kW and 0 VAR to 10 VAR. The transient is also observed in the three-phase grid current in Fig.5.21 and in the phase voltage and current response represented in Fig. 5.22. The spikes noticed during this transition is essential in order to have a fast response to the step input.

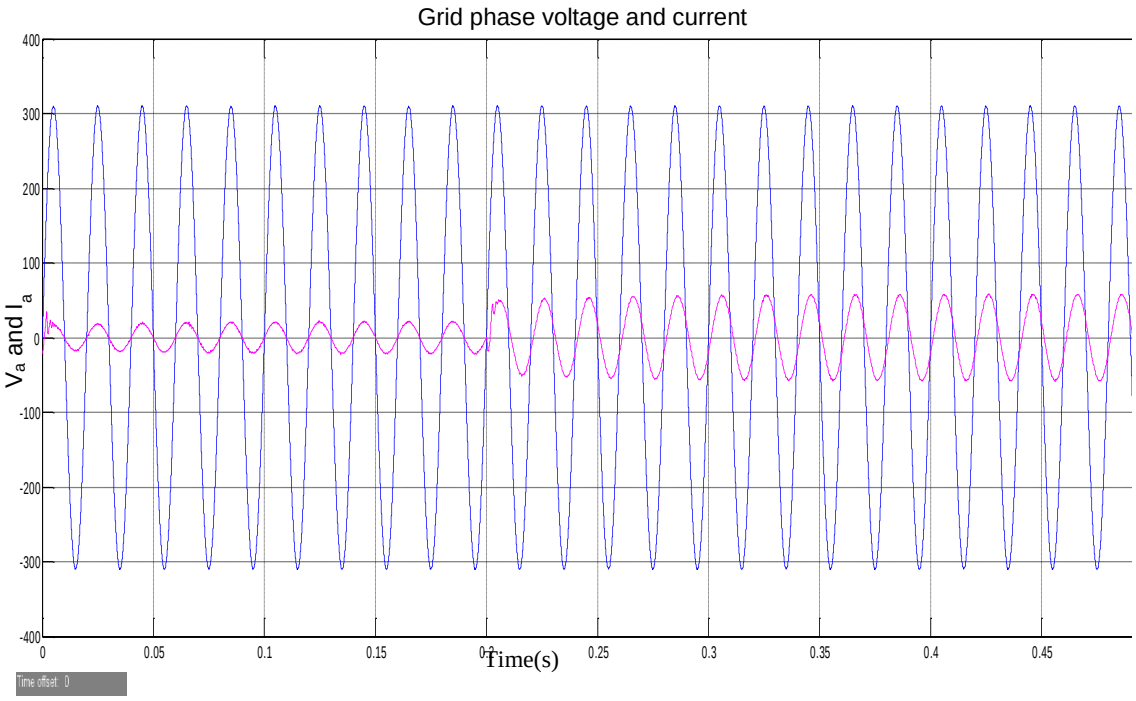

Figure 5.22: Phase voltage and grid current response to change in step reference command of active and reactive power

The set power reference for the active power is set to 30 kW at a simulation time step of 0.2 s as shown in Fig 5.23 while the grid-connected VSI reactive power reference is 10 kVAR represented in Fig 5.24 which means the grid is required to deliver reactive power to the GCI. The dc link voltage is maintained at 800 V_{dc} for this set of simulations.

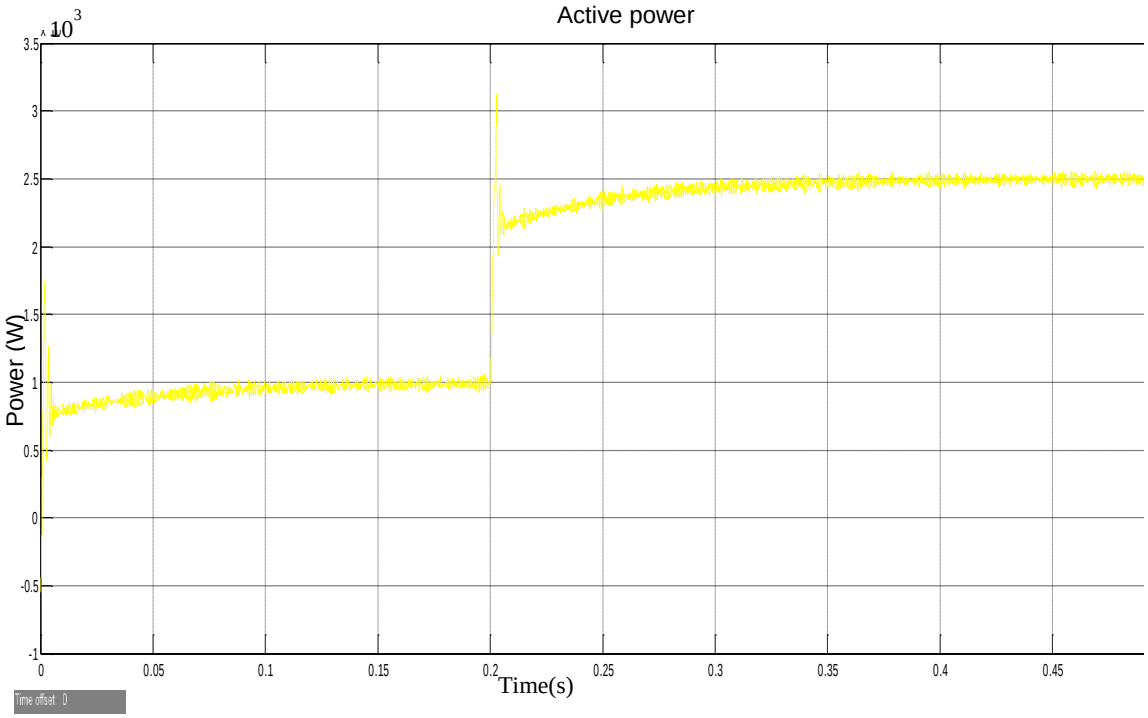

Figure 5.23: Active power 'P' injected into the grid

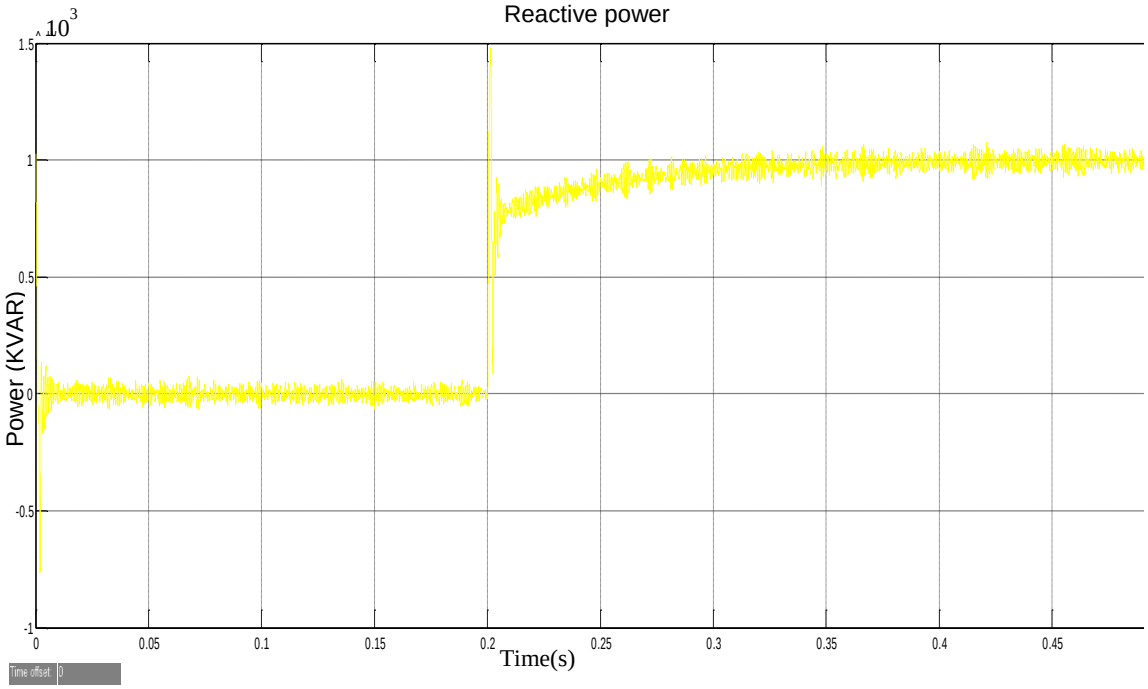

Figure 5.24: Reactive power 'Q' injected into the grid

The tracking response of the d current component is plotted in Fig 5.25. It shows the capability of the controller for the d axis in adequately tracking the set power with a steady state which is nearly zero as seen in the plot for the control loop error in Fig. 5.26 below. Some spikes are noticed at 0.2s when the step change occurred which is required for rapid response to the step reference input.

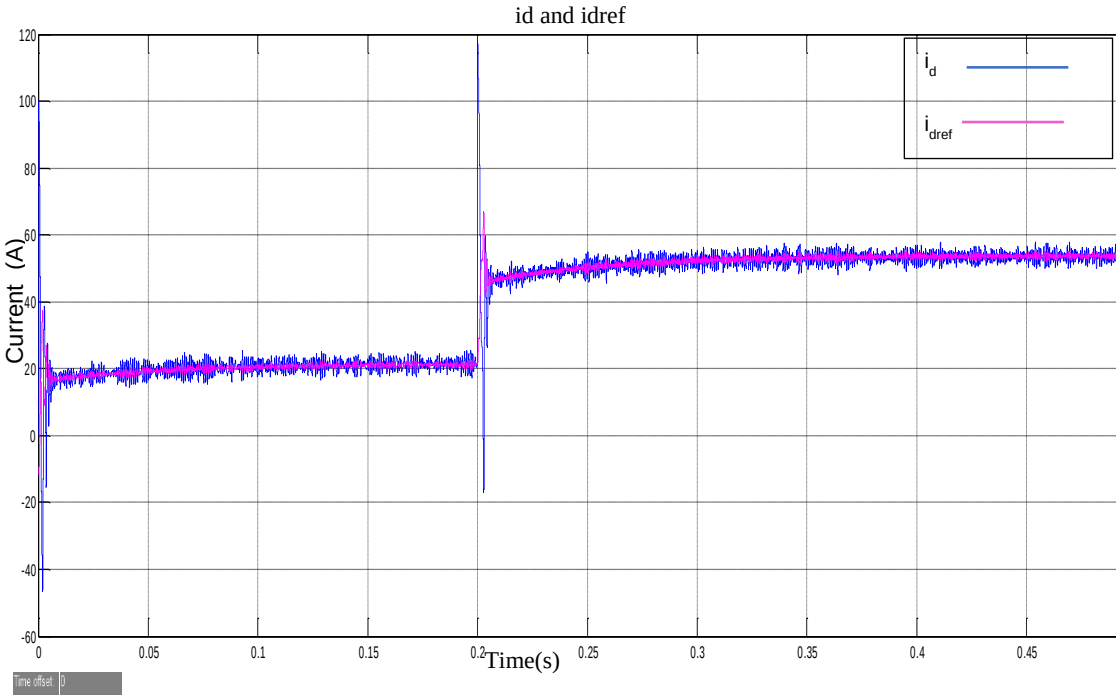

Figure 5.25: i_d current response to change in reference command

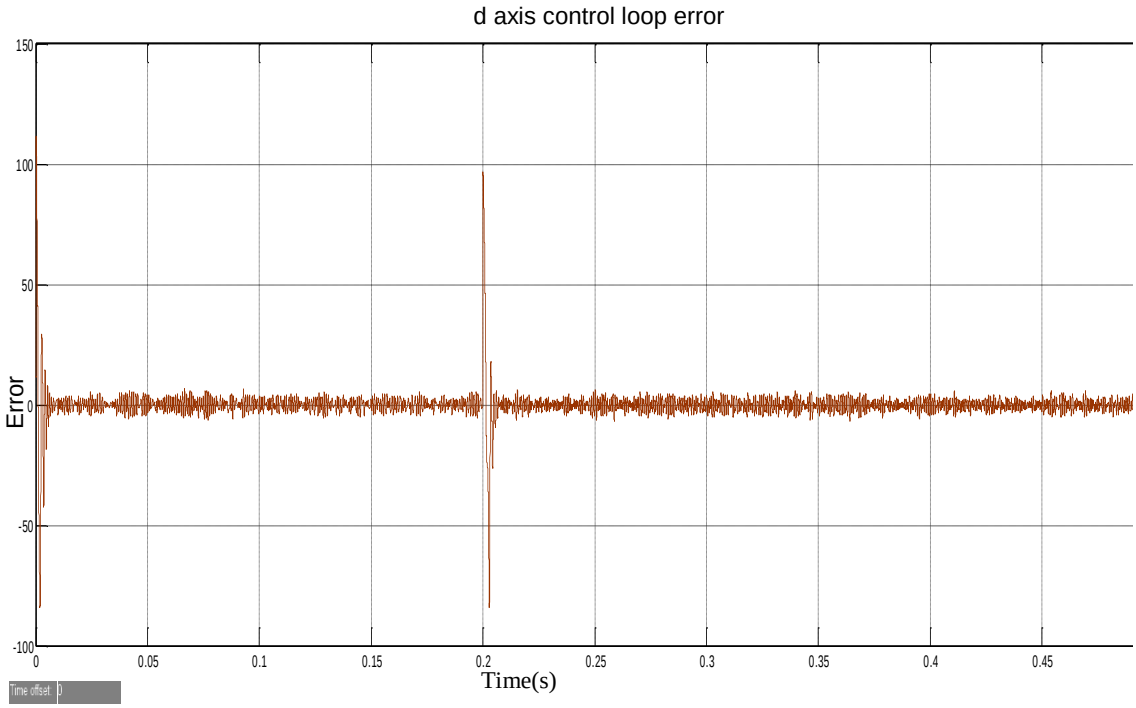

Figure 5.26: current control loop error for i_d current

The tracking response of the q current component is plotted in Fig 5.27. The capability of the controller for the d axis to adequately track the set power is shown with a steady state which is nearly zero as seen in the plot for the control loop error in Fig. 5.28 below. Some spikes are also noticed required for prompt response to the step input

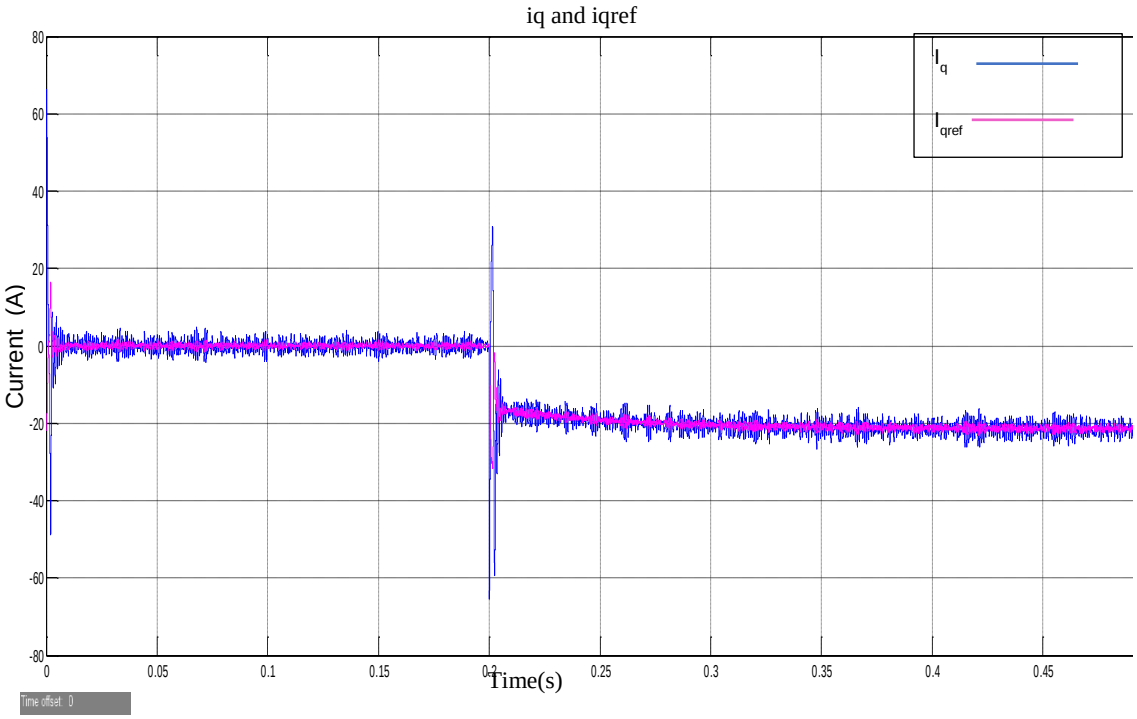

Figure 5.27: i_q current response to change in reference command

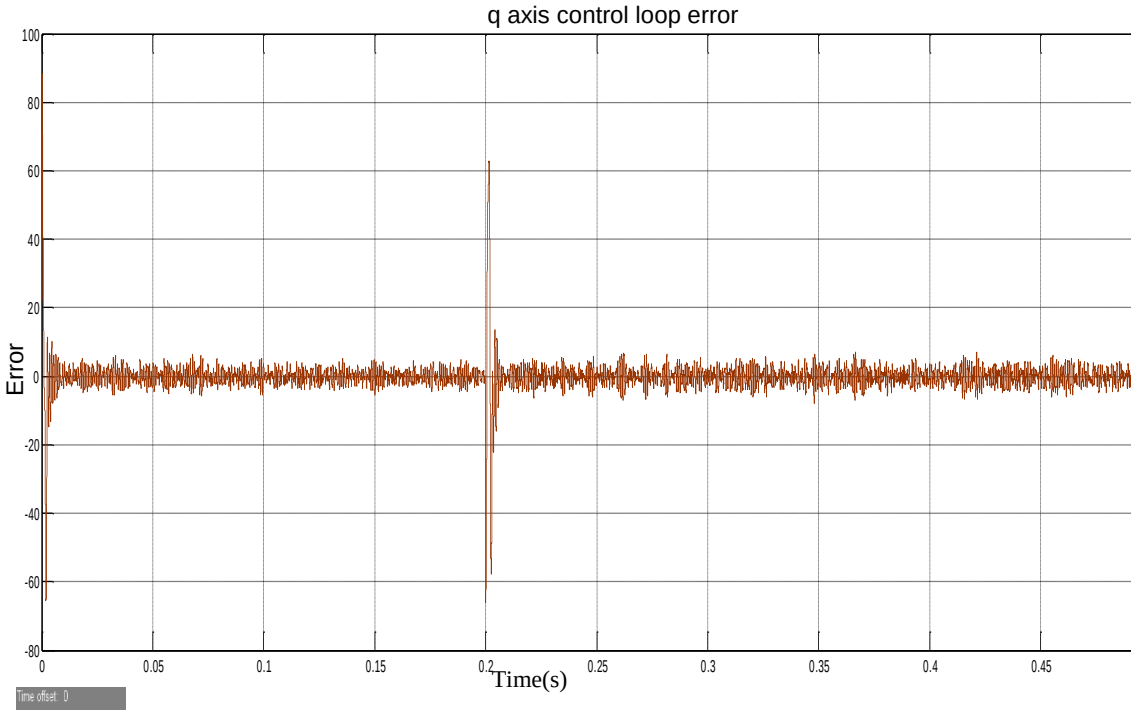

Figure 5.28: Current control loop error for i_q current

The performance analysis of the PI controllers for the d axis current and q axis current components can be examined from the simulation results displayed in Fig. 5.25 and Fig. 5.27 where i_d and i_q reference tracking corresponds to the active and reactive power respectively (Reznik 2012). The d and q current also experiences transient at 0.2 s in response to the step change in power injected into the grid. A transient was also noticed in the errors of both axes at this time as well as seen in Fig. 5.26 and Fig. 5.28. However, the d and q voltage components as represented in Fig. 5.29 does not experience transient at this time which confirms the performance of the system since the designed controller is a current control algorithm. The injected d and q components directed to the PWM are presented in Fig. 5.30.

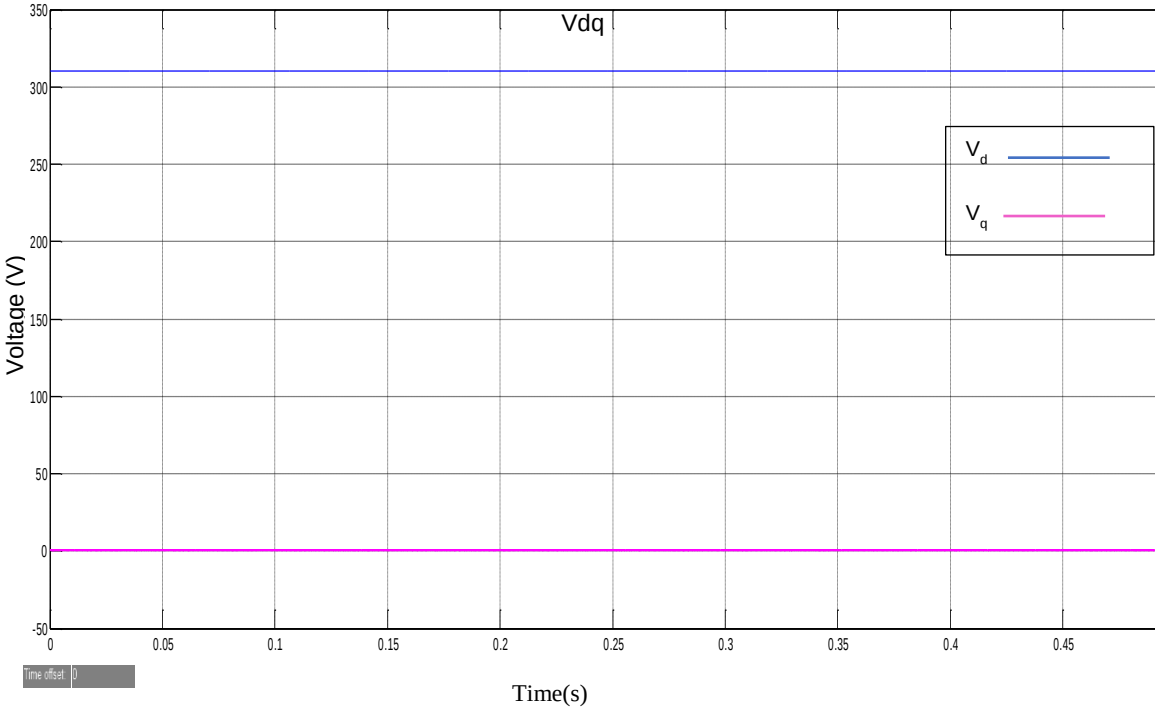

Figure 5.29: d and q components of voltage measured

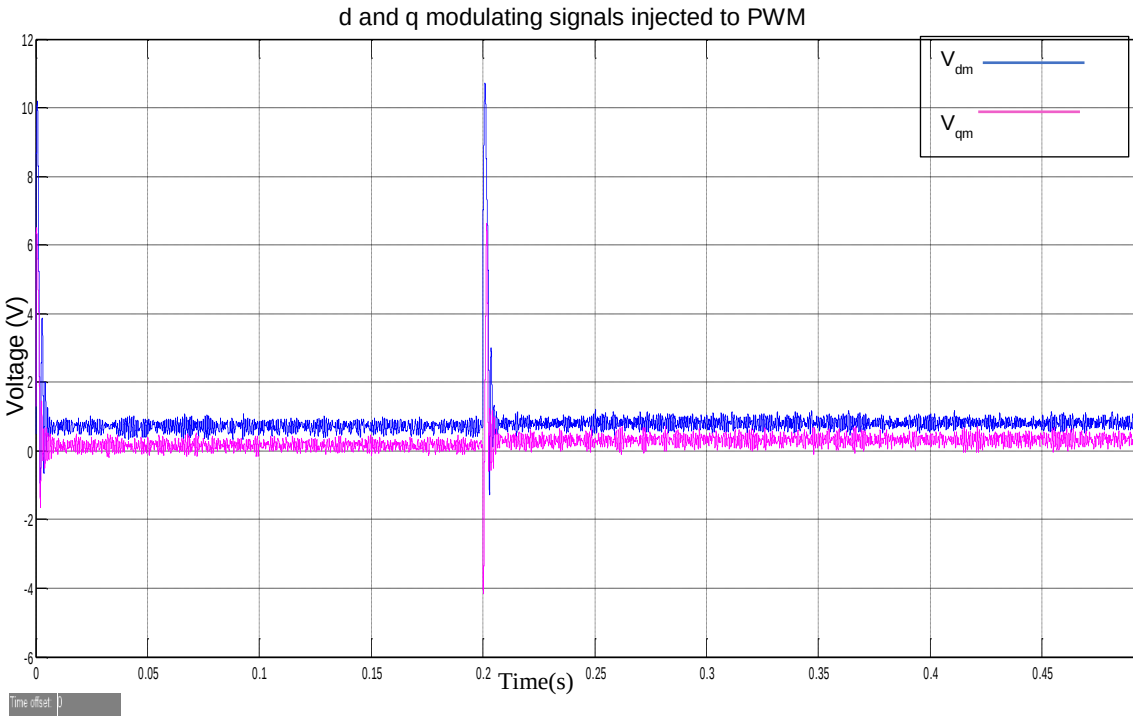

Figure 5.30: d and q components of the modulating signals directed to the PWM

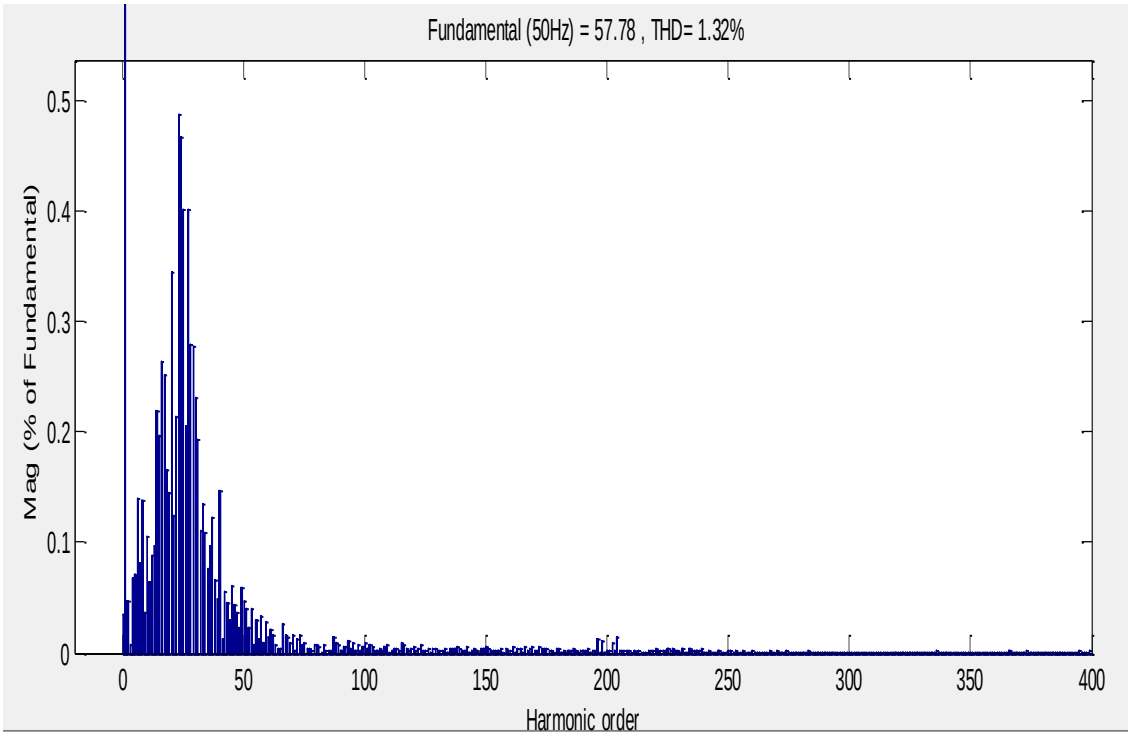

Figure 5.31: FFT Analysis showing THD of line current injected to the grid

In Fig. 5.31, the THD of the current injected into the grid is displayed. It shows that THD of 1.32% is injected into the grid which implies that THD is minimized when the system operates with higher load.

The step reference command of active power at time 0.3 s provides 35 kW and reactive power of 15 kVAR. The response of the system is displayed in the following results.

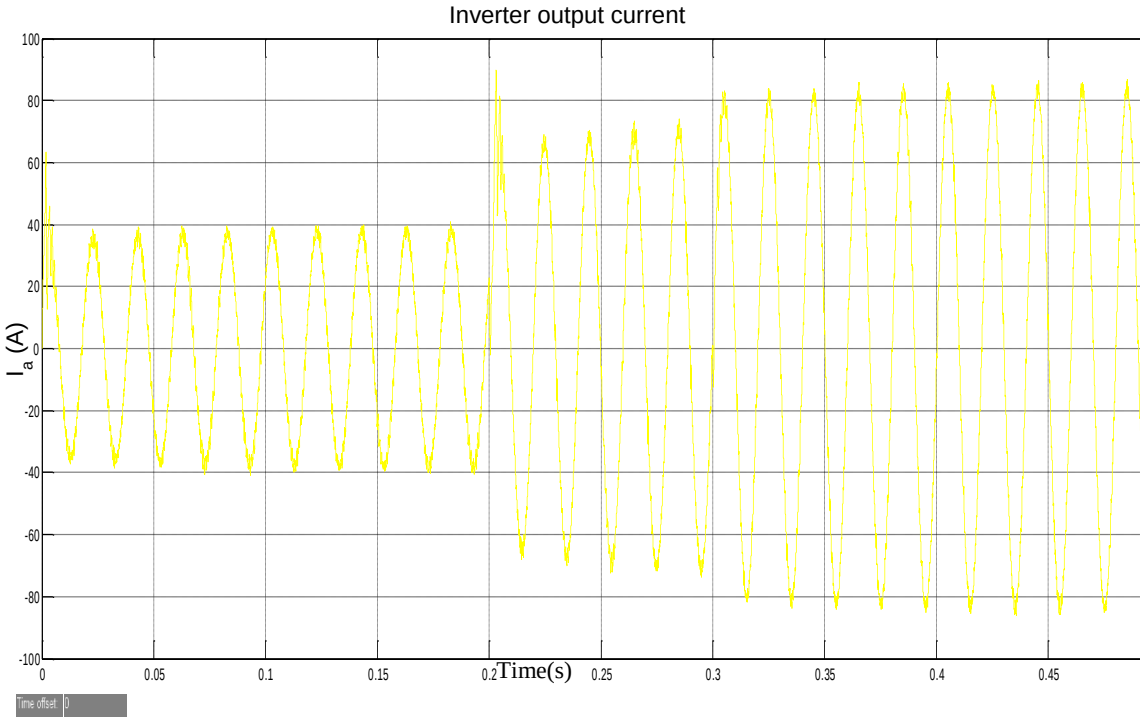

Figure 5.32: Inverter output current i_a

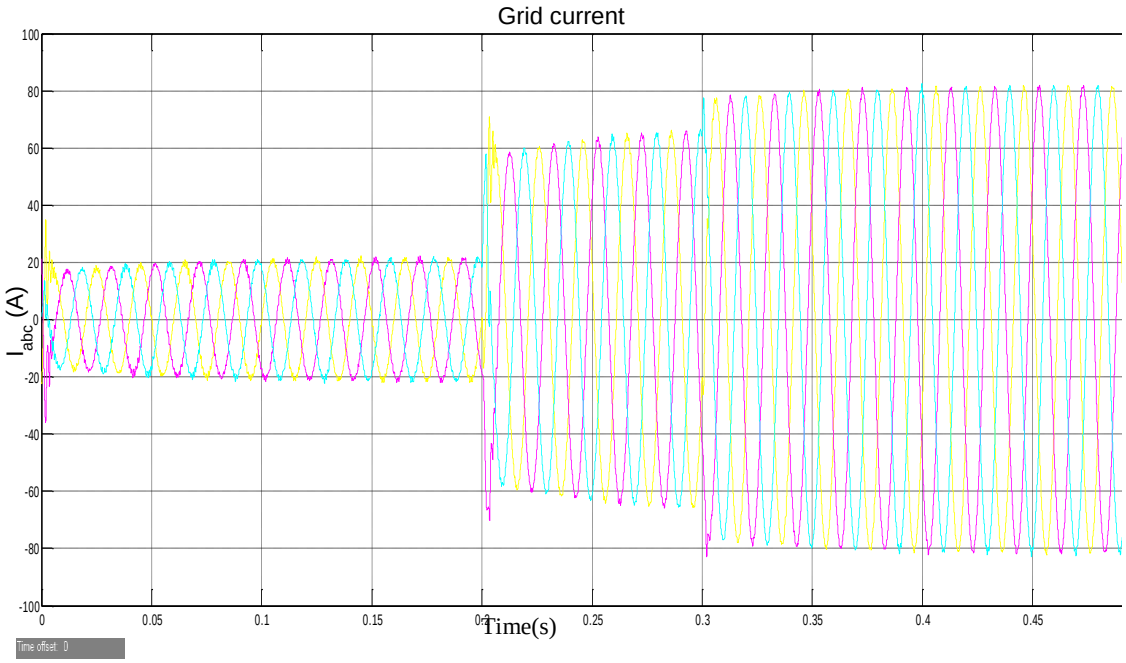

Figure 5.33: Grid current response to change in reference command of active and reactive power

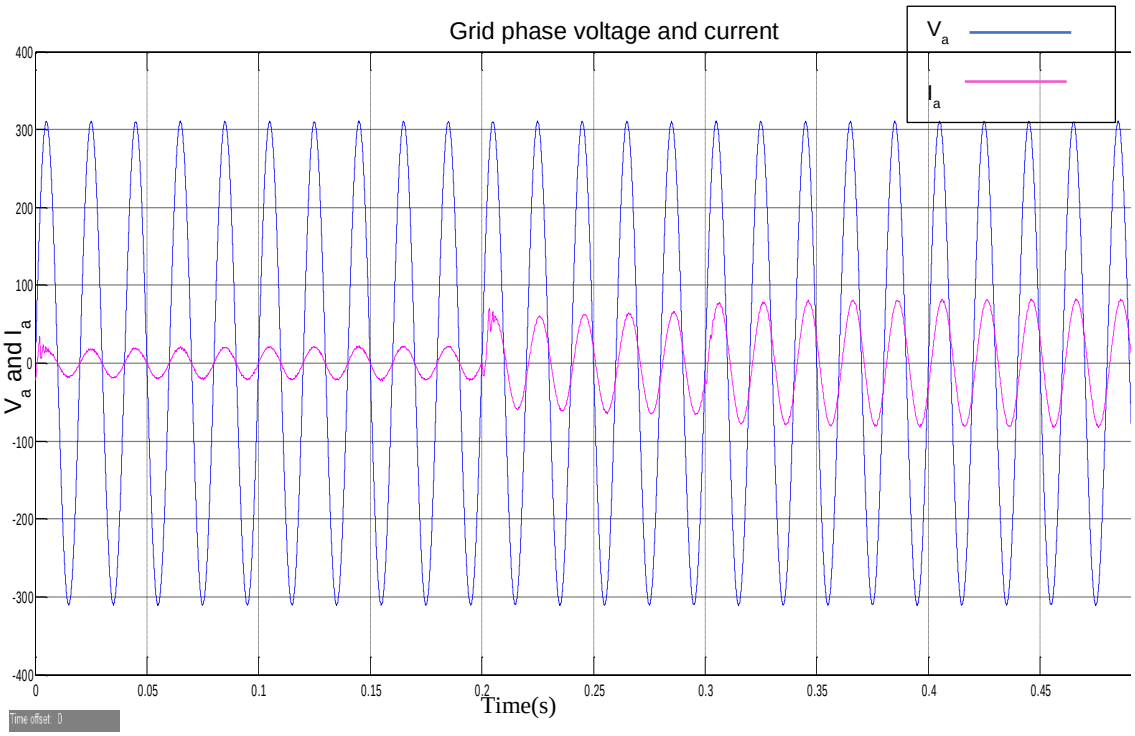

Figure 5.34: Phase voltage and grid current response to change in step reference command of active and reactive power

The response of the inverter line current at 0.3 s is indicated in Fig. 5.32 showing a little transient spikes occurring at that time due to step change in active power from 30 kW to 35 kW and 10 VAR to 15 VAR. the transient is also very little when observed in the three-phase grid current in Fig.5.33 and in the phase voltage and current response represented in Fig. 5.34.

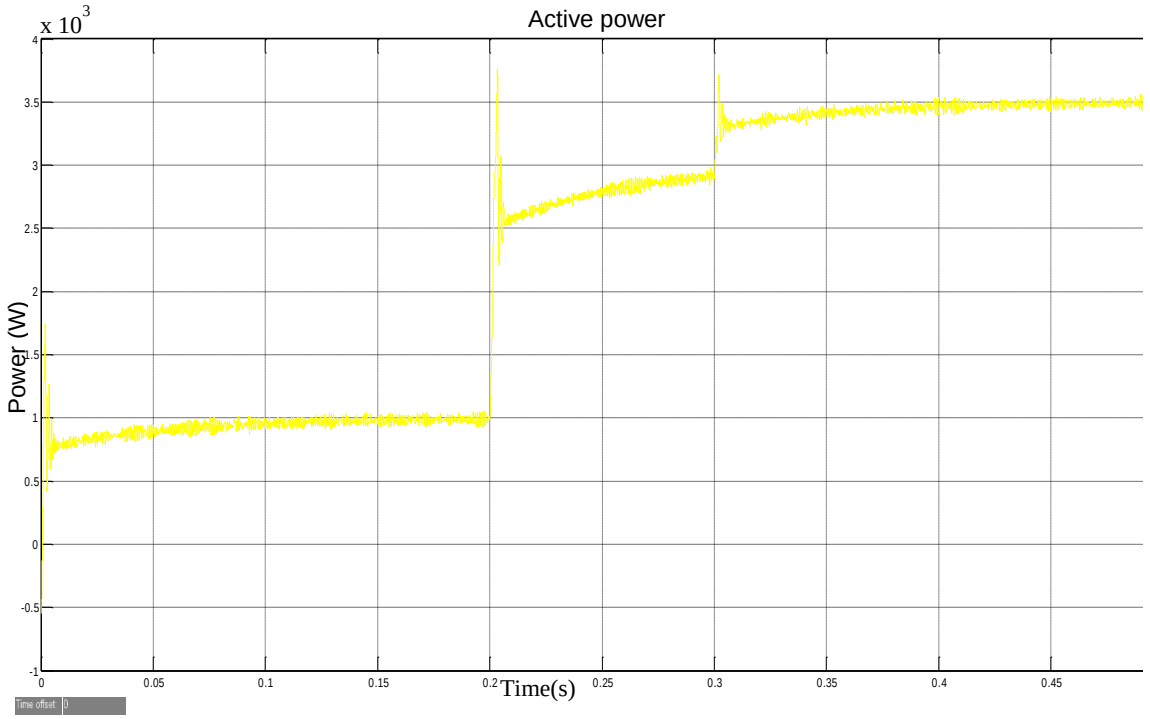

Figure 5.35: Active power 'P' injected into the grid

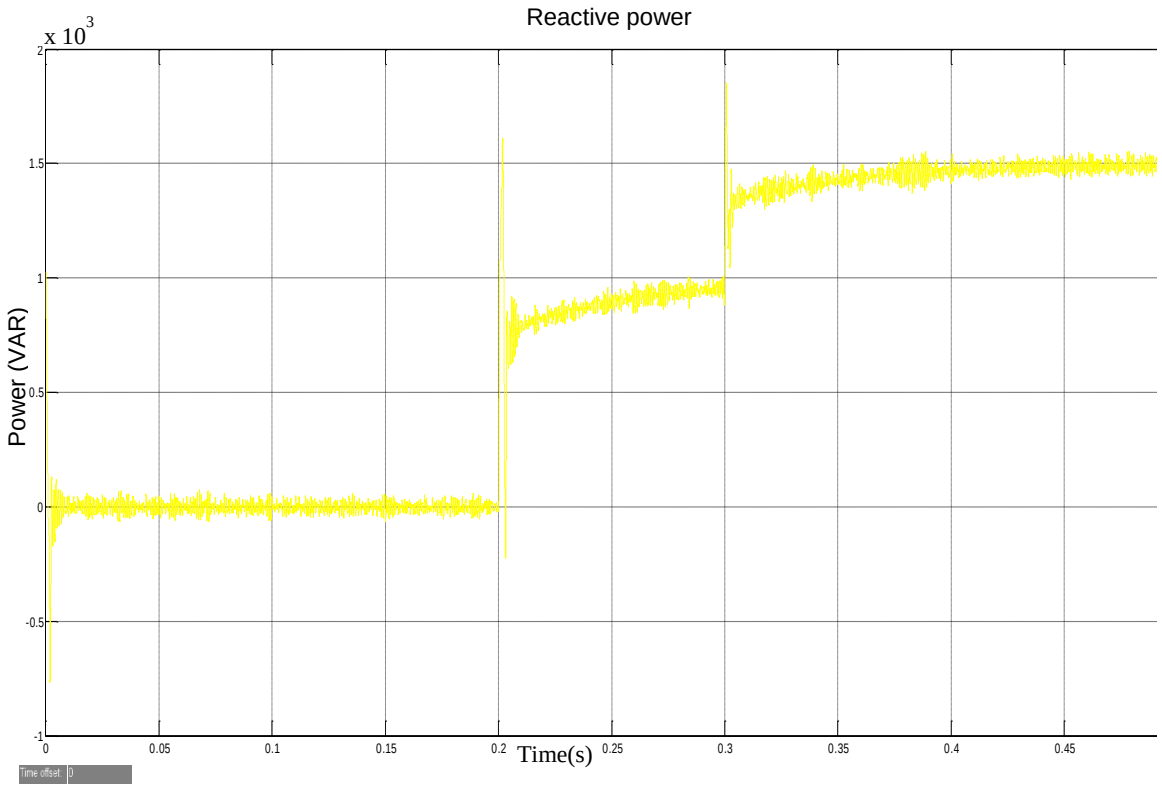

Figure 5.36: Reactive power 'Q' injected into the grid

The active and reactive power injected to the grid are shown in Fig. 5.35 and Fig. 5.36 respectively while the d component and q component of the current is represented in Fig. 5.37 and Fig. 5.39 respectively.

The tracking response of the d current component which is represented in Fig 5.37 shows the proficiency of the controller for the d axis in adequately tracking the set power with a steady state which is nearly zero as seen in the plot for the control loop error in Fig. 5.38 below. A slight overshoot is also noticed at the step change occurring at 0.3 s compared to the transient spikes induced at 0.2 s.

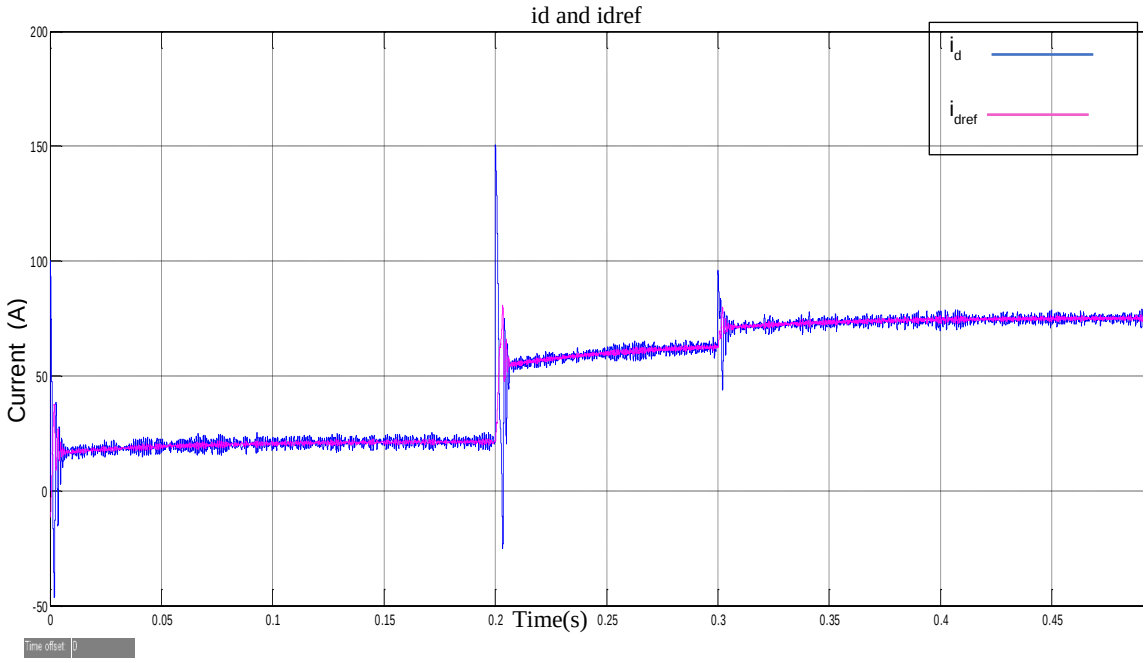

Figure 5.37: i_d current response to change in reference command

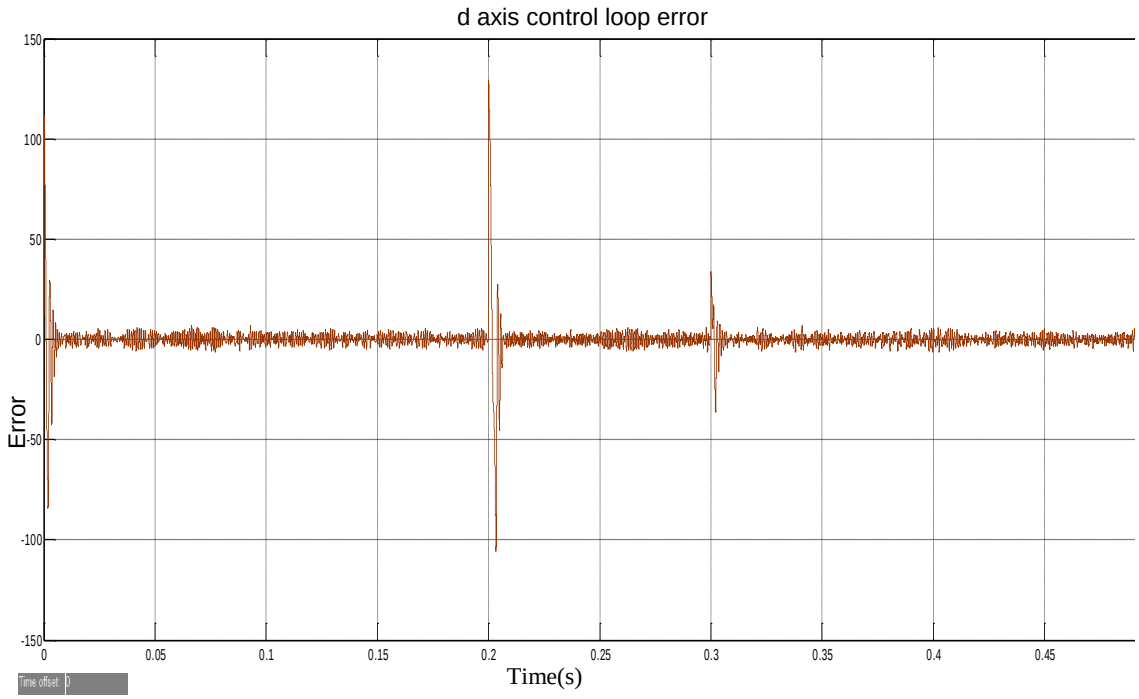

Figure 5.38: current control loop error for i_d current

The tracking response of the q current component has been represented in Fig 5.39 showing the proficiency of the controller for the q axis in effectively tracking the set power with a steady state which is nearly zero as seen in the plot for the control loop error in Fig. 5.40 below. A slight overshoot is also noticed at the step change occurring at 0.3 s compared to the transient spikes induced at 0.2 s.

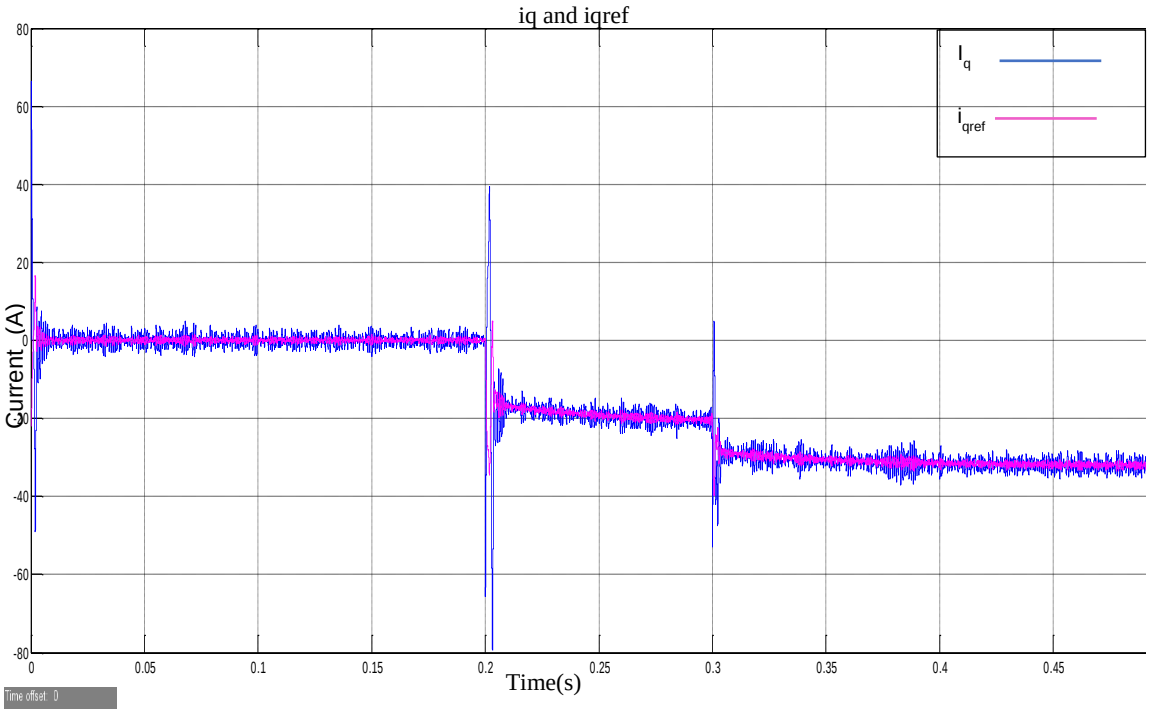

Figure 5.39: i_q current response to change in reference command

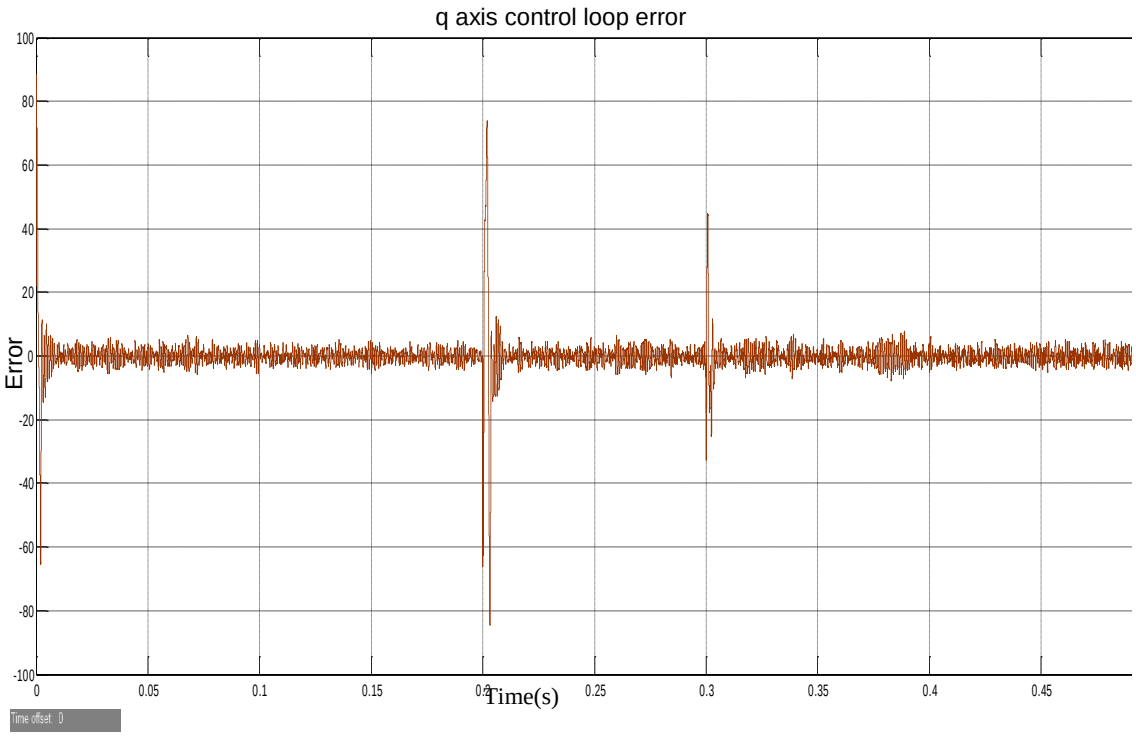

Figure 5.40: current control loop error for i_q current

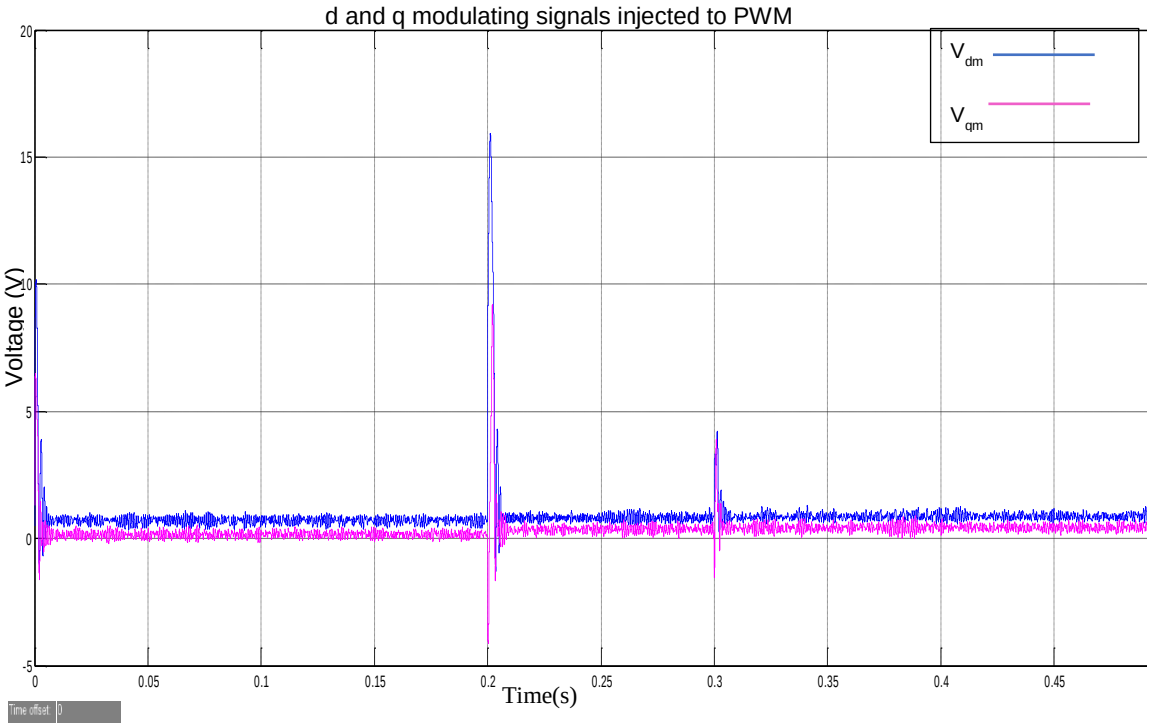

Figure 5.41: d and q components of the modulating signals directed to the PWM

The Fig. 5.41 above showing the d and q components of the modulating signals directed to the PWM generator also shows little spikes indicating the response to step change at 0.3 s.

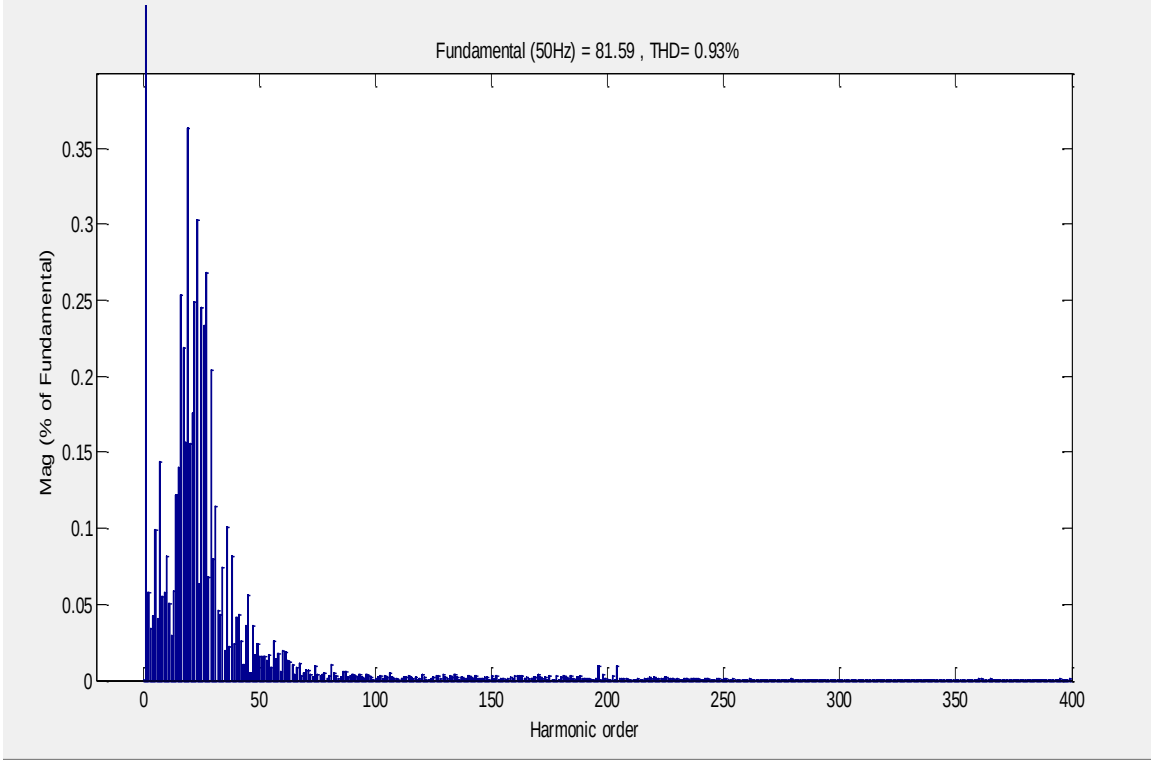

Figure 5.42: FFT Analysis showing THD of line current injected to the grid

Using the FFT analysis to determine the THD of line current injected into the grid, it can be seen from Fig. 5.42 that the total harmonic distortion has reduced to 0.93% which verifies that the THD reduces when the power load increases. This is correct when compared with the previous analysis that has been done in this chapter.

5.3.2 Bidirectional flow of power from the Utility grid to dc-link

The capability of the grid-connected VSI to supply power in the reverse direction that is from the grid to dc-link is verified from the following simulation results. For time 0.3 s, the GCI is initially set to supply active power of 20 kW and 10 kVAR. However, there is a reference command for active power to consume 10 kW and reactive power of 30 kW. The following simulation results displayed below shows the transition process at time 0.3 s.

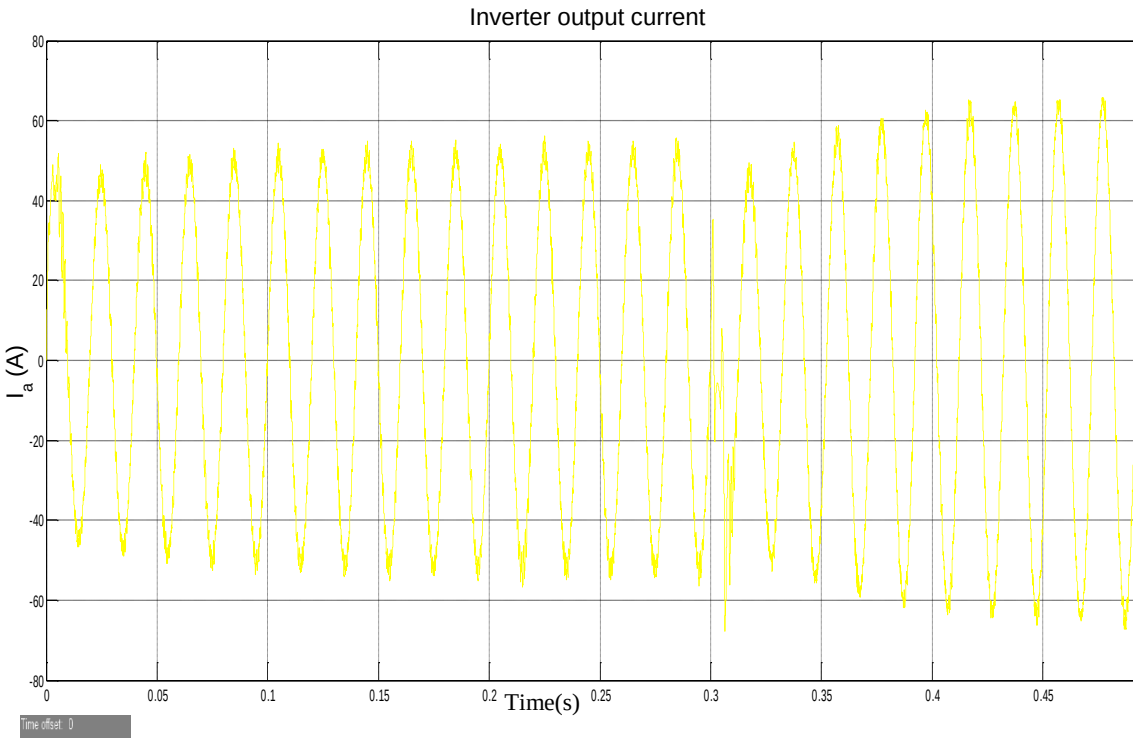

Figure 5.43: Inverter output current i_a

The response of the inverter line current indicated in Fig 5.43 shows The transition process which can be observed at 0.3 s with the presence of little spikes at that time due to change in command reference as seen in the in the inverter output current.

The transition process can also be noticed in the three-phase current injected into the grid after the LCL filter with the presence of transition spikes at 0.3 s as shown in Fig. 5.44 and also in the comparison of phase voltage and current response displayed in Fig. 5.45.

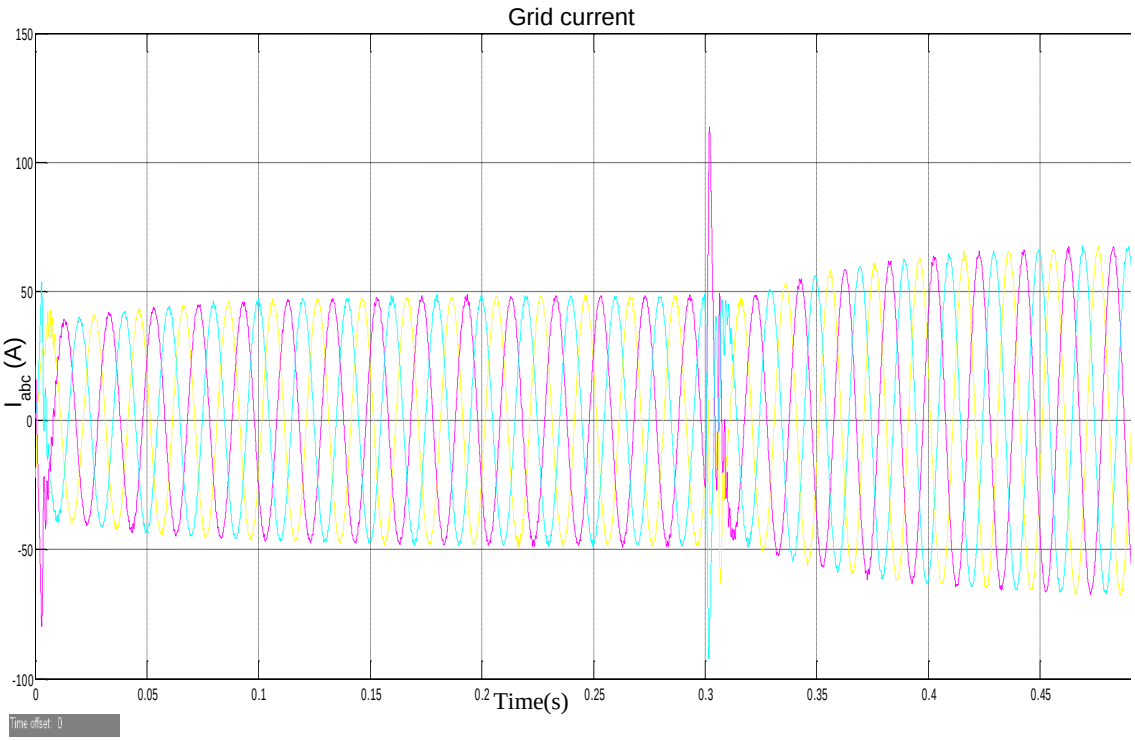

Figure 5.44: Grid current response to change in reference command of active and reactive power

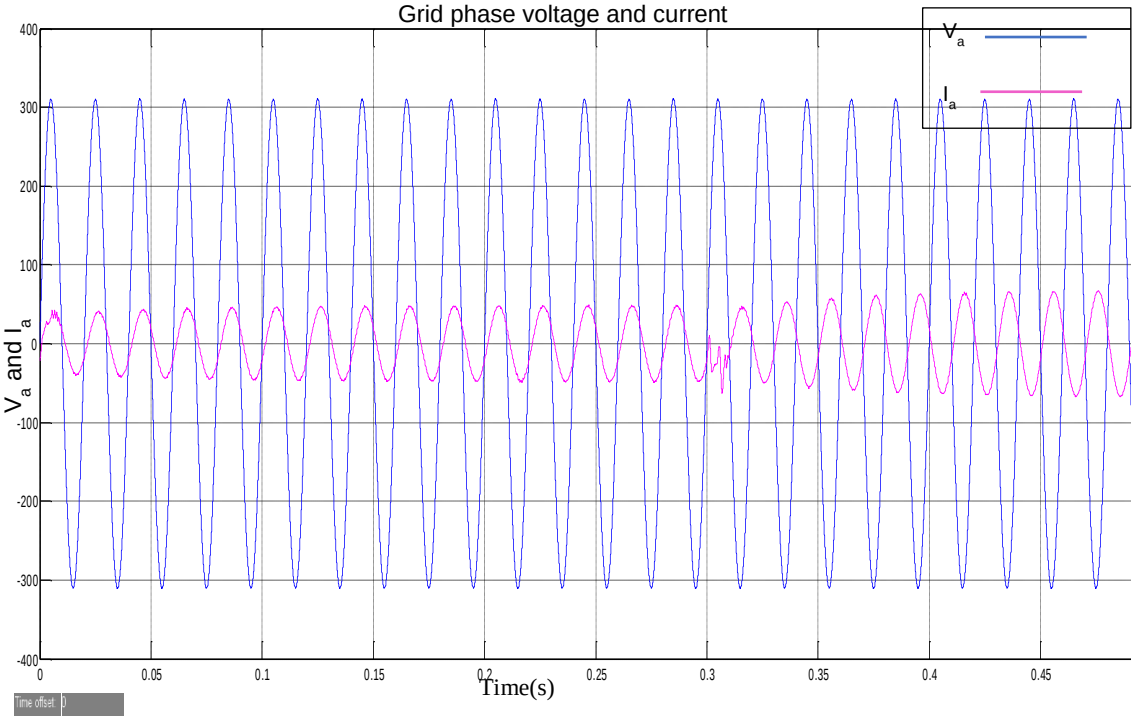

Figure 5.45: Phase voltage and grid current response to change in step reference command of active and reactive power

The transition process can also be noticed in the injected active and reactive power in Fig. 5.46. The transient also appears in the current reference tracking presented in Fig 5.47 and Fig. 5.49. However, large spikes are noticed from the control loop errors of both axis due to the transition process of 0.3 s as displayed in Fig. 5.48 and Fig. 5.50 respectively.

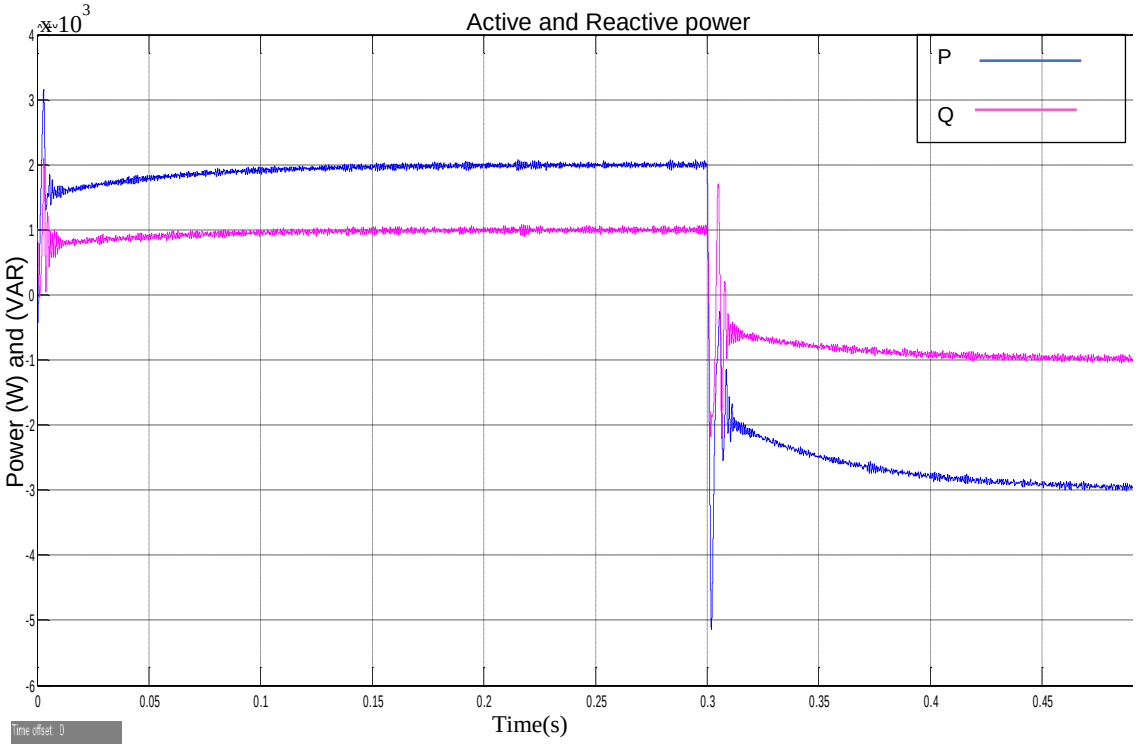

Figure 5.46: Active power and reactive power injected into the grid

The tracking response of the d current component plotted in Fig 5.47 shows the capability of the controller for the d axis in adequately tracking the set power with a steady state which is nearly zero as seen in the plot for the control loop error in Fig. 5.48 below. Some spikes are also noticed at 0.3 s when the transient process occurred which is required for rapid response to the step reference input.

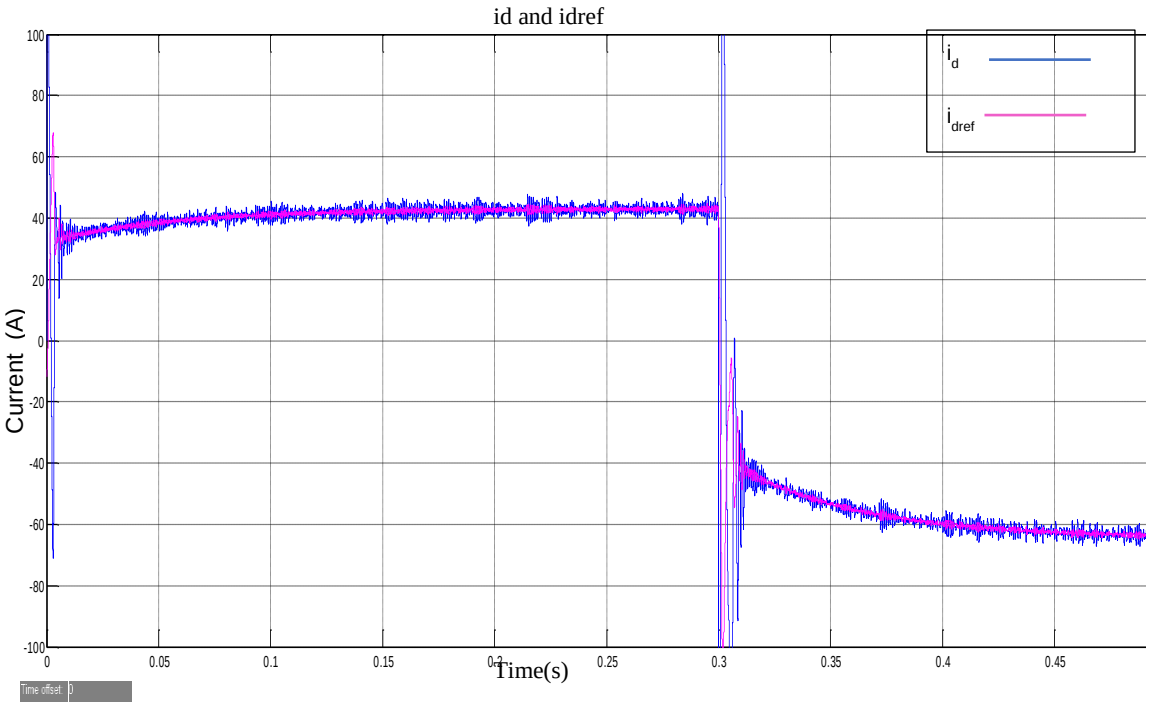

Figure 5.47: i_d current response to change in reference command

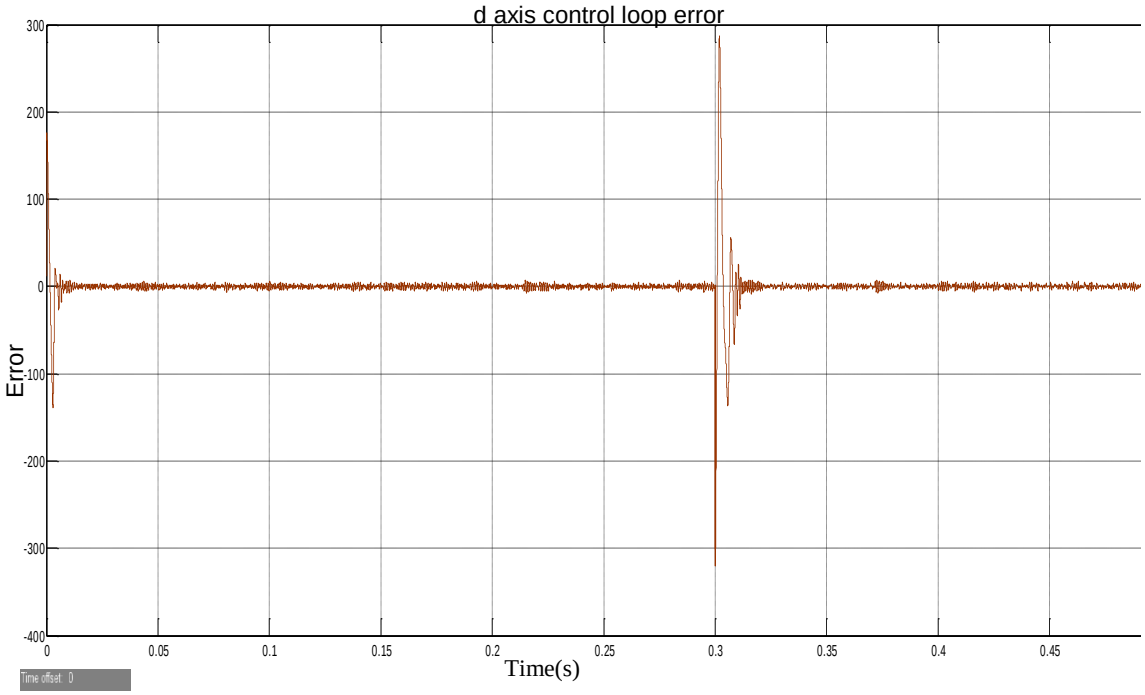

Figure 5.48: current control loop error for i_d current

The transition is also observed in the tracking response of the q current component with the spikes induced at 0.3 s with a steady state error that is nearly zero also experiencing transient spikes at 0.3 s.

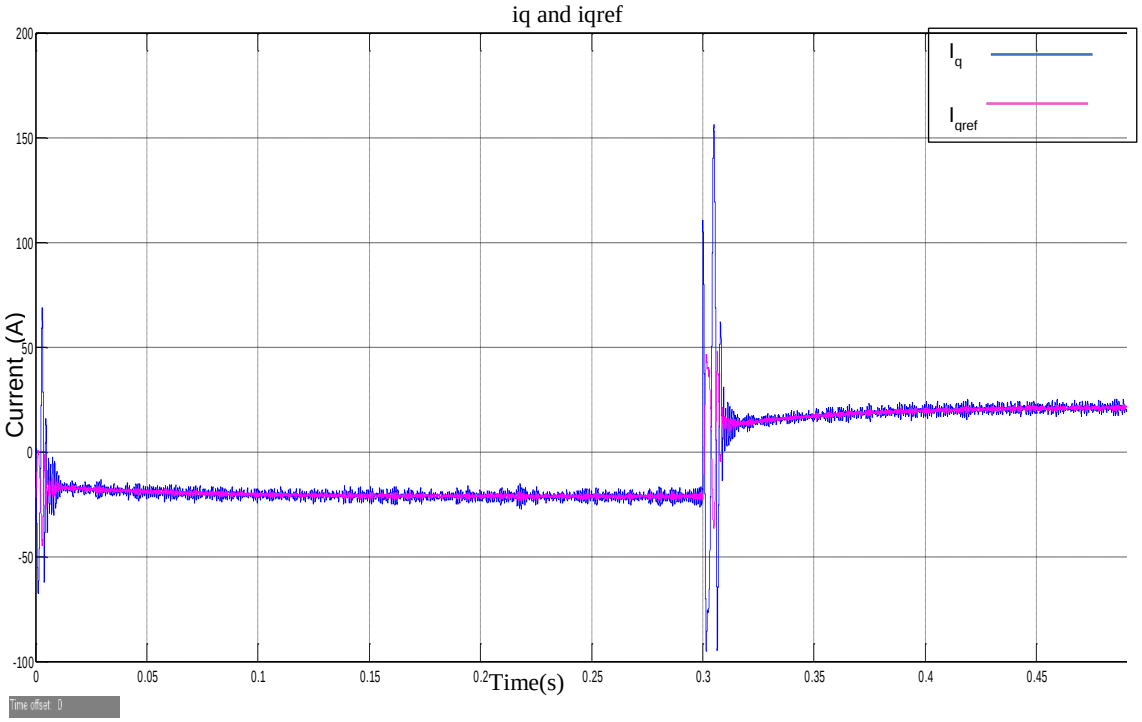

Figure 5.49: i_q current response to change in reference command

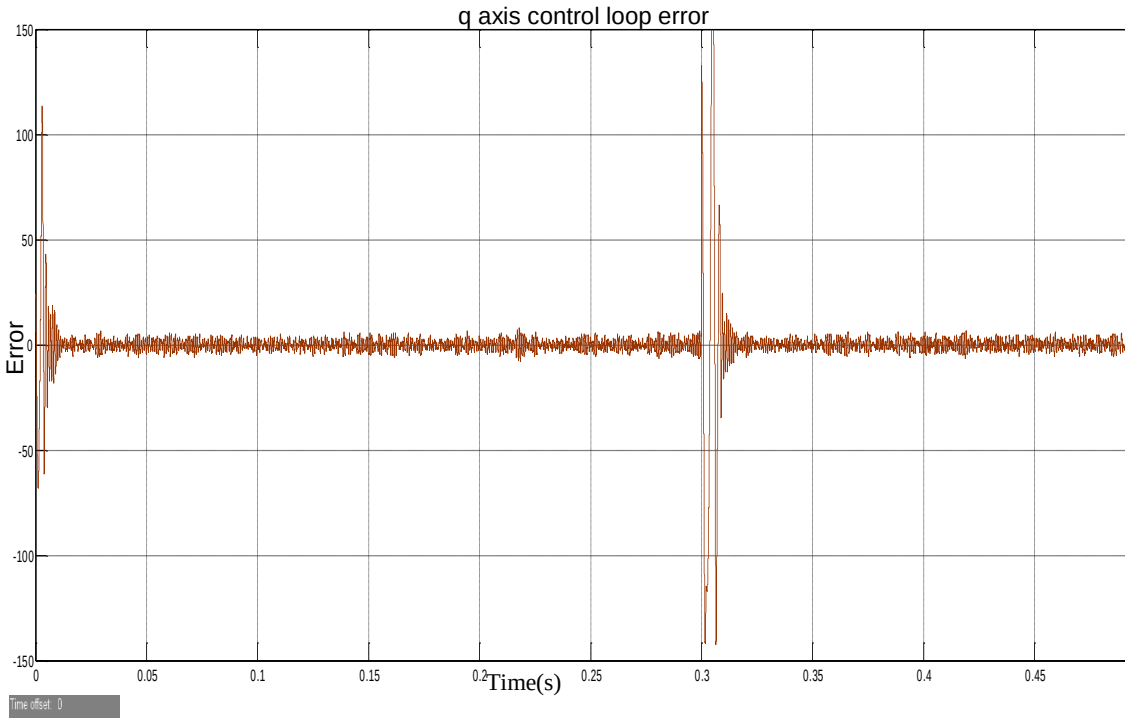

Figure 5.50: current control loop error for i_q current

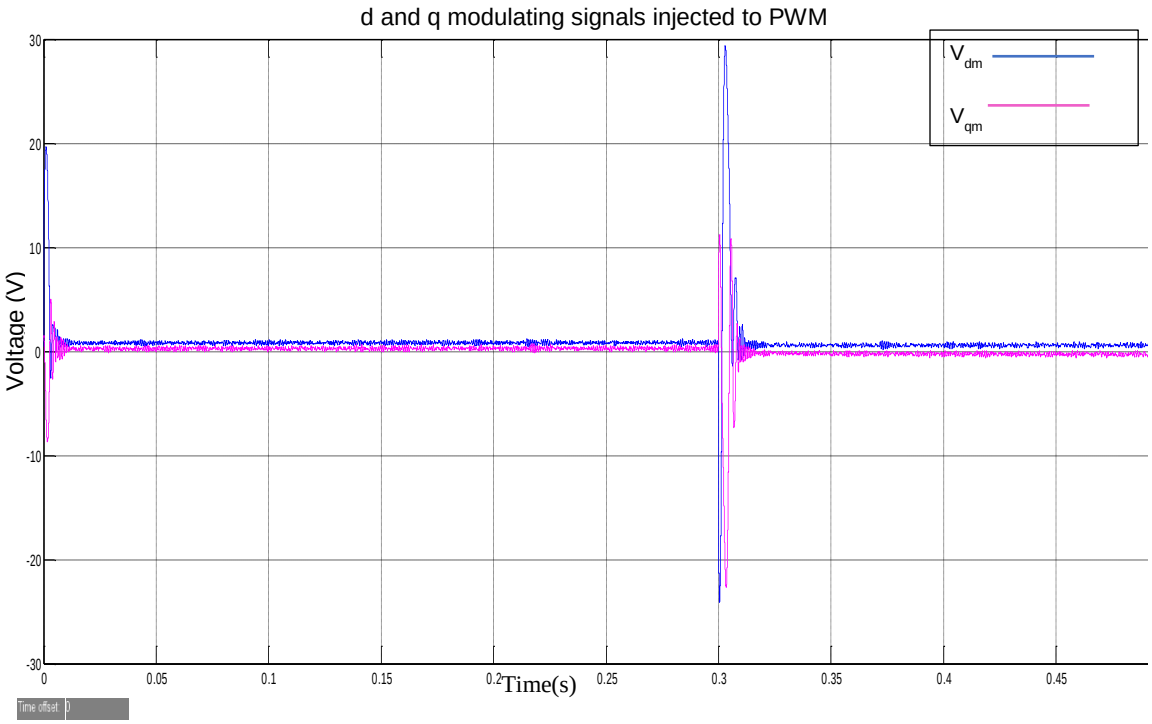

Figure 5.51: d and q components of the modulating signals directed to the PWM

The PWM generator will receive d and q modulating signals with some transient which is induced at 0.3 s. When the FFT analysis was carried out on the line current injected into the grid, a total harmonic distortion of 1.16% was observed as seen in the harmonic spectrum in Fig. 5.52. The THD observed in this analysis is still acceptable under the IEEE 1547 standards requirements for injected current which allows a THD of up to 5%.

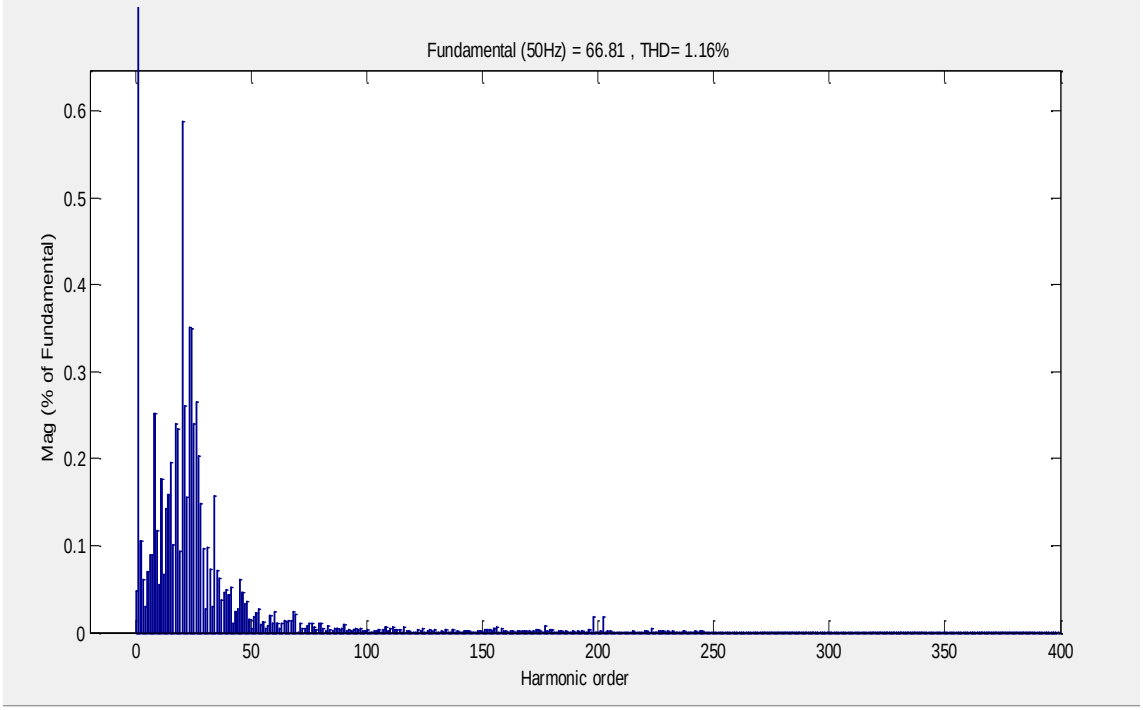

Figure 5.52: FFT Analysis showing THD of line current injected to the grid

5.4 Conclusion

The operation of the three-phase grid-connected VSI model has been studied in this chapter. The design done in the previous chapter was implemented in the developed model and the simulation results show that the design procedures are suitable. The effectiveness of the designed LCL filter was verified as low current harmonics which satisfy the IEEE standards were injected into the grid. The designed current control system has also been analysed in this chapter to verify its capability to operate perfectly when the inverter is connected to the grid by carrying out various simulations.

CHAPTER 6

CONCLUSION AND FUTURE WORK

6.1 Conclusion

The comprehensive overview of power electronics inverter was studied at the beginning of this thesis. The complete design and development of the three-phase grid-connected VSI was presented in this thesis. Through designing, analysis, modelling and simulations, this thesis was able to achieve its objectives. The smart inverter has been modelled and simulated in Matlab/Simulink environment to test the design of the model and develop the control resolutions proposed in this work.

In order to achieve the aims of this research, the design of the power stage and output filter of the three phase GCI system has been done. The low pass LCL filter was chosen for the purpose of this work due to its improved ripple attenuation characteristics. The designed LCL filter and the controller was implemented in the developed model and the simulation results indicate that the design procedures are suitable. The effectiveness of the designed LCL filter was confirmed as low current harmonics which satisfy the IEEE standards were injected into the grid. The effectiveness of the PI current controllers to operate in grid-connected mode have also been shown through the tracking capability of the active and reactive power references which were both varied to test the response of the system. Through various simulations of the developed model under different ratings of power injected into the system, the efficiency of the system, robustness of the proposed controller and improved power quality of the system were verified.

6.2 Future work

- Other control procedures should be designed and developed to compare between the control methods
- Experimental setup to compare with the simulation results
- Integration of communication interface with the system
- Modelling of the system in other software platforms to compare simulated results.

REFERENCES

Abo-Al-Ez, K.M., Xia, X. and Zhang, J., 2012, August. Smart interconnection of a PV/wind DG micro grid with the utility distribution network. In *Industrial and Commercial Use of Energy Conference (ICUE), 2012 Proceedings of the 9th* (pp. 1-8). IEEE.

Abu-Rub, H., Iqbal, A. & Guzinski, J., 2012. *HIGH PERFORMANCE CONTROL OF AC DRIVES WITH MATLAB/SIMULINK MODELS* first edit., New York: John Wiley & Sons Ltd. Publication.

Adekola, O.I. & Raji, A.K., 2015. Functionalities of Smart Inverter System for Grid-Connected Applications. In *Industrial and Commercial Use of Energy (ICUE), International Conference on the. IEEE,*. pp. 340–344.

Agirman, I. & Blasko, V., 2003. A novel control method of a VCS without AC line voltage sensors. *IEEE Transactions on Industry Applications*, 39(2), pp.519–524.

Ahmed, K.H., Finney, S.J. & Williams, B.W., 2007. Passive filter design for three-phase inverter interfacing in distributed generation. In *5th International Conference-Workshop Compatibility in Power Electronics, CPE 2007*.

Alatrash, H., Mensah, A., Mark, E., Haddad, G. and Enslin, J., 2012. Generator emulation controls for photovoltaic inverters. *Smart Grid, IEEE Transactions on*, *3*(2), pp.996-1011.

Alepuz, S., Busquets-Monge, S., Bordonau, J., Gago, J., González, D. and Balcells, J., 2006. Interfacing renewable energy sources to the utility grid using a three-level inverter. *Industrial Electronics, IEEE Transactions on*, *53*(5), pp.1504-1511.

Al-Saedi, W., Lachowicz, S.W. and Habibi, D., 2011, September. An optimal current control strategy for a three-phase grid-connected photovoltaic system using particle swarm optimization. In *Power Engineering and Automation Conference (PEAM), 2011 IEEE* (Vol. 1, pp. 286-290). IEEE.

Americans for a clean energy grid, 2014. Smart Solar Inverters. , (Dc), pp.1–5. Available at: http://cleanenergytransmission.org.

Amin, M.M. and Mohammed, O., 2011. Development of high-performance grid-connected wind energy conversion system for optimum utilization of variable speed wind turbines. *Sustainable Energy, IEEE Transactions on*,*2*(3), pp.235-245.

Arai, J., Iba, K., Funabashi, T., Nakanishi, Y., Koyanagi, K. and Yokoyama, R., 2008. Power electronics and its applications to renewable energy in Japan.*Circuits and Systems Magazine, IEEE*, *8*(3), pp.52-66.

Bacha, S., Antoneta, I.M. & Bratcu, I., 2013. *Advanced Textbooks in Control and Signal*

Processing Power Electronic Converters Modeling and Control G. Michael & J. M. (University of Strathclyde), eds., France: springer.

Baliga, B.J., 2001. The future of power semiconductor device technology.*Proceedings of the IEEE*, *89*(6), pp.822-832.

Balu, N.J. and Lauby, M.G. eds., 1994. *Power system stability and control*(Vol. 7). New York: McGraw-hill.

Banks, D. & Schaffler, J., 2006. The potential contribution of renewable energy in South Africa. *Draft Update Report*, (February).

Bellini, A., Bifaretti, S., Iacovone, V. and Cornaro, C., 2009, September. Simplified model of a photovoltaic module. In *Applied Electronics, 2009. AE 2009* (pp. 47-51). IEEE.

Beser, E., Arifoglu, B., Camur, S. and Beser, E.K., 2010. A grid-connected photovoltaic power conversion system with single-phase multilevel inverter. *Solar Energy*, *84*(12), pp.2056-2067.

Bhutia, B., Ali, M. & Tiadi, N., 2014. Design of Three Phase PWM Voltage Source Inverter For Photovoltaic Application. *International Journal Of Innovative Research In Electrical, Electronics, Instrumentation And Control Engineering*, 2(4), pp.2321–2004. Available at: www.ijireeice.com

Bhutia, B., Ali, S.M. & Tiadi, N., 2014. Design of Three Phase PWM Voltage Source Inverter For Photovoltaic Application. , 2(4), pp.1364–1367.

Blaabjerg, F. et al., 2006. Overview of Control and Grid Synchronization for Distributed Power Generation Systems. *IEEE Transactions on Industrial Electronics*, 53(5), pp.1398–1409.

Blasko, V., & Kaura, V. (1997). A novel control to actively damp resonance in input LC filter of a three-phase voltage source converter. *Industry Applications, IEEE Transactions on*, *33*(2), 542-550.

Borgonovo, D., 2001. Modelling and control of the three-phase PWM rectifier using park transformation. *Master's Thesis, Federal University of Santa Catarina, Florian6polis*.

Bose, B.K., 2002. *Modern Power Electronics And Ac Drives.pdf*,

Boulder, C., 2012. Workshop On Technology,Measurement,And Standards Challenges For The Smart Grid. *National Institute of standards and technology. U.S. Department of commerce*.

Bouzguenda, M. et al., 2011. Solar photovoltaic inverter requirements for smart grid applications. In *2011 IEEE PES Conference on Innovative Smart Grid Technologies - Middle*

East, ISGT Middle East 2011.

Braun, M. 2007. Technological control capabilities of DER to provide future ancillary services. *International Journal of Distributed Energy Resources*, *3*(3), 191-206.

Braun, M. et al., 2012. Is the distribution grid ready to accept large-scale photovoltaic deployment? State of the art, progress, and future prospects. *Progress in Photovoltaics: Research and Applications*, 20(1), pp.6–11. Available at: http://dx.doi.org/10.1002/pip.1160.

Buticchi, G., Barater, D., Lorenzani, E. and Franceschini, G., 2012. Digital control of actual grid-connected converters for ground leakage current reduction in PV transformerless systems. *Industrial Informatics, IEEE Transactions on*, *8*(3), pp.563-572.

Carnieletto, R., Suryanarayanan, S., Simões, M. G., & Farret, F. 2009. A multifunctional single-phase voltage source inverter in perspective of the Smart Grid Initiative. In *Industry Applications Society Annual Meeting, 2009. IAS 2009. IEEE*: pp. 1-7.

Carrasco, J.M. et al., 2006. Power-Electronic Systems for the Grid Integration of Renewable Energy Sources : A Survey. *IEEE Transactions on industrial electronics*, 53(4), pp.1002–1016.

Chen, X., Fu, Q. and Infield, D.G., 2009, April. PV grid-connected power conditioning system with Z-source network. In *Sustainable Power Generation and Supply, 2009. SUPERGEN'09. International Conference on* (pp. 1-6). IEEE.

Chen, Z., Blaabjerg, F. and Pedersen, J.K., 2005, June. A multi-functional power electronic converter in distributed generation power systems. In *Power Electronics Specialists Conference, 2005. PESC'05. IEEE 36th* (pp. 1738-1744). IEEE.

Chetty, L. & Ijumba, N.M., 2009. Design of a Filter For a Spwm Vsi Connected to the Grid Via The ∆-Winding Of A ∆-Y Transformer. In *Proceedings of the 16th International Symposium on High Voltage Engineering*.

Chitti Babu, B., Mohapatra, M., Jena, S. and Naik, A., 2010, December. Dynamic performance of adaptive hysteresis current controller for mains-connected inverter system. In *Industrial Electronics, Control & Robotics (IECR), 2010 International Conference on* (pp. 95-100). IEEE.

Chung, S.K., 2000. Power conversion systems for ducks. *IEEE Proc-Electr. Power App*, 147(3), pp.213–219. Available at: http://adsabs.harvard.edu/abs/1979fec..conf..100S.

Craciun, B. et al., 2012. Improved Voltage Regulation Strategies by PV Inverters in LV Rural Networks. *3rd IEEE International Symposium on Power Electronics for Distributed Generation Systems (PEDG)*, pp.775–781.

Craciun, B.I. et al., 2012. Control of Grid Connected PV Systems with Grid Support Functions. , pp.2011–2012.

Crăciun, B. I., Kerekes, T., Séra, D., & Teodorescu, R. 2012. Overview of recent grid codes for PV power integration. In *Optimization of Electrical and Electronic Equipment (OPTIM), 2012 13th International Conference on IEEE* (pp. 959-965).

Dai, J., Xu, D.D. and Wu, B., 2009. A novel control scheme for current-source-converter-based PMSG wind energy conversion systems. *Power Electronics, IEEE Transactions on*, *24*(4), pp.963-972.

Dasgupta, S., Mohan, S.N., Sahoo, S.K. and Panda, S.K., 2011, May. Derivation of instantaneous current references for three phase PV inverter connected to grid with active and reactive power flow control. In *Power Electronics and ECCE Asia (ICPE & ECCE), 2011 IEEE 8th International Conference on* (pp. 1228-1235). IEEE.

Dasgupta, S., Mohan, S.N., Sahoo, S.K. and Panda, S.K., 2011, December. Evaluation of current reference generation methods for a three-phase inverter interfacing renewable energy sources to generalized micro-grid. In *Power Electronics and Drive Systems (PEDS), 2011 IEEE Ninth International Conference on* (pp. 316-321). IEEE.

Dasgupta, S., Mohan, S.N., Sahoo, S.K. and Panda, S.K., 2013. Lyapunov function-based current controller to control active and reactive power flow from a renewable energy source to a generalized three-phase microgrid system.*Industrial Electronics, IEEE Transactions on*, *60*(2), pp.799-813.

Dasgupta, S., Mohan, S.N., Sahoo, S.K. and Panda, S.K., 2013. Lyapunov function-based current controller to control active and reactive power flow from a renewable energy source to a generalized three-phase microgrid system.*Industrial Electronics, IEEE Transactions on*, *60*(2), pp.799-813.

Dash, A. R., Babu, B. C., Mohanty, K. B., & Dubey, R. 2011. Analysis of PI and PR controllers for distributed power generation system under unbalanced grid faults. In *Power and Energy Systems (ICPS), 2011 International Conference on* (pp. 1-6). IEEE.

Davari, M., Salabeigi, I., Gharehpetian, G.B., Fathi, S.H. and Kaviani, K., 2009, January. Optimal tuning of multifunction current controller for sigma delta modulation inverter-based distributed generation using PSO method. In*TENCON 2009-2009 IEEE Region 10 Conference* (pp. 1-6). IEEE.

Delfino, F., Procopio, R., Rossi, M. and Ronda, G., 2010. Integration of large-size photovoltaic systems into the distribution grids: a P–Q chart approach to assess reactive support capability. *IET Renewable Power Generation*, *4*(4), pp.329-340.

Denholm, P. & Margolis, R.M., 2007. Evaluating the limits of solar photovoltaics (PV) in electric power systems utilizing energy storage and other enabling technologies. *Energy Policy*, 35(9), pp.4424–4433.

Doukas, H. et al., 2006. Renewable energy sources and rationale use of energy development in the countries of GCC: Myth or reality? *Renewable Energy*, 31(6), pp.755–770.

Eltamaly, A.M., 2012. A novel harmonic reduction technique for controlled converter by third harmonic current injection. *Electric Power Systems Research*, *91*, pp.104-112.

Eren, S., Bakhshai, A. and Jain, P., 2012, February. Control of grid-connected voltage source inverter with LCL filter. In *Applied Power Electronics Conference and Exposition (APEC), 2012 Twenty-Seventh Annual IEEE* (pp. 1516-1520). IEEE.

Evju, S. E. 2007. Fundamentals of Grid Connected Photo-Voltaic Power Electronic Converter Design.

Fukuda, S., & Yoda, T. 2001. A novel current-tracking method for active filters based on a sinusoidal internal model for PWM inverters. *Industry Applications, IEEE Transactions on*, *37*(3), 888-895.

Gabe, I. J., Montagner, V. F., & Pinheiro, H. 2009. Design and implementation of a robust current controller for VSI connected to the grid through an LCL filter. *Power Electronics, IEEE Transactions on*, *24*(6), 1444-1452.

Gajanayake, C.J., Vilathgamuwa, D.M., Loh, P.C., Blaabjerg, F. and Teodorescu, R., 2007, June. A z-source inverter based flexible DG system with P+ resonance and repetitive controllers for power quality improvement of a weak grid. In *Power Electronics Specialists Conference, 2007. PESC 2007. IEEE* (pp. 2457-2463). IEEE.

Gajanayake, C.J., Vilathgamuwa, D.M., Loh, P.C., Teodorescu, R. and Blaabjerg, F., 2009. Z-source-inverter-based flexible distributed generation system solution for grid power quality improvement. *Energy Conversion, IEEE Transactions on*, *24*(3), pp.695-704.

Geibel, D. et al., 2009. Improvement of Power Quality and Reliability with Multifunctional PV-Inverters in Distributed Energy Systems. *Electric power quality and utilisation (EPQU)*.

Gidwani, L., Tiwari, H. and Bansal, R.C., 2013. Improving power quality of wind energy conversion system with unconventional power electronic interface. *International Journal of Electrical Power & Energy Systems*, *44*(1), pp.445-453.

Gonzalez, D. et al., 2012. Modeling and control of grid connected photovoltaic systems. *Revista Facultad De Ingenieria-Universidad De Antioquia*, pp.145–156. Available at: <Go to

ISI>://WOS:000302266900015.

Gow, J.A. and Manning, C.D., 1999, March. Development of a photovoltaic array model for use in power-electronics simulation studies. In *Electric Power Applications, IEE Proceedings-* (Vol. 146, No. 2, pp. 193-200). IET.

Goyal, S., Ghosh, A. and Ledwich, G., 2009. Active power flow control in a distribution system using discontinuous voltage controller. *Electric Power Systems Research*, *79*(1), pp.255-264.

Güngör, V.C. et al., 2011. Smart Grid Technologies : Communication Technologies and Standards. *IEEE Transactions on Industrial Informatics*, 7(4), pp.529–539.

Hadjidemetriou, L., Kyriakides, E., & Blaabjerg, F. 2013. A new hybrid PLL for interconnecting renewable energy systems to the grid. *Industry Applications, IEEE Transactions on*, *49*(6), 2709-2719.

Hamadi, A., Rahmani, S., Al-Haddad, K. and Al-Turki, Y., 2011, November. A three-phase three wire grid-connect photovoltaic energy source with sepic converter to track the maximum power point. In *IECON 2011-37th Annual Conference on IEEE Industrial Electronics Society* (pp. 3087-3092). IEEE.

Hassan, F.A., 2005. On Power Electronics Interface for Distributed Generation Applications and its Impact on System Reliability to Customers On Power Electronics Interface for Distributed Generation Applications and its Impact on System Reliability to Customers.

Hassan, M. & Bhuiyan, A.H., 2010. Design and performance evaluation of three-phase inverter for grid-connected photovoltaic system. *Journal of Electrical Engineering*, pp.1–8.

He, C., Xie, X., Yan, H., Xie, C. and Chen, G., 2011. A novel grid-connected converter with active power filtering function. *Energy Procedia*, *12*, pp.348-354.

Hoffmann, W., 2006. PV solar electricity industry: Market growth and perspective. *Solar Energy Materials and Solar Cells*, 90(18-19), pp.3285–3311.

IEEEStandards, 2009. *IEEE Std 1547.2-2008 IEEE Application Guide for IEEE Std 1547, IEEE Standard for Interconnecting Distributed Resources with Electric Power Systems*.

Khadkikar, V., Varma, R.K., Seethapathy, R., Chandra, A. and Zeineldin, H., 2012, June. Impact of distributed generation penetration on grid current harmonics considering non-linear loads. In *Power Electronics for Distributed Generation Systems (PEDG), 2012 3rd IEEE International Symposium on*(pp. 608-614). IEEE.

Jena, S., Babu, B.C. and Naik, A., 2011. Experimental study on reactive power management in inverter-interfaced distributed generation system.

Jena, S. and Babu, B.C., 2011, May. Power quality improvement of 1-Φ grid-connected PWM inverter using fuzzy with hysteresis current controller. In *Environment and Electrical Engineering (EEEIC), 2011 10th International Conference on* (pp. 1-4). IEEE.

Jena, S., Babu, B.C., Naik, A.K. and Mishra, G., 2011, December. Performance improvement of single-phase grid—Connected PWM inverter using PI with hysteresis current controller. In *Energy, Automation, and Signal (ICEAS), 2011 International Conference on* (pp. 1-5). IEEE.

Jena, S., Babu, B.C., Mishra, G. and Naik, A.K., 2011, December. Reactive power compensation in inverter-interfaced distributed generation. In *Energy, Automation, and Signal (ICEAS), 2011 International Conference on* (pp. 1-6). IEEE.

Johnson, B.A., 2013. MODELING AND ANALYSIS OF A PV GRID-TIED SMART INVERTER'S SUPPORT FUNCTIONS. *Master's Thesis*.

Kadri, R., Gaubert, J.-P. & Champenois, G., 2011. An Improved Maximum Power Point Tracking for Photovoltaic Grid-Connected Inverter Based on Voltage-Oriented Control. *IEEE Transactions On Industrial Electronics*, 58(1), pp.66–75. Available at: http://ieeexplore.ieee.org/lpdocs/epic03/wrapper.htm?arnumber=6617987.

Karimi, H., Yazdani, A. and Iravani, R., 2011. Robust control of an autonomous four-wire electronically-coupled distributed generation unit. *Power Delivery, IEEE Transactions on*, *26*(1), pp.455-466.

Karmiris, G., Tsengenes, G. and Adamidis, G., 2012. A multifunction control scheme for current harmonic elimination and voltage sag mitigation using a three phase three level flying capacitor inverter. *Simulation Modelling Practice and Theory*, *24*, pp.15-34.

Kaura, V. & Blasko, V., 1997. Operation of a phase locked loop system under distorted utility\nconditions. *IEEE Transactions on Industry Applications*, 33(1), pp.58–63.

Kazmierkowski, M. P., & Malesani, L. 1998. Current control techniques for three-phase voltage-source PWM converters: a survey. *Industrial Electronics, IEEE Transactions on*, *45*(5), 691-703.

Khadkikar, V., 2012. Enhancing electric power quality using UPQC: a comprehensive overview. *Power Electronics, IEEE Transactions on*, *27*(5), pp.2284-2297.

Kim, H., Yu, T. and Choi, S., 2008. Indirect current control algorithm for utility interactive inverters in distributed generation systems. *Power Electronics, IEEE Transactions on*, *23*(3), pp.1342-1347.

Lamchich, M. R. M. T. 2004. Average current mode control of a voltage source inverter

connected to the grid: application to different filter cells. *Journal of Electrical Engineering*, *55*(3-4), 77-82.

Leslie Jr, L. G. 2003. *Design And Analysis Of A Grid Connected Photovoltaic Generation System With Active Filtering Function* (Master's dissertation, Virginia Polytechnic Institute and State University).

Lettl, J., Bauer, J. & Linhart, L., 2011. Comparison of Different Filter Types for Grid Connected Inverter. In *PIERS Proceedings*. MOROCCO, pp. 1426–1429.

Li, F., Wang, X., Chen, Z., Zhang, X. and Hu, Y., 2011, November. A control strategy for multi-functional converter to improve grid power quality. In *IECON 2011-37th Annual Conference on IEEE Industrial Electronics Society* (pp. 790-795). IEEE.

Lin, B.R. and Chen, J.J., 2006, November. Three-phase two-leg inverter for stand-alone and grid-connected renewable energy systems. In *TENCON 2006. 2006 IEEE Region 10 Conference* (pp. 1-4). IEEE.

Liserre, M., Teodorescu, R., & Blaabjerg, F. 2004. Stability of grid-connected PV inverters with large grid impedance variation. In *Power Electronics Specialists Conference, 2004. PESC 04. 2004 IEEE 35th Annual*(Vol. 6, pp. 4773-4779). IEEE.

Liserre, M., Blaabjerg, F., & Hansen, S. 2005. Design and control of an LCL-filter-based three-phase active rectifier. *Industry Applications, IEEE Transactions on*, *41*(5), 1281-1291.

Lopes, J.A.P., Moreira, C.L. & Madureira, A.G., 2006. Defining control strategies for microgrids islanded operation. *IEEE Transactions on Power Systems*.

Macken, K.J., Vanthournout, K., Van den Keybus, J., Deconinck, G. and Belmans, R.J., 2004. Distributed control of renewable generation units with integrated active filter. *Power Electronics, IEEE Transactions on*, *19*(5), pp.1353-1360.

Mahmood, H. and Jiang, J., 2012. Modeling and control system design of a grid connected VSC considering the effect of the interface transformer type.*Smart Grid, IEEE Transactions on*, *3*(1), pp.122-134.

Makhlouf, M Messai, Nabti, K and Benalla, H., 2012. Modeling and Simulation of Grid-connected Photovoltaic Distributed Generation System. In *First International Conference on Renewable Energies and Vehicular Technology Modeling*. pp. 187–193.

Malek, H., 2014. *Control of Grid-Connected Photovoltaic Systems Using Fractional Order Operators*,

Marafia, a. H., 2001. Feasibility study of photovoltaic technology in Qatar. *Renewable Energy*, 24(3-4), pp.565–567.

Marei, M., El-Saadany, E.F. and Salama, M., 2004. A novel control algorithm for the DG interface to mitigate power quality problems. *Power Delivery, IEEE Transactions on*, *19*(3), pp.1384-1392.

Maris, T.I., Ekonomou, L. and Fotis, G.P., 2007. Modeling of a single-phase photovoltaic inverter. *Solar energy materials and solar cells*, *91*(18), pp.1713-1725.

Marwali, M.N. and Keyhani, A., 2004. Control of distributed generation systems-Part I: Voltages and currents control. *Power Electronics, IEEE Transactions on*, *19*(6), pp.1541-1550.

Massawe, H.B., 2013. Grid Connected Photovoltaic Systems with SmartGrid functionality. *Master's Thesis; NTNU*, (June).

Mataifa, H., Raji, A. & Tzoneva, R., 2015. Grid-mode Controller Design for a Dual-mode Inverter Interface for a Distributed Generation Source. In *Industrial and Commercial Use of Energy (ICUE), International Conference on the. IEEE,*. pp. 317–324.

Mazumder, S.K. et al., 2010. A universal grid-connected fuel-cell inverter for residential application. *IEEE Transactions on Industrial Electronics*, 57(10), pp.3431–3447.

Meersman, B., De Kooning, J., Vandoorn, T., Degroote, L., Renders, B., & Vandevelde, L. 2010. Overview of PLL methods for distributed generation units. In *Universities Power Engineering Conference (UPEC), 2010 45th International* (pp. 1-6). IEEE.

Mohamed, Y. A. R., & El-Saadany, E. F. 2007. An improved deadbeat current control scheme with a novel adaptive self-tuning load model for a three-phase PWM voltage-source inverter. *Industrial Electronics, IEEE Transactions on*,*54*(2), 747-759.

Mohamed, Y.A.R.I., 2011. Mitigation of dynamic, unbalanced, and harmonic voltage disturbances using grid-connected inverters with LCL filter. *IEEE Transactions on Industrial Electronics*.

Mohan, N. and Undeland, T.M., 2007. *Power electronics: converters, applications, and design*. John Wiley & Sons.

Ned Mohan, 2003. *First Courses On Power Electronics And Drives - Ned Mohan.pdf* 2003rd ed., Minneapolis: MNPERE P.O Box 14503, Minneapolis, MN 55414 USA.

Paál, E., Weitzl, Z. & Choi, C.S., 2011. Grid Management Functions built in PV Inverters for Distributed Power Generation. *8th International Conference on Power Electronics*, (11).

Paál, E. and Tatai, Z., 2010, September. Grid Connected Inverters influence on power quality of Smart Grid. In *Power Electronics and Motion Control Conference (EPE/PEMC), 2010 14th International* (pp. T6-35). IEEE.

Pádua, M. S., Deckmann, S. M., & Marafão, F. P. 2005. Frequency-adjustable positive sequence detector for power conditioning applications. In*Power Electronics Specialists Conference, 2005. PESC'05. IEEE 36th* (pp. 1928-1934). IEEE.

Panda, S., Mishra, A. & Srinivas, B., for Adjustable Speed Drive Applications. 2009.

Park, S. et al., 2003. A New Single-Phase Five-Level PWM Inverter Employing a Deadbeat Control Scheme. , 18(3), pp.831–843.

Parkpoom, S., Harrison, G.P. & Bialek, J.W., 2004. Climate change impacts on electricity demand. *39th International Universities Power Engineering Conference, 2004. UPEC 2004.*, 3(Table I), pp.1342–1346.

Pastor, M. & Dudrik, J., 2013. Design of output LCL filter for 15-level cascade inverter. *Elektronika ir Elektrotechnika*, 19(8).

Pegels, A. 2010. Renewable energy in South Africa: Potentials, barriers and options for support. *Energy policy*, *38*(9), 4945-4954.

Peng, F.Z., 2003. Z-source inverter. *IEEE Transactions on Industry Applications*.

Petrone, G., Spagnuolo, G. and Vitelli, M., 2007. Analytical model of mismatched photovoltaic fields by means of Lambert W-function. *Solar Energy Materials and Solar Cells*, *91*(18), pp.1652-1657

Pouresmaeil, E., Miguel-Espinar, C., Massot-Campos, M., Montesinos-Miracle, D. and Gomis-Bellmunt, O., 2013. A control technique for integration of DG units to the electrical networks. *Industrial Electronics, IEEE Transactions on*, *60*(7), pp.2881-2893.

Powertech & Creamer Media's research channel Africa, 2014. ELECTRICITY. *A review of South Africa's electricity sector*, (February).

Renders, B., De Gussemé, K., Ryckaert, W.R. and Vandevelde, L., 2009. Converter-connected distributed generation units with integrated harmonic voltage damping and harmonic current compensation function. *Electric power systems research*, *79*(1), pp.65-70.

Reznik, A. et al., 2012. LCL filter design and performance analysis for small wind turbine systems. In *Power Electronics and Machines in Wind Applications (PEMWA), 2012 IEEE*.

Reznik, A. 2012. *Analysis and Design of a Smart-inverter for Renewable Energy Interconnection to the Grid* (Masters dissertation, Colorado School of Mines).

Rocabert, J., Luna, A., Blaabjerg, F., & Rodríguez, P. 2012. Control of power converters in AC microgrids. *Power Electronics, IEEE Transactions on*, *27*(11), 4734-4749.

Rodriguez, P., Timbus, A., Teodorescu, R., Liserre, M. and Blaabjerg, F., 2009. Reactive

power control for improving wind turbine system behavior under grid faults. *IEEE Transactions on Power Electronics*, *24*(7-8), pp.1798-1801.

Ross, K. & Jordan, B., 2012. Renewable Energy for a Cleaner Future. *earthdaynetwork*.

Rowan, T.M. and Kerkman, R.J., 1986. A new synchronous current regulator and an analysis of current-regulated PWM inverters. *Industry Applications, IEEE Transactions on*, (4), pp.678-690.

Saccomando, G. & Svensson, J., 2001. Transient operation of grid-connected voltage source converterunder unbalanced voltage conditions. *Conference Record of the 2001 IEEE Industry Applications Conference. 36th IAS Annual Meeting (Cat. No.01CH37248)*, 4, pp.1–6.

Saeedifard, M., Nikkhajoei, H., Iravani, R. and Bakhshai, A., 2007. A space vector modulation approach for a multimodule HVDC converter system. *Power Delivery, IEEE Transactions on*, *22*(3), pp.1643-1654.

Salam, A.A. et al., 2010. An Improved Inverter Control Scheme for Managing the Distributed Generation Units in a Microgrid. *International Review of Electrical Engineering (I.R.E.E)*, 5(3).

Sangita Nandurkar, M.R. & Rajeev, M., 2012. Design and Simulation of three phase Inverter for grid connected Photovoltic systems. *Proceedings of Third Biennial National Conference*.

Satoh, K. and Yamamoto, M., 2001. The present state of the art in high-power semiconductor devices. *Proceedings of the IEEE*, *89*(6), pp.813-821.

Savaghebi, M., Vasquez, J.C., Jalilian, A., Guerrero, J.M. and Lee, T.L., 2013. Selective compensation of voltage harmonics in grid-connected microgrids.*Mathematics and Computers in Simulation*, *91*, pp.211-228.

Schauder, C.D. and Caddy, R., 1982. Current control of voltage-source inverters for fast four-quadrant drive performance. *IEEE Transactions on Industry Applications*, *2*(IA-18), pp.163-171.

Scheuer, G. and Stemmler, H., 1996. Analysis of a 3-level-VSI neutral-point-control for fundamental frequency modulated SVC-applications.

Schonardie, M.F. & Martins, D.C., 2008. Application of the dq0 transformation in the three-phase grid-connected PV systems with active and reactive power control. *2008 IEEE International Conference on Sustainable Energy Technologies*, pp.18–23.

Selvaraj, J. & Rahim, N. a., 2009. Multilevel Inverter For Grid-Connected PV System Employing Digital PI Controller. *IEEE Transactions on Industrial Electronics*, 56(1), pp.149–158.

Serban, I. and Marinescu, C., 2010, July. Active power decoupling circuit for a single-phase battery energy storage system dedicated to autonomous microgrids. In *Industrial Electronics (ISIE), 2010 IEEE International Symposium on* (pp. 2717-2722). IEEE.

Shen, G. et al., 2009. A new current feedback PR control strategy for grid-connected VSI with an LCL filter. *Conference Proceedings - IEEE Applied Power Electronics Conference and Exposition - APEC*, pp.1564–1569.

Singh, M., Khadkikar, V., Chandra, A. and Varma, R.K., 2011. Grid interconnection of renewable energy sources at the distribution level with power-quality improvement features. *Power Delivery, IEEE Transactions on*,*26* (1), pp.307-315.

Singh, M., Khadkikar, V. and Chandra, A., 2011. Grid synchronisation with harmonics and reactive power compensation capability of a permanent magnet synchronous generator-based variable speed wind energy conversion system. *Power Electronics, IET*, *4*(1), pp.122-130.

Sissine, F., 2007. Renewable Energy : Background and Issues for the 110 th Congress Resources , Science , and Industry Division. *CRS Report*.

Smith, J., 2013. Modeling High-Penetration PV for Distribution Interconnection Studies. *Electric power research institute*.

Solangi, K. H., Islam, M. R., Saidur, R., Rahim, N. A., & Fayaz, H. 2011. A review on global solar energy policy. *Renewable and sustainable energy reviews*, *15*(4), 2149-2163.

Song, Y.H. and Johns, A., 1999. *Flexible ac transmission systems (FACTS)*(No. 30). IET.

Su, L., Li, G. and Jin, Z., 2011, July. Modeling, control and testing of a voltage-source-inverter-based microgrid. In *Electric Utility Deregulation and Restructuring and Power Technologies (DRPT), 2011 4th International Conference on* (pp. 724-729). IEEE.

Sun, Z., & Zhang, X. Y. 2012. Advances on distributed generation technology.*Energy Procedia*, *17*, 32-38.

Tang, Y., Loh, P. C., Wang, P., Choo, F. H., Gao, F., & Blaabjerg, F. 2012. Generalized design of high performance shunt active power filter with output LCL filter. *Industrial Electronics, IEEE Transactions on*, *59*(3), 1443-1452.

Teke, A., & Latran, M. B. 2014. Review of Multifunctional Inverter Topologies and Control Schemes Used in Distributed Generation Systems. *Journal of Power Electronics*, *14*(2), 324-340.

Teodorescu, R. & Blaabjerg, F., 2004. Flexible Control of Small Wind Turbines With Grid Failure Detection Operating in. *IEEE TRANSACTIONS ON POWER ELECTRONICS*, 19(5),

pp.1323–1332.

Teodorescu, R., Liserre, M. & Rodriguez, P., 2011. *GRID CONVERTERS FOR PHOTOVOLTAIC AND WIND POWER SYSTEMS* 1st ed., A John Wiley and Sons, Ltd., Publication.

Timbus, A. et al., 2005. Synchronization methods for three phase distributed power generation systems. An overview and evaluation. *PESC Record - IEEE Annual Power Electronics Specialists Conference*, 2005, pp.2474–2481.

Trabelsi, M. & Ben-Brahim, L., 2011. Experimental photovoltaic power supply based on flying capacitors multilevel inverter. *3rd International Conference on Clean Electrical Power: Renewable Energy Resources Impact, ICCEP 2011*, (Figure 1), pp.578–583.

Trabelsi, M., Ben-Brahim, L., & Ghazi, K. A. (2013, November). An improved Real-Time Digital Feedback Control for grid-tie multilevel inverter. In *Industrial Electronics Society, IECON 2013-39th Annual Conference of the IEEE* (pp. 5776-5781). IEEE.

Trejos, A., Gonzalez, D. & Ramos-Paja, C.A., 2012. Modeling of step-up grid-connected photovoltaic systems for control purposes. *Energies*, 5(6), pp.1900–1926.

Trujillo, C.L., Velasco, D., Figueres, E. and Garcerá, G., 2010. Analysis of active islanding detection methods for grid-connected microinverters for renewable energy processing. *Applied Energy*, *87*(11), pp.3591-3605.

Tsengenes, G. and Adamidis, G., 2011. Investigation of the behaviour of a three phase grid-connected photovoltaic system to control active and reactive power. *Electric Power Systems Research*, *81*(1), pp.177-184.

Twining, E. & Holmes, D.G., 2003. Grid current regulation of a three-phase voltage source inverter with an LCL input filter. *IEEE Transactions on Power Electronics*.

Ullah, N.R., Thiringer, T. & Karlsson, D., 2007. Voltage and Transient Stability Support by Wind Farms Complying With the E . ON Netz Grid Code. *IEEE Transactions on Power Electronics*, 22(4), pp.1647–1656.

Umland, J. W., & Safiuddin, M. (1990). Magnitude and symmetric optimum criterion for the design of linear control systems: what is it and how does it compare with the others?. *Industry Applications, IEEE Transactions on*, *26*(3), 489-497.

Vasquez, J.C., Guerrero, J.M., Savaghebi, M., Eloy-Garcia, J. and Teodorescu, R., 2013. Modeling, analysis, and design of stationary-reference-frame droop-controlled parallel three-phase voltage source inverters.*Industrial Electronics, IEEE Transactions on*, *60*(4), pp.1271-1280.

Ventosa, M. et al., 2005. Electricity market modeling trends. *Elsevier Energy Policy*, 33(7), pp.897–913. Available at: http://linkinghub.elsevier.com/retrieve/pii/S0301421503003161 [Accessed July 11, 2014].

Verhoeven, B. & KEMA, B.V., 1998. Utility Aspects of Grid Connected. *International energy agency*, p.168. Available at: http://www.hme.ca/gridconnect/IEA_PVPS_Task_5-01_Utility_aspects_of_PV_grid-connection.pdf.

Vijayapriya, T. & Kothari, D.P., 2011. Smart Grid : An Overview. *scientific research*, (November), pp.305–311.

Vodyakho, O., & Mi, C. C. 2009. Three-level inverter-based shunt active power filter in three-phase three-wire and four-wire systems. *Power Electronics, IEEE Transactions on*, *24*(5), 1350-1363.

Wang, F., Duarte, J.L. and Hendrix, M.A., 2011. Grid-interfacing converter systems with enhanced voltage quality for microgrid application—concept and implementation. *Power Electronics, IEEE Transactions on*, *26*(12), pp.3501-3513.

Walling, R.A., Clark, K. & Member, S., 2010. Grid Support Functions Implemented in Utility-Scale PV Systems. , pp.1–5.

Weedall, M., 2000. BPA Smart Grid Overview Smart Grid. , pp.1–18.

Winkler, H., 2005. Renewable energy policy in South Africa: Policy options for renewable electricity. *Energy Policy*, 33(1), pp.27–38.

Wu, B., 2006. *High-power converters and AC drives*. John Wiley & Sons.

Xiao-Hong, Z., 2009. Electricity demand side management and its different promotion measures. *Asia-Pacific Power and Energy Engineering Conference, APPEEC*.

Xue, Y. et al., 2011. Towards next generation photovoltaic inverters. *IEEE Energy Conversion Congress and Exposition*, pp.2467–2474. Available at: http://ieeexplore.ieee.org/lpdocs/epic03/wrapper.htm?arnumber=6064096.

Yafaoui, A., Wu, B. and Kouro, S., 2012. Improved active frequency drift anti-islanding detection method for grid connected photovoltaic systems. *Power Electronics, IEEE Transactions on*, *27*(5), pp.2367-2375.

Yang, Y. & Blaabjerg, F., 2015. Overview of Single-Phase Grid-Connected Photovoltaic Systems.

Yazdani, A. & Iravani, R., 2010. *Voltage-Sourced Converters in Power Systems: Modeling, Control, and Applications*, Available at: http://books.google.com/books?id=_x_4Cu-BKwkC&pgis=1.

Yoo, D. K., & Wang, L. 2011. A model predictive resonant controller for grid-connected voltage source converters. In *IECON 2011-37th Annual Conference on IEEE Industrial Electronics Society* (pp. 3082-3086). IEEE.

Zamani, M.A., Yazdani, A. and Sidhu, T.S., 2012. A control strategy for enhanced operation of inverter-based microgrids under transient disturbances and network faults. *Power Delivery, IEEE Transactions on*, *27*(4), pp.1737-1747.

Zeng, Z., Yang, H., Zhao, R., & Cheng, C. (2013). Topologies and control strategies of multi-functional grid-connected inverters for power quality enhancement: A comprehensive review. *Renewable and Sustainable Energy Reviews*, *24*, 223-270. Available at: http://linkinghub.elsevier.com/retrieve/pii/S1364032113001925 [Accessed June 13, 2014].

APPENDICES

Appendix 1

Inverter before the integration of the controller

The Simulink model of the grid-connected inverter before the controller was connected is shown below. The internal generation of modulating signals was selected for the PWM block in this model at this stage since the controller is yet to be integrated in the model.

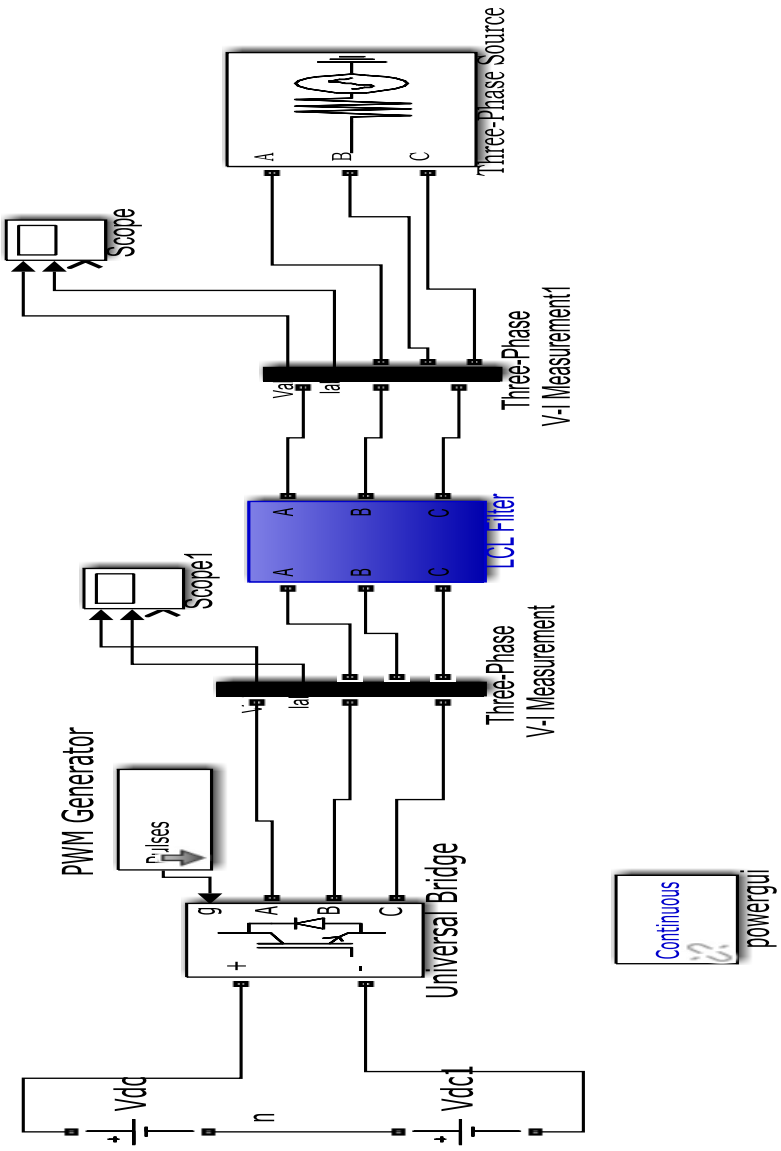

Appendix 2

Inverter with the controller

The complete grid connected inverter system with the integration of the control system simulated in Simulink is shown below. The signal builder block is used to vary the active and reactive power reference for this model.

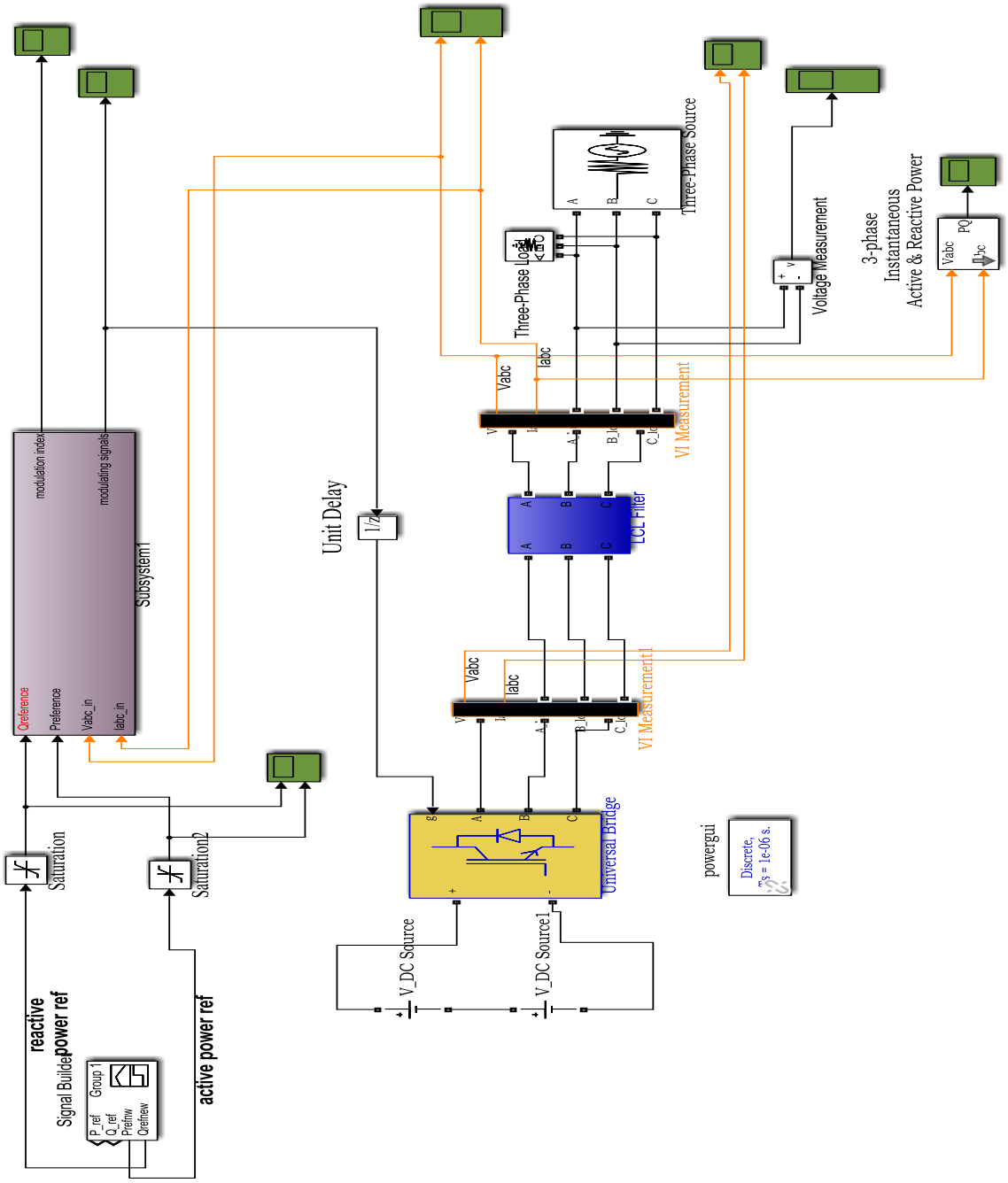

Appendix 3

The grid-connected inverter controller

The control model employed for the grid-connected inverter system which is the current control algorithm using the synchronous (dq) reference frame is represented below.

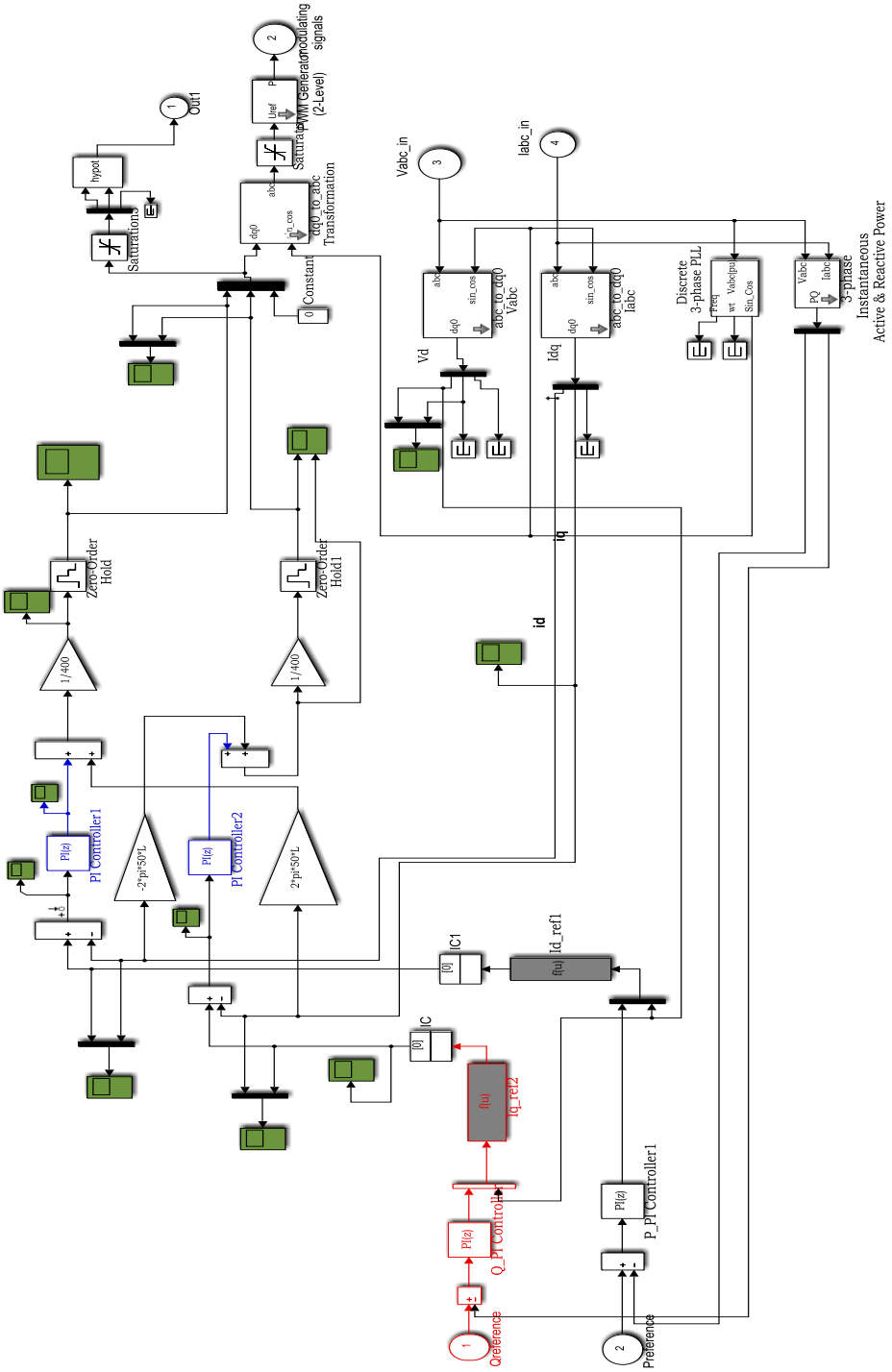

Appendix 4

Linearized model of the grid connected inverter system

The main model comprises of non-linear components such as the three-phase IGBT VSC block due to the switching characteristics of the IGBTs present in the block, the average model based VSC block has been used for the purpose of linearizing the system and tuning of the PI controllers afterwards.